

# Event-Triggered Robust Model Predictive Control

by

**Li Deng**

A thesis submitted in partial fulfillment of the requirements for the degree of

Doctor of Philosophy

in

Control Systems

Department of Electrical and Computer Engineering  
University of Alberta

©Li Deng 2023

# Abstract

Model predictive control (MPC) is one of the most popular control strategies in modern control systems and has been used in a variety of applications due to its ability to handle hard constraints. As a significant branch of MPC, robust MPC is an effective strategy to deal with external disturbances or system uncertainties, and guarantee robust stability of uncertain systems. However, with the increase of system complexity and various demands, robust MPC optimization problems become more and more complicated, leading to high computational loads. By contrast, event-triggered control, which executes control actions only when some events occur, has shown advantages over traditional periodic control in dealing with resource constraints in energy, computation, and communication. Hence, this thesis is concerned with the combination of robust MPC and event-triggered control to address the challenges in traditional MPC.

Three research topics are considered. Firstly, from a deterministic point of view, a two-step triggering scheme involving a tentative verification of a deterministic triggering condition and a delayed triggering with a waiting horizon is proposed to ensure necessary events and reduce the number of times of solving the MPC optimization problem. Secondly, the stochasticity is considered into the design of event-triggered schemes, which is investigated in two aspects: i) Based on the probability density function of disturbances, an event-triggered scheme related to a designed minimal robust positively invariant set of tube-

based MPC is constructed to generate dynamic triggering sets, leading to a prescribed expectation of inter-execution times and a reduction of computational burden, while not sacrificing the quadratic performance significantly.

ii) With an updating law for the transition probabilities of a Markov chain, a stochastic triggering scheme involving a prescribed triggering function and a checking function is proposed to achieve aperiodic and non-persistent event verification and enlarge the inter-execution time. Both tube-based MPC and linear matrix inequality-based (LMI-based) MPC are presented with such a stochastic triggering scheme. Thirdly, for unknown systems with initially measured input-output data, a robust data-driven MPC with a terminal inequality constraint is developed to complete the analysis of recursive feasibility and stability, and an event-triggered scheme is designed based on a mismatch between the data-driven model and the original plant to reduce computational burden. Finally, an event-triggered stochastic MPC approach is applied to constrained queueing networks with a dynamic topology for the scheduling problem.

Different from most existing results which focus on only triggering action, the proposed approaches also incorporate event checking into the event-triggered scheme design and make use of optimal control sequences of MPC, resulting in more flexible triggering schemes with longer inter-execution times. The effectiveness of the proposed approaches is verified by numerical examples and comparative studies with existing work. Recursive feasibility of MPC and robust stability of linear discrete-time systems are theoretically analyzed. These results provide some new insights for the design of event-triggered robust MPC.

# Preface

The ideas in Chapters 2-6 were from discussions with Prof. Tongwen Chen and Prof. Zhan Shu. The algorithms, mathematical derivations and proofs, and numerical simulations were my original work, as well as the introduction in Chapter 1.

- Chapter 2 has been published as: Li Deng, Zhan Shu, and Tongwen Chen, Event-triggered robust model predictive control for linear discrete-time systems with a guaranteed average inter-execution time. *International Journal of Robust & Nonlinear Control*, vol. 32, no. 6, pp. 3969-3985, Apr. 2022.
- Chapter 3 has been published as: Li Deng, Zhan Shu, and Tongwen Chen, Robust model predictive control using a two-step triggering scheme. *IEEE Transactions on Automatic Control*, vol. 68, no. 3, pp. 1934-1940, Apr. 2022. An extension of this Chapter has been published as: Li Deng, Zhan Shu, and Tongwen Chen, Event-triggered robust distributed MPC for multi-agent systems with a two-step event verification. *8th IFAC Symposium on System Structure and Control*, vol. 55, no. 34, pp. 144-149, Sep. 2022.
- Chapter 4 has been published as: Li Deng, Zhan Shu, and Tongwen Chen, Event-triggered robust MPC with stochastic event verification. *Automatica*, vol. 146, Dec. 2022.
- Chapter 5 has been submitted to *IEEE Transactions on Automatic Control* as: Li Deng, Zhan Shu, and Tongwen Chen, Event-triggered ro-

bust MPC with terminal inequality constraints: A data-driven approach, Aug. 2022.

- Chapter 6 has been submitted to *IEEE Transactions on Network Science and Engineering* as: Li Deng, Zhan Shu, and Tongwen Chen, Event-triggered stochastic model predictive control for constrained queueing networks, Jun. 2023.

# Acknowledgements

First and foremost, I would like to express my appreciation to my supervisors, Prof. Tongwen Chen and Prof. Zhan Shu, for their valuable guidance and kind support throughout this work. Their profound knowledge and experience in control theory, alongside with encouragement and patience for me, not only helped me to find the right research path and cope with the problems I encountered during my Ph.D. program, but also enriched my knowledge and improved my qualification as a researcher. I have been fortunate enough to work with the two nice supervisors. I would also like to thank my committee member Prof. Qing Zhao for her precious time and valuable feedback.

Furthermore, I am deeply grateful to Drs. Jun Shang, Hao Yu, and Jing Zhou for their valuable comments and suggestions. Their passion for scientific research and self-discipline have inspired me to work harder and make better achievements. I would like to thank all previous and current members of the research group, Boyuan Zhou, Junyi Yang, Mani Hemanth Dhullipalla, Haniyeh Seyed Alinezhad, Harikrishna Rao Mohan Rao, Jinyuan Wei, and Ziyi Guo for their kindness, encouragement, and help.

I also wish to acknowledge the financial support from the China Scholarship Council (CSC) and Natural Sciences and Engineering Research Council of Canada (NSERC).

Last but not the least, greatest thanks also go to my family members and friends for their unconditional support and understanding over the past years. Again, to people mentioned or not, my thankfulness and gratitude are beyond words and can never be written well enough.

# Contents

<b>1</b>	<b>Introduction</b>	<b>1</b>
1.1	Research Background . . . . .	1
1.1.1	Robust Model Predictive Control . . . . .	2
1.1.2	Event-Triggered Control . . . . .	3
1.2	Literature Review . . . . .	4
1.2.1	Event-Triggered Robust MPC with Known System Models	4
1.2.2	Event-Triggered Data-Driven MPC . . . . .	8
1.3	Research Motivation and Contributions . . . . .	10
1.4	Thesis Outline . . . . .	12
<b>2</b>	<b>Event-Triggered Robust MPC with Guaranteed Average Inter-Execution Times</b>	<b>14</b>
2.1	Problem Formulation . . . . .	15
2.2	Event-Triggered Robust MPC . . . . .	17
2.2.1	Setup of Tube-Based MPC . . . . .	17
2.2.2	Event-Triggered Scheme Design . . . . .	20
2.3	Recursive Feasibility and Stability Analysis . . . . .	25
2.3.1	Recursive Feasibility . . . . .	26
2.3.2	Robust Stability . . . . .	27
2.4	Simulation Examples . . . . .	29
2.5	Summary . . . . .	34
<b>3</b>	<b>Robust MPC Using A Two-Step Triggering Scheme</b>	<b>35</b>
3.1	Tube-Based MPC with Two-Step Triggering . . . . .	36

3.1.1	Problem Formulation . . . . .	36
3.1.2	Two-Step Triggering MPC Design . . . . .	38
3.1.3	Recursive Feasibility and Stability Analysis . . . . .	45
3.1.4	Simulation Examples . . . . .	46
3.2	An Extension to Multi-Agent Systems . . . . .	50
3.2.1	Problem Formulation . . . . .	50
3.2.2	Distributed MPC with Two-Step Triggering . . . . .	52
3.2.3	Stability and Consensus Analysis . . . . .	54
3.2.4	Simulation Example . . . . .	57
3.3	Summary . . . . .	59
<b>4</b>	<b>Event-Triggered Robust MPC with Stochastic Event Verifi-</b>	
	<b>cation</b>	<b>60</b>
4.1	Problem Formulation . . . . .	61
4.2	Stochastic Event-Triggered Scheme Design . . . . .	62
4.2.1	Triggering Function $g$ . . . . .	63
4.2.2	Triggering Indicator $\xi_{t_i}$ and Generated Random Process $\xi_t$ . . . . .	64
4.2.3	Checking Function $\mu$ . . . . .	67
4.2.4	Inter-Execution Time . . . . .	69
4.3	Stochastic Event-Triggered Tube-Based MPC Design . . . . .	71
4.3.1	Tube-Based MPC Design . . . . .	72
4.3.2	Recursive Feasibility and Stability Analysis . . . . .	74
4.4	Stochastic Event-Triggered LMI-Based MPC Design . . . . .	76
4.4.1	LMI-Based MPC Design . . . . .	76
4.4.2	Recursive Feasibility and Stability Analysis . . . . .	82
4.5	Simulation Examples . . . . .	83
4.6	Summary . . . . .	87
<b>5</b>	<b>Event-Triggered Robust MPC: A Data-Driven Approach</b>	<b>88</b>
5.1	Problem Formulation . . . . .	89



5.2	Terminal Set $\mathcal{Z}_f$ Design . . . . .	95
5.2.1	Data-Based Closed-Loop Representation . . . . .	96
5.2.2	Terminal Weighting Matrix $P$ and Control Gain $\hat{K}$ . . . . .	99
5.2.3	The Value of $\alpha$ . . . . .	101
5.2.4	Terminal Inequality Constraint . . . . .	101
5.3	Event-Triggered Scheme Design . . . . .	103
5.3.1	Triggering Threshold . . . . .	104
5.3.2	Event-Triggered Controller . . . . .	105
5.4	Recursive Feasibility and Stability Analysis . . . . .	106
5.4.1	Recursive Feasibility . . . . .	107
5.4.2	Input-to-State Stability . . . . .	109
5.5	Simulation Example . . . . .	112
5.6	Summary . . . . .	116
<b>6</b>	<b>An Application to Constrained Queueing Networks</b>	<b>117</b>
6.1	Problem Formulation . . . . .	118
6.1.1	Constraints . . . . .	118
6.1.2	Control Strategy . . . . .	120
6.2	Main Results . . . . .	122
6.2.1	MPC Optimization Problem . . . . .	123
6.2.2	Event-Triggered Scheme with An Adaptive Checking S- trategy . . . . .	125
6.2.3	Event-Triggered Controller . . . . .	128
6.3	Stability of Queueing Networks . . . . .	129
6.3.1	Stability Region . . . . .	129
6.3.2	Terminal Feasible Control Set . . . . .	130
6.3.3	Stability Analysis . . . . .	131
6.4	Simulation Examples . . . . .	135
6.5	Summary . . . . .	141

<b>7</b>	<b>Conclusions and Future Work</b>	<b>142</b>
7.1	Conclusions . . . . .	142
7.2	Future Work . . . . .	144
	<b>Bibliography</b>	<b>146</b>

# List of Tables

2.1	Distribution of inter-execution times based on $K_1$ . . . . .	30
2.2	Distribution of inter-execution times based on $K_2$ . . . . .	30
2.3	Comparison results with [67] in Case A . . . . .	30
2.4	Distribution of inter-execution times . . . . .	33
2.5	Comparison results with [67] . . . . .	33
3.1	Comparison results of parameters $\mu, \tau$ . . . . .	47
3.2	Comparison results with [60] . . . . .	47
3.3	Comparison results with [67] in Case A . . . . .	49
3.4	Comparison results with [67] in Case B . . . . .	49
3.5	Comparison results with one-step triggering . . . . .	58
4.1	Average inter-execution time $\bar{\Delta}$ and performance cost $\bar{J}$ . . . . .	84
4.2	Triggering results with $\theta = 0.2$ . . . . .	85
4.3	Running results . . . . .	85
4.4	Comparison results with existing results . . . . .	87
4.5	Triggering results . . . . .	87
6.1	Triggering results for $t \in [50, 200]$ . . . . .	138
6.2	Comparison results with [97] . . . . .	140

# List of Figures

2.1	Feasible regions $\mathcal{X}_N$ . . . . .	30
2.2	Control input and state trajectories (The circles represent event-triggered instants). . . . .	33
3.1	Illustration of triggering instant sequences. . . . .	37
3.2	The accuracy of the estimation of $\kappa$ . . . . .	48
3.3	State trajectories. . . . .	48
3.4	The distributions of triggering instants (The red crosses represent unnecessary events). . . . .	58
3.5	State trajectories. . . . .	58
4.1	The evolutions of $\alpha$ and $\beta$ for different Hill coefficients. . . . .	67
4.2	Architecture of the proposed stochastic event-triggered scheme. . . . .	68
4.3	Illustration of inter-execution time. . . . .	70
4.4	Triggering instants of the proposed LMI-based MPC. . . . .	84
4.5	Triggering instants of the proposed tube-based MPC. . . . .	84
4.6	State trajectories of the proposed LMI-based MPC. . . . .	86
5.1	Architecture of the proposed event-triggered data-driven MPC. . . . .	94
5.2	Feasible regions with different terminal constraints. . . . .	113
5.3	Evolutions of $J$ with different terminal constraints. . . . .	113
5.4	Output trajectories with different triggering strategies. . . . .	114
5.5	Control input trajectories with different triggering strategies. . . . .	114
5.6	Evolutions of $J$ with different triggering strategies. . . . .	114
5.7	Average inter-execution time comparison. . . . .	115

5.8	Performance cost comparison. . . . .	115
6.1	An example of a queueing network. . . . .	120
6.2	Architecture with the proposed event-triggered scheme. . . . .	122
6.3	Illustration of inter-execution time. . . . .	127
6.4	Airport scheduling. . . . .	135
6.5	Stability region. . . . .	136
6.6	The number of customers at airports in one realization. . . . .	136
6.7	Evolution of $J^*(q(t_j))$ in one realization. . . . .	137
6.8	Checking time slots in one realization. . . . .	137
6.9	A product line. . . . .	138
6.10	Trajectories of buffers in one realization. . . . .	140
6.11	The amount of materials in all buffers in one realization. . . . .	141

# List of Symbols

$\mathbb{R}$	Set of real numbers
$\mathbb{Z}$ ( $\mathbb{Z}^+$ )	Set of (nonnegative) integers
$\mathbb{C}$	Set of complex numbers
$I_n$	$n$ by $n$ identity matrix
$\mathbf{0}_{n \times m}$ ( $\mathbf{0}_n$ )	$n$ by $m$ ( $n$ by $n$ ) zero matrix
$\ x\ $	Euclidean norm or induced matrix norm
$x^{[\ell]}$	$\ell$ th element of $x \in \mathbb{R}^n$
$P \succ (\succeq) 0$	Positive (semi-)definiteness of $P \in \mathbb{R}^{n \times n}$
$\lambda_{\min}(P)$ ( $\lambda_{\max}(P)$ )	Minimum (Maximum) eigenvalue of $P \in \mathbb{R}^{n \times n}$
$ a $	Absolute value of a scalar $a$
$\lceil a \rceil$	Nearest integer of a scalar $a$
*	A term that can be inferred by symmetry
$X^\dagger$	Moore-Penrose pseudoinverse of $X$
$\text{diag}\{\cdot\}$	Block diagonal matrix
$\mathbb{E}\{x\}$	Expectation of a random variable $x$
$d(x, \mathcal{Z})$	$\min\{\ x - z\  \mid z \in \mathcal{Z}\}$ , where $x \in \mathbb{R}^n$ , $\mathcal{Z} \subseteq \mathbb{R}^n$
$\mathbb{Z}_{[a,b]}$	Set $\{r \in \mathbb{Z} \mid a \leq r \leq b\}$ , where $a, b \in \mathbb{Z}$
$a\mathcal{Z}$	Set $\{az \mid z \in \mathcal{Z}\}$ , where $a \in \mathbb{R}$ , $\mathcal{Z} \subseteq \mathbb{R}^n$
$\mathcal{Z}_1 \oplus \mathcal{Z}_2$	Set $\{z_1 + z_2 \mid z_1 \in \mathcal{Z}_1, z_2 \in \mathcal{Z}_2\}$ , where $\mathcal{Z}_1, \mathcal{Z}_2 \subseteq \mathbb{R}^n$
$\mathcal{Z}_1 \ominus \mathcal{Z}_2$	Set $\{z \in \mathbb{R}^n \mid z \oplus \mathcal{Z}_2 \subseteq \mathcal{Z}_1\}$ , where $\mathcal{Z}_1, \mathcal{Z}_2 \subseteq \mathbb{R}^n$

# List of Acronyms

MPC	Model predictive control
ISS	Input-to-state stable
NCSs	Networked control systems
DoS	Denial-of-service
LMI	Linear matrix inequality
DTMC	Discrete-time Markov chain
LQR	Linear quadratic regulator

# Chapter 1

## Introduction

This thesis explores the design and analysis of event-triggered robust model predictive control (MPC) for linear time-invariant systems with bounded disturbances. In this chapter, the research background for event-triggered robust MPC is introduced and a literature review is provided to summarize the recent development in this area. Thereafter, the contributions of the thesis are listed, followed by a thesis outline.

### 1.1 Research Background

Model predictive control (MPC) is a modern optimal control method to predict optimized future control actions based on online numerical optimization. A main advantage of MPC is to deal with constraints on the operating region and control inputs, and optimize the closed-loop performance. It depends on the cost function to impose control objectives, such as stabilizing a system, tracking a reference trajectory or a setpoint, and approaching state estimation of a complex model. The key idea behind MPC is to utilize a dynamical model to predict the future behavior for a control input sequence over a finite time horizon. This input sequence is optimized at each time step in order to satisfy hard constraints and achieve optimal performance, and only the first element of the optimized input sequence is applied to the dynamical system; then the whole procedure is repeated at the next time step using latest available information on the system state. Since it delivers a great many



advantages such as a simple control policy for dynamic systems, generic consideration of constraints, and recursive feasibility of optimization problems, MPC has received considerable attention from academia and industry in the past decades.

### 1.1.1 Robust Model Predictive Control

As is well known, uncertainty is ubiquitous and inevitable in control applications [1, 2]. Hence, robust control techniques have been incorporated into MPC to deal with external disturbances or system uncertainties, resulting in robust MPC, which has become a main branch of MPC. In robust MPC, the bound of the uncertainty is assumed to be known, which is necessary to determine robust invariant sets limiting future states and control inputs, and is a basis for guaranteeing robust satisfaction of constraints. Although a comprehensive theory for analyzing stability, robustness, and optimality of robust MPC is available, with the increase of system complexity and various demands, robust MPC optimization problems become more and more complicated, leading to high computational loads, a large number of control parameters, and other disadvantages.

Many early approaches took account of reducing the on-line computational burden of robust MPC by introducing off-line strategies. References [3, 4, 5] designed a feedback control law off-line, and merely optimized some additional perturbations on the feedback law on-line. In [6, 7], the only on-line computation was to search a suitable feedback gain in a look-up table which was constructed off-line by solving MPC optimization problems. References [8, 9] extended the idea in [7] to off-line output feedback robust MPC. Although the above-mentioned methods obtained some promising results by using off-line methods to alleviate the on-line computation load in robust MPC, few of them can be applied to a wide range of applications since they are very complicated and inflexible. Hence, more advanced strategies need to be explored.

### 1.1.2 Event-Triggered Control

Nowadays, the majority of control systems are typically implemented over shared communication media and thus how to design effective scheduling strategies for such control systems has been a challenging problem. With conventional controllers, the information is transmitted between system components (such as actuators, sensors, and plants) in a periodic manner, regardless of whether the measured output changes or not. This approach is the so-called time-triggered control, which may lead to some unnecessary transmissions and then cause a waste of communication and computation resources. To circumvent this, event-triggered control, which releases and transmits data only when some events occur, has been developed to reduce computation and communication [10]. In event-triggered control, the system decides when to execute an action based on a well-designed triggering condition on the measured signals, leading to aperiodic communication and computation that only take place when needed. In other words, some action is executed unless some triggering condition is satisfied.

A natural question is how to design an effective triggering condition to make an event triggered at the appropriate time. Actually, such a triggering condition can be designed in different forms, such as the error between the predicted state/output and the actual state/output exceeding a given value [11, 12, 13], a function derived from stability analysis crossing a pre-defined threshold [14, 15], the actual state leaving a certain triggering set [16, 17], or a dynamic strategy depending on an internal dynamical variable [18, 19]. These triggering schemes have been effectively applied in linear systems [11, 12, 14, 20], uncertain systems [21, 22], stochastic systems [23, 24, 25], and multi-agent systems [26, 27]. Furthermore, different performance specifications have been analyzed under event-triggered control, including bounded-input bounded-output stability [28], input-to-state stability [25, 29, 30], mean square stability [31], and finite-gain  $\mathcal{L}_2$  stability [15]. Some improved event-triggered control schemes have been combined with different controller designs,

such as sliding mode controllers [23, 32],  $H_\infty$  controllers [33, 34], and model predictive controllers [27, 35, 36]. Although a great many triggering schemes have been designed for reducing data transmission in networked control systems (NCSs) [22, 26, 28, 33, 35, 36], much progress for other purposes has been made for event-triggered control, such as achieving efficient task scheduling [37], generating desirable switching rules in switched systems [38, 39, 40], and leader-following consensus problems [41, 42]. Moreover, the implementation of event-triggered control in different practical applications has been explored in, e.g., urban traffic networks [43], wastewater treatment plants [44], and large-scale transport systems [45].

## 1.2 Literature Review

Due to the potential advantages of event-triggered control over traditional time-triggered control and its wide use in various fields, it is a natural choice to combine MPC and event-triggered control to address the challenges in traditional MPC. For known system models with external disturbances or parameter uncertainties, a great deal of effort has been devoted to event-triggered robust MPC. In recent years, for unknown systems with initially measured data, data-driven techniques have been introduced to the design of robust MPC and event-triggered control, and some preliminary results have begun to appear.

### 1.2.1 Event-Triggered Robust MPC with Known System Models

With known nominal system models, research on event-triggered robust MPC has achieved extensive meaningful maturity. Typically, the results are either based on deterministic or stochastic triggering conditions.

### 1.2.1.1 Event-Triggered Robust MPC Based on Deterministic Triggering Conditions

Most existing triggering schemes used in robust MPC are based on deterministic criteria. These results have shown the benefits of event-triggered robust MPC in two aspects.

On the one hand, to alleviate the burden of communication, events are used to decide if data transmissions occur or not. For example, reference [46] presented an event-triggered robust MPC approach for discrete-time linear systems with exogenous disturbances and the state information would be sent from the sensor to the controller only if the event condition would be satisfied, reducing the communication effort while guaranteeing a desired performance. In order to mitigate the unnecessary waste of communication between the sensor and the controller, references [47, 48, 49] proposed an event-triggered output feedback robust MPC where only when the output error exceeded a given threshold, the current measured output could be transmitted to the controller. Reference [50] designed an event-triggered combined scheme of MPC and integral sliding mode control to reduce the number of transmissions of the actual plant state and avoid network congestion. From a geometrical viewpoint, a sequence of triggering hyperrectangles was constructed on-line around the optimal state sequence of a robust MPC problem in [51], leading to reduced data transmission. More complicated problems have been incorporated into the design of event-triggered robust MPC, such as, network-induced delays [52], packet dropouts [53, 54], and denial-of-service (DoS) attacks [55].

On the other hand, to reduce the burden of computation, namely, reducing the amount of solving optimization problems, events are used to determine when it is necessary to solve optimization problems. In [56, 57], an event-triggered condition was derived based on the Lipschitz property to decide whether the optimization problem should be solved or not. An aperiodic formulation of event-triggered MPC was provided in [58] based on new feasibility and stability results by imposing a terminal constraint. Reference [59]

extended the dynamic event-triggered scheme in [18] to robust MPC to reduce resource consumption more significantly. A co-design of the event-triggered condition and feedback policy was proposed in [60], achieving a larger attraction region and better control performance. More complicated but efficient event-triggered robust MPC strategies have been presented in recent years. In [61], two different event-triggered strategies were constructed in the sensor and controller nodes for reducing communication and computational loads, respectively. Reference [62] combined event-triggered and self-triggered mechanisms to save on-line computational resources from two aspects: reducing the frequency of solving the MPC optimization control problem and decreasing the prediction horizon adaptively.

Although above mentioned triggering schemes can alleviate the burden of communication and computation for robust MPC, most of them are dependent on the current states or measurement errors only. From the conservatism point of view, such deterministic triggering schemes with one-step checking may lead to occasional events that are unnecessary to be treated. In addition, due to the uncertainties in practical systems, false events may be generated, resulting in some unnecessary triggering. Hence, designing an effective triggering scheme to ensure that the triggered events are necessary is still an open problem.

### **1.2.1.2 Event-Triggered Robust MPC Based on Stochastic Triggering Conditions**

Another type of event design based on stochastic conditions or criteria has emerged due to the flexibility and analyzability associated with stochastic distributions. In [23], an event-triggered sliding mode control was employed to keep receiving and sending the delayed measurement to update control actions for uncertain stochastic systems subject to limited communication capacity. In [24], a framework of event-triggered stabilization was established for the stochastic systems by applying a powerful stochastic convergence theorem. Reference [25] derived some sufficient conditions on an event-triggered control protocol for stochastic multi-agent systems with state-dependent noises

and achieved the desired consensus for the closed-loop system in probability. For discrete-time linear systems subject to Gaussian white noise disturbances, reference [63] proposed a stochastic event-triggered control scheme that theoretically and numerically outperformed a periodic one. By using the ergodicity property of a homogeneous Markov chain, an event-triggered control design was proposed in [64], and the trade-off between the communication rate and the control performance was quantified analytically. A Gaussianity-preserving event-based sensor was adopted in [65, 66] to reduce the communication rate and maintain the estimation performance.

Relevantly, based on the knowledge of probability density functions, some triggering sets were designed to achieve a desired expectation of inter-execution times for a tube-based robust MPC scheme in [67]. A stochastic event-triggered predictive control scheme was proposed in [68] which allowed non-uniformly sampled measurements and large delays involved in outputs. However, reference [68] just considered a predictive feedback law, which is not standard robust MPC with guaranteed hard constraints and recursive feasibility. Up to now, the stochasticity of most stochastic event-triggered control schemes is from stochastic systems. Although stochastic distributions make the design of triggering conditions flexible, they may cause loss of recursive feasibility and stability in MPC design. This is the main reason why few results on stochastic event-triggered MPC can be found. Hence, how to design a stochastic event-triggered condition for robust MPC with guaranteed recursive feasibility and stability is worth exploring.

### **1.2.1.3 Problems in Deterministic and Stochastic Triggering Conditions**

Apart from the problems mentioned in deterministic and stochastic event-triggered robust MPC approaches, there are two common problems. First, although the introduction of event-triggered control leads to reduced communication and computation loads in robust MPC, these benefits are at the cost of control performance. How to achieve the trade-off between control per-

formance and computational burden has not been further investigated and is still a challenging problem in event-triggered robust MPC. Second, both deterministic and stochastic event-triggered robust MPC approaches mentioned above require persistent event monitoring and verification, which are resource-intensive, and the connection between event verification and action triggering is usually overlooked. As a matter of fact, monitoring the system state and verifying the triggering condition at the next sampling instant should depend on the system state and the feasibility of the triggering condition at the current sampling instant. If the system is triggered at the current sampling instant, the waiting time for the subsequent event verification and triggering could be longer, as the updated control action may regulate the system state well. More advanced and effective strategies should be designed to link event verification with action triggering.

### 1.2.2 Event-Triggered Data-Driven MPC

Typical MPC requires explicit knowledge of the underlying system models which are usually obtained from first principles or system identification. However, with the increase of system complexity in real-world applications, obtaining an accurate system model becomes computationally demanding and even impossible, posing grand challenges for the practical implementation of MPC. To tackle the modeling issue, data-driven approaches have been considered for MPC, which can implement MPC controllers directly from measured data without prior knowledge of an accurate model. The existing results are typically divided into two categories. One is to improve an inaccurate initial model continuously through online measurements, which are expected to capture the uncertainties in the initial model, such as learning-based or adaptive MPC schemes [69, 70, 71]. Another category is to directly predict future trajectories according to Willems’ fundamental lemma from behavioral systems theory [72]. Compared with the first category, this type of data-driven MPC, also called purely data-driven MPC, is completely based on initial measure-

ment data and does not require system identification or online state estimation, thus drawing growing interests. Recently, some primary issues arisen from this category have been investigated, for instance, an optimal problem of the weights in linear combinations of past trajectories for unconstrained systems [73], a distributionally robust constrained problem with probabilistic guarantees on performance [74], and an application to power system oscillation damping [75].

Despite remarkable developments in [73, 74, 75], there are still two challenging problems that need to be solved. On the one hand, for a data-driven approach, it is challenging to construct appropriate terminal constraints such that recursive feasibility and closed-loop stability are guaranteed. The aforementioned work [73, 74, 75] does not provide any results regarding this problem. Very recently, reference [76] utilized terminal equality constraints and provided the first analysis on recursive feasibility and stability of purely data-driven MPC. However, as pointed out in model-based MPC [77], a terminal equality constraint is rather restrictive, because it is generally difficult to drive a state to a specified point. Further, it always requires a long prediction horizon so as to make the optimization problem feasible. On the other hand, although the proposed data-driven MPC approaches in [73, 74, 75] can greatly lower the model requirements and simplify the implementation of MPC, they may bring heavier computational burden and require more computational resources than that of model-based MPC due to the introduction of a large amount of data. To circumvent this issue, reference [76] provided a multistep strategy, that is, solving a data-driven MPC optimization problem for every fixed  $n$  steps. Since this strategy is unconcerned about any performance of the controlled system, it undoubtedly shows some conservatism.

Recently, some work devoting to enabling event-triggered control to data-driven MPC has started to appear. With training data samples, reference [78] applied a statistical learning to event-triggered MPC, which showed better tracking performance with less frequent event triggers when compared with



classical event-triggered MPC. In [79], a subspace predictive control method with a novel event-triggered law was developed based on data of linear time-invariant systems. However, references [78, 79] considered only a simple case, that is, based on state and input data without disturbances only, and no complete analysis of recursive feasibility and stability were presented.

### 1.3 Research Motivation and Contributions

Despite the remarkable progress in the above-mentioned literature, there are still some challenges which require further research before event-triggered robust MPC can be applied widely in practice:

- In event-triggered robust MPC, the reduction of computation loads is at the cost of control performance. How to achieve the trade-off between control performance and computational burden?
- Most existing triggering conditions depend on the current states or measurement errors only, leading to occasional or false events that are unnecessary to be treated. How to design an effective triggering scheme to ensure that the triggered events are necessary?
- As a matter of fact, like when to trigger the event, when to check the triggering condition should also be dependent on the system dynamics and be carefully designed. How to link event verification with action triggering?
- For data-driven MPC, how to utilize event-triggered control to alleviate the issue of computational resources and how to provide complete analysis of recursive feasibility and stability?

Motivated by the above problems, this thesis focuses on the design of event-triggered robust MPC to reduce computational burden as well as guarantee recursive feasibility of MPC and robust stability of linear discrete-time sys-

tems with bounded disturbances. The main contributions are summarized as follows:

1. According to the probability distribution of disturbances, an event-triggered scheme related to a designed minimal robust positively invariant set is constructed to generate dynamic triggering sets. With the designed event-triggered scheme, a tube-based MPC that allows the initially predicted state different from the current actual state of the plant is considered to preserve the control performance, and the optimization problem subject to hard constraints is solved only when the current state is outside the corresponding triggering set. The designed event-triggered controller can achieve a prescribed expectation of inter-execution times, while not sacrificing the quadratic performance significantly.
2. A two-step scheme involving a tentative verification of a triggering condition and a delayed triggering with a waiting horizon is proposed to ensure necessary events and reduce the average triggering rate. The triggering condition and the waiting horizon are synthesized based on a prediction model of the plant and a robust positively invariant set associated with it. Furthermore, the proposed two-step triggering scheme is extended to multi-agent systems, and a theoretical condition associated with closed-loop stability and consensus is derived for each agent.
3. Based on the ergodicity of a purposely designed Markov chain, a stochastic triggering scheme including a prescribed triggering function, an updating law for the transition probabilities of the Markov chain, and a checking function is investigated to achieve aperiodic and non-persistent event verification and enlarge the inter-execution time. Both tube-based MPC and linear matrix inequality-based (LMI-based) MPC are considered, and they show complementary merits with such a stochastic triggering scheme. Under mild conditions, recursive feasibility and closed-loop robust stability of both approaches are guaranteed theoretically.

4. Using initially measured input-output data of unknown systems, a terminal inequality constraint is developed for the data-driven MPC optimization problem without any prior identification, resulting in a larger feasible region and a lower bound for the prediction horizon when compared with a terminal equality constraint. An event-triggered scheme associated with a local controller is designed to trigger the solution of the data-driven MPC optimization problem when necessary, leading to the reduction of resource consumption. A complete analysis of recursive feasibility and stability is presented based on the designed terminal ingredients.
5. An event-triggered stochastic MPC approach is studied for the scheduling problem of constrained queueing networks with a dynamic topology. A discrete-time Markov chain (DTMC) in combination with a Bernoulli trial is used to model the time-varying routing of queueing networks. The constituency and positiveness constraints on queue lengths together with a dynamic topology and the stochasticity in packet arrival are incorporated into a stochastic MPC optimization problem. An event-triggered scheme with adaptive event checking involving an estimated waiting horizon is designed to trigger the solution of the optimization problem when necessary, leading to reduced computational burden and improved utilization of communication resources. With a constructed stability region of arrival rates, the stability of queueing networks is discussed by the relation between the inter-execution time and objective function.

## 1.4 Thesis Outline

The remainder of the thesis is organized as follows:

- In Chapter 2, based on a probability density function of disturbances, an event-triggered scheme related to a designed minimal robust positively

invariant set of tube-based MPC is constructed to generate dynamic triggering sets.

- In Chapter 3, a two-step triggering scheme involving a tentative verification of a triggering condition and a delayed triggering with a waiting horizon is proposed and an extension of this approach is applied to multi-agent systems.
- In Chapter 4, a stochastic triggering scheme involving a prescribed triggering function, an updating law for the transition probabilities of the Markov chain, and a checking function is designed to achieve aperiodic and non-persistent event verification and enlarge the inter-execution time.
- In Chapter 5, a data-driven MPC with a terminal inequality constraint is developed for unknown systems with initially measured input-output data and an event-triggered scheme is considered to reduce computational burden.
- In Chapter 6, an event-triggered stochastic MPC approach is applied to constrained queueing networks with a dynamic topology for the scheduling problem.
- In Chapter 7, concluding remarks of the thesis and some potential directions of future work are provided.

## Chapter 2

# Event-Triggered Robust MPC with Guaranteed Average Inter-Execution Times\*

This chapter investigates an event-triggered robust MPC controller involving a set-valued triggering function to achieve a prescribed expectation of inter-execution times. In [60, 67], a restrictive condition that the initially predicted state is equal to the current actual state is always required in the MPC optimization problem, which makes it hard to preserve control performance if the optimization problem is only solved at triggering instants. To avoid this, tube-based MPC is considered to remove this requirement and incorporated into the design of the event-triggered scheme, achieving the trade-off between control performance and computational burden. According to the probability distribution of bounded disturbances, the dynamic triggering sets which can limit the state error between the actual state and the predicted state are derived based on the concept of robust positively invariant sets. The optimization problem is solved only at event-triggered instants when the state is outside the corresponding set.

This chapter is organized as follows. Section 2.1 describes the system model and formulates an event-triggered robust MPC problem. Section 2.2

---

\*A version of this chapter has been published as: Li Deng, Zhan Shu, and Tongwen Chen, Event-triggered robust model predictive control for linear discrete-time systems with a guaranteed average inter-execution time. *International Journal of Robust & Nonlinear Control*, vol. 32, no. 6, pp. 3969-3985, Apr. 2022.

studies tube-based MPC and designs the event-triggered scheme. Section 2.3 analyzes recursive feasibility and robust stability. Section 2.4 verifies the proposed approach by numerical examples. Section 2.5 concludes this chapter.

## 2.1 Problem Formulation

Consider the following linear discrete-time system with bounded disturbances:

$$x(t+1) = Ax(t) + Bu(t) + \omega(t), \quad (2.1)$$

where  $t \in \mathbb{Z}^+$ ;  $x(t) \in \mathbb{R}^{n_x}$  is the system state;  $u(t) \in \mathbb{R}^{n_u}$  is the control input;  $\omega(t) \in \mathbb{R}^{n_x}$  is the persistent unknown disturbance; the matrix pair  $(A, B)$  is stabilizable. The disturbance  $\omega(t)$  is bounded, i.e.,  $\omega(t) \in \mathcal{W}$ , where  $\mathcal{W}$  is a compact and convex set containing the origin.

**Assumption 2.1.** *The disturbance  $\omega(t)$  for all  $t \in \mathbb{Z}^+$  is independently and identically distributed with a bounded probability density function  $f_\omega$ .*

The system is subject to the following constraints:

$$x(t) \in \mathcal{X}, \quad u(t) \in \mathcal{U}, \quad (2.2)$$

where  $\mathcal{X} \subseteq \mathbb{R}^{n_x}$  and  $\mathcal{U} \subseteq \mathbb{R}^{n_u}$  are compact and convex sets containing the origin.

The nominal system corresponding to (2.1) is

$$\hat{x}(t+1) = A\hat{x}(t) + B\hat{u}(t), \quad (2.3)$$

where  $\hat{x}(t) \in \mathbb{R}^{n_x}$  and  $\hat{u}(t) \in \mathbb{R}^{n_u}$  are the state and control input of the nominal system.

In this chapter, we consider a tube-based MPC approach to handle state and control constraints in (2.2) by using the concept of robust positively invariant sets. Before proceeding, we have the following notations: Given two sets  $\mathcal{Z}_1, \mathcal{Z}_2 \subseteq \mathbb{R}^n$ , the Minkowski set addition is defined by  $\mathcal{Z}_1 \oplus \mathcal{Z}_2 \triangleq \{z_1 + z_2 \mid z_1 \in \mathcal{Z}_1, z_2 \in \mathcal{Z}_2\}$  and the Pontryagin set difference is defined by  $\mathcal{Z}_1 \ominus \mathcal{Z}_2 \triangleq \{z \in \mathbb{R}^n \mid z \oplus \mathcal{Z}_2 \subseteq \mathcal{Z}_1\}$ .

**Definition 2.1.** [80] A set  $\mathcal{Z}$  is a robust positively invariant set for the system in (2.1) with a state feedback control law if  $(A + BK)\mathcal{Z} \oplus \mathcal{W} \subseteq \mathcal{Z}$ , where  $K \in \mathbb{R}^{n_u \times n_x}$  is a stabilizing feedback gain.

For the system in (2.1), we will adopt the following definition of robust stability.

**Definition 2.2.** [80] A set  $\mathcal{Z}$  is robustly exponentially stable for the system in (2.1) with a feasible region  $\mathcal{X}_N$  and an initial state  $x(0) \in \mathcal{X}_N$  if there exist  $\theta \in (0, 1)$  and  $\delta > 0$  such that  $d(x(t), \mathcal{Z}) \leq \delta \sqrt{\theta^t} d(x(0), \mathcal{Z})$  for all  $t \in \mathbb{Z}^+$ , where  $d(x(t), \mathcal{Z}) \triangleq \min\{\|x(t) - z\| \mid z \in \mathcal{Z}\}$ .

In order to save computational resources, an event-triggered controller is designed as

$$\begin{aligned} u(t) &= \kappa(\tilde{x}(t_j), t - t_j), \quad t \in \mathbb{Z}_{[t_j, t_{j+1}-1]}, \\ t_{j+1} &= \min\{t \in \mathbb{Z}_{\geq t_j+1} \mid x(t) \notin \phi(\tilde{x}(t_j), t - t_j)\}, \end{aligned}$$

where  $\{t_j : j \in \mathbb{Z}^+\} \subseteq \mathbb{Z}^+$  denotes the triggering instant sequence; the function  $\kappa : \mathbb{R}^{n_x} \times \mathbb{R} \rightarrow \mathbb{R}^{n_u}$  is to be designed; the set-valued function  $\phi$  will be designed by  $\phi(\tilde{x}(t_j), t - t_j) = \tilde{x}(t - t_j | t_j) \oplus \mathcal{Q}_{t-t_j}$ , where  $\tilde{x}(t - t_j | t_j)$  is the predicted state at instant  $t$  based on the measurement at the event-triggered instant  $t_j$  and  $\tilde{x}(t_j) = \tilde{x}(0 | t_j)$ ; the closed sets  $\mathcal{Q}_{t-t_j} \subseteq \mathbb{R}^{n_x}$ ,  $t \in \mathbb{Z}_{[t_j, t_{j+1}-1]}$ , are to be designed. That is, an event should be triggered if the actual states deviate too much from the predicted states.

To satisfy the constraints in (2.2) and reduce the amount of computation in solving the optimization problem while not sacrificing the quadratic performance significantly, this chapter is to design an event-triggered robust MPC controller  $\kappa$  involving a set-valued triggering function  $\phi$  such that the optimization problem is solved at event-triggered instants only and a given expected value of inter-execution times  $\Delta \triangleq \mathbb{E}\{t_{j+1} - t_j\}$  is achieved based on Assumption 2.1. Besides, the recursive feasibility and closed-loop stability are guaranteed.

## 2.2 Event-Triggered Robust MPC

In [60, 67], a restrictive condition that the initially predicted state  $\tilde{x}(t)$  is equal to the actual state  $x(t)$  is required to simplify the design. In general, the actual state converges to the predicted value after solving the optimization problem rather than equals it instantaneously. However, removing such a requirement is not an easy thing. Firstly, when  $x(t) \neq \tilde{x}(t)$  is considered, how to describe the uncertainty between  $x(t)$  and  $\tilde{x}(t)$  is challenging. Secondly, as  $x(t) - \tilde{x}(t) = 0$  no longer holds, design simplification based on this relationship cannot be employed. Moreover, it undoubtedly poses a grand challenge to prove recursive feasibility and robust stability. In this section, we are devoted to removing such a restrictive requirement by using a robust positively invariant set  $\mathcal{Z}$ , leading to tube-based MPC.

### 2.2.1 Setup of Tube-Based MPC

Given a stabilizing feedback gain  $K \in \mathbb{R}^{n_u \times n_x}$ , a robust positively invariant set  $\mathcal{Z}$  is designed by following the method in [81]. Then, the terminal set  $\mathcal{X}_f$  should be designed to satisfy the following conditions:

$$\mathcal{X}_f \subseteq \mathcal{X} \ominus \mathcal{Z} \tag{2.4a}$$

$$(A + BK)\mathcal{X}_f \subseteq \mathcal{X}_f \tag{2.4b}$$

$$K\mathcal{X}_f \subseteq \mathcal{U} \ominus K\mathcal{Z}. \tag{2.4c}$$

Define the terminal cost function as:  $V_f(\tilde{x}) = \tilde{x}^T P \tilde{x}$ ,  $P \succ 0$ , and a control law  $\tilde{u} = K\tilde{x}$ ,  $K \in \mathbb{R}^{n_u \times n_x}$  such that

$$V_f((A + BK)\tilde{x}) - V_f(\tilde{x}) \leq -\tilde{x}^T(Q + K^T R K)\tilde{x} \tag{2.5}$$

for  $\tilde{x} \in \mathcal{X}_f$ , where  $Q \succ 0$  and  $R \succ 0$ .

**Remark 2.1.** *In order to guarantee (2.5), one can obtain  $P$  and  $K$  by using the LQR technique directly or firstly design a stabilizing feedback gain  $K$  by one of many standard approaches, such as pole assignment, and then solve (2.5) to obtain  $P$ .*



Moreover, the following lemma describes the relationship between a robust positively invariant set and the state trajectory, which will be used to design an event-triggered controller later.

**Lemma 2.1.** [80] *Suppose that  $\mathcal{Z}$  is a robust positively invariant set of the system in (2.1). If  $x(t) \in \hat{x}(t) \oplus \mathcal{Z}$  and  $u(t) = \hat{u}(t) + K(x(t) - \hat{x}(t))$ , then  $x(t+1) \in \hat{x}(t+1) \oplus \mathcal{Z}$  for all  $\omega(t) \in \mathcal{W}$ .*

At the event-triggered instant  $t_j$ , a robust MPC optimization problem for the current actual state  $x(t_j)$  is described as:

$$\begin{aligned} & \min_{\tilde{\mathbf{x}}(t_j), \tilde{\mathbf{u}}(t_j)} J_N(\tilde{\mathbf{x}}(t_j), \tilde{\mathbf{u}}(t_j)) \\ \text{s.t. } & x(t_j) - \tilde{x}(t_j) \in \mathcal{Z}, \end{aligned} \quad (2.6a)$$

$$\tilde{x}(i+1|t_j) = A\tilde{x}(i|t_j) + B\tilde{u}(i|t_j), \quad i \in \mathbb{Z}_{[0, N-1]}, \quad (2.6b)$$

$$\tilde{x}(i|t_j) \in \mathcal{X} \ominus \mathcal{Z}, \quad i \in \mathbb{Z}_{[0, N-1]}, \quad (2.6c)$$

$$\tilde{u}(i|t_j) \in \mathcal{U} \ominus K\mathcal{Z}, \quad i \in \mathbb{Z}_{[0, N-1]}, \quad (2.6d)$$

$$\tilde{x}(N|t_j) \in \mathcal{X}_f \subseteq \mathcal{X} \ominus \mathcal{Z}, \quad (2.6e)$$

where  $\tilde{x}(i|t_j)$  is the predicted state at instant  $t_j + i$  based on the measurement at the event-triggered instant  $t_j$  and  $\tilde{x}(t_j) = \tilde{x}(0|t_j)$ ;  $\tilde{u}(i|t_j)$  is the predicted control input at  $t_j + i$  and  $\tilde{u}(t_j) = \tilde{u}(0|t_j)$ ;  $N \in \mathbb{Z}_{\geq 1}$  denotes the prediction horizon;  $\mathbb{Z}_{[0, N-1]} \triangleq \{i \in \mathbb{Z} \mid 0 \leq i \leq N-1\}$ . Let  $\mathcal{H}_N(x(t_j)) \triangleq \{\tilde{\mathbf{x}}(t_j), \tilde{\mathbf{u}}(t_j) \in \mathbb{H}_N \mid (2.6a) \text{ to } (2.6e)\}$  be the set of feasible decision variables, where  $\mathbb{H}_N \triangleq \mathbb{R}^{n_x} \times \dots \times \mathbb{R}^{n_x} \times \mathbb{R}^{n_u} \times \dots \times \mathbb{R}^{n_u}$ . Then, the feasible region is defined as  $\mathcal{X}_N \triangleq \{x(t_j) \in \mathbb{R}^{n_x} \mid \mathcal{H}_N(x(t_j)) \neq \emptyset\}$ .

In (2.6), instead of imposing the constraint  $x(t_j) = \tilde{x}(t_j)$  as in [60, 67], we consider the constraint in (2.6a), which was proposed to reduce conservatism in [80]. The state and control input constraints in (2.6c)-(2.6d) are based on a robust positively invariant set  $\mathcal{Z}$ . Equation (2.6e) is the terminal constraint. The solutions of the optimization problem are the optimal control sequence  $\tilde{\mathbf{u}}^*(t_j) \triangleq \{\tilde{u}^*(0|t_j), \tilde{u}^*(1|t_j), \dots, \tilde{u}^*(N-1|t_j)\}$  and the optimal state sequence  $\tilde{\mathbf{x}}^*(t_j) \triangleq \{\tilde{x}^*(0|t_j), \tilde{x}^*(1|t_j), \dots, \tilde{x}^*(N|t_j)\}$ . The corresponding optimal cost is  $J_N^*(x(t_j))$ .

The cost function in (2.6) is given by

$$J_N(\tilde{\mathbf{x}}(t_j), \tilde{\mathbf{u}}(t_j)) \triangleq \sum_{i=0}^{N-1} l(\tilde{x}(i|t_j), \tilde{u}(i|t_j)) + V_f(\tilde{x}(N|t_j)),$$

where  $l(\tilde{x}(i|t_j), \tilde{u}(i|t_j)) \triangleq \tilde{x}(i|t_j)^\top Q \tilde{x}(i|t_j) + \tilde{u}(i|t_j)^\top R \tilde{u}(i|t_j)$ ,  $i \in \mathbb{Z}_{[0, N-1]}$  is the stage cost, and  $V_f(\tilde{x}(N|t_j)) \triangleq \tilde{x}(N|t_j)^\top P \tilde{x}(N|t_j)$  is the terminal cost. Motivated by Lemma 2.1, the event-triggered control law applied to the system in (2.1) is given by

$$u(t) = \tilde{u}(t - t_j|t_j) + K(x(t) - \tilde{x}(t - t_j|t_j)), \quad t \in \mathbb{Z}_{[t_j, t_{j+1}-1]}. \quad (2.7)$$

The designed event-triggered controller is dependent on the actual state  $x(t)$  and the disturbance  $\omega(t)$ , leading to a closed-loop control at the instants when the on-line optimization is absent.

Then, the closed-loop system with the event-triggered controller is given by

$$x(t+1) = Ax(t) + Bu(t) + \omega(t), \quad t \in \mathbb{Z}_{[t_j, t_{j+1}-1]} \quad (2.8)$$

$$t_{j+1} = \min\{t \in \mathbb{Z}_{\geq t_j+1} \mid x(t) \notin \tilde{x}(t - t_j|t_j) \oplus \mathcal{Q}_{t-t_j}\}. \quad (2.9)$$

Without loss of generality, set  $t_0 = 0$  and suppose that the initial state  $x(0)$  is triggered automatically at instant  $t_0$ . Assume that the event-triggered controller transmits a whole sequence  $\tilde{\mathbf{u}}^*(t_j)$  to the actuator at the event-triggered instant  $t_j$ . According to (2.7)-(2.9), if the event-triggered condition in (2.9) is not satisfied, the elements  $\{\tilde{u}^*(0|t_j), \tilde{u}^*(1|t_j), \dots, \tilde{u}^*(t - t_j|t_j)\}$  of the control sequence  $\tilde{\mathbf{u}}^*(t_j)$  would be applied; otherwise, the optimization problem in (2.6) would be solved, and a new control sequence  $\tilde{\mathbf{u}}^*(t_{j+1})$  would be transmitted to the actuator. From the perspective of practical implementation, we set  $t_{j+1} = t_j + N$  if there is no event triggered after  $N - 1$  steps, which guarantees that an event will be triggered within the prediction horizon  $N$ , that is,  $t_{j+1} - t_j \leq N$  for all  $j \in \mathbb{Z}^+$ .

**Remark 2.2.** In [67], the event-triggered control input is designed as  $u(t) = \tilde{u}(t - t_j|t_j)$ ,  $t \in \mathbb{Z}_{[t_j, t_{j+1}-1]}$ , which means that the term  $K(x(t) - \tilde{x}(t - t_j|t_j))$  is

neglected and the control inputs are deterministic and invariant between two event-triggered instants. Since  $x(t_j) = \tilde{x}(t_j)$  is considered in the optimization problem of [67], the control law is valid at the event-triggered instant  $t_j$ . However, when the event-triggered condition is not satisfied and the optimization problem is not solved, if  $u(t) = \tilde{u}(t - t_j|t_j)$  is still applied to the system between two event-triggered instants, in the presence of disturbances, it is difficult to achieve effective control and preserve the control performance since  $x(t) = \tilde{x}(t - t_j|t_j)$ ,  $t \in \mathbb{Z}_{[t_j+1, t_{j+1}-1]}$ , is not always satisfied in general.

### 2.2.2 Event-Triggered Scheme Design

In this section, triggering sets  $\mathcal{Q}_i$ ,  $i \in \mathbb{Z}_{[1, N-1]}$ , are designed to guarantee a given average inter-execution time based on the probability density functions defined as follows.

**Definition 2.3.** [82] Let  $\mathbf{Y} \triangleq [\mathbf{Y}_1^T, \dots, \mathbf{Y}_i^T]^T \in \mathbb{R}^i$  be a continuous random vector with a joint probability density function  $f_{\mathbf{Y}}(\mathbf{y})$ . For a set  $\mathcal{D} \subseteq \mathbb{R}^i$ , the probability that the continuous random vector  $\mathbf{Y}$  falls inside  $\mathcal{D}$  is

$$\mathbb{P}\{\mathbf{Y} \in \mathcal{D}\} \triangleq \int_{\mathcal{D}} f_{\mathbf{Y}}(\mathbf{y}) d\mathbf{y}.$$

If  $F_{\mathbf{Y}}(\mathbf{y}) \triangleq \mathbb{P}\{\mathbf{Y}_1 \leq y_1, \dots, \mathbf{Y}_i \leq y_i\}$  is the cumulative distribution function of  $\mathbf{Y}$ , the joint probability density function  $f_{\mathbf{Y}}(\mathbf{y})$  can be computed as a partial derivative

$$f_{\mathbf{Y}}(\mathbf{y}) = \frac{\partial^i F_{\mathbf{Y}}(\mathbf{y})}{\partial y_1 \cdots \partial y_i}.$$

According to the event-triggered condition in (2.9), we define the following probability that an event is triggered at instant  $t + i$  after event-triggered instant  $t$ :

$$\hat{\mathcal{P}}_i \triangleq \mathbb{P}\{x(t+i) \notin \tilde{x}(i|t) \oplus \mathcal{Q}_i, x(t+\ell) \in \tilde{x}(\ell|t) \oplus \mathcal{Q}_\ell, \ell \in \mathbb{Z}_{[1, i-1]}\}. \quad (2.10)$$

To ensure that an event is triggered within the prediction horizon  $N$ , we assume that  $\sum_{i=1}^N \hat{\mathcal{P}}_i = 1$  and  $\hat{\mathcal{P}}_i \geq 0$ . Then, the expectation of inter-execution

times is determined as

$$\hat{\Delta} \triangleq \mathbb{E}\{t_{j+1} - t_j\} = \sum_{i=1}^N i\hat{\mathcal{P}}_i. \quad (2.11)$$

Hence, by choosing  $\hat{\mathcal{P}}_i$  and designing corresponding triggering sets  $\mathcal{Q}_i$ , we can achieve any desirable value of  $\hat{\Delta}$ . However, since

$$x(t + \ell) - \tilde{x}(\ell|t) = \sum_{s=0}^{\ell-1} (A + BK)^s \omega(t + \ell - s - 1) + (A + BK)^\ell (x(t) - \tilde{x}(t))$$

for  $\ell \in \mathbb{Z}_{[1,i]}$ , the probability in (2.10) is related to the uncertain error between  $x(t)$  and  $\tilde{x}(t)$ . It is numerically intractable to construct suitable triggering sets  $\mathcal{Q}_i$ ,  $i \in \mathbb{Z}_{[1,N-1]}$ , to satisfy (2.10) for given  $\hat{\mathcal{P}}_i$ . Hence, to specify this uncertainty, we define another probability to design triggering sets  $\mathcal{Q}_i$ ,  $i \in \mathbb{Z}_{[1,N-1]}$ , by using the robust positively invariant set  $\mathcal{Z}$  in the following form

$$\mathcal{P}_i \triangleq \mathbb{P} \left\{ \sum_{s=0}^{i-1} (A + BK)^s \omega(i - s - 1) \notin \mathcal{Q}_i \ominus (A + BK)^i \mathcal{Z}, \right. \\ \left. \sum_{s=0}^{\ell-1} (A + BK)^s \omega(\ell - s - 1) \in \mathcal{Q}_\ell \ominus (A + BK)^\ell \mathcal{Z}, \ell \in \mathbb{Z}_{[1,i-1]} \right\}. \quad (2.12)$$

According to Assumption 2.1, the probability in (2.12) is independent of  $t$ . Note that  $\sum_{i=1}^N \mathcal{P}_i = 1$ ,  $\mathcal{P}_i \geq 0$ , and the expected value of inter-execution times  $\Delta = \mathbb{E}\{t_{j+1} - t_j\} = \sum_{i=1}^N i\mathcal{P}_i$ . Since the set  $\mathcal{Z}$  contains all uncertainties between  $x(t)$  and  $\tilde{x}(t)$ , the designed  $\mathcal{Q}_i$  through (2.12) by giving  $\mathcal{P}_i$  will lead to a mismatch between  $\hat{\mathcal{P}}_i$  and  $\mathcal{P}_i$ . Hence, instead of specifying  $\mathcal{P}_i$ , we give a desired value  $\Delta$  directly, and then obtain some triggering sets  $\mathcal{Q}_i$  through (2.12) to execute the event-triggered condition in (2.9). The details of this strategy are as follows.

Assume that  $t_{j+1} = t_j + N$  if there is no event triggered after  $N - 1$  steps, which means  $\mathcal{Q}_N = (A + BK)^N \mathcal{Z}$ . It is known from (2.12) that the condition  $(A + BK)^i \mathcal{Z} \subseteq \mathcal{Q}_i$ ,  $i \in \mathbb{Z}_{[1,N-1]}$ , needs to be satisfied. Hence, to facilitate the discussion, we design  $\mathcal{Q}_i \triangleq \gamma(A + BK)^i \mathcal{Z}$ ,  $i \in \mathbb{Z}_{[1,N-1]}$ , where  $\gamma \in \mathbb{R}_{\geq 1}$ . Define

the following function  $\mathcal{P}_i : \mathbb{R}_{\geq 1} \longrightarrow \mathbb{R}_{[0,1]}$

$$\mathcal{P}_i(\gamma) \triangleq \mathbb{P} \left\{ \sum_{s=0}^{i-1} (A + BK)^s \omega(i - s - 1) \notin (\gamma - 1)(A + BK)^i \mathcal{Z}, \right. \\ \left. \sum_{s=0}^{\ell-1} (A + BK)^s \omega(\ell - s - 1) \in (\gamma - 1)(A + BK)^\ell \mathcal{Z}, \ell \in \mathbb{Z}_{[1, i-1]} \right\}.$$

Then, let  $\tilde{\mathcal{Q}}_i(\gamma) \triangleq (\gamma - 1)(A + BK)^i \mathcal{Z}$  for  $\gamma \in \mathbb{R}_{\geq 1}$  and  $i \in \mathbb{Z}_{[1, N-1]}$ . The following lemmas provide some important properties of  $\tilde{\mathcal{Q}}_i(\gamma)$  and  $\mathcal{P}_i(\gamma)$ .

**Lemma 2.2.** *For all  $\gamma_1, \gamma_2 \in \mathbb{R}_{\geq 1}$  with  $\gamma_1 \leq \gamma_2$ ,  $\tilde{\mathcal{Q}}_i(\gamma_1) \subseteq \tilde{\mathcal{Q}}_i(\gamma_2)$ .*

**Proof.** Let  $\gamma_1, \gamma_2 \in \mathbb{R}_{\geq 1}$  with  $\gamma_1 \leq \gamma_2$ . It follows that

$$\tilde{\mathcal{Q}}_i(\gamma_1) = (\gamma_1 - 1)(A + BK)^i \mathcal{Z} \subseteq (A + BK)^i ((\gamma_1 - 1)\mathcal{Z} \oplus (\gamma_2 - \gamma_1)\mathcal{Z})$$

for all  $i \in \mathbb{Z}_{[1, N-1]}$ . Since  $\mathcal{Z}$  is a compact and convex set containing the origin, then if  $z \in (\gamma_1 - 1)\mathcal{Z} \oplus (\gamma_2 - \gamma_1)\mathcal{Z}$ , there must exist  $z_1, z_2 \in \mathcal{Z}$  such that  $z = (\gamma_1 - 1)z_1 + (\gamma_2 - \gamma_1)z_2$ . Then,

$$z = (\gamma_2 - 1) \left( \frac{(\gamma_1 - 1)}{(\gamma_2 - 1)} z_1 + \frac{(\gamma_2 - \gamma_1)}{(\gamma_2 - 1)} z_2 \right) \in (\gamma_2 - 1)\mathcal{Z}.$$

Thus, we have  $(\gamma_1 - 1)\mathcal{Z} \oplus (\gamma_2 - \gamma_1)\mathcal{Z} = (\gamma_2 - 1)\mathcal{Z}$ . Hence,

$$\tilde{\mathcal{Q}}_i(\gamma_1) \subseteq (\gamma_2 - 1)(A + BK)^i \mathcal{Z} = \tilde{\mathcal{Q}}_i(\gamma_2).$$

■

Define the following function  $\tilde{\mathcal{P}}_i : \mathbb{R}_{\geq 1} \longrightarrow \mathbb{R}_{[0,1]}$  as

$$\tilde{\mathcal{P}}_i(\gamma) \triangleq \mathbb{P} \left\{ \sum_{s=0}^{i-1} (A + BK)^s \omega(i - s - 1) \in \tilde{\mathcal{Q}}_i(\gamma), \right. \\ \left. \sum_{s=0}^{\ell-1} (A + BK)^s \omega(\ell - s - 1) \in \tilde{\mathcal{Q}}_\ell(\gamma), \ell \in \mathbb{Z}_{[1, i-1]} \right\} \quad (2.13)$$

for  $\gamma \in \mathbb{R}_{\geq 1}$  and  $i \in \mathbb{Z}_{[1, N-1]}$ . Then, according to Definition 2.3, the monotonicity of  $\tilde{\mathcal{P}}_i(\gamma)$  is shown in the following lemma.

**Lemma 2.3.**  $\tilde{\mathcal{P}}_i(\gamma)$  is a continuous and monotonically nondecreasing function with respect to  $\gamma$ , where  $\gamma \in \mathbb{R}_{\geq 1}$  and  $i \in \mathbb{Z}_{[1, N-1]}$ .

**Proof.** Define  $\tilde{\mathcal{P}}_0(\gamma) = 1$ . Since an event is triggered within the prediction horizon  $N$ , define  $\tilde{\mathcal{P}}_N(\gamma) = 0$ . Let  $z(\ell - 1) = \sum_{s=0}^{\ell-1} (A + BK)^s \omega(\ell - s - 1)$  for  $\ell \in \mathbb{Z}_{[1, i]}^+$ , then there exists a nonsingular matrix  $T \in \mathbb{R}^{in_x \times in_x}$  as

$$T = \begin{bmatrix} I & 0 & \cdots & 0 \\ (A + BK) & I & \cdots & 0 \\ \vdots & \vdots & \ddots & \vdots \\ (A + BK)^{i-1} & (A + BK)^{i-2} & \cdots & I \end{bmatrix}$$

such that  $\mathbf{z} = T\boldsymbol{\omega}$ , where  $\mathbf{z} \triangleq [z(0)^T, \dots, z(i-1)^T]^T$ ,  $\boldsymbol{\omega} \triangleq [\omega(0)^T, \dots, \omega(i-1)^T]^T$ . Based on the probability density function  $f_{\boldsymbol{\omega}}$ , the joint probability density function of  $\mathbf{z}$  is obtained as  $f_{\mathbf{z}}(\mathbf{z}) = |\det(T^{-1})| f_{\boldsymbol{\omega}}(T^{-1}(\mathbf{z}))$  for all  $\mathbf{z} \in \mathbb{R}^{in_x}$ . Then, it follows that

$$\begin{aligned} \tilde{\mathcal{P}}_i(\gamma) &= \int_{\{\boldsymbol{\omega} \in \mathbb{R}^{in_x} \mid \sum_{s=0}^{\ell-1} (A+BK)^s \omega(\ell-s-1) \in \tilde{\mathcal{Q}}_{\ell}(\gamma), \ell \in \mathbb{Z}_{[1, i]}^+\}} f_{\boldsymbol{\omega}}(\boldsymbol{\omega}) d\boldsymbol{\omega} \\ &= \int_{\{\mathbf{z} \in \mathbb{R}^{in_x} \mid z(\ell-1) \in \tilde{\mathcal{Q}}_{\ell}(\gamma), \ell \in \mathbb{Z}_{[1, i]}^+\}} f_{\mathbf{z}}(\mathbf{z}) d\mathbf{z} \\ &= \int_{\tilde{\mathcal{Q}}_i(\gamma) \times \tilde{\mathcal{Q}}_{i-1}(\gamma) \times \cdots \times \tilde{\mathcal{Q}}_1(\gamma)} f_{\mathbf{z}}(\mathbf{z}) d\mathbf{z}, \end{aligned}$$

where  $d\boldsymbol{\omega}$ ,  $d\mathbf{z}$  denote  $in_x$ -dimensional volume differentials. Let  $\text{vol}(\mathcal{X})$  denote the Lebesgue measure of  $\mathcal{X}$ . Based on Lemma 2.2, it is easy to show that  $\text{vol}(\tilde{\mathcal{Q}}_i(\gamma))$  is continuous and monotonically nondecreasing with respect to  $\gamma$ . Then, for any arbitrary  $\gamma_1, \gamma_2 \in \mathbb{R}_{\geq 1}$  with  $\gamma_1 \leq \gamma_2$ , it follows that

$$\begin{aligned} \tilde{\mathcal{P}}_i(\gamma_2) &= \int_{\tilde{\mathcal{Q}}_i(\gamma_2) \times \cdots \times \tilde{\mathcal{Q}}_1(\gamma_2)} f_{\mathbf{z}}(\mathbf{z}) d\mathbf{z} \\ &= \int_{\tilde{\mathcal{Q}}_i(\gamma_1) \times \cdots \times \tilde{\mathcal{Q}}_1(\gamma_1)} f_{\mathbf{z}}(\mathbf{z}) d\mathbf{z} + \int_{(\tilde{\mathcal{Q}}_i(\gamma_2) \times \cdots \times \tilde{\mathcal{Q}}_1(\gamma_2)) \setminus (\tilde{\mathcal{Q}}_i(\gamma_1) \times \cdots \times \tilde{\mathcal{Q}}_1(\gamma_1))} f_{\mathbf{z}}(\mathbf{z}) d\mathbf{z} \\ &\leq \tilde{\mathcal{P}}_i(\gamma_1) + h(\gamma_1, \gamma_2), \end{aligned}$$

where

$$\begin{aligned} h(\gamma_1, \gamma_2) &= \sup_{\mathbf{z} \in \mathbb{R}^{inx}} f_{\mathbf{z}}(\mathbf{z}) \text{vol}((\tilde{\mathcal{Q}}_i(\gamma_2) \times \cdots \times \tilde{\mathcal{Q}}_1(\gamma_2)) \setminus (\tilde{\mathcal{Q}}_i(\gamma_1) \times \cdots \times \tilde{\mathcal{Q}}_1(\gamma_1))) \\ &= \sup_{\mathbf{z} \in \mathbb{R}^{inx}} f_{\mathbf{z}}(\mathbf{z}) \left( \prod_{\ell=1}^i \text{vol}(\tilde{\mathcal{Q}}_{\ell}(\gamma_2)) - \prod_{\ell=1}^i \text{vol}(\tilde{\mathcal{Q}}_{\ell}(\gamma_1)) \right). \end{aligned}$$

It follows that  $h(\gamma, \gamma) = 0$  for any  $\gamma \in \mathbb{R}_{\geq 1}$ . Furthermore,

$$\begin{aligned} \tilde{\mathcal{P}}_i(\gamma_1) &\leq \tilde{\mathcal{P}}_i(\gamma_2) \leq \tilde{\mathcal{P}}_i(\gamma_1) + h(\gamma_1, \gamma_2), \\ \tilde{\mathcal{P}}_i(\gamma_2) - h(\gamma_1, \gamma_2) &\leq \tilde{\mathcal{P}}_i(\gamma_1) \leq \tilde{\mathcal{P}}_i(\gamma_2). \end{aligned}$$

Thus,  $\tilde{\mathcal{P}}_i(\gamma)$  is a continuous function with respect to  $\gamma$ . It is shown that (2.13) is equal to

$$\tilde{\mathcal{P}}_i(\gamma) = \mathbb{P} \left\{ \sum_{s=0}^{\ell-1} (A + BK)^s \omega(\ell - s - 1) \in \tilde{\mathcal{Q}}_{\ell}(\gamma), \ell \in \mathbb{Z}_{[1, i]}^+ \right\}. \quad (2.14)$$

Then, according to Lemma 2.2, for any  $\gamma_1, \gamma_2 \in \mathbb{R}_{\geq 1}$  with  $\gamma_1 \leq \gamma_2$ ,  $\tilde{\mathcal{P}}_i(\gamma_1) \leq \tilde{\mathcal{P}}_i(\gamma_2)$  for  $i \in \mathbb{Z}_{[1, N-1]}^+$ , which implies that  $\tilde{\mathcal{P}}_i(\gamma)$  is monotonically nondecreasing.  $\blacksquare$

Then, define the expected function  $\Delta : \mathbb{R}_{\geq 1} \rightarrow \mathbb{R}_{[1, N]}$  of inter-execution times as

$$\Delta(\gamma) = \mathbb{E}\{t_{j+1} - t_j\} = \sum_{i=1}^N iP_i(\gamma)$$

for  $\gamma \in \mathbb{R}_{\geq 1}$ . Based on the results of Lemmas 2.2 and 2.3, we can obtain the following lemma to show the monotonicity of  $\Delta(\gamma)$ .

**Lemma 2.4.**  $\Delta(\gamma)$  is a monotonically nondecreasing and continuous function with respect to  $\gamma$ . Moreover,  $\Delta(1) = 1$ , and  $\Delta(\gamma) = N$  for a sufficiently large  $\gamma$ .

**Proof.** The probability  $\mathcal{P}_i(\gamma)$  that an event is triggered at the  $i$ th step after the last event-triggered instant is given as

$$\begin{aligned} \mathcal{P}_i(\gamma) &= \mathbb{P} \left\{ \sum_{s=0}^{i-1} (A + BK)^s \omega(i - s - 1) \notin \tilde{\mathcal{Q}}_i(\gamma), \right. \\ &\quad \left. \sum_{s=0}^{\ell-1} (A + BK)^s \omega(\ell - s - 1) \in \tilde{\mathcal{Q}}_{\ell}(\gamma), \ell \in \mathbb{Z}_{[1, i-1]} \right\}. \end{aligned} \quad (2.15)$$

Note that  $\mathcal{P}_i(\gamma) = \tilde{\mathcal{P}}_{i-1}(\gamma) - \tilde{\mathcal{P}}_i(\gamma)$ . According to Lemma 2.3,  $\tilde{\mathcal{P}}_i(\gamma)$  is a continuous function with respect to  $\gamma$ , thus  $\Delta(\gamma)$  is also a continuous function with respect to  $\gamma$ . Moreover, for any  $\gamma_1, \gamma_2 \in \mathbb{R}_{\geq 1}$  with  $\gamma_1 \leq \gamma_2$ , it follows that

$$\begin{aligned} \Delta(\gamma_1) &= \sum_{i=1}^N iP_i(\gamma_1) = \sum_{i=1}^N i(\tilde{\mathcal{P}}_{i-1}(\gamma_1) - \tilde{\mathcal{P}}_i(\gamma_1)) \\ &= \tilde{\mathcal{P}}_0(\gamma_1) + \sum_{i=1}^{N-1} \tilde{\mathcal{P}}_i(\gamma_1) \\ &= 1 + \sum_{i=1}^{N-1} \tilde{\mathcal{P}}_i(\gamma_1) \\ &\leq 1 + \sum_{i=1}^{N-1} \tilde{\mathcal{P}}_i(\gamma_2) = \Delta(\gamma_2). \end{aligned}$$

It is shown that  $\Delta(\gamma)$  is monotonically nondecreasing with respect to  $\gamma$ . Since  $\mathcal{Z}$  is a nonempty set, then  $\tilde{\mathcal{Q}}_i(1) = \emptyset$  for all  $i \in \mathbb{Z}_{[1, N-1]}$ , implying  $\mathcal{P}_1(1) = 1$  in (2.15). Hence,  $\Delta(1) = 1$ ; furthermore, since the probability density function  $f_\omega$  is bounded, there exists a sufficiently large  $\gamma$  such that  $\mathcal{P}_i(\gamma) = 0$  for  $i \in \mathbb{Z}_{[1, N-1]}$  and  $\mathcal{P}_N(\gamma) = 1$ , implying  $\Delta(\gamma) = N$ .  $\blacksquare$

According to Lemma 2.4, for a given expected value of inter-execution times  $\Delta$ , there exists an appropriate  $\gamma$ . Since the set  $\mathcal{Z}$  contains all uncertainties between  $x(t)$  and  $\tilde{x}(t)$ , there is a possibility that when  $\sum_{s=0}^{i-1} (A + BK)^s \omega(i-s-1) \notin \mathcal{Q}_i \ominus (A + BK)^i \mathcal{Z}$  is satisfied at instant  $t_j + i$ , the event-triggered condition in (2.9) may be satisfied at instant  $t \geq t_j + i$ , which implies  $\hat{\Delta} \geq \Delta$ . That is, the designed event-triggered scheme may reduce the communication more than expected.

## 2.3 Recursive Feasibility and Stability Analysis

In this section, recursive feasibility of the proposed event-triggered robust MPC and robust stability of the closed-loop system are analyzed.



### 2.3.1 Recursive Feasibility

The following theorem ensures that if the optimization problem in (2.6) is feasible at the initial event-triggered instant, then it remains feasible for all future event-triggered instants.

**Theorem 2.1.** *Suppose that  $(\tilde{\mathbf{x}}^*(t_j), \tilde{\mathbf{u}}^*(t_j))$  is the optimal solution of the optimization problem in (2.6) for  $x(t_j) \in \mathcal{X}_N$  at any event-triggered instant  $t_j \in \mathbb{Z}^+$ . Then, under the event-triggered condition in (2.9), for the system in (2.1),  $(\tilde{\mathbf{x}}(t_{j+1}), \tilde{\mathbf{u}}(t_{j+1}))$  with  $\tilde{\mathbf{u}}(t_{j+1}) \triangleq \{\tilde{u}(0|t_{j+1}), \dots, \tilde{u}(N-1|t_{j+1})\}$  and  $\tilde{\mathbf{x}}(t_{j+1}) \triangleq \{\tilde{x}(0|t_{j+1}), \dots, \tilde{x}(N|t_{j+1})\}$  defined by*

$$\tilde{x}(i|t_{j+1}) = \begin{cases} \tilde{x}^*(t_{j+1} - t_j + i|t_j), & i \in \mathbb{Z}_{[0, t_j + N - t_{j+1}]} \\ (A + BK)^{i - (t_j + N - t_{j+1})} \tilde{x}^*(N|t_j), & i \in \mathbb{Z}_{[t_j + N + 1 - t_{j+1}, N]}. \end{cases} \quad (2.16)$$

$$\tilde{u}(i|t_{j+1}) = \begin{cases} \tilde{u}^*(t_{j+1} - t_j + i|t_j), & i \in \mathbb{Z}_{[0, t_j + N - t_{j+1} - 1]} \\ K\tilde{x}(i|t_{j+1}), & i \in \mathbb{Z}_{[t_j + N - t_{j+1}, N - 1]}. \end{cases} \quad (2.17)$$

is feasible for the optimization problem at the triggering instant  $t_{j+1}$ .

**Proof.** According to Lemma 2.1, since  $x(t_j) \in \tilde{x}^*(t_j) \oplus \mathcal{Z}$ , it follows that  $x(t_j + i) \in \tilde{x}^*(i|t_j) \oplus \mathcal{Z}$ ,  $i \in \mathbb{Z}_{[0, N]}$ , implying  $x(t_{j+1}) \in \tilde{x}^*(t_{j+1} - t_j|t_j) \oplus \mathcal{Z}$ . Hence, according to (2.16), we have that

$$x(t_{j+1}) \in \tilde{x}(t_{j+1}) \oplus \mathcal{Z}.$$

Then, the constraint in (2.6a) is satisfied. To prove that the constraints in (2.6c)-(2.6e) are feasible, firstly, consider  $i \in \mathbb{Z}_{[0, t_j + N - t_{j+1} - 1]}$ . Since  $\tilde{x}^*(t_{j+1} - t_j + i|t_j) \in \mathcal{X} \ominus \mathcal{Z}$  and  $\tilde{u}^*(t_{j+1} - t_j + i|t_j) \in \mathcal{U} \ominus K\mathcal{Z}$ , then according to (2.16) and (2.17), we have that

$$\begin{aligned} \tilde{x}(i|t_{j+1}) &\in \mathcal{X} \ominus \mathcal{Z}, \quad i \in \mathbb{Z}_{[0, t_j + N - t_{j+1} - 1]}, \\ \tilde{u}(i|t_{j+1}) &\in \mathcal{U} \ominus K\mathcal{Z}, \quad i \in \mathbb{Z}_{[0, t_j + N - t_{j+1} - 1]}. \end{aligned}$$

Secondly, consider  $i \in \mathbb{Z}_{[t_j + N - t_{j+1}, N - 1]}$ . Since  $\tilde{x}^*(N|t_j) \in \mathcal{X}_f \subseteq \mathcal{X} \ominus \mathcal{Z}$ , according to (2.4b), we have that

$$(A + BK)^{i - (t_j + N - t_{j+1})} \tilde{x}^*(N|t_j) \in \mathcal{X}_f \subseteq \mathcal{X} \ominus \mathcal{Z}, \quad i \in \mathbb{Z}_{[t_j + N - t_{j+1}, N - 1]},$$

which implies  $\tilde{x}(i|t_{j+1}) \in \mathcal{X} \ominus \mathcal{Z}$  and  $\tilde{x}(N|t_{j+1}) \in \mathcal{X}_f \subseteq \mathcal{X} \ominus \mathcal{Z}$ . According to (2.4c), we have that

$$K\tilde{x}(i|t_{j+1}) \in K\mathcal{X}_f \subseteq \mathcal{U} \ominus K\mathcal{Z}, \quad i \in \mathbb{Z}_{[t_j+N-t_{j+1}, N-1]},$$

which implies  $\tilde{u}(i|t_{j+1}) \in \mathcal{U} \ominus K\mathcal{Z}$ . It is concluded that  $(\tilde{\mathbf{x}}(t_{j+1}), \tilde{\mathbf{u}}(t_{j+1}))$  constructed by the optimal solution of the optimization problem, is feasible at the triggering instant  $t_{j+1}$ . Therefore, recursive feasibility of the optimization problem is guaranteed.  $\blacksquare$

### 2.3.2 Robust Stability

According to (2.5), the following lemma is obtained by induction to show the decreasing of  $V_f(\tilde{x}(t))$ . It will be used to ensure the decreasing of the optimal cost function  $J_N^*(x(t_j))$  later.

**Lemma 2.5.** *For all  $\tilde{x}(t) \in \mathcal{X}_f$ ,  $t \in \mathbb{Z}^+$ , we have that*

$$V_f((A + BK)^i \tilde{x}(t)) \leq V_f(\tilde{x}(t)) - \sum_{h=0}^{i-1} l(\tilde{x}(h|t), K\tilde{x}(h|t)), \quad i \in \mathbb{Z}_{\geq 1}. \quad (2.18)$$

**Proof.** According to the condition in (2.5), we have that

$$V_f((A + BK)\tilde{x}(t)) \leq V_f(\tilde{x}(t)) - l(\tilde{x}(t), K\tilde{x}(t)), \quad (2.19)$$

$$V_f((A + BK)^2\tilde{x}(t)) \leq V_f((A + BK)\tilde{x}(t)) - l(\tilde{x}(1|t), K\tilde{x}(1|t)), \quad (2.20)$$

$\vdots$

$$V_f((A + BK)^i \tilde{x}(t)) \leq V_f((A + BK)^{i-1} \tilde{x}(t)) - l(\tilde{x}(i-1|t), K\tilde{x}(i-1|t)). \quad (2.21)$$

Then, equation (2.18) is obtained by summing from (2.19) to (2.21).  $\blacksquare$

**Lemma 2.6.** *Suppose that  $J_N^*(x(t_j))$  is the optimal cost of the optimization problem in (2.6) for  $x(t_j) \in \mathcal{X}_N$  at any event-triggered instant  $t_j \in \mathbb{Z}^+$ . Then, under the event-triggered condition in (2.9), the optimal cost  $J_N^*(x(t_{j+1}))$  satisfies*

$$J_N^*(x(t_{j+1})) \leq J_N^*(x(t_j)) - \sum_{i=0}^{t_{j+1}-t_j-1} l(\tilde{x}^*(i|t_j), \tilde{u}^*(i|t_j)). \quad (2.22)$$

**Proof.** Since recursive feasibility of the MPC optimization problem is guaranteed, a feasible cost  $J_N(x(t_{j+1}))$  at the event-triggered instant  $t_{j+1}$  is constructed based on the optimal solution of the optimization problem as

$$\begin{aligned} J_N(x(t_{j+1})) &= J_N^*(x(t_j)) - V_f(\tilde{x}^*(N|t_j)) - \sum_{i=0}^{t_{j+1}-t_j-1} l(\tilde{x}^*(i|t_j), \tilde{u}^*(i|t_j)) \\ &\quad + V_f(\tilde{x}(N|t_{j+1})) + \sum_{i=t_j+N-t_{j+1}}^{N-1} l(\tilde{x}(i|t_{j+1}), \tilde{u}(i|t_{j+1})) \\ &\geq J_N^*(x(t_{j+1})). \end{aligned} \quad (2.23)$$

According to Lemma 2.5, we have

$$\begin{aligned} V_f(\tilde{x}(N|t_{j+1})) &= V_f((A+BK)^{(t_{j+1}-t_j)}\tilde{x}^*(N|t_j)) \\ &\leq V_f(\tilde{x}^*(N|t_j)) - \sum_{i=t_j+N-t_{j+1}}^{N-1} l(\tilde{x}(i|t_{j+1}), \tilde{u}(i|t_{j+1})). \end{aligned} \quad (2.24)$$

Substituting (2.24) into (2.23) yields (2.22). ■

**Lemma 2.7.** *Under the event-triggered condition in (2.9), for the system in (2.1), there exist constants  $c_2 > c_1 > 0$  such that*

$$J_N^*(x(t_j)) \geq c_1 \|\tilde{x}^*(t_j)\|^2, \quad \forall x(t_j) \in \mathcal{X}_N, \quad (2.25)$$

$$J_N^*(x(t_{j+1})) \leq J_N^*(x(t_j)) - \sum_{i=0}^{t_{j+1}-t_j-1} c_1 \|\tilde{x}^*(i|t_j)\|^2, \quad \forall x(t_j) \in \mathcal{X}_N, \quad (2.26)$$

$$J_N^*(x(t_j)) \leq c_2 \|\tilde{x}^*(t_j)\|^2, \quad \forall x(t_j) \in \mathcal{X}_f \oplus \mathcal{Z}. \quad (2.27)$$

**Proof.** Equations (2.25)-(2.27) can be easily obtained by induction based on (2.22) in Lemma 2.6. ■

Based on Lemma 2.7, the main stability theorem is obtained below.

**Theorem 2.2.** *For the system in (2.1) with  $x(0) \in \mathcal{X}_N$  and  $\omega(t) \in \mathcal{W}$ ,  $t \in \mathbb{Z}^+$ , the set  $\mathcal{Z}$  is robustly exponentially stable.*

**Proof.** According to (2.26), if  $t_{j+1} = t_j + 1$ , we have that

$$J_N^*(x(t_j + 1)) \leq J_N^*(x(t_j)) - c_1 \|\tilde{x}^*(t_j)\|^2, \quad \forall x(t_j) \in \mathcal{X}_f \oplus \mathcal{Z}.$$

Then, it follows from (2.25) and (2.27) that

$$J_N^*(x(t_j + 1)) \leq (1 - \frac{c_1}{c_2})J_N^*(x(t_j)),$$

which implies that

$$J_N^*(x(t_{j+1})) \leq (1 - \frac{c_1}{c_2})^{(t_{j+1}-t_j)} J_N^*(x(t_j)). \quad (2.28)$$

For all  $\beta \geq 0$ , let  $\mathcal{S}_\beta \triangleq \{x(t) \mid J_N^*(x(t)) \leq \beta, t \in \mathbb{Z}\}$ . Since  $J_N^*(x(t)) = 0$  for all  $x(t) \in \mathcal{Z}$  [80],  $\mathcal{S}_0 = \mathcal{Z}$  and there exists a  $\beta > 0$  such that  $\mathcal{S}_\beta \subseteq \mathcal{X}_f \oplus \mathcal{Z}$ . Then, from (2.28), in general, we have that

$$J_N^*(x(t)) \leq \theta^t J_N^*(x(0)) \quad (2.29)$$

for all  $x(0) \in \mathcal{S}_\beta$  and  $t \in \mathbb{Z}^+$ , where  $\theta = 1 - c_1/c_2$ . Based on (2.29), there must exist some  $0 < c < \infty$  satisfying

$$\|\tilde{x}(t)\| \leq c\sqrt{\theta^t}\|\tilde{x}(0)\|. \quad (2.30)$$

Then, for all  $x(0) \in \mathcal{X}_N$  and  $\omega(t) \in \mathcal{W}$ , there exists an  $\epsilon \in \mathbb{Z}^+_{>0}$  such that  $x(i) \in \mathcal{S}_\beta$  for all  $i > \epsilon$ . Hence, from (2.30), there must exist a  $\mu > c$  such that  $\|\tilde{x}(t)\| \leq \mu\sqrt{\theta^t}\|\tilde{x}(0)\|$  for all  $x(0) \in \mathcal{X}_N$ . Since  $x(t) \in \tilde{x}(t) \oplus \mathcal{Z}$ ,  $d(x(t), \mathcal{Z}) \leq \mu\sqrt{\theta^t}d(x(0), \mathcal{Z})$ . Hence, according to Definition 2.2, the set  $\mathcal{Z}$  is robustly exponentially stable for the system in (2.1) with the feasible region  $\mathcal{X}_N$ . ■

## 2.4 Simulation Examples

**Example 2.1.** Consider the linear system provided in [67]:

$$x(t+1) = \begin{bmatrix} 1.1 & 0.2 \\ 0 & 1.2 \end{bmatrix} x(t) + \begin{bmatrix} 0 \\ 1 \end{bmatrix} u(t) + \omega(t),$$

where  $\omega(t)$  is independently uniformly distributed on  $\mathcal{W} = [-1, 1] \times [-1, 1]$  for all  $t \in \mathbb{Z}^+$ . The state constraint is  $\mathcal{X} = [-30, 30] \times [-30, 30]$ , and the control constraint is  $\mathcal{U} = [-10, 10]$ . The horizon length is set as  $N = 10$ . The weighting matrices of the stage cost are chosen as  $Q = I_2$  and  $R = I$ . In this example, 50 random realizations of the disturbance sequence are considered.

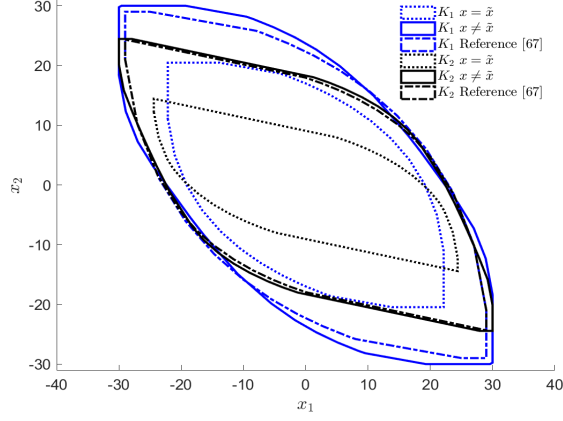


Figure 2.1: Feasible regions  $\mathcal{X}_N$ .

Table 2.1: Distribution of inter-execution times based on  $K_1$

Inter-execution time	Count	Frequency
2	814	3.00%
3	11350	41.78%
4	11127	40.96%
5	3446	12.69%
6	406	1.49%
7	21	0.08%

Table 2.2: Distribution of inter-execution times based on  $K_2$

Inter-execution time	Count	Frequency
2	3438	11.21%
3	17166	55.99%
4	8714	28.42%
5	1265	4.13%
6	74	0.24%

Table 2.3: Comparison results with [67] in Case A

	$K_1$		$K_2$	
	$\bar{J}_{\text{perf}}$	$\bar{T}_c$	$\bar{J}_{\text{perf}}$	$\bar{T}_c$
Time-triggered controller	5.7709	501.23s	7.2608	521.65s
Time-triggered controller in [67]	5.7705	492.75s	7.2593	493.27s
Event-triggered controller	5.7811	153.69s	7.2796	179.36s
Event-triggered controller in [67]	6.7682	181.03s	8.9162	182.51s

### A. Comparisons with different feedback gains

Consider the following two feedback gains and the corresponding weighting matrices of the terminal cost:

$$K_1 = \begin{bmatrix} -1.0042 & -1.0788 \end{bmatrix}, P_1 = \begin{bmatrix} 2.6093 & 0.2100 \\ 0.2100 & 2.1837 \end{bmatrix},$$

$$K_2 = \begin{bmatrix} -1.7500 & -1.3000 \end{bmatrix}, P_2 = \begin{bmatrix} 17.5385 & 4.5894 \\ 4.5894 & 3.2404 \end{bmatrix},$$

where  $K_1$  is the LQR gain and  $K_2$  is an arbitrarily stabilizing feedback gain. Given an expected value of inter-execution times  $\Delta = 3$ , then we can find  $\gamma_1 = 3.7368$  and  $\gamma_2 = 4.5368$  by using a stochastic approximation approach as provided in [83]. Set the initial state  $x(0) = [-27.19, 18.74]^T$  and the simulation steps  $T_{\text{sim}} = 10^5$ . Consider the following performance index:

$$J_{\text{perf}} = \frac{1}{T_{\text{sim}}} \sum_{t=0}^{T_{\text{sim}}-1} x(t)^T Q x(t) + u(t)^T R u(t). \quad (2.31)$$

To show the advantages of the proposed method, comparisons with the method in [67] have been carried out. Let  $\bar{J}_{\text{perf}}$  and  $\bar{T}_c$  be the average performance index and on-line computation time of these 50 random disturbance realizations, respectively. It is seen from Figure 2.1 that, robust MPC with  $x(t) \neq \tilde{x}(t)$  can bring a larger feasible region  $\mathcal{X}_N$  than that with  $x(t) = \tilde{x}(t)$ . For one of realizations, the distributions of inter-execution times in  $10^5$  steps are listed in Table 2.1 and Table 2.2, which present the resulted average inter-execution times  $\hat{\Delta}_1 = 3.6813$  and  $\hat{\Delta}_2 = 3.2619$ , respectively. As shown in Table 2.3, there is no significant increase of the performance index for the designed event-triggered controller when compared with time-triggered (periodical) controller, but there is a 17.29% increase of the performance index by employing the method in [67] based on the LQR gain. Moreover, when the LQR gain is not considered, it is shown that the control performance in [67] will become worse, but the proposed method can still keep the control performance close to that of time-triggered (periodical) controller. Furthermore, the proposed event-triggered scheme requires less computation time than that of [67]. Hence, it is shown that the proposed event-triggered robust MPC not

only achieves better reduction of transmission costs, but also preserves the desired control performance.

### B. Transient behavior analysis

To analyze the transient behavior brought by the event-triggered controllers, the disturbances  $\omega(t)$  are set to be  $[0, 0]^T$  for  $t \in [21, 50]$  and uniformly distributed on  $\mathcal{W} = [-1, 1] \times [-1, 1]$  for other sampling instants. It is assumed that the disturbances keep the same for the simulation with these two methods. Set the simulation steps  $T_{\text{sim}} = 70$  and the initial state  $x(0) = [0, 0]^T$  which is regarded as the stable point of the nominal system. Consider the error performance index:

$$J_{\text{error}} = \frac{1}{T_{\text{sim}}} \sum_{t=0}^{T_{\text{sim}}-1} \sqrt{(x(t) - x(0))^T (x(t) - x(0))}. \quad (2.32)$$

Then, we obtain  $J_{\text{error}} = 1.0079$  by using the proposed method, which is smaller than that in [67] in which the error performance index is  $J_{\text{error}} = 1.0655$ . For one of disturbance realizations, it is seen from Figure 2.2, the control inputs fluctuate in a smaller range than that of [67], and the speed of convergence to the origin is faster when the disturbances disappear. Similar results can be also observed on state trajectories. Therefore, for this example, the transient behavior of the closed-loop system in the proposed event-triggered robust MPC is better than that in [67].

**Example 2.2.** Consider the decentralized interconnected system (DIS2) provided in [84]:

$$\dot{x}(t) = \begin{bmatrix} -4 & 2 & 1 \\ 3 & -2 & 5 \\ -7 & 0 & 3 \end{bmatrix} x(t) + \begin{bmatrix} 1 & 0 \\ 1 & 0 \\ 0 & 1 \end{bmatrix} u(t) + \omega(t). \quad (2.33)$$

Let the sampling instant  $T_s = 0.2s$ . The constraint sets are  $\mathcal{X} = [-40, 40] \times [-40, 40] \times [-40, 40]$  and  $\mathcal{U} = [-25, 25] \times [-25, 25]$ . Set the horizon length  $N = 8$ . The weighting matrices of the stage cost are chosen as  $Q = I_3$  and  $R = I_2$ . The feedback gain and weighting matrix of the terminal cost are

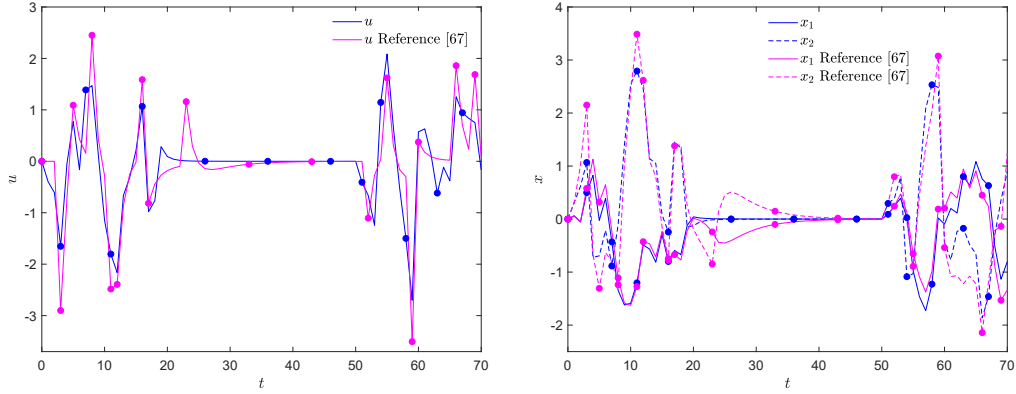


Figure 2.2: Control input and state trajectories (The circles represent event-triggered instants).

Table 2.4: Distribution of inter-execution times

Inter-execution time	Count	Frequency
2	1654	5.43%
3	19441	63.82%
4	8504	27.91%
5	838	2.75%
6	27	0.09%

Table 2.5: Comparison results with [67]

	$\bar{J}_{\text{perf}}$	$\bar{T}_c$
Time-triggered controller	13.2980	1405.86s
Time-triggered controller in [67]	13.2878	1011.29s
Event-triggered controller	13.3237	315.71s
Event-triggered controller in [67]	22.9653	295.08s

given as:

$$K = \begin{bmatrix} -2.1123 & -0.9940 & 0.7995 \\ 2.3691 & 0.1225 & -2.8873 \end{bmatrix}, P = \begin{bmatrix} 15.5988 & 2.6096 & -13.8923 \\ 2.6096 & 3.1475 & 0.6272 \\ -13.8923 & 0.6272 & 20.4932 \end{bmatrix}.$$

Set the initial state  $x(0) = [-1.18, 8.74, 12.87]^T$ . We can obtain  $\gamma = 8.5020$  for a given expected value of inter-execution times  $\Delta = 3$ . Consider 50 random realizations of the disturbance sequence. For one of realizations, the distribution of inter-execution times is displayed in Table 2.4, which presents



the resulted average inter-execution time  $\hat{\Delta} = 3.2825$ . From the comparison results in Table 2.5, it is concluded that the proposed event-triggered robust MPC can achieve a better balance between computational burden and control performance than [67]. In order to analyze the transient behavior, we set the disturbances  $\omega(t) = [0, 0, 0]^T$  for  $t \in [21, 40]$  and the initial state  $x(0) = [0, 0, 0]^T$ . The error performance index  $J_{\text{error}} = 0.9071$  is obtained by using the proposed method, which is smaller than that in [67] ( $J_{\text{error}} = 1.3312$ ). It is concluded that the proposed method provides a better transient behavior than that in [67].

## 2.5 Summary

In this chapter, an event-triggered robust MPC approach based on the concept of minimal robust positively invariant sets has been proposed for linear discrete-time systems with bounded disturbances. Tube-based MPC has been incorporated into the design of the event-triggered scheme, achieving the trade-off between control performance and computational burden. According to the known probability distribution of bounded disturbances, an event-triggered condition which can limit the state error between the predicted state and the actual state has been derived to reduce the amount of computation in solving the optimization problem. Both recursive feasibility and robust stability of the proposed event-triggered robust MPC are guaranteed. Simulation results have shown the benefits of the designed event-triggered MPC controller.

# Chapter 3

## Robust MPC Using A Two-Step Triggering Scheme\*

This chapter investigates a two-step triggering scheme involving a tentative verification of a triggering condition and a delayed triggering to ensure necessary events for tube-based MPC constructed in Chapter 2. In practical situations, events may be triggered occasionally or falsely. Under such circumstances, existing control actions may remain effective, and solving the optimization problem could be unnecessary. Hence, to avoid unnecessary events and reduce resource consumption further, we propose a two-step triggering scheme, which ensures that the triggered events are necessary. A triggering function is proposed based on the distances between actual states and a robust positively invariant set. With a constructed two-step verification, the optimization problem is solved and the triggering instant is updated if the triggering conditions are satisfied at both checking instants, leading to a further reduction of computational burden. Moreover, the designed two-step triggering scheme can be extended to multi-agent systems.

This chapter is organized as follows. Section 3.1 designs a two-step trig-

---

\*A version of this chapter has been published as: Li Deng, Zhan Shu, and Tongwen Chen, Robust model predictive control using a two-step triggering scheme. *IEEE Transactions on Automatic Control*, vol. 68, no. 3, pp. 1934-1940, Apr. 2022. An extension of this Chapter has been published as: Li Deng, Zhan Shu, and Tongwen Chen, Event-triggered robust distributed MPC for multi-agent systems with a two-step event verification. *8th IFAC Symposium on System Structure and Control*, vol. 55, no. 34, pp. 144-149, Sep. 2022.

gering scheme for tube-based MPC, analyzes recursive feasibility and robust stability, and verifies the proposed approach by numerical examples. Section 3.2 extends the designed two-step triggering scheme to a multi-agent system and discusses stability and consensus of the overall multi-agent system. Section 3.3 concludes this chapter.

## 3.1 Tube-Based MPC with Two-Step Triggering

Consider the linear discrete-time system with bounded disturbances in (2.1). According to [80] and [81], a robust positively invariant set can be regarded as the “origin” of the systems with disturbances. Hence, we take the following assumption in the remaining analysis and design of this chapter.

**Assumption 3.1.**  $x(t) \notin \mathcal{Z}$ , where  $\mathcal{Z}$  is a robust positively invariant set designed as in Algorithm A.1.

In this section, we will design a two-step triggering scheme for the tube-based MPC optimization problem shown in (2.6). In the existing event-triggered MPC, the optimization problem is solved at each triggering instant, and less computational resources are required compared with periodic computation. However, events in practical situations may be triggered occasionally or falsely. Under such circumstances, existing control actions may remain effective, and solving the optimization problem could be unnecessary. Hence, to avoid unnecessary events and reduce resource consumption further, we propose a two-step triggering scheme, which can ensure that the triggered events are necessary.

### 3.1.1 Problem Formulation

Define the triggering instant sequence as  $\{t_l : l \in \mathbb{Z}^+\} \subseteq \mathbb{Z}^+$ . First, a tentative checking condition is given by

$$t_j^1 = \min \{ \min \{ t \in \mathbb{Z}_{>t_l} \mid g(t, x(t), x(t_l)) > 0 \}, t_l + N \}, \quad (3.1)$$

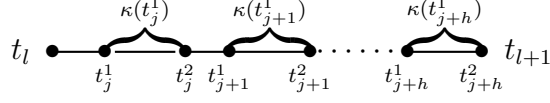


Figure 3.1: Illustration of triggering instant sequences.

where  $g : \mathbb{Z}^+ \times \mathbb{R}^{n_x} \times \mathbb{R}^{n_x} \rightarrow \mathbb{R}$  is a triggering function to be designed, and  $\{t_j^1 : j \in \mathbb{Z}^+\} \subseteq \mathbb{Z}^+$  is the first checking instant sequence. At  $t_j^1$ , instead of triggering immediately, we generate a waiting horizon  $\kappa(t_j^1) \in \mathbb{Z}_{[1, N-1]}$ , that is, the most likely instant when the condition in (3.1) is violated again. Define the second checking instant sequence as  $\{t_j^2 : j \in \mathbb{Z}^+\} \subseteq \mathbb{Z}^+$  and  $t_j^2 = t_j^1 + \kappa(t_j^1)$ . Then, the triggering instant is determined by

$$t_{l+1} = \begin{cases} t_j^2, & \text{if } t_j^2 = t_l + N \\ \min\{t_j^2 \in \mathbb{Z}^+ \mid g(t_j^2, x(t_j^2), x(t_j^1)) > 0\}, & \text{otherwise} \end{cases}. \quad (3.2)$$

Assume that the initial instants  $t_0 = t_0^1 = t_0^2 = 0$ . Here,  $N$  is regarded as the maximum of the inter-execution time, i.e., if the inter-execution time exceeds it, then the system will be triggered automatically. Clearly, it follows that  $\{t_l : l \in \mathbb{Z}^+\} \subseteq \{t_j^2 : j \in \mathbb{Z}^+\}$ . A relation between these sequences is illustrated in Figure 3.1, where  $h \in \mathbb{Z}^+$ .

Combining (3.1) and (3.2), two kinds of events are considered in this two-step triggering scheme: one is unnecessary events, for which (3.1) is satisfied but (3.2) is not; the other is necessary events, for which both (3.1) and (3.2) are satisfied.

**Remark 3.1.** *Setting the prediction horizon  $N$  as the maximum of the inter-execution time plays a critical role in preserving the control performance and guaranteeing robust stability for the proposed two-step triggering scheme.*

An event-triggered controller to be designed is of the form

$$u(t) = \varphi(x(t), \tilde{x}(t), \tilde{u}(t)), \quad t \in \mathbb{Z}_{[t_l, t_{l+1})}, \quad (3.3)$$

where the function  $\varphi : \mathbb{R}^{n_x} \times \mathbb{R}^{n_x} \times \mathbb{R}^{n_u} \rightarrow \mathbb{R}^{n_u}$  is to be determined.

The main purpose is to design a controller of the form (3.3) with a triggering function  $g$  and a waiting horizon  $\kappa$  such that the optimization problem in (2.6) is solved at  $t_l$ .

### 3.1.2 Two-Step Triggering MPC Design

In this subsection, the triggering Function  $g$  and the waiting horizon  $\kappa$  are designed, and the effects of triggering parameters on the inter-execution time are analyzed.

#### 3.1.2.1 Triggering Function $g$

To ensure robust stability when the optimization problem in (2.6) is not solved, according to Definition 2.2, for  $t \in \mathbb{Z}_{>t_l}$ , the triggering function  $g$  is designed as

$$g(t, x(t), x(t_l)) = d(x(t), \tau\mathcal{Z}) - \mu\sqrt{\theta^{t-t_l}}d(x(t_l), \tau\mathcal{Z}),$$

where  $\tau \in (0, 1]$ ,  $\mu \in (0, \eta]$ ,  $\theta = 1 - c_1/c_2$  and

$$\eta = \min\left\{1, \frac{z_{\min}}{z_{\max}\sqrt{\theta}}\right\}, \quad (3.4a)$$

$$c_1 = \lambda_{\min}(Q + K^T R K), \quad (3.4b)$$

$$c_2 = \lambda_{\max}(P), \quad (3.4c)$$

$z_{\min}$  and  $z_{\max}$  are the shortest and longest distances between the points on the boundary of  $\mathcal{Z}$  and the origin.

Let  $z^*(x(t), \mathcal{Z}) \triangleq \arg \min\{\|x(t) - z\| \mid z \in \mathcal{Z}\}$ . According to the definition of the distance, we have that  $d(x(t), \tau\mathcal{Z}) = \|x(t) - z^*(x(t), \tau\mathcal{Z})\|$ . Since  $\tau\mathcal{Z}$  is a homogeneous convex subset of  $\mathcal{Z}$ ,  $z^*(x(t), \tau\mathcal{Z}) = \tau z^*(x(t), \mathcal{Z})$  holds. Then, the triggering function  $g$  is equivalent to the following form

$$g(t, x(t), x(t_l)) = \|x(t) - \tau z^*(x(t), \mathcal{Z})\| - \mu\sqrt{\theta^{t-t_l}}\|x(t_l) - \tau z^*(x(t_l), \mathcal{Z})\|.$$

For notational simplicity, let  $z^*(x(t))$  stand for  $z^*(x(t), \mathcal{Z})$ . Then, we have the following two lemmas, which are helpful for our analysis later.

**Lemma 3.1.** For a stabilizing feedback gain  $K \in \mathbb{R}^{n_u \times n_x}$ , we have that  $\frac{\rho(A+BK)}{\sqrt{\theta}} \leq 1$ , where  $\rho(A+BK)$  is the spectral radius of  $A+BK$ .

**Proof.** According to (2.5), we have that

$$P \succeq (A+BK)^T P (A+BK) + (Q + K^T R K). \quad (3.5)$$

Let  $\xi \in \mathbb{C}^{n_x}$  be the corresponding eigenvector of  $\rho(A+BK)$  and  $\bar{\xi}$  be the complex conjugate transpose of  $\xi$ . Pre- and post-multiplying (3.5) by  $\bar{\xi}$  and  $\xi$ , respectively, yields that

$$\bar{\xi} P \xi \geq [\rho(A+BK)]^2 \bar{\xi} P \xi + \bar{\xi} (Q + K^T R K) \xi.$$

Since  $K$  is a stabilizing gain, i.e.,  $\rho(A+BK) < 1$ , we have that

$$(1 - [\rho(A+BK)]^2) \lambda_{\max}(P) \geq \lambda_{\min}(Q + K^T R K).$$

Then, it follows that

$$\frac{\lambda_{\max}(P) - \lambda_{\min}(Q + K^T R K)}{\lambda_{\max}(P)} \geq [\rho(A+BK)]^2. \quad (3.6)$$

Note that  $\theta = 1 - c_1/c_2$ . Then, from (3.4b)-(3.4c), equation (3.6) implies that  $\frac{\rho(A+BK)}{\sqrt{\theta}} \leq 1$ . ■

**Lemma 3.2.** If  $\mu \in (0, \eta]$ , then  $\mu\sqrt{\theta^{t-t_l}} \|z^*(x(t_l))\| - \|z^*(x(t))\| \leq 0$  for  $t > t_l$ .

**Proof.** If  $\mu \in (0, \eta]$ , from (3.4a), then we have that

$$\mu\sqrt{\theta^{t-t_l}} \|z^*(x(t_l))\| - \|z^*(x(t))\| \leq \frac{z_{\min}}{z_{\max}\sqrt{\theta}} \sqrt{\theta} z_{\max} - z_{\min} = 0. \quad (3.7)$$

■

### 3.1.2.2 Waiting Horizon $\kappa$

At  $t_j^1$ , the tentative checking condition in (3.1) is satisfied. Instead of triggering immediately, we would like to estimate the most likely instant when the tentative checking condition in (3.1) is violated again as follows:

$$\kappa^*(t_j^1) = \min\{k \in \mathbb{Z}_{>0} \mid d(x(t_j^1 + k), \tau \mathcal{Z}) \leq \mu\sqrt{\theta^k} d(x(t_j^1), \tau \mathcal{Z})\}. \quad (3.8)$$

Due to the presence of uncertain disturbances, it is difficult to predict  $d(x(t_j^1 + k), \tau\mathcal{Z})$  at  $t_j^1$ . Thus, it is numerically intractable to obtain  $\kappa^*(t_j^1)$  based on (3.8). Since  $\tau\mathcal{Z}$  is a homogeneous convex subset of  $\mathcal{Z}$ , we have that  $d(x(t_j^1 + k), \tau\mathcal{Z}) = d(x(t_j^1 + k), \mathcal{Z}) + (1 - \tau)\|z^*(x(t_j^1 + k))\|$ . Then, the condition in (3.8) can be written as

$$d(x(t_j^1 + k), \mathcal{Z}) \leq \mu\sqrt{\theta^k}d(x(t_j^1), \tau\mathcal{Z}) - (1 - \tau)\|z^*(x(t_j^1 + k))\|. \quad (3.9)$$

Since  $\tau \in (0, 1]$ , we can obtain a necessary condition of (3.9) as

$$d(x(t_j^1 + k), \mathcal{Z}) \leq \mu\sqrt{\theta^k}d(x(t_j^1), \tau\mathcal{Z}). \quad (3.10)$$

Accordingly, we consider an alternative, that is, estimating a lower bound  $\underline{\kappa}(t_j^1)$  of  $\kappa^*(t_j^1)$  as

$$\underline{\kappa}(t_j^1) = \min\{k \in \mathbb{Z}_{>0} \mid d(x(t_j^1 + k), \mathcal{Z}) \leq \mu\sqrt{\theta^k}d(x(t_j^1), \tau\mathcal{Z})\}. \quad (3.11)$$

Although  $d(x(t_j^1 + k), \mathcal{Z})$  remains uncomputable, we have the following lemma to facilitate the computation.

**Lemma 3.3.** *For a stabilizing feedback gain  $K \in \mathbb{R}^{n_u \times n_x}$ , there always exist a  $\bar{k} \in \mathbb{Z}_{>0}$ , a sufficiently small  $\sigma_{\min} > 0$ , and a  $\sigma_{\max} > 0$  which is dependent on  $A + BK$  such that*

$$\sigma_{\min}[\rho(A + BK)]^k \|\tilde{x}(t)\| \leq d(x(t + k), \mathcal{Z}) \leq \sigma_{\max}[\rho(A + BK)]^k \|\tilde{x}(t)\| \quad (3.12)$$

for  $k \in \mathbb{Z}_{(0, \bar{k})}$ .

**Proof.** Since  $x(t) \in \tilde{x}(t) \oplus \mathcal{Z}$ ,  $x(t + k) \in \tilde{x}(k|t) \oplus \mathcal{Z}$  according to Lemma 2.1. Then, we have that  $d(x(t + k), \mathcal{Z}) \leq \|\tilde{x}(k|t)\|$ . According to the prediction model in (2.6b),  $\tilde{x}(k|t) = (A + BK)^k \tilde{x}(t)$  by using the control law  $\tilde{u} = K\tilde{x}$ . Since  $A + BK$  is Schur,  $\|(A + BK)^k \tilde{x}(t)\| \leq \sigma_{\max}[\rho(A + BK)]^k \|\tilde{x}(t)\|$ , where  $\sigma_{\max} > 0$  is dependent on  $A + BK$ . On the other hand, for a sufficiently small  $\sigma_{\min}$ , we can always find a  $\bar{k}$  such that  $\sigma_{\min}[\rho(A + BK)]^k \|\tilde{x}(t)\| \leq d(x(t + k), \mathcal{Z})$  for  $k \in \mathbb{Z}_{(0, \bar{k})}$ . ■

Here,  $\sigma_{\min}$  is trivial, and  $\sigma_{\max}$  can be estimated by a generalized eigenvalue problem subject to LMIs as follows:

$$\begin{aligned} & \min_{\sigma_{\max}^2, M} \sigma_{\max}^2 \\ \text{s.t. } & I \preceq M \preceq \sigma_{\max}^2 I \end{aligned} \quad (3.13a)$$

$$\frac{\epsilon}{[\rho(A+BK)]^2} (A+BK)^T M (A+BK) - M \prec 0 \quad (3.13b)$$

where  $M \succ 0$ ;  $\epsilon > 0$  is a given scalar which is sufficiently close to 1, but not equal to 1.

According to Lemma 3.3,  $d(x(t_j^1 + k), \mathcal{Z})$  can be roughly described by  $\sigma[\rho(A+BK)]^k \|\tilde{x}(t_j^1)\|$ , where  $\sigma \in (\sigma_{\min}, \sigma_{\max})$ , and  $\underline{\kappa}(t_j^1)$  in (3.11) can be estimated correspondingly by

$$\underline{\kappa}_{\text{est}}(t_j^1) = \min \left\{ k \in \mathbb{Z}_{>0} \mid \left( \frac{\rho(A+BK)}{\sqrt{\theta}} \right)^k \leq \frac{\mu d(x(t_j^1), \tau \mathcal{Z})}{\sigma \|\tilde{x}(t_j^1)\|} \right\}. \quad (3.14)$$

On the other hand, since  $N$  is the maximum of the inter-execution time, the waiting horizon  $\kappa(t_j^1)$  is consequently determined by

$$\kappa(t_j^1) = \min \{ \underline{\kappa}_{\text{est}}(t_j^1), t_l + N - t_j^1 \}. \quad (3.15)$$

As  $\underline{\kappa}$  is a lower bound of  $\kappa^*$ , i.e.,  $\underline{\kappa} \leq \kappa^*$ , and the estimation  $\underline{\kappa}_{\text{est}}$  in (3.14) may not be accurate due to the choice of  $\sigma$ , we need to check the triggering condition again at  $t_j^2$ .

**Remark 3.2.** *From the above analysis, the values of  $\sigma_{\min}$  and  $\sigma_{\max}$  have an effect on the determination of the waiting horizon. However, how to design  $\sigma_{\min}$  and  $\sigma_{\max}$  to generate a tight estimation and how to update these two parameters as the system operates remain challenging, and are left for future study.*

### 3.1.2.3 Two-Step Triggering Scheme

Combining (3.1) and (3.2), the proposed two-step triggering scheme is summarized as Algorithm 3.1, and an event-triggered controller is designed



**Algorithm 3.1:** Two-step triggering scheme.

---

```

1: Initialize all parameters.
2: At  $t_l$ , solve the optimization problem in (2.6). Let  $t = t_l + 1$ .
3: if  $t < t_l + N$ , then
4:   if  $g(t, x(t), x(t_l)) > 0$  is satisfied, then
5:     let  $t_j^1 = t$ , calculate  $\kappa(t_j^1)$ , and wait until  $t_j^2$ .
6:     if  $t_j^2 = t_l + N$ , then
7:       let  $t_{l+1} = t_l + N$ ,  $l = l + 1$ , and go back to step 2.
8:     else
9:       if  $g(t_j^2, x(t_j^2), x(t_j^1)) > 0$  is satisfied, then
10:        let  $t_{l+1} = t_j^2$ ,  $l = l + 1$ , and go back to step 2.
11:       else
12:        let  $t = t_j^2 + 1$ , and go back to step 3.
13:       end
14:     end
15:   else
16:     let  $t = t + 1$ , and go back to step 3.
17:   end
18: else
19: let  $t_{l+1} = t_l + N$ ,  $l = l + 1$ , and go back to step 2.
20: end

```

---

based on Lemma 2.1:

$$u(t) = \tilde{u}(t - t_l|t_l) + K(x(t) - \tilde{x}(t - t_l|t_l)), \quad t \in \mathbb{Z}_{[t_l, t_{l+1})}, \quad (3.16)$$

where  $\tilde{u}(t - t_l|t_l)$  and  $\tilde{x}(t - t_l|t_l)$  are the solutions to the optimization problem in (2.6) at the triggering instant  $t_l$ . In tube-based MPC, the tightened input constraint in (2.6d) may lead to some conservativeness. To reduce it, instead of directly applying the optimal control sequence to the system, we consider a term  $K(x(t) - \tilde{x}(t - t_l|t_l))$  in (3.16), which can be regarded as a feedback compensation for the tightened input constraints and disturbances.

### 3.1.2.4 Parameters Analysis

According to Figure 3.1, the inter-execution time between two triggering instants is given by

$$\Delta \triangleq t_{l+1} - t_l = \sum_{s=0}^h (t_{j+s}^1 - t_{j+s-1}^2) + \kappa(t_{j+s}^1). \quad (3.17)$$

Equation (3.17) shows that  $\Delta$  is related to the checking instant sequences  $\{t_j^1 : j \in \mathbb{Z}^+\}$ ,  $\{t_j^2 : j \in \mathbb{Z}^+\}$  and the waiting horizon  $\kappa$ . In view of this, we provide the following two propositions to analyze the effects of  $\mu$  and  $\tau$  on  $\kappa$  and  $t_j^1$  so that their effects on  $\Delta$  can be quantified.

**Proposition 3.1.** *At  $t_j^1$ , we have the following results:*

- (i) *If there exist  $\mu_1, \mu_2 \in (0, \eta]$  with  $\mu_1 \leq \mu_2$  and  $\kappa_1, \kappa_2 \in \mathbb{Z}_{[1, N-1]}$  satisfying the condition in (3.14), then  $\kappa_1 \geq \kappa_2$ .*
- (ii) *If there exist  $\tau_1, \tau_2 \in (0, 1]$  with  $\tau_1 \leq \tau_2$  and  $\kappa_3, \kappa_4 \in \mathbb{Z}_{[1, N-1]}$  satisfying the condition in (3.14), then  $\kappa_3 \leq \kappa_4$ .*

**Proof.** (i) Note that  $\frac{\rho(A+BK)}{\sqrt{\theta}} \leq 1$  according to Lemma 3.1. If  $\mu_1 \leq \mu_2$ , according to (3.14), we have that

$$\left[ \frac{\rho(A+BK)}{\sqrt{\theta}} \right]^{\kappa_1} \leq \left[ \frac{\rho(A+BK)}{\sqrt{\theta}} \right]^{\kappa_2},$$

which implies that  $\kappa_1 \geq \kappa_2$ .

(ii) If  $\tau_1 \leq \tau_2$ , then we have that  $d(x(t_j^1), \tau_1 \mathcal{Z}) \geq d(x(t_j^1), \tau_2 \mathcal{Z})$ . Under the satisfaction of the tentative checking condition in (3.1), according to (3.14), we have that

$$\left[ \frac{\rho(A+BK)}{\sqrt{\theta}} \right]^{\kappa_3} \geq \left[ \frac{\rho(A+BK)}{\sqrt{\theta}} \right]^{\kappa_4},$$

which implies that  $\kappa_3 \leq \kappa_4$ . ■

**Proposition 3.2.** *Let  $t_l$  be the last triggering instant.*

- (i) *If there exist  $\mu_1, \mu_2 \in (0, \eta]$  with  $\mu_1 \leq \mu_2$  satisfying the condition in (3.1) at  $\hat{t}_1, \hat{t}_2$ , respectively, that is,*

$$\hat{t}_1 = \min\{t \in \mathbb{Z}_{>t_l} \mid \|x(t) - \tau z^*(x(t))\| > \mu_1 \sqrt{\theta^{t-t_l}} \|x(t_l) - \tau z^*(x(t_l))\|\}, \quad (3.18)$$

$$\hat{t}_2 = \min\{t \in \mathbb{Z}_{>t_l} \mid \|x(t) - \tau z^*(x(t))\| > \mu_2 \sqrt{\theta^{t-t_l}} \|x(t_l) - \tau z^*(x(t_l))\|\}, \quad (3.19)$$

then  $\hat{t}_1 \leq \hat{t}_2$ .

- (ii) If there exist  $\tau_1, \tau_2 \in (0, 1]$  with  $\tau_1 \leq \tau_2$  satisfying the condition in (3.1) at  $\hat{t}_3, \hat{t}_4$ , respectively, that is,

$$\hat{t}_3 = \min\{t \in \mathbb{Z}_{>t_l} \mid \|x(t) - \tau_1 z^*(x(t))\| > \mu\sqrt{\theta^{t-t_l}}\|x(t_l) - \tau_1 z^*(x(t_l))\|\}, \quad (3.20)$$

$$\hat{t}_4 = \min\{t \in \mathbb{Z}_{>t_l} \mid \|x(t) - \tau_2 z^*(x(t))\| > \mu\sqrt{\theta^{t-t_l}}\|x(t_l) - \tau_2 z^*(x(t_l))\|\}, \quad (3.21)$$

then  $\hat{t}_3 \leq \hat{t}_4$ .

**Proof.** (i) Assume that  $\hat{t}_1 > \hat{t}_2$ . Then, the condition in (3.18) is not satisfied at  $\hat{t}_2$ . Combining this with (3.18)-(3.19) yields that

$$\begin{aligned} \mu_2 \sqrt{\theta^{\hat{t}_2-t_l}}\|x(t_l) - \tau z^*(x(t_l))\| &< \|x(\hat{t}_2) - \tau z^*(x(\hat{t}_2))\| \\ &\leq \mu_1 \sqrt{\theta^{\hat{t}_2-t_l}}\|x(t_l) - \tau z^*(x(t_l))\|. \end{aligned} \quad (3.22)$$

Obviously,  $\mu_1 > \mu_2$ , which contradicts the pre-specified condition  $\mu_1 \leq \mu_2$ . Hence,  $\hat{t}_1 \leq \hat{t}_2$ .

(ii) Since  $\tau\mathcal{Z}$  is a homogeneous convex subset of  $\mathcal{Z}$ , we have that  $\|x(t) - \tau z^*(x(t))\| = \|x(t) - z^*(x(t))\| + (1 - \tau)\|z^*(x(t))\|$ . Then, the conditions in (3.20) and (3.21) can be written as

$$\begin{aligned} \|x(\hat{t}_3) - z^*(x(\hat{t}_3))\| - \mu\sqrt{\theta^{\hat{t}_3-t_l}}\|x(t_l) - z^*(x(t_l))\| \\ > (1 - \tau_1)(\mu\sqrt{\theta^{\hat{t}_3-t_l}}\|z^*(x(t_l))\| - \|z^*(x(\hat{t}_3))\|), \end{aligned} \quad (3.23)$$

$$\begin{aligned} \|x(\hat{t}_4) - z^*(x(\hat{t}_4))\| - \mu\sqrt{\theta^{\hat{t}_4-t_l}}\|x(t_l) - z^*(x(t_l))\| \\ > (1 - \tau_2)(\mu\sqrt{\theta^{\hat{t}_4-t_l}}\|z^*(x(t_l))\| - \|z^*(x(\hat{t}_4))\|). \end{aligned} \quad (3.24)$$

Suppose that  $\hat{t}_3 > \hat{t}_4$ . Then, equation (3.23) is not satisfied at  $\hat{t}_4$ . Combining this with (3.23)-(3.24) yields that

$$\begin{aligned} (1 - \tau_2)(\mu\sqrt{\theta^{\hat{t}_4-t_l}}\|z^*(x(t_l))\| - \|z^*(x(\hat{t}_4))\|) \\ < (1 - \tau_1)(\mu\sqrt{\theta^{\hat{t}_4-t_l}}\|z^*(x(t_l))\| - \|z^*(x(\hat{t}_4))\|). \end{aligned} \quad (3.25)$$

From (3.7) in Lemma 3.2, it follows that  $\tau_1 > \tau_2$ , which contradicts the pre-specified condition  $\tau_1 \leq \tau_2$ . Hence,  $\hat{t}_3 \leq \hat{t}_4$ . ■

Propositions 3.1 and 3.2 indicate that a bigger  $\mu$  may lead to a smaller  $\kappa$  and a larger  $t_j^1$ ; a bigger  $\tau$  may lead to a larger  $\kappa$  and a larger  $t_j^1$ . Therefore, according to (3.17), a larger  $\Delta$  may be obtained by picking a bigger  $\tau$ . Theoretical analysis of the relationship between  $\Delta$  and  $\mu$  is challenging, but some numerical evaluations are provided in the simulation.

### 3.1.3 Recursive Feasibility and Stability Analysis

In this section, recursive feasibility of the proposed event-triggered robust MPC and robust stability of the closed-loop system are analyzed.

#### 3.1.3.1 Recursive Feasibility

At  $t_l$ , the optimization problem in (2.6) is solved, and the optimal control sequence  $\tilde{\mathbf{u}}^*(t_l) \triangleq \{\tilde{u}^*(0|t_l), \tilde{u}^*(1|t_l), \dots, \tilde{u}^*(N-1|t_l)\}$  and the corresponding optimal state sequence  $\tilde{\mathbf{x}}^*(t_l) \triangleq \{\tilde{x}^*(0|t_l), \tilde{x}^*(1|t_l), \dots, \tilde{x}^*(N|t_l)\}$  are obtained. Then, at  $t_j^2 \in \mathbb{Z}_{>t_l}$ , if the condition in (3.2) is satisfied, then let  $t_{l+1} = t_j^2$  be the latest triggering instant, and the optimization problem is solved; else, the candidate predicted state and control input are constructed as

$$\tilde{x}(i|t) = \begin{cases} \tilde{x}^*(t - t_l + i|t_l), & i \in \mathbb{Z}_{[0, t_l + N - t]} \\ (A + BK)^{i - (t_l + N - t)} \tilde{x}^*(N|t_l), & i \in \mathbb{Z}_{[t_l + N + 1 - t, N]}. \end{cases} \quad (3.26)$$

$$\tilde{u}(i|t) = \begin{cases} \tilde{u}^*(t - t_l + i|t_l), & i \in \mathbb{Z}_{[0, t_l + N - 1 - t]} \\ K\tilde{x}(i|t), & i \in \mathbb{Z}_{[t_l + N - t, N - 1]}. \end{cases} \quad (3.27)$$

**Theorem 3.1.** *Under the proposed two-step triggering scheme, for all  $x(t+1) = Ax(t) + Bu(t) + \omega(t)$ ,  $t \in \mathbb{Z}_{[t_l, t_{l+1}]}$ ,  $(\tilde{\mathbf{x}}(t_{l+1}), \tilde{\mathbf{u}}(t_{l+1}))$  constructed by  $(\tilde{\mathbf{x}}^*(t_l), \tilde{\mathbf{u}}^*(t_l))$  is feasible for the optimization problem at the triggering instant  $t_{l+1}$ , where  $\tilde{\mathbf{u}}(t_{l+1}) \triangleq \{\tilde{u}(0|t_{l+1}), \dots, \tilde{u}(N-1|t_{l+1})\}$  and  $\tilde{\mathbf{x}}(t_{l+1}) \triangleq \{\tilde{x}(0|t_{l+1}), \dots, \tilde{x}(N|t_{l+1})\}$ .*

**Proof.** Similar to the proof of Theorem 2.1, and thus omitted. ■

#### 3.1.3.2 Robust Stability

**Theorem 3.2.** *For the system in (2.1) with an initial state  $x(0) \in \mathcal{X}_N$  and  $\omega(t) \in \mathcal{W}$ ,  $t \in \mathbb{Z}^+$ , the set  $\mathcal{Z}$  is robustly exponentially stable under the proposed*

two-step triggering scheme.

**Proof.** At  $t_l$ , according to Lemmas 2.5-2.7, we have that

$$c_1 \|\tilde{x}^*(t_l)\|^2 \leq J_N^*(x(t_l)) \leq c_2 \|\tilde{x}^*(t_l)\|^2, \quad \forall x(t_l) \in \mathcal{X}_f \oplus \mathcal{Z}. \quad (3.28)$$

Then, at  $t \in \mathbb{Z}_{>t_l}$ , two cases should be considered under the proposed two-step triggering scheme.

First, if the condition in (3.2) is satisfied, then the optimization problem in (2.6) is solved and a new optimal cost  $J_N^*(x(t))$  is obtained. According to (2.22) in Lemma 2.6, the following condition is satisfied

$$J_N^*(x(t)) \leq J_N^*(x(t_l)) - \sum_{i=0}^{t-t_l-1} c_1 \|\tilde{x}^*(i|t_l)\|^2. \quad (3.29)$$

Combining (3.28) and (3.29) yields that  $J_N^*(x(t)) \leq \theta^{(t-t_l)} J_N^*(x(t_l))$ . Then, there must exist a  $\varsigma_1 > 0$  satisfying  $\|\tilde{x}^*(t)\| \leq \varsigma_1 \sqrt{\theta^{t-t_l}} \|\tilde{x}^*(t_l)\|$ . Since  $x \in \tilde{x} \oplus \mathcal{Z}$ , we have that  $d(x(t), \mathcal{Z}) \leq \varsigma_2 \sqrt{\theta^{t-t_l}} d(x(t_l), \mathcal{Z})$  for  $\varsigma_2 > 0$ . Second, if the condition in (3.1) or (3.2) is not satisfied, then we have that

$$\begin{aligned} & \|x(t) - z^*(x(t))\| - \mu \sqrt{\theta^{t-t_l}} \|x(t_l) - z^*(x(t_l))\| \\ & \leq (1 - \tau) (\mu \sqrt{\theta^{t-t_l}} \|z^*(x(t_l))\| - \|z^*(x(t))\|). \end{aligned} \quad (3.30)$$

According to (3.7) in Lemma 3.2, it follows that  $d(x(t), \mathcal{Z}) \leq \mu \sqrt{\theta^{t-t_l}} d(x(t_l), \mathcal{Z})$ . Hence, combining these two cases, there must exist a  $\delta \geq \varsigma_2$  always satisfying  $d(x(t), \mathcal{Z}) \leq \delta \sqrt{\theta^t} d(x(0), \mathcal{Z})$  for all  $x(0) \in \mathcal{X}_N$  and  $\omega(t) \in \mathcal{W}$ ,  $t \in \mathbb{Z}_{>0}$ . According to Definition 2.2, the set  $\mathcal{Z}$  is robustly exponentially stable for the system in (2.1) with the proposed two-step triggering scheme.  $\blacksquare$

### 3.1.4 Simulation Examples

To show the advantages of the proposed method, we compare the commonly used one-step triggering scheme with the condition in (3.1) and the proposed two-step triggering scheme in the following examples.

**Example 3.1.** Consider the linear system provided in [60]:

$$x(t+1) = \begin{bmatrix} 1.1 & 1 \\ 0 & 1.3 \end{bmatrix} x(t) + \begin{bmatrix} 1 \\ 1 \end{bmatrix} u(t) + \omega(t). \quad (3.31)$$

Table 3.1: Comparison results of parameters  $\mu, \tau$

	$\tilde{\Delta}_1$	$\underline{\Delta}_1$	$\bar{\Delta}_1$	$\tilde{\Delta}_2$	$\underline{\Delta}_2$	$\bar{\Delta}_2$	$\tilde{\kappa}$	$L$
$\mu = 0.1$	1.34	1	5	3.76	2	5	1.12	69
$\mu = 0.6$	1.72	1	5	4.06	3	5	1.00	78
$\tau = 0.1$	1.12	1	4	3.28	3	5	1.02	21
$\tau = 0.5$	3.44	1	5	4.92	3	5	1.16	52

Table 3.2: Comparison results with [60]

	$\tilde{\Delta}$	$J$
One-step triggering scheme	1.72	3.2808
Two-step triggering scheme	4.06	3.3293
Triggering scheme in [60]	1.15	3.2695

By using the LQR technique, we obtain

$$K = [-0.4991 \quad -0.9546], \quad P = \begin{bmatrix} 2.6093 & 0.2100 \\ 0.2100 & 2.1837 \end{bmatrix}.$$

Accordingly,  $\theta = 0.6290$ .  $\sigma_{\max} = 6.6786$  is obtained by solving (3.13); then choose  $\sigma = 1$ . As with [60], we set the simulation steps  $T_{\text{sim}} = 1000$  and the initial state  $x(0) = [-30, 10]^T$ , and consider the performance index in (2.31).

To show the effects of parameters  $\mu$  and  $\tau$  on the average waiting horizon  $\tilde{\kappa}$ , the average inter-execution time  $\tilde{\Delta}$ , and the number of unnecessary events  $L$ , different values of  $\mu$  and  $\tau$  are considered, and the results are presented in Table 3.1, where  $\underline{\Delta}$  and  $\bar{\Delta}$  represent the minimum and maximum of inter-execution times, respectively; the subscripts “1” and “2” are used to emphasize the one-step triggering scheme and the two-step triggering scheme, respectively. It is shown that the average inter-execution time becomes larger with the increase of parameter  $\mu$  or  $\tau$  in the one-step triggering scheme, which coincides with theoretical analysis in Proposition 3.2. By using the two-step triggering scheme, it is seen from Table 3.1 that a smaller  $\mu$  leads to a little longer average waiting horizon  $\tilde{\kappa}$ , but the resulting average inter-execution time may become smaller; a larger  $\mu$  or  $\tau$  avoids more unnecessary event triggering and reduces resource consumption further.

In addition, to show the effect of  $\sigma$  on the estimation of  $\kappa$ , we compare

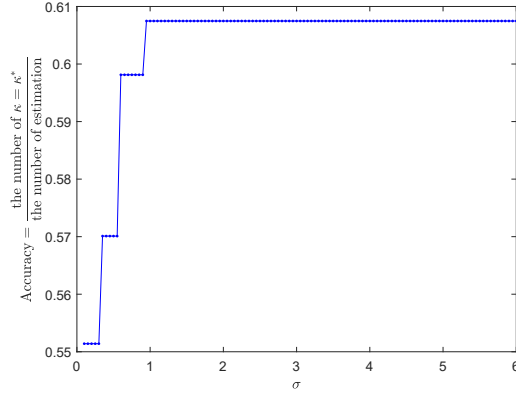


Figure 3.2: The accuracy of the estimation of  $\kappa$ .

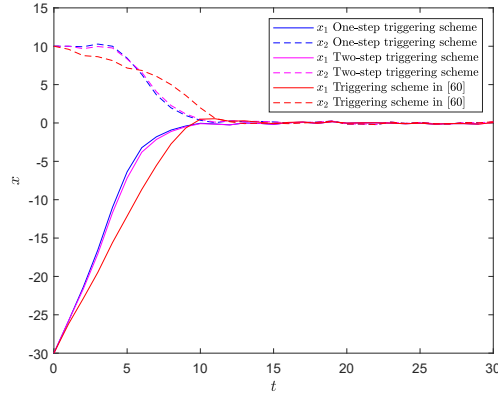


Figure 3.3: State trajectories.

$\kappa$  with  $\kappa^*$  for different values of  $\sigma$ , and calculate the accuracy of estimation, namely, the ratio of the number of  $\kappa = \kappa^*$  to the total number of estimation. From Figure 3.2, initially, the accuracy tends to increase with respect to  $\sigma$ , and when  $\sigma$  exceeds some value, the accuracy becomes stable. Moreover, from Figure 3.3 and Table 3.2, the two proposed event-triggered robust MPC controllers obtain a larger average inter-execution time with slight control performance loss when compared with [60].

**Example 3.2.** Consider the decentralized interconnected system in (2.33). Let the sampling period be  $T_s = 0.2s$ . The constraint sets are  $\mathcal{X} = [-40, 40] \times [-40, 40] \times [-40, 40]$  and  $\mathcal{U} = [-25, 25] \times [-25, 25]$ . The weighting matrices of the stage cost are chosen as  $Q = I_3$  and  $R = I_2$ .  $\sigma_{\max} = 3.9171$  is obtained by solving (3.13); then choose  $\sigma = 0.5$ . Set  $\mu = 0.2$ ,  $\tau = 0.5$ , and  $N = 8$ .

Table 3.3: Comparison results with [67] in Case A

	$\tilde{\Delta}$	$J$
One-step triggering scheme	3.32	71.1341
Two-step triggering scheme	7.11	73.2351
Triggering scheme in [67]	1.38	72.0724

Table 3.4: Comparison results with [67] in Case B

	$\tilde{\Delta}$	$J$	$J_{\text{error}}$	$T_{\text{step}}$
One-step triggering scheme	5.16	8.9491	1.0821	10.96
Two-step triggering scheme	7.25	9.4559	1.1069	11.03
Triggering scheme in [67]	1.79	9.8695	1.1978	11.70

We consider 50 random realizations of the disturbance sequence on  $\mathcal{W} = [-1, 1] \times [-1, 1] \times [-1, 1]$  and compare the proposed methods with event-triggered MPC in Section V-C of [67].

**Case A:** Set the simulation steps  $T_{\text{sim}} = 30$  and the initial state  $x(0) = [10, 10, 10]^T$ . From Table 3.3, the one-step event-triggered robust MPC outperforms [67] in terms of the inter-execution time and control performance, and the two-step triggering scheme brings the greatest reduction of computational burden with slight control performance loss. It is shown that the designed event-triggered controller in (3.16) preserves the control performance even if the optimization problem is not solved.

**Case B:** Set the simulation steps  $T_{\text{sim}} = 60$  and the initial state  $x(0) = [0, 0, 0]^T$ . The disturbance  $\omega(t)$  is set to be  $[0, 0, 0]^T$  for  $t \in [16, 30]$ . Consider the error performance index in (2.32). Let  $T_{\text{step}}$  represent the average step-size interval that the states return to around the origin after the disturbance disappears. From Table 3.4, all the indexes  $(\tilde{\Delta}, J, J_{\text{error}}, T_{\text{step}})$  with the two proposed event-triggered MPC controllers are better than that in [67], showing a superior performance.



## 3.2 An Extension to Multi-Agent Systems

In this section, we will extend the designed two-step triggering scheme in Section 3.1 to multi-agent systems.

### 3.2.1 Problem Formulation

Consider a linear discrete-time multi-agent system with  $M$  agents. Each agent  $\mathcal{A}_i$  ( $i = 1, \dots, M$ ) is described as

$$x_i(t+1) = A_i x_i(t) + B_i u_i(t) + \omega_i(t), \quad t \in \mathbb{Z}^+, \quad (3.32)$$

where  $x_i(t) \in \mathbb{R}^{n_x}$  is the system state;  $u_i(t) \in \mathbb{R}^{n_u}$  is the control input;  $\omega_i(t) \in \mathbb{R}^{n_x}$  is the persistent unknown disturbance and  $\omega_i(t) \in \mathcal{W}_i$ ; the matrix pair  $(A_i, B_i)$  is stabilizable. The topology of these  $M$  agents is constructed by an undirected graph. Let  $\mathcal{N}_i$  be the set that collects the neighbours of agent  $\mathcal{A}_i$ . Each agent  $\mathcal{A}_i$  ( $i = 1, \dots, M$ ) is subject to the following constraints:

$$x_i(t) \in \mathcal{X}_i, \quad u_i(t) \in \mathcal{U}_i, \quad (3.33)$$

where  $\mathcal{X}_i \subseteq \mathbb{R}^{n_x}$  and  $\mathcal{U}_i \subseteq \mathbb{R}^{n_u}$  are compact and convex sets containing the origin.

To handle the constraints in (3.33) for each agent, we use a distributed MPC approach. Define a terminal cost function:  $V_{f,i}(\tilde{x}_i(k|t)) = \tilde{x}_i(k|t)^T P_i \tilde{x}_i(k|t)$ ,  $k, t \in \mathbb{Z}^+$ , where  $\tilde{x}_i(k|t)$  is the predicted state at  $t+k$  and  $\tilde{x}_i(t) = \tilde{x}_i(0|t)$ ;  $P_i \succ 0$  should be designed to satisfy

$$P_i - (A_i + B_i K_i)^T P_i (A_i + B_i K_i) \succeq (Q_i + K_i^T R_i K_i) + \sum_{j \in \mathcal{N}_i} 2(Q_{ij} + Q_{ji}), \quad (3.34)$$

where  $K_i \in \mathbb{R}^{n_u \times n_x}$  is to be designed;  $Q_i \succ 0$  and  $R_i \succ 0$  are given weighting matrices;  $Q_{ij} \succ 0$  and  $Q_{ji} \succ 0$  are cooperation matrices between agent  $\mathcal{A}_i$  and agent  $\mathcal{A}_j$ . Based on the obtained feedback gain  $K_i$  by (3.34), the terminal set

$\mathcal{X}_{f,i}$  is constructed by the following conditions:

$$\mathcal{X}_{f,i} \subseteq \mathcal{X}_i \ominus \mathcal{Z}_i, \quad (3.35a)$$

$$(A_i + B_i K_i) \mathcal{X}_{f,i} \subseteq \mathcal{X}_{f,i}, \quad (3.35b)$$

$$K_i \mathcal{X}_{f,i} \subseteq \mathcal{U}_i \ominus K_i \mathcal{Z}_i. \quad (3.35c)$$

For agent  $\mathcal{A}_i$ , a distributed tube-based MPC optimization problem is formulated as:

$$\begin{aligned} & \min_{\tilde{\mathbf{x}}_i(t), \tilde{\mathbf{u}}_i(t)} J_i(t) \\ \text{s.t. } & x_i(t) \in \tilde{x}_i(t) \oplus \mathcal{Z}_i, \end{aligned} \quad (3.36a)$$

$$\tilde{x}_i(k+1|t) = A_i \tilde{x}_i(k|t) + B_i \tilde{u}_i(k|t), \quad k \in \mathbb{Z}_{[0, N-1]}, \quad (3.36b)$$

$$\tilde{x}_i(k|t) \in \mathcal{X}_i \ominus \mathcal{Z}_i, \quad k \in \mathbb{Z}_{[0, N-1]}, \quad (3.36c)$$

$$\tilde{u}_i(k|t) \in \mathcal{U}_i \ominus K_i \mathcal{Z}_i, \quad k \in \mathbb{Z}_{[0, N-1]}, \quad (3.36d)$$

$$\tilde{x}_i(N|t) \in \mathcal{X}_{f,i}, \quad (3.36e)$$

$$\|\tilde{x}_i(k|t) - \hat{x}_i(k|t)\| \leq \zeta_i(t), \quad k \in \mathbb{Z}_{[0, N-1]}, \quad (3.36f)$$

where  $\tilde{\mathbf{u}}_i(t) \triangleq \{\tilde{u}_i(0|t), \dots, \tilde{u}_i(N-1|t)\}$  and  $\tilde{\mathbf{x}}_i(t) \triangleq \{\tilde{x}_i(0|t), \dots, \tilde{x}_i(N|t)\}$ ;  $\tilde{u}_i(k|t)$  is the predicted control input at  $t+k$  and  $\tilde{u}_i(t) = \tilde{u}_i(0|t)$ ;  $N \in \mathbb{Z}_{\geq 1}$  is the prediction horizon. In this optimization problem, equation (3.36a) is the error constraint between  $x_i(t)$  and  $\tilde{x}_i(t)$  based on  $\mathcal{Z}_i$ ; equations (3.36c)-(3.36e) are the tightened state, control input, and terminal constraints for the prediction model in (3.36b), respectively. Equation (3.36f) is the compatibility constraint to ensure that the actual states of agents do not deviate too much from their latest transmitted states to neighbors, where  $\hat{x}_i(k|t)$  is the transmitted state to neighbors, i.e.,  $\hat{x}_i(k|t) = \tilde{x}_i(k|t-1)$ ;  $\zeta_i(t)$  is a given upper bound of the difference between  $\tilde{x}_i(k|t)$  and  $\hat{x}_i(k|t)$ . The cost function is defined as

$$\begin{aligned} J_i(t) = & \sum_{k=0}^{N-1} [l_i(\tilde{x}_i(k|t), \tilde{u}_i(k|t)) + \sum_{j \in \mathcal{N}_i} (\tilde{x}_i(k|t) - \hat{x}_j(k|t))^T Q_{ij} \\ & \times (\tilde{x}_i(k|t) - \hat{x}_j(k|t))] + V_{f,i}(\tilde{x}_i(N|t)), \end{aligned}$$

where  $l_i(\tilde{x}_i(k|t), \tilde{u}_i(k|t)) = \tilde{x}_i(k|t)^T Q_i \tilde{x}_i(k|t) + \tilde{u}_i(k|t)^T R_i \tilde{u}_i(k|t)$  is the stage cost;  $\sum_{j \in \mathcal{N}_i} (\tilde{x}_i(k|t) - \hat{x}_j(k|t))^T Q_{ij} (\tilde{x}_i(k|t) - \hat{x}_j(k|t))$  is a cooperation term.

For agent  $\mathcal{A}_i$ , denote the triggering instant sequence as  $\{t_i^l : l \in \mathbb{Z}^+\} \subseteq \mathbb{Z}^+$ . Given a triggering instant  $t_i^l$ , we introduce a first checking instant sequence  $\{t_i^d : d \in \mathbb{Z}^+\} \subseteq \mathbb{Z}^+$  and a triggering function  $g_i : \mathbb{Z}^+ \times \mathbb{R}^{n_x} \times \mathbb{R}^{n_x} \rightarrow \mathbb{R}$  to be designed. Accordingly, the first checking instant is updated by

$$t_i^d = \min \left\{ \min \{t \in \mathbb{Z}_{>t_i^l} \mid g_i(t, x_i(t), x_i(t_i^l)) > 0\}, t_i^l + N \right\}, \quad (3.37)$$

where  $t_i^0 = 0$  as  $d = 0$ . By continuously checking the condition in (3.37), the first checking instant  $t_i^d$  will be determined only if the checked condition is satisfied. Then, instead of triggering immediately, we generate a waiting horizon  $\kappa_i(t_i^d) \in \mathbb{Z}_{[1, N-1]}$ , that is, the most likely instant when the condition in (3.37) is violated again. Define a second checking instant sequence as  $\{\hat{t}_i^d : d \in \mathbb{Z}^+\} \subseteq \mathbb{Z}^+$  and let

$$\hat{t}_i^d = t_i^d + \kappa_i(t_i^d), \quad (3.38)$$

where  $\hat{t}_i^0 = 0$  as  $d = 0$ . Then, the triggering instant is determined by

$$t_i^{l+1} = \begin{cases} \hat{t}_i^d, & \text{if } \hat{t}_i^d = t_i^l + N, \\ \min \{\hat{t}_i^d \mid g_i(\hat{t}_i^d, x_i(\hat{t}_i^d), x_i(t_i^d)) > 0\}, & \text{otherwise,} \end{cases} \quad (3.39)$$

where  $t_i^0 = 0$  as  $l = 0$ . Clearly, it follows that  $\{t_i^l : l \in \mathbb{Z}^+\} \subseteq \{\hat{t}_i^d : d \in \mathbb{Z}^+\}$ .

Under the two-step triggering scheme in (3.37)-(3.39), an event-triggered controller is designed as

$$u_i(t) = \varphi_i(t - t_i^l, x_i(t)), \quad t \in \mathbb{Z}_{[t_i^l, t_i^{l+1})},$$

where the function  $\varphi_i : \mathbb{Z}^+ \times \mathbb{R}^{n_x} \rightarrow \mathbb{R}^{n_u}$  is to be determined.

Similar to Section 3.1, the objective of this section is to design a two-step triggering scheme with a triggering condition  $g_i$  and a waiting horizon  $\kappa_i$  for each agent  $\mathcal{A}_i$  ( $i = 1, \dots, M$ ) such that the distributed tube-based MPC optimization problem in (3.36) subject to the constraints in (3.33) is solved at the triggering instant  $t_i^l$  only.

### 3.2.2 Distributed MPC with Two-Step Triggering

In this subsection, the weighting matrix of the terminal cost function is obtained and a two-step triggering scheme for distributed MPC is designed.

### 3.2.2.1 Terminal Cost Function $V_{f,i}$

To guarantee recursive feasibility and achieve closed-loop stability and consensus of the overall multi-agent system in robust distributed MPC, the influences from neighbouring agents are incorporated into the design of the terminal cost function  $V_{f,i}$  by cooperation matrices  $Q_{ij}$  and  $Q_{ji}$  in the following lemma.

**Lemma 3.4.** *For each agent  $\mathcal{A}_i$  ( $i = 1, \dots, M$ ) with given weighting matrices  $Q_i \succ 0$  and  $R_i \succ 0$ , and cooperation matrices  $Q_{ij} \succ 0$  and  $Q_{ji} \succ 0$ , if there exist matrices  $\bar{P}_i \succ 0$  and  $Y_i$  such that*

$$\begin{bmatrix} \bar{P}_i & * & * & * & * \\ A_i \bar{P}_i + B_i Y_i & \bar{P}_i & * & * & * \\ \bar{P}_i & 0 & Q_i^{-1} & * & * \\ Y_i & 0 & 0 & R_i^{-1} & * \\ \bar{P}_i & 0 & 0 & 0 & (\sum_{j \in \mathcal{N}_i} 2(Q_{ij} + Q_{ji}))^{-1} \end{bmatrix} \succeq 0, \quad (3.40)$$

then (3.34) can be guaranteed, and the weighting matrix and corresponding controller gain are obtained by  $P_i = \bar{P}_i^{-1}$  and  $K_i = Y_i \bar{P}_i^{-1}$ .

**Proof.** For (3.40), let  $Y_i \triangleq K_i \bar{P}_i$ . Then, pre- and post-multiplying (3.40) by  $\bar{P}_i^{-1}$  and using the Schur complement equivalence yield that

$$\bar{P}_i^{-1} - (A_i + B_i K_i)^T \bar{P}_i^{-1} (A_i + B_i K_i) \succeq (Q_i + K_i^T R_i K_i) + \sum_{j \in \mathcal{N}_i} 2(Q_{ij} + Q_{ji}).$$

Let  $\bar{P}_i^{-1} = P_i$ , then (3.34) is guaranteed. ■

### 3.2.2.2 Two-Step Triggering Scheme

For agent  $\mathcal{A}_i$ , at  $t \in \mathbb{Z}_{>t_i^l}$ , the triggering function  $g_i$  is constructed as

$$g_i(t, x_i(t), x_i(t_i^l)) = d(x_i(t), \tau_i \mathcal{Z}_i) - \mu_i \sqrt{\theta_i^{t-t_i^l}} d(x_i(t_i^l), \tau_i \mathcal{Z}_i),$$

where  $\tau_i \in (0, 1]$ ,  $\mu_i \in (0, \eta_i]$ ,  $\theta_i = 1 - p_i/q_i$ , and

$$\begin{aligned} \eta_i &= \min \left\{ 1, \frac{z_{i,\min}}{z_{i,\max} \sqrt{\theta_i}} \right\}, \\ p_i &= \lambda_{\min} (Q_i + K_i^T R_i K_i + \sum_{j \in \mathcal{N}_i} 2(Q_{ij} + Q_{ji})), \\ q_i &= \lambda_{\max} (P_i), \end{aligned}$$

**Lemma 3.5.** For agent  $\mathcal{A}_i$  with a stabilizing feedback gain  $K_i \in \mathbb{R}^{n_u \times n_x}$ , there always exist a lower bound  $\sigma_i^{\min} > 0$  and an upper bound  $\sigma_i^{\max} > 0$  such that

$$\begin{aligned} \sigma_i^{\min} [\rho(A_i + B_i K_i)]^{k_i} \|\tilde{x}_i(t)\| &\leq d(x_i(t + k_i), \mathcal{Z}_i) \\ &\leq \sigma_i^{\max} [\rho(A_i + B_i K_i)]^{k_i} \|\tilde{x}_i(t)\| \end{aligned}$$

for  $k_i \in \mathbb{Z}_{(0, \bar{k}_i)}$ , where  $\bar{k}_i \in \mathbb{Z}_{>0}$ ;  $\sigma_i^{\min}$  is sufficiently small;  $\sigma_i^{\max}$  is decided by the following generalized eigenvalue problem subject to LMIs:

$$\begin{aligned} \min_{(\sigma_i^{\max})^2, \mathcal{H}_i} (\sigma_i^{\max})^2 \\ \text{s.t. } I \preceq \mathcal{H}_i \preceq (\sigma_i^{\max})^2 I \end{aligned} \quad (3.42a)$$

$$\frac{\epsilon_i}{[\rho(A_i + B_i K_i)]^2} (A_i + B_i K_i)^T \mathcal{H}_i (A_i + B_i K_i) - \mathcal{H}_i \prec 0 \quad (3.42b)$$

where  $\mathcal{H}_i \succ 0$ ;  $\epsilon_i > 0$  is a prescribed scalar which should be chosen to infinitely close to 1.

**Proof.** Similar to the proof of Lemma 3.3, and thus omitted. ■

According to Lemma 3.5, for a suitable  $\sigma_i \in (\sigma_i^{\min}, \sigma_i^{\max})$ , we have that  $d(x_i(t_i^d + k_i), \mathcal{Z}_i) = \sigma_i [\rho(A_i + B_i K_i)]^{k_i} \|\tilde{x}_i(t_i^d)\|$ . Hence, we can estimate  $\underline{\kappa}_i(t_i^d)$  in (3.11) by

$$\underline{\kappa}_i^{\text{est}}(t_i^d) = \min \left\{ k_i \in \mathbb{Z}_{>0} \mid \left( \frac{\rho(A_i + B_i K_i)}{\sqrt{\theta_i}} \right)^{k_i} \leq \frac{\mu_i d(x_i(t_i^d), \tau_i \mathcal{Z}_i)}{\sigma_i \|\tilde{x}_i(t_i^d)\|} \right\}.$$

According to (3.37) and (3.39), the waiting horizon  $\kappa_i(t_i^d)$  is decided by

$$\kappa_i(t_i^d) = \min \{ \underline{\kappa}_i^{\text{est}}(t_i^d), t_i^l + N - t_i^d \}. \quad (3.43)$$

### 3.2.3 Stability and Consensus Analysis

For agent  $\mathcal{A}_i$ , at  $t_i^l$ , let  $\tilde{\mathbf{u}}_i^*(t_i^l) \triangleq \{\tilde{u}_i^*(0|t_i^l), \tilde{u}_i^*(1|t_i^l), \dots, \tilde{u}_i^*(N-1|t_i^l)\}$  and  $\tilde{\mathbf{x}}_i^*(t_i^l) \triangleq \{\tilde{x}_i^*(0|t_i^l), \tilde{x}_i^*(1|t_i^l), \dots, \tilde{x}_i^*(N|t_i^l)\}$  be the corresponding optimal control and state sequences, respectively. At  $t \in \mathbb{Z}_{>t_i^l}$ , if there is no necessary event triggered, then the feasible control inputs could be applied to the system

and the feasible predicted states could be sent to its neighbors, which are constructed based on the optimal solution  $(\tilde{\mathbf{x}}_i^*(t_i^l), \tilde{\mathbf{u}}_i^*(t_i^l))$  as follows:

$$\tilde{x}_i(k|t) = \begin{cases} \tilde{x}_i^*(t - t_i^l + k|t_i^l), & k \in \mathbb{Z}_{[0, t_i^l + N - t]}, \\ (A_i + B_i K_i)^{k - (t_i^l + N - t)} \tilde{x}_i^*(N|t_i^l), & k \in \mathbb{Z}_{[t_i^l + N + 1 - t, N]}. \end{cases} \quad (3.44)$$

$$\tilde{u}_i(k|t) = \begin{cases} \tilde{u}_i^*(t - t_i^l + k|t_i^l), & k \in \mathbb{Z}_{[0, t_i^l + N - 1 - t]}, \\ K_i \tilde{x}_i^*(k|t), & k \in \mathbb{Z}_{[t_i^l + N - t, N - 1]}. \end{cases} \quad (3.45)$$

**Theorem 3.3.** *For agent  $\mathcal{A}_i$ , under the two-step triggering scheme in (3.37)-(3.39),  $(\tilde{\mathbf{x}}_i(t_i^{l+1}), \tilde{\mathbf{u}}_i(t_i^{l+1}))$  constructed by  $(\tilde{\mathbf{x}}_i^*(t_i^l), \tilde{\mathbf{u}}_i^*(t_i^l))$  is feasible for the optimization problem in (3.36) at the triggering instant  $t_i^{l+1}$ , where  $\tilde{\mathbf{u}}_i(t_i^{l+1}) \triangleq \{\tilde{u}_i(0|t_i^{l+1}), \dots, \tilde{u}_i(N-1|t_i^{l+1})\}$  and  $\tilde{\mathbf{x}}_i(t_i^{l+1}) \triangleq \{\tilde{x}_i(0|t_i^{l+1}), \dots, \tilde{x}_i(N|t_i^{l+1})\}$ .*

**Proof.** Similar to the proof of Theorem 2.1, and thus omitted. ■

**Definition 3.1.** *A set  $\mathcal{Z}$  is robustly exponentially stable for the overall multi-agent system in (3.32), if for each agent  $\mathcal{A}_i$  ( $i = 1, \dots, M$ ) with a robust positively invariant set  $\mathcal{Z}_i$ , a feasible region  $\tilde{\mathcal{X}}_i$ , and an initial state  $x_i(0) \in \tilde{\mathcal{X}}_i$ , there exist  $\theta \in (0, 1)$  and  $\delta > 0$  such that  $d(x_i(t), \mathcal{Z}) \leq \delta \sqrt{\theta^t} d(x_i(0), \mathcal{Z})$  for all  $t \in \mathbb{Z}^+$ , where  $\mathcal{Z} \triangleq \text{Co}(\bigcup_{i=1}^q \mathcal{Z}_i)$  represents a convex hull for the union of some convex sets  $\mathcal{Z}_i$ ,  $i = 1, \dots, q$ .*

To show consensus among all agents, in the presence of disturbances, we prove that all states finally converge to  $\mathcal{Z}$  based on Definition 3.1. Before proceeding, the following useful lemma is derived from (3.34) by induction.

**Lemma 3.6.** *For each agent  $\mathcal{A}_i$  ( $i = 1, \dots, M$ ), assume that  $J_i^*(x_i(t_i^l))$  is the optimal cost of the optimization problem in (3.36) for  $x_i(t_i^l) \in \tilde{\mathcal{X}}_i$  at any triggering instant  $t_i^l \in \mathbb{Z}^+$ . Then, the optimal cost  $J_i^*(x_i(t_i^{l+1}))$  satisfies*

$$\begin{aligned} & \sum_{i=1}^M J_i^*(x_i(t_i^{l+1})) - \sum_{i=1}^M J_i^*(x_i(t_i^l)) \\ & \leq \sum_{i=1}^M \left( \sum_{k=0}^{t_i^{l+1} - t_i^l - 1} -l_i(\tilde{x}_i^*(k|t_i^l), \tilde{u}_i^*(k|t_i^l)) \right. \\ & \quad \left. - \sum_{j \in \mathcal{N}_i} (\tilde{x}_i(k|t_i^l) - \hat{x}_j(k|t_i^l))^T Q_{ij} (\tilde{x}_i(k|t_i^l) - \hat{x}_j(k|t_i^l)) \right) \end{aligned}$$

$$+ (N - 1) \sum_{j \in \mathcal{N}_i} \lambda_{\max}(Q_{ij}) (2(\zeta_i(k|t_i^l) + \xi_{ij}(k|t_i^l))\zeta_j(k|t_i^l) + \zeta_j^2(k|t_i^l)).$$

where  $\xi_{ij}(k|t_i^l) = \|\hat{x}_i(k|t_i^l) - \hat{x}_j(k|t_i^l)\|$ .

**Proof.** The proof can be found in [27]. ■

**Theorem 3.4.** *For the overall multi-agent system in (3.32), under the proposed two-step triggering scheme in (3.37)-(3.39), the set  $\mathcal{Z}$  is robustly exponentially stable. Moreover, the consensus is achieved among all agents.*

**Proof.** For each agent  $\mathcal{A}_i$  ( $i = 1, \dots, M$ ), let  $t_i^l$  be its latest triggering instant. At  $t \in \mathbb{Z}_{>t_i^l}$ , two cases should be considered under the proposed two-step triggering scheme in (3.37)-(3.39). On one hand, if there is a necessary event triggered, then the optimization problem in (3.36) is solved. According to Lemma 3.6, the optimal cost  $J_i^*(x_i(t))$  should satisfy

$$\sum_{i=1}^M J_i^*(x_i(t)) \leq \sum_{i=1}^M v_i J_i^*(x_i(t_i^l)),$$

where  $v_i > 0$ . Then, it follows that  $\sum_{i=1}^M \|\tilde{x}_i^*(t)\| \leq \sum_{i=1}^M v_i \sqrt{\theta_i^{t-t_i^l}} \|\tilde{x}_i^*(t_i^l)\|$ . Since  $x_i \in \tilde{x}_i \oplus \mathcal{Z}_i$ , there must exist a  $\gamma_i > 0$  such that

$$\sum_{i=1}^M d(x_i(t), \mathcal{Z}) \leq \sum_{i=1}^M \gamma_i \sqrt{\theta_i^{t-t_i^l}} d(x_i(t_i^l), \mathcal{Z}),$$

where  $\mathcal{Z} \triangleq \text{Co}(\bigcup_{i=1}^q \mathcal{Z}_i)$ . Accordingly, we have that

$$d(x_i(t), \mathcal{Z}) \leq \gamma \sqrt{\theta^{t-t_i^l}} d(x_i(t_i^l), \mathcal{Z}), \quad (3.46)$$

where  $\gamma = \max_{i \in M} \{\gamma_i\}$  and  $\theta = \max_{i \in M} \{\theta_i\}$ .

On the other hand, if there is no necessary event triggered, then we have that

$$\begin{aligned} & \|x_i(t) - z(x_i(t))\| - \mu_i \sqrt{\theta_i^{t-t_i^l}} \|x_i(t_i^l) - z(x_i(t_i^l))\| \\ & \leq (1 - \tau_i) (\mu_i \sqrt{\theta_i^{t-t_i^l}} \|z(x_i(t_i^l))\| - \|z(x_i(t))\|). \end{aligned}$$

Since  $\mu_i \sqrt{\theta_i^{t-t_i^l}} \|z(x_i(t_i^l))\| - \|z(x_i(t))\| \leq 0$ , we have that

$$d(x_i(t), \mathcal{Z}) \leq \mu \sqrt{\theta^{t-t_i^l}} d(x_i(t_i^l), \mathcal{Z}), \quad (3.47)$$

where  $\mu = \max_{i \in M} \{\mu_i\}$ . Combining (3.46) and (3.47) yields that  $d(x_i(t), \mathcal{Z}) \leq \delta \sqrt{\theta^t} d(x_i(0), \mathcal{Z})$  for all  $x_i(0) \in \tilde{\mathcal{X}}_i$ , where  $\delta > 0$ . According to Definition 3.1, the set  $\mathcal{Z}$  is robustly exponentially stable for the overall multi-agent system in (3.32) with the proposed two-step triggering scheme. Furthermore, it is concluded that all states finally converge to the set  $\mathcal{Z}$ , that is, the consensus being achieved among all agents.  $\blacksquare$

### 3.2.4 Simulation Example

**Example 3.3.** Consider a linear discrete-time multi-agent system with 3 agents ( $M = 3$ ). The system matrices are as follows:

$$\begin{aligned} A_1 &= \begin{bmatrix} 1.6 & 1.1 \\ -0.7 & 1.2 \end{bmatrix}, \quad B_1 = \begin{bmatrix} 1 \\ 1 \end{bmatrix}, \\ A_2 &= \begin{bmatrix} 1.5 & 1.1 \\ 0 & 1.2 \end{bmatrix}, \quad B_2 = \begin{bmatrix} 0.8 \\ 0.9 \end{bmatrix}, \\ A_3 &= \begin{bmatrix} 1.4 & 1.1 \\ -0.3 & 1.1 \end{bmatrix}, \quad B_3 = \begin{bmatrix} 1.2 \\ 0.8 \end{bmatrix}. \end{aligned}$$

The constraint sets are  $\mathcal{X}_i = [-30, 30] \times [-30, 30]$ ,  $\mathcal{U}_i = [-20, 20]$ , and  $\mathcal{W}_i = [-0.5, 0.5] \times [-0.5, 0.5]$ . The neighbouring sets are  $\mathcal{N}_1 = \{2, 3\}$ ,  $\mathcal{N}_2 = \{1\}$ , and  $\mathcal{N}_3 = \{1\}$ . Let  $Q_i = I_2$ ,  $R_i = 1$ ,  $Q_{12} = Q_{13} = I_2$ ,  $Q_{21} = 0.5I_2$ , and  $Q_{31} = 0.8I_2$ . By solving (3.42), we can obtain  $\sigma_1^{\max} = 32.7603$ ,  $\sigma_2^{\max} = 7.2682$ , and  $\sigma_3^{\max} = 6.1472$ , respectively. Then, choose triggering parameters  $\sigma_i = 1$ ,  $\tau_i = 0.1$ ,  $\mu_i = 0.05$ , the prediction horizon  $N = 6$ , and the initial states  $x_1(0) = [-6, 15]^T$ ,  $x_2(0) = [-3, 22]^T$ , and  $x_3(0) = [-5, 25]^T$ . Consider the following indexes: the overall cost  $\tilde{J} = \frac{1}{M} \sum_{i=1}^M J_i$ , the overall average waiting horizon  $\tilde{\kappa} = \frac{1}{M} \sum_{i=1}^M \tilde{\kappa}_i$ , and the overall average inter-execution time  $\tilde{\Delta} = \frac{1}{M} \sum_{i=1}^M \tilde{\Delta}_i$ , where  $J_i = 1/T_{\text{sim}} \sum_{t=0}^{T_{\text{sim}}-1} \|x_i(t)\|_{Q_i}^2 + \|u_i(t)\|_{R_i}^2 + \sum_{j \in \mathcal{N}_i} \|x_i(t) - x_j(t)\|_{Q_{ij}}^2$ ;  $\tilde{\kappa}_i$  is the average waiting horizon and  $\tilde{\Delta}_i$  is the average inter-execution time for agent  $\mathcal{A}_i$ .



Table 3.5: Comparison results with one-step triggering

	$\tilde{\kappa}$	$\tilde{\Delta}$	$\tilde{J}$
One-step triggering scheme	-	1.27	28.0541
Two-step triggering scheme	1.15	2.97	28.8777

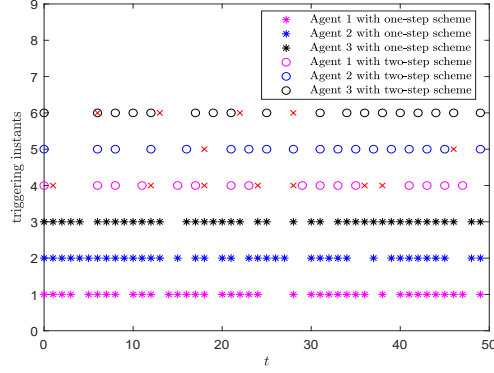


Figure 3.4: The distributions of triggering instants (The red crosses represent unnecessary events).

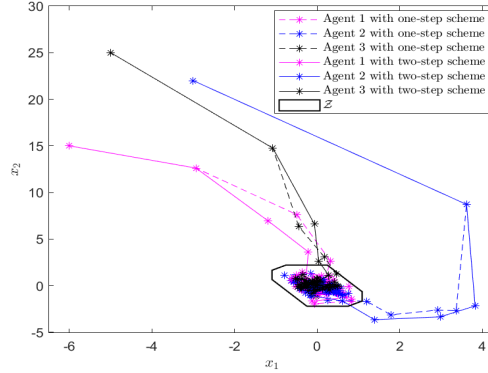


Figure 3.5: State trajectories.

To show the effectiveness of the proposed two-step triggering scheme in (3.37)-(3.39), we compare it with the commonly used one-step triggering scheme in (3.37). From Table 3.5, both the average waiting horizon and inter-execution time of the two-step triggering scheme are longer than that of the one-step triggering scheme. All the distributions of triggering instants are depicted in Figure 3.4. It is shown that the proposed two-step event verification can avoid unnecessary events triggering and reduce resource consumption further. Seen from Figure 3.5, the states of each agent finally converge to the

set  $\mathcal{Z}$ , which shows that the proposed event-triggered robust distributed MPC can achieve consensus for this multi-agent system.

### 3.3 Summary

In this chapter, a two-step triggering scheme to ensure necessary events for tube-based MPC has been investigated. Based on the distances between actual states and a robust positively invariant set, a novel event trigger including two-step checks has been designed, resulting in a larger average inter-execution time. The effects of designed parameters on the inter-execution time have been analyzed. Both recursive feasibility and robust stability have been proven. An extension of the designed two-step triggering scheme has been applied to multi-agent systems. Robust stability and consensus among all agents have been achieved. Simulation results have shown the effectiveness of the designed event-triggered robust MPC controllers.

# Chapter 4

## Event-Triggered Robust MPC with Stochastic Event Verification\*

As a matter of fact, like when to trigger the event, when to check the triggering condition should also be dependent on the system dynamics and carefully designed. This chapter investigates a novel event-triggered robust MPC approach to link event verification with action triggering and achieve adaptive and non-persistent state monitoring and event verification. Based on the ergodicity of a purposely designed Markov chain, a stochastic triggering scheme involving a prescribed triggering function, an updating law for the transition probabilities of the Markov chain, and a checking function is proposed to determine when to solve the underlying optimization problem. Both tube-based MPC and LMI-based MPC are considered, and they show complementary merits with the proposed stochastic triggering scheme. Recursive feasibility of both approaches and robust stability of the closed-loop system are guaranteed theoretically.

This chapter is organized as follows. Section 4.1 formulates a stochastic event verification problem. Section 4.2 studies the stochastic event-triggered scheme to link event verification with action triggering. Section 4.3 and

---

\*A version of this chapter has been published as: Li Deng, Zhan Shu, and Tongwen Chen, Event-triggered robust MPC with stochastic event verification. *Automatica*, vol. 146, Dec. 2022.

Section 4.4 present stochastic event-triggered tube-based MPC design and stochastic event-triggered LMI-based MPC design, respectively. Section 4.5 verifies the two proposed approaches by numerical examples. Section 4.6 concludes this chapter.

## 4.1 Problem Formulation

Consider the linear discrete-time system with bounded disturbances in (2.1). The system is subject to the following state and control constraints:

$$x(t) \in \mathcal{X}, \quad u(t) \in \mathcal{U}, \quad t \in \mathbb{Z}^+, \quad (4.1)$$

where  $\mathcal{X} \triangleq \{x \in \mathbb{R}^{n_x} \mid |x^{[\iota]}| \leq \bar{x}^{[\iota]}, \iota = 1, 2, \dots, n_x\}$  and  $\bar{x} \triangleq [\bar{x}^{[1]}, \bar{x}^{[2]}, \dots, \bar{x}^{[n_x]}]^T$  with  $\bar{x}^{[\iota]} > 0$ ;  $\mathcal{U} \triangleq \{u \in \mathbb{R}^{n_u} \mid |u^{[\ell]}| \leq \bar{u}^{[\ell]}, \ell = 1, 2, \dots, n_u\}$  and  $\bar{u} \triangleq [\bar{u}^{[1]}, \bar{u}^{[2]}, \dots, \bar{u}^{[n_u]}]^T$  with  $\bar{u}^{[\ell]} > 0$ .

In this chapter, robust MPC is used to handle the state and control constraints in (4.1). Let  $N \in \mathbb{Z}_{\geq 1}$  be the prediction horizon of MPC. An event-triggered controller is designed to solve a robust MPC optimization problem at the triggering instants only. Unlike persistent event verification and self-triggered event verification, this work is devoted to constructing a flexible event verification and linking it with action triggering.

Denote the checking instant sequence as  $\{t_l : l \in \mathbb{Z}^+\} \subseteq \mathbb{Z}^+$ . Given a checking instant  $t_l$ , we introduce a checking function  $\mu : \mathbb{Z}^+ \times \mathbb{Z}_{[0,1]} \rightarrow \mathbb{Z}_{[1,N]}$ , to determine the next checking instant, that is,

$$t_{l+1} = t_l + \mu(t_l, \xi_{t_l}), \quad (4.2)$$

where  $t_0 = 0$  as  $l = 0$ , and  $\xi_{t_l}$  is a triggering indicator to be designed showing if the system is triggered at  $t_l$ .

Denote the triggering instant sequence  $\{t_j : j \in \mathbb{Z}^+\} \subseteq \mathbb{Z}^+$ . Accordingly, the triggering instant is generated by

$$t_{j+1} = \begin{cases} \min\{t_l \mid g(t_l, x(t_l), x(t_j)) > 0\}, & \text{if } t_l < t_j + N, \\ t_l, & \text{if } t_l = t_j + N, \end{cases} \quad (4.3)$$

where  $g : \mathbb{Z}^+ \times \mathbb{R}^{n_x} \times \mathbb{R}^{n_x} \rightarrow \mathbb{R}$  is a triggering function which will be designed later based on the latest checking and triggering information, and  $t_0 = 0$  as  $j = 0$ . Here, the MPC prediction horizon  $N$  is regarded as a time-out triggering interval, i.e., if the inter-execution time exceeds it, then the system is triggered automatically at this instant. Clearly,  $\{t_j : j \in \mathbb{Z}^+\} \subseteq \{t_l : l \in \mathbb{Z}^+\}$ .

Then, an event-triggered controller  $\kappa : \mathbb{Z}^+ \times \mathbb{R}^{n_x} \rightarrow \mathbb{R}^{n_u}$  to be designed is of the form

$$u(t) = \kappa(t_j, x(t)), \quad t \in \mathbb{Z}_{[t_j, t_{j+1})}. \quad (4.4)$$

The main objective of this chapter is to design the checking function  $\mu$  together with corresponding triggering function  $g$  and triggering indicator  $\xi_{t_l}$  such that the triggering condition is checked at some specific instants and control action is updated accordingly through on-line optimization if the condition is satisfied at these instants. Based on the designed event verification and triggering scheme, two robust MPC approaches, tube-based MPC and LMI-based MPC, are to be used to synthesize the event-triggered controller in (4.4).

## 4.2 Stochastic Event-Triggered Scheme Design

As we know, traditional event-triggered MPC, on the one hand, requires persistent event monitoring and verification, and ignores the connection between event verification and action triggering, that is,

$$t_{l+1} = t_l + 1. \quad (4.5)$$

Self-triggered MPC, on the other hand, operates in an open-loop way so that triggering instants are generated without considering the uncertain disturbances between triggering instants, that is,

$$t_{j+1} = t_j + \Gamma(t_j),$$

where  $\Gamma(t_j)$  is a priori maximum of the inter-execution time related to the current triggering information. In this chapter, we plan to develop a novel

event verification and triggering scheme in (4.2) and (4.3) that links event verification and triggering. The key idea of our design is that the next event verification instant  $t_{l+1}$  should be dependent on the event triggering information at the current instant,  $\xi_{t_l}$ , as shown in (4.2). To this end, we will construct a Markov chain with adaptive transition probabilities to design the checking function  $\mu$  such that  $t_{l+1}$  and  $\xi_{t_l}$  are linked.

### 4.2.1 Triggering Function $g$

At the checking instant  $t_l \in \mathbb{Z}_{[t_j, t_{j+1})}$ , the triggering function  $g$  is constructed in term of the current state  $x(t_l)$  and the latest triggering state  $x(t_j)$  as follows:

$$g(t_l, x(t_l), x(t_j)) = (x(t_l) - x(t_j))^T \Omega_0 (x(t_l) - x(t_j)) - \theta x(t_j)^T \Omega_1 x(t_j), \quad (4.6)$$

where  $t_l \in \mathbb{Z}_{[t_j, t_{j+1})}$ , the triggering parameter  $0 < \theta < 1$  is a prescribed scalar which can be used to tune the trade-off between inter-execution time and control performance, and the matrices  $\Omega_0 \succ 0$  and  $\Omega_1 \succ 0$  reacting to uncertain disturbances are to be designed in the next section. To facilitate the remaining derivations, define the following two functions to characterize the variation of  $g$ :

$$f_0(t_l, x(t_l), x(t_j)) \triangleq \frac{(x(t_l) - x(t_j))^T \Omega_0 (x(t_l) - x(t_j))}{\theta x(t_j)^T \Omega_1 x(t_j)}, \quad (4.7)$$

$$f_1(t_l, x(t_l), x(t_j)) \triangleq \frac{1}{f_0(t_l, x(t_l), x(t_j))}. \quad (4.8)$$

$f_0, f_1$  are used to design adaptive transition probabilities of the Markov chain later. Based on the triggering function  $g$ , the triggering indicator  $\xi_{t_l}$  defined on the checking instants  $t_l$  is designed as follows:

$$\xi_{t_l} \triangleq \begin{cases} 1, & g(t_l, x(t_l), x(t_j)) > 0, \\ 0, & \text{otherwise.} \end{cases} \quad (4.9)$$

Then, combining (4.6)-(4.9) yields that

$$\xi_{t_l} = \begin{cases} 1, & \text{if } 0 < f_1(t_l, x(t_l), x(t_j)) < 1, \\ 0, & \text{if } 0 < f_0(t_l, x(t_l), x(t_j)) \leq 1. \end{cases} \quad (4.10)$$

The triggering indicator  $\xi_{t_l}$  is determined by the variation of the triggering function, namely,  $f_0(t_l, x(t_l), x(t_j))$  and  $f_1(t_l, x(t_l), x(t_j))$ , which will be used to link event verification with action triggering later.

**Remark 4.1.** *In the presence of disturbances, it is regarded that the actual states cannot come to the origin directly. Hence, the denominator of (4.7), i.e.,  $x(t_j)^T \Omega_1 x(t_j)$ , is not equal to zero for  $\Omega_1 > 0$ .*

#### 4.2.2 Triggering Indicator $\xi_{t_l}$ and Generated Random Process $\xi_t$

To construct the checking function  $\mu$  such that the next checking instant  $t_{l+1}$  and the triggering indicator  $\xi_{t_l}$  are linked, a random variable  $\xi_t$  is generated from  $\xi_{t_l}$  in (4.9) and the union of a collection of homogenous Markov chains  $\{\xi_t\}_{t \in (t_l, t_{l+1})}$  with a state space  $\mathcal{B} = \{0, 1\}$  to be designed. Define the one-step transition matrix dependent on  $t_l$  as

$$T_{t_l} \triangleq \begin{bmatrix} 1 - \alpha_{t_l} & \alpha_{t_l} \\ \beta_{t_l} & 1 - \beta_{t_l} \end{bmatrix},$$

where  $0 < \alpha_{t_l} \triangleq \mathbb{P}\{\xi_{t+1} = 1 \mid \xi_t = 0\} < 1$  and  $0 < \beta_{t_l} \triangleq \mathbb{P}\{\xi_{t+1} = 0 \mid \xi_t = 1\} < 1$  for  $t \in (t_l, t_{l+1})$ .

If the system is triggered at  $t_l$ , the triggering condition in (4.9) is less likely to be satisfied at  $t_l + 1$ , as the updated control action may regulate the system well. Consequently, the waiting time for the subsequent event verification and triggering can be longer. Otherwise, the triggering condition in (4.9) is more likely to be satisfied due to possible disturbances, and the waiting time for the subsequent event verification and triggering should be shorter. Inspired by this idea,  $\beta_{t_l}$  should be set to a large number if  $\xi_{t_l} = 1$ , and  $\alpha_{t_l}$  should be set to a large number if  $\xi_{t_l} = 0$ . To this end, an updating law of the transition probabilities is proposed below:

$$\begin{cases} \alpha_{t_l} = \alpha_{t_{l-1}}, \beta_{t_l} = \tilde{\beta}_{t_l}, & \text{if } \xi_{t_l} = 1, \\ \alpha_{t_l} = \tilde{\alpha}_{t_l}, \beta_{t_l} = \beta_{t_{l-1}}, & \text{if } \xi_{t_l} = 0, \end{cases} \quad (4.11)$$

where

$$\tilde{\beta}_{t_l} \triangleq \frac{2(\psi_{t_l} - \beta_0)(f_1(t_l, x(t_l), x(t_j)))^n}{1 + (f_1(t_l, x(t_l), x(t_j)))^n} + \beta_0, \quad (4.12)$$

$$\tilde{\alpha}_{t_l} \triangleq \frac{2(\alpha_0 - \frac{1}{N})(f_0(t_l, x(t_l), x(t_j)))^n}{1 + (f_0(t_l, x(t_l), x(t_j)))^n} + \frac{1}{N}, \quad (4.13)$$

$$\psi_{t_l} \triangleq \min(\alpha_{t_l}(N - 1), 1), \quad (4.14)$$

and  $n > 0$  is a known scalar;  $\alpha_0$  and  $\beta_0$  are given initial values and should satisfy

$$\alpha_0 \in [\frac{1}{N}, 1), \quad (4.15)$$

$$\beta_0 \in (0, 1 - \frac{1}{N}]. \quad (4.16)$$

**Lemma 4.1.** *For given initial values  $\alpha_0$  and  $\beta_0$ , the updating law for Markov transition probabilities in (4.11) can guarantee that*

$$\frac{1}{N} \leq \alpha_{t_l} \leq \alpha_0, \quad t_l \in \mathbb{Z}^+, \quad (4.17)$$

$$\beta_0 \leq \beta_{t_l} \leq \psi_{t_l}, \quad t_l \in \mathbb{Z}^+. \quad (4.18)$$

**Proof.** To facilitate the proof,  $f_0$  and  $f_1$  are considered as independent variables of (4.13) and (4.12), respectively. Obviously,  $\alpha_{t_l}$  and  $\beta_{t_l}$  are continuous with respect to  $f_0$  and  $f_1$ , respectively. Then, the first-order derivative of  $\alpha_{t_l}$  with respect to  $f_0$  is derived as

$$\alpha'_{t_l} = \frac{2n(\alpha_0 - \frac{1}{N})(f_0)^{n-1}}{(1 + (f_0)^n)^2}, \quad (4.19)$$

and the first-order derivative of  $\beta_{t_l}$  with respect to  $f_1$  is derived as

$$\beta'_{t_l} = \frac{2n(\psi_{t_l} - \beta_0)(f_1)^{n-1}}{(1 + (f_1)^n)^2}. \quad (4.20)$$

Since  $\{\xi_t\}_{t \in (t_l, t_{l+1})}$  is a homogenous Markov chain, we just discuss the following two cases according to (4.10). First, if  $\xi_{t_l} = 0$ , i.e.,  $0 < f_0 \leq 1$ , then combining (4.15) and (4.19) yields that  $\alpha'_{t_l} \geq 0$ . Specifically, if  $\alpha_0 \in (\frac{1}{N}, 1)$ , then  $\alpha'_{t_l} > 0$  and  $\alpha_{t_l}$  is monotonically increasing with respect to  $f_0$ , and thus we have  $\frac{1}{N} < \alpha_{t_l} \leq \alpha_0$ ; else,  $\alpha_0 = \frac{1}{N}$ , then  $\alpha'_{t_l} = 0$  and  $\alpha_{t_l} = \alpha_0 = \frac{1}{N}$  for any  $f_0$ .



Consequently, we have (4.17). Then, it follows that  $1 - \frac{1}{N} \leq \alpha_{t_l}(N - 1) \leq \alpha_0(N - 1)$ , which implies that

$$\psi_{t_l} \geq 1 - \frac{1}{N}, \quad t_l \in \mathbb{Z}^+. \quad (4.21)$$

Second, if  $\xi_{t_l} = 1$ , i.e.,  $0 < f_1 < 1$ , then combining (4.16) and (4.21) with (4.20) yields that  $\beta'_{t_l} \geq 0$ . Specifically, if  $\beta_0 \in (0, 1 - \frac{1}{N})$ , then  $\beta'_{t_l} > 0$  and  $\beta_{t_l}$  is monotonically increasing with respect to  $f_1$ , and thus we have  $\beta_0 < \beta_{t_l} < \psi_{t_l}$ ; else,  $\beta_0 = 1 - \frac{1}{N}$  and  $\alpha_0 = \frac{1}{N}$ , then  $\psi_{t_l} = \alpha_0(N - 1)$ , and thus  $\beta'_{t_l} = 0$  and  $\beta_{t_l} = \psi_{t_l} = \beta_0$  for any  $f_1$ . Consequently, we have (4.18).  $\blacksquare$

Based on Lemma 4.1, combining (4.15) and (4.17) yields that

$$\frac{1}{N} \leq \alpha_{t_l} < 1, \quad t_l \in \mathbb{Z}^+.$$

Note that for  $t_l \in \mathbb{Z}_{>0}$ ,  $\beta_{t_l} = \psi_{t_l}$  holds only when  $\psi_{t_l} = \beta_0$ . Then, combining (4.14), (4.16), and (4.18) yields that

$$\beta_0 \leq \beta_{t_l} < 1, \quad t_l \in \mathbb{Z}_{>0}. \quad (4.22)$$

Hence, the updating law in (4.11) can guarantee the probability requirement  $\alpha_{t_l}, \beta_{t_l} \in (0, 1)$ .

**Remark 4.2.** *The updating law in (4.11) is derived from the Hill function which has the form of  $\frac{f^n}{1+f^n}$  and is often used to reflect the ligand concentration in biochemistry, and  $n$  is called the Hill coefficient. To illustrate the benefits of employing the Hill function,  $f_0$  and  $f_1$  are considered as independent variables ranging from 0 to 1. The evolutions of  $\alpha_{t_l}$  and  $\beta_{t_l}$  for different Hill coefficients are depicted in Figure 4.1. It is shown that, firstly, the form of the Hill function can easily guarantee the requirement  $\alpha_{t_l}, \beta_{t_l} \in (0, 1)$ ; secondly, it can limit  $\alpha_{t_l}$  and  $\beta_{t_l}$  in the lower and upper bounds, which is verified in Lemma 4.1; furthermore, we can use the Hill coefficient  $n$  to adjust the sensitivity of  $f_0$  ( $f_1$ ) on  $\alpha_{t_l}$  ( $\beta_{t_l}$ ).*

According to the designed updating law for Markov transition probabilities in (4.11) and Lemma 4.1, the ergodicity property of the homogeneous Markov

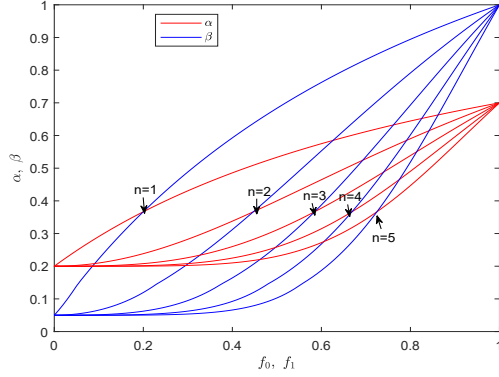


Figure 4.1: The evolutions of  $\alpha$  and  $\beta$  for different Hill coefficients.

chain  $\{\xi_t\}_{t \in (t_l, t_{l+1})}$ , which is essential for the design of  $\mu$ , is established in the following lemma.

**Lemma 4.2.** *The homogeneous Markov chain  $\{\xi_t\}_{t \in (t_l, t_{l+1})}$  with the state space  $\mathcal{B}$  is ergodic.*

**Proof.** Since the transition probabilities of the Markov chain  $\{\xi_t\}_{t \in (t_l, t_{l+1})}$  satisfy  $\alpha_{t_l}, \beta_{t_l} \in (0, 1)$ , it follows from Lemma 4.1 that every state can be reached from every other state, and thus this chain is evidently irreducible and aperiodic. Accordingly, this irreducible chain with the state space  $\mathcal{B}$  is positive recurrent. Since  $\{\xi_t\}_{t \in (t_l, t_{l+1})}$  is irreducible, aperiodic, and positive recurrent, it is ergodic. ■

### 4.2.3 Checking Function $\mu$

For the Markov chain  $\{\xi_t\}_{t \in (t_l, t_{l+1})}$ , denote the first-return step to the state “1” as  $\mu_{11}$  and the first-arrival step from the state “0” to the state “1” as  $\mu_{01}$ . At the checking instant  $t_l$ , if the triggering condition is satisfied, i.e.,  $\xi_{t_l} = 1$ , then the most likely instant when it is to be satisfied again can be estimated by the first-return step  $\mu_{11}$ ; else, the first-arrival step  $\mu_{01}$  can be used to estimate when  $\xi_{t_l}$  would visit the state “1” from the state “0”. Therefore, the checking function  $\mu(t_l, \xi_{t_l})$  of determining the next checking instant can be constructed

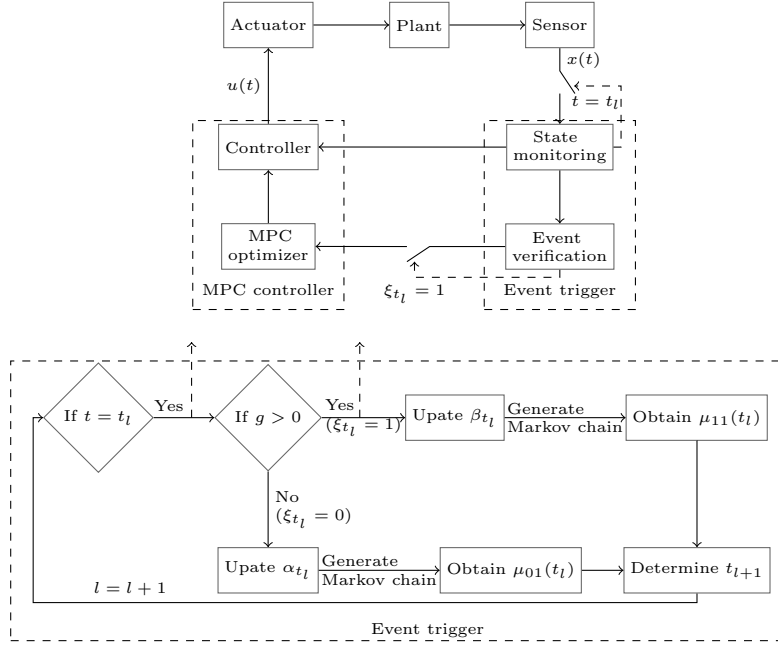


Figure 4.2: Architecture of the proposed stochastic event-triggered scheme.

accordingly as

$$\mu(t_l, \xi_{t_l}) = \begin{cases} \min \{ \lceil \mu_{11}(t_l) \rceil, t_j + N - t_l \}, & \text{if } \xi_{t_l} = 1, \\ \min \{ \lfloor \mu_{01}(t_l) \rfloor, t_j + N - t_l \}, & \text{if } \xi_{t_l} = 0, \end{cases} \quad (4.23)$$

where  $\lceil \mu_{11}(t_l) \rceil$  is the rounding half up of  $\mu_{11}(t_l)$ , that is, the nearest integer of  $\mu_{11}(t_l)$ .

The control structure with the proposed stochastic event-triggered scheme is illustrated in Figure 4.2. It is seen that the designed event trigger contains two parts. The ‘State monitoring’ part is used to decide whether the current sampling instant  $t$  is the checking instant  $t_l$ . If it is, i.e.,  $t = t_l$ , then the triggering condition will be checked; else, a feasible control input constructed by the optimal solution of the optimization problem at triggering instant  $t_j$  and stored in the ‘Controller’ will be applied. At the ‘Event verification’ part, if the triggering condition is satisfied, i.e.,  $\xi_{t_l} = 1$ , the value of  $\beta_{t_l}$  will be updated by the event trigger and then the optimization problem will be solved by the ‘MPC optimizer’; else, the value of  $\alpha_{t_l}$  will be updated and the feasible control input will be applied. Accordingly, a new Markov chain will be generated based on the updated Markov transition probabilities to obtain

$\mu_{11}(t_l)$  or  $\mu_{01}(t_l)$ , and then the next checking instant will be determined.

By virtue of the ergodicity property of a homogeneous Markov chain in [85], the following lemma can be used to determine the mean first-return step and the mean first-arrival step.

**Lemma 4.3.** [85, Section 3.4] *For the homogenous ergodic Markov chain  $\{\xi_t\}_{t \in (t_l, t_{l+1})}$  with the state space  $\mathcal{B}$ , the mean first-return step to the state “1” is*

$$\mathbb{E}\{\mu_{11}(t_l)\} = 1 + \frac{\beta_{t_l}}{\alpha_{t_l}} \quad (4.24)$$

and the mean first-arrival step from the state “0” to the state “1” is

$$\mathbb{E}\{\mu_{01}(t_l)\} = \frac{1}{\alpha_{t_l}}. \quad (4.25)$$

Combining (4.23) with (4.24)-(4.25), the designed checking function  $\mu(t_l, \xi_{t_l})$  is dependent on Markov transition probabilities  $\alpha_{t_l}$  and  $\beta_{t_l}$  which are associated with the variation of the triggering function  $g$ . It is seen that, if  $\xi_{t_l} = 1$ ,  $\beta_{t_l}$  could be larger and thus  $\mathbb{E}\{\mu_{11}(t_l)\}$  could become larger, i.e., the average waiting time for the subsequent event verification and triggering may become longer; else,  $\alpha_{t_l}$  could be larger and thus  $\mathbb{E}\{\mu_{01}(t_l)\}$  could become smaller, i.e., the average waiting time may become shorter. Hence, the proposed stochastic event-triggered scheme in (4.2) and (4.3) follows the fact that the waiting time is dependent on the system state and the feasibility of the triggering condition. It links event verification with action triggering and achieves adaptive and non-persistent state monitoring and event verification.

#### 4.2.4 Inter-Execution Time

Define  $\Delta_j \triangleq t_{j+1} - t_j$ ,  $j \in \mathbb{Z}^+$  as the inter-execution time between the triggering instant  $t_j$  and  $t_{j+1}$ . Then, we have the following theorem to quantify the bounds of the mean inter-execution time  $\mathbb{E}\{\Delta_j\}$ .

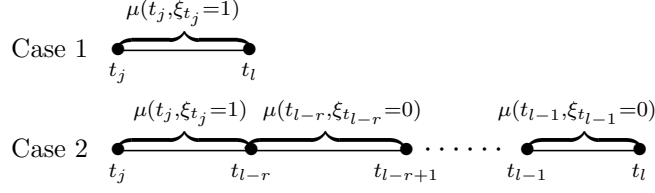


Figure 4.3: Illustration of inter-execution time.

**Theorem 4.1.** *For given initial values  $\alpha_0$ ,  $\beta_0$ , and the updating law for Markov transition probabilities in (4.11), we have that*

$$1 + \frac{\beta_0}{\alpha_0} \leq \mathbb{E}\{\mu_{11}(t_l)\} \leq N, \quad t_l \in \mathbb{Z}^+, \quad (4.26)$$

$$\frac{1}{\alpha_0} \leq \mathbb{E}\{\mu_{01}(t_l)\} \leq N, \quad t_l \in \mathbb{Z}^+. \quad (4.27)$$

Furthermore, the mean inter-execution time  $\mathbb{E}\{\Delta_j\}$  satisfies

$$1 + \frac{\beta_0}{\alpha_0} \leq \mathbb{E}\{\Delta_j\} \leq N, \quad j \in \mathbb{Z}^+. \quad (4.28)$$

**Proof.** From (4.24), it is observed that a larger  $\alpha_{t_l}$  and a smaller  $\beta_{t_l}$  lead to a smaller  $\mathbb{E}\{\mu_{11}(t_l)\}$ , and a smaller  $\alpha_{t_l}$  and a larger  $\beta_{t_l}$  lead to a larger  $\mathbb{E}\{\mu_{11}(t_l)\}$ . Thus, based on (4.17) and (4.18), we have that

$$1 + \frac{\beta_0}{\alpha_0} \leq \mathbb{E}\{\mu_{11}(t_l)\} \leq 1 + \frac{\psi_{t_l}}{\alpha_{t_l}}, \quad t_l \in \mathbb{Z}^+.$$

According to (4.14),  $\psi_{t_l} \leq \alpha_{t_l}(N-1)$  holds, implying that  $1 + \frac{\psi_{t_l}}{\alpha_{t_l}} \leq N$ . Hence, we have (4.26). From (4.25), it is observed that  $\mathbb{E}\{\mu_{01}(t_l)\}$  is non-increasing with respect to  $\alpha_{t_l}$ . Thus, based on (4.17), we have (4.27).

At the checking instant  $t_l \in \mathbb{Z}_{(t_j, t_{j+1}]}$ , two cases should be considered as in Figure 4.3, where  $r \in \mathbb{Z}_{\geq 1}$ . For case 1,  $\xi_{t_l} = 1$ , i.e.,  $t_{j+1} = t_l$ , then

$$\Delta_j = t_l - t_j = \mu(t_j, \xi_{t_j} = 1).$$

For case 2,  $\xi_{t_{l-r}} = 0$ ,  $\xi_{t_{l-r+1}} = 0$ ,  $\dots$ ,  $\xi_{t_{l-1}} = 0$ , and  $\xi_{t_l} = 1$ , i.e.,  $t_{j+1} = t_l$ , then

$$\Delta_j = t_l - t_j = \mu(t_j, \xi_{t_j} = 1) + \mu(t_{l-r}, \xi_{t_{l-r}} = 0) + \dots + \mu(t_{l-1}, \xi_{t_{l-1}} = 0).$$

Based on the above two cases, we have that

$$\Delta_j = \begin{cases} \mu(t_j, \xi_{t_j} = 1) + \sum_{s=1}^r \mu(t_{l-s}, \xi_{t_{l-s}} = 0), & \text{if } r \in \mathbb{Z}_{\geq 1}, \\ \mu(t_j, \xi_{t_j} = 1), & \text{otherwise.} \end{cases} \quad (4.29)$$

From (4.23), we have that  $\mu(t_j, \xi_{t_j} = 1) = \mu_{11}(t_j)$  since  $\mu_{11}(t_j) \leq N$ . Then, combining it with (4.29) yields that

$$\mathbb{E}\{\Delta_j\} \geq \mathbb{E}\{\mu_{11}(t_j)\}. \quad (4.30)$$

It is seen from (4.3) that  $N$  is a time-out triggering interval, thus  $\mathbb{E}\{\Delta_j\} \leq N$ . Combining it with (4.30) yields that (4.28).  $\blacksquare$

As can be seen in Theorem 4.1, the prediction horizon  $N$  of MPC has a critical impact on the implementation of the designed stochastic event-triggered scheme. Such an upper bound of inter-execution time is essential in event-triggered robust MPC to preserve the optimality and closed-loop stability. The problem of selecting the prediction horizon is beyond the scope of this chapter due to its complexity and is left for our future study.

The designed law in (4.11) not only provides a flexible way to update  $\alpha_{t_l}$  and  $\beta_{t_l}$  with the evolution of the system states and builds a connection between event verification and action triggering, but also plays an important role in the design of the terminal cost function and the guarantee of recursive feasibility and closed-loop stability in event-triggered robust MPC as will be shown in the next two sections.

### 4.3 Stochastic Event-Triggered Tube-Based MPC Design

Based on the stochastic event-triggered scheme proposed in Section 4.2, tube-based MPC is to be developed in this section.

### 4.3.1 Tube-Based MPC Design

Given a stabilizing feedback gain  $K_T \in \mathbb{R}^{n_u \times n_x}$ , the local controller is constructed by

$$\kappa_T(\tilde{x}(i|t)) = K_T \tilde{x}(i|t), \quad i, t \in \mathbb{Z}^+, \quad (4.31)$$

and the corresponding prediction model is given by

$$\tilde{x}(i+1|t) = A\tilde{x}(i|t) + B\kappa_T(\tilde{x}(i|t)), \quad i, t \in \mathbb{Z}^+, \quad (4.32)$$

where  $\tilde{x}(i|t)$  is the predicted state at  $t+i$  and  $\tilde{x}(t) = \tilde{x}(0|t)$ ; the subscript  $T$  is used to emphasize the variables related to tube-based MPC. Then, the terminal set  $\mathcal{X}_T$  should be designed to satisfy the conditions in (2.4a)-(2.4c). Define the terminal cost function as

$$V_T(\tilde{x}(i|t)) = \tilde{x}(i|t)^\top \Omega_{\xi(i|t)} \tilde{x}(i|t), \quad i, t \in \mathbb{Z}^+, \quad (4.33)$$

where

$$\Omega_{\xi(i|t)} = \begin{cases} \Omega_1, & \text{if } \xi(i|t) = 1, \\ \Omega_0, & \text{if } \xi(i|t) = 0. \end{cases}$$

To guarantee the closed-loop stability,  $\Omega_0$  and  $\Omega_1$  need to be designed such that the following condition holds:

$$\mathbb{E}\{V_T(\tilde{x}(i+1|t)) - V_T(\tilde{x}(i|t))\} \leq -\mathbb{E}\{l(\tilde{x}(i|t), \kappa_T(\tilde{x}(i|t)))\}, \quad (4.34)$$

where  $\tilde{x}(i|t) \in \mathcal{X}_T$ ;  $l(\tilde{x}(i|t), \kappa_T(\tilde{x}(i|t))) \triangleq \tilde{x}(i|t)^\top Q \tilde{x}(i|t) + \kappa_T(\tilde{x}(i|t))^\top R \kappa_T(\tilde{x}(i|t))$ ;  $Q \succ 0$  and  $R \succ 0$  are given weighting matrices. The following theorem gives the desirable  $\Omega_0$  and  $\Omega_1$ .

**Theorem 4.2.** *Under the stochastic event-triggered scheme in (4.2) and (4.3), if there exist two matrices  $\Omega_0 \succ 0$  and  $\Omega_1 \succ 0$  such that*

$$(A + BK_T)^\top (\beta_0 \Omega_0 + (1 - \beta_0) \Omega_1) (A + BK_T) - \Omega_1 \preceq -(Q + K_T^\top R K_T), \quad (4.35)$$

$$(A + BK_T)^\top ((1 - \alpha_0) \Omega_0 + \alpha_0 \Omega_1) (A + BK_T) - \Omega_0 \preceq -(Q + K_T^\top R K_T), \quad (4.36)$$

$$\Omega_0 \preceq \Omega_1, \quad (4.37)$$

then the condition in (4.34) holds.

**Proof.** Substituting (4.31) and (4.32) into (4.34) yields that

$$(A + BK_T)^T \mathbb{E}\{\Omega_{\xi_{(i+1|t)}}\} (A + BK_T) - \mathbb{E}\{\Omega_{\xi_{(i|t)}}\} \preceq -(Q + K_T^T R K_T). \quad (4.38)$$

At  $t \in \mathbb{Z}^+$ , two cases should be considered under the stochastic event-triggered scheme in (4.2) and (4.3). First, if  $\xi_{(i|t)} = 1$ , then  $\mathbb{E}\{\Omega_{\xi_{(i|t)}}\} = \Omega_1$ ,  $\mathbb{E}\{\Omega_{\xi_{(i+1|t)}}\} = \beta_{t_i} \Omega_0 + (1 - \beta_{t_i}) \Omega_1$ ; else,  $\mathbb{E}\{\Omega_{\xi_{(i|t)}}\} = \Omega_0$ ,  $\mathbb{E}\{\Omega_{\xi_{(i+1|t)}}\} = (1 - \alpha_{t_i}) \Omega_0 + \alpha_{t_i} \Omega_1$ . Accordingly, equation (4.38) is guaranteed by the following conditions:

$$(A + BK_T)^T (\beta_{t_i} \Omega_0 + (1 - \beta_{t_i}) \Omega_1) (A + BK_T) - \Omega_1 \preceq -(Q + K_T^T R K_T), \quad (4.39)$$

$$(A + BK_T)^T ((1 - \alpha_{t_i}) \Omega_0 + \alpha_{t_i} \Omega_1) (A + BK_T) - \Omega_0 \preceq -(Q + K_T^T R K_T). \quad (4.40)$$

Note that (4.39) and (4.40) are dependent on the transition probabilities  $\alpha_{t_i}$  and  $\beta_{t_i}$  associated with  $t_i$ . Since (4.22) holds, if (4.35) and (4.37) are satisfied, we have that

$$\begin{aligned} & (A + BK_T)^T (\beta_{t_i} \Omega_0 + (1 - \beta_{t_i}) \Omega_1) (A + BK_T) - \Omega_1 \\ &= (A + BK_T)^T (\beta_0 \Omega_0 + (1 - \beta_0) \Omega_1) (A + BK_T) - \Omega_1 + (A + BK_T)^T \\ & \quad \times (\beta_{t_i} - \beta_0) (\Omega_0 - \Omega_1) (A + BK_T) \\ & \preceq -(Q + K_T^T R K_T). \end{aligned}$$

Hence, equation (4.39) is guaranteed. Likewise, if (4.36) and (4.37) are satisfied, equation (4.40) is guaranteed for  $0 < \alpha_{t_i} \leq \alpha_0$ . Therefore, equation (4.34) can be guaranteed by (4.35)-(4.37).  $\blacksquare$

$\Omega_0$  and  $\Omega_1$  obtained by solving the conditions in Theorem 4.2 off-line are closely related to the local controller gain  $K_T$  and the corresponding robust positively invariant set  $\mathcal{Z}$  containing all uncertainties. Hence, an implicit connection is built between the checking function  $\mu$  and uncertain disturbances through the local controller gain  $K_T$ , the triggering function  $g$ , the triggering indicator  $\xi_{t_i}$ , and the updating law for Markov transition probabilities in (4.11), resulting in a ‘‘closed-loop’’ operation from disturbances to event verification.



Based on the solved  $\Omega_0$  and  $\Omega_1$  in Theorem 4.2, at each triggering instant  $t_j$ , an event-triggered tube-based MPC optimization problem is formulated by:

$$\begin{aligned} & \min_{\tilde{\mathbf{x}}(t_j), \tilde{\mathbf{u}}(t_j)} J_N(t_j), \\ \text{s.t. } & (2.6a), (2.6b), (2.6c), (2.6d), \text{ and } (2.6e) \end{aligned} \quad (4.41)$$

The performance cost associated with predicted states and control inputs is designed as

$$J_N(t_j) \triangleq \mathbb{E} \left\{ \sum_{i=0}^{N-1} l(\tilde{x}(i|t_j), \tilde{u}(i|t_j)) + V_T(\tilde{x}(N|t_j)) \right\}. \quad (4.42)$$

According to Lemma 2.1, to steer the states into the robust positively invariant set  $\mathcal{Z}$ , an event-triggered tube-based MPC should be designed by

$$u_T(t) = \tilde{u}(t - t_j|t_j) + K_T(x(t) - \tilde{x}(t - t_j|t_j)), \quad (4.43)$$

where  $t \in \mathbb{Z}_{[t_j, t_{j+1})}$ ;  $\tilde{x}(t - t_j|t_j)$  and  $\tilde{u}(t - t_j|t_j)$  are the solutions of the optimization problem in (4.41) at the triggering instant  $t_j$ . Due to the implicit link between uncertain disturbances and event verification, the controller in (4.43) has the potential to keep the actual states close to the predicted states and preserve the control performance even if the optimization problem is not solved.

### 4.3.2 Recursive Feasibility and Stability Analysis

**Definition 4.1.** *The system in (2.1) is said to be exponentially mean-square stable with a feasible region  $\mathcal{X}_N$  and an initial state  $x(0) \in \mathcal{X}_N$  if there exist  $\theta \in (0, 1)$  and  $\delta > 0$  such that  $\mathbb{E}\{\|x(t)\|^2\} < \delta\theta^t\|x(0)\|^2$  for  $t \in \mathbb{Z}^+$ .*

**Theorem 4.3.** *Suppose that  $(\tilde{\mathbf{x}}^*(t_j), \tilde{\mathbf{u}}^*(t_j))$  is the optimal solution of the optimization problem in (4.41) at any triggering instant  $t_j$ . For the system in (2.1) with the event-triggered controller in (4.43) and the stochastic event-triggered scheme in (4.2) and (4.3),  $(\tilde{\mathbf{x}}(t_{j+1}), \tilde{\mathbf{u}}(t_{j+1}))$  with  $\tilde{\mathbf{u}}(t_{j+1}) \triangleq \{\tilde{u}(0|t_{j+1}), \dots,$*

$\tilde{u}(N-1|t_{j+1})\}$  and  $\tilde{\mathbf{x}}(t_{j+1}) \triangleq \{\tilde{x}(0|t_{j+1}), \dots, \tilde{x}(N|t_{j+1})\}$  defined by

$$\tilde{x}(i|t_{j+1}) = \begin{cases} \tilde{x}^*(\Delta_j + i|t_j), & i \in \mathbb{N}_{[0, N-\Delta_j]}, \\ (A + BK_T)^{i+\Delta_j-N} \tilde{x}^*(N|t_j), & i \in \mathbb{N}_{[N+1-\Delta_j, N]}, \end{cases} \quad (4.44)$$

$$\tilde{u}(i|t_{j+1}) = \begin{cases} \tilde{u}^*(\Delta_j + i|t_j), & i \in \mathbb{N}_{[0, N-1-\Delta_j]}, \\ \kappa_T(\tilde{x}(i|t_{j+1})), & i \in \mathbb{N}_{[N-\Delta_j, N-1]}, \end{cases} \quad (4.45)$$

is feasible for the optimization problem at the triggering instant  $t_{j+1}$ . Moreover, the closed-loop system is exponentially mean-square stable.

**Proof.** (Recursive feasibility) Similar to the proof of Theorem 2.1, and thus omitted.

(Stability) According to the stochastic event-triggered scheme in (4.2) and (4.3), two cases should be considered to prove closed-loop stability at the checking instant  $t_l \in \mathbb{Z}_{>t_j}$ . If the triggering condition is not satisfied, i.e.,  $\xi_{t_l} = 0$ , a feasible cost  $J_N(x(t_l))$  is constructed as

$$\begin{aligned} J_N(x(t_l)) = & \mathbb{E}\left\{ J_N^*(x(t_j)) - V_T(\tilde{x}^*(N|t_j)) + V_T(\tilde{x}(N|t_l)) \right. \\ & \left. - \sum_{i=0}^{t_l-t_j-1} l(\tilde{x}^*(i|t_j), \tilde{u}^*(i|t_j)) + \sum_{i=t_j+N-t_l}^{N-1} l(\tilde{x}(i|t_l), \kappa_T(\tilde{x}(i|t_l))) \right\}. \end{aligned} \quad (4.46)$$

According to (4.34), using the candidate states in (4.44) and control inputs in (4.45), we have that

$$\mathbb{E}\{V_T(\tilde{x}(N|t_l))\} \leq \mathbb{E}\left\{V_T(\tilde{x}^*(N|t_j)) - \sum_{i=t_j+N-t_l}^{N-1} l(\tilde{x}(i|t_l), \kappa_T(\tilde{x}(i|t_l)))\right\}.$$

Substituting it into (4.46) yields that

$$J_N(x(t_l)) - J_N^*(x(t_j)) \leq -\mathbb{E}\left\{ \sum_{i=0}^{t_l-t_j-1} l(\tilde{x}^*(i|t_j), \tilde{u}^*(i|t_j)) \right\}. \quad (4.47)$$

Then, there exists a scalar  $0 < \theta < 1$  satisfying

$$\begin{aligned} J_N(x(t_j+1) \mid \xi_{t_j} = 1) & \leq \theta J_N^*(x(t_j)), \\ & \vdots \\ J_N(x(t_l) \mid \xi_{t_l-1} = 0) & \leq \theta J_N(x(t_l-1)). \end{aligned} \quad (4.48)$$

By induction based on (4.48), we have that

$$J_N(x(t_l)) \leq \theta^{(t_l-t_j)} J_N^*(x(t_j)).$$

Then, we have that  $\mathbb{E}\{\|\tilde{x}(t_l)\|^2\} \leq c\theta^{(t_l-t_j)}\|\tilde{x}^*(t_j)\|^2$ , where  $c > 0$ . Since  $x \in \tilde{x} \oplus \mathcal{Z}$ , it follows that

$$\mathbb{E}\{\|x(t)\|^2\} \leq \delta\theta^t\|x(0)\|^2, \quad t \in \mathbb{Z}_{>0} \quad (4.49)$$

for initial state  $x(0)$ , where  $\delta > 0$ .

If the triggering condition is satisfied, i.e.,  $\xi_{t_l} = 1$ , then a new solution  $(\tilde{\mathbf{x}}^*(t_l), \tilde{\mathbf{u}}^*(t_l))$  and an optimal cost  $J_N^*(x(t_l))$  can be obtained, and  $J_N^*(x(t_l))$  satisfies

$$J_N^*(x(t_l)) - J_N^*(x(t_j)) \leq J_N(x(t_l)) - J_N^*(x(t_j)). \quad (4.50)$$

Combining (4.50) with (4.47), we also have (4.49). According to Definition 4.1, the exponential mean-square stability of the closed-loop system is guaranteed. ■

## 4.4 Stochastic Event-Triggered LMI-Based MPC Design

Based on the stochastic event-triggered scheme proposed in Section 4.2, LMI-based MPC is to be developed in this section.

### 4.4.1 LMI-Based MPC Design

In this subsection, we will use the concept of quadratic boundedness to address the recursive feasibility and stability issues arisen from stochastic event verification and triggering.

**Definition 4.2.** [86] *The system in (2.1) with Lyapunov matrix  $P \succ 0$  is quadratically bounded if  $x(t)^T P x(t) \geq 1$  implies that  $x(t+1)^T P x(t+1) \leq x(t)^T P x(t)$ ,  $t \in \mathbb{Z}^+$ .*

The following two lemmas will be used later to show a robust positively invariant set.

**Lemma 4.4.** [86] *The system in (2.1) with Lyapunov matrix  $P \succ 0$  is quadratically bounded if  $x(t)^\top P x(t) \geq \frac{1}{\omega} \omega(t)^\top \omega(t)$  implies that  $x(t+1)^\top P x(t+1) \leq x(t)^\top P x(t)$ ,  $t \in \mathbb{Z}^+$ .*

**Lemma 4.5.** [86] *The following facts are equivalent: (i) The system in (2.1) is quadratically bounded with Lyapunov matrix  $P$ . (ii) The set  $\Phi \triangleq \{x | x^\top P x \leq 1\}$  is a robust positively invariant set.*

With LMI-based MPC, the solution of the optimization problem is no longer an optimal control sequence as tube-based MPC, but a feedback gain. Hence, the local controller and corresponding terminal set are removed since all the control actions in the whole infinite horizon are determined based on this solved feedback gain. According to the triggering indicator, the structure of the robust event-triggered MPC controller is given by

$$u_L(i|t) = \begin{cases} K_1(t)x(i|t), & \text{if } \xi_{(i|t)} = 1, \\ K_0(t)x(i|t), & \text{if } \xi_{(i|t)} = 0 \end{cases} \quad (4.51)$$

for  $i, t \in \mathbb{Z}^+$ , where  $K_0(t)$  and  $K_1(t)$  will be designed later; the subscript  $L$  is used to emphasize the variables related to LMI-based MPC. Different from (4.33), we consider a cost function related to the actual state  $x(i|t)$  as

$$V_L(x(i|t)) = x(i|t)^\top \Omega_{\xi_{(i|t)}} x(i|t), \quad i, t \in \mathbb{Z}^+$$

and an infinite performance cost

$$J_\infty(t) \triangleq \mathbb{E} \left\{ \sum_{i=0}^{\infty} (l(x(i|t), u(i|t)) - \varsigma \omega(i|t)^\top \omega(i|t)) \right\},$$

where  $\varsigma > 0$  is a prescribed weight associated with disturbances and sufficiently small. This type of performance cost was first proposed for the systems with bounded disturbances in [87], which differs from (4.42) in tube-based MPC. Then, the following theorem gives a suboptimal design of  $K_0(t)$  and  $K_1(t)$  to minimize  $J_\infty(t)$  and a related performance bound.

**Theorem 4.4.** *Under the stochastic event-triggered scheme in (4.2) and (4.3), if there exist scalars  $\gamma, \vartheta$ , matrices  $\bar{\Omega}_0 \succ 0, \bar{\Omega}_1 \succ 0, U \succ 0, X \succ 0, Y_0, Y_1$  such that*

$$s.t. \begin{bmatrix} \min_{\gamma, \vartheta, \bar{\Omega}_0, \bar{\Omega}_1, Y_0, Y_1, U, X} \gamma \\ \bar{\Omega}_1 & * & * & * & * & * & * \\ 0 & \vartheta I & * & * & * & * & * \\ A\bar{\Omega}_1 + BY_1 & \gamma I & \beta_0^{-1}\bar{\Omega}_0 & * & * & * & * \\ A\bar{\Omega}_1 + BY_1 & \gamma I & 0 & (1 - \beta_0)^{-1}\bar{\Omega}_1 & * & * & * \\ \bar{\Omega}_1 & 0 & 0 & 0 & \gamma Q^{-1} & * & * \\ Y_1 & 0 & 0 & 0 & 0 & \gamma R^{-1} & * \end{bmatrix} \succeq 0, \quad (4.52a)$$

$$\begin{bmatrix} \bar{\Omega}_0 & * & * & * & * & * & * \\ 0 & \vartheta I & * & * & * & * & * \\ A\bar{\Omega}_0 + BY_0 & \gamma I & (1 - \alpha_0)^{-1}\bar{\Omega}_0 & * & * & * & * \\ A\bar{\Omega}_0 + BY_0 & \gamma I & 0 & \alpha_0^{-1}\bar{\Omega}_1 & * & * & * \\ \bar{\Omega}_0 & 0 & 0 & 0 & \gamma Q^{-1} & * & * \\ Y_0 & 0 & 0 & 0 & 0 & \gamma R^{-1} & * \end{bmatrix} \succeq 0, \quad (4.52b)$$

$$\bar{\Omega}_0 \succeq \bar{\Omega}_1, \quad (4.52c)$$

$$\begin{bmatrix} 1 & * \\ x(t_j) & \bar{\Omega}_1 \end{bmatrix} \succeq 0, \quad (4.52d)$$

$$\begin{bmatrix} (1 - \varepsilon)\bar{\Omega}_1 & * & * \\ 0 & \frac{\varepsilon}{\bar{\omega}}I & * \\ A\bar{\Omega}_1 + BY_1 & I & \bar{\Omega}_1 \end{bmatrix} \succeq 0, \quad (4.52e)$$

$$\begin{bmatrix} U & * \\ Y_s^T & \bar{\Omega}_s \end{bmatrix} \succeq 0, \quad U^{[\ell\ell]} \preceq (\bar{u}^{[\ell]})^2, \quad (\ell = 1, 2, \dots, n_u; s = 0, 1), \quad (4.52f)$$

$$\begin{bmatrix} \frac{1}{1+\bar{\omega}}X & * & * \\ (A\bar{\Omega}_s + BY_s)^T & \bar{\Omega}_s & * \\ I & 0 & I \end{bmatrix} \succeq 0, \quad X^{[\iota\iota]} \preceq (\bar{x}^{[\iota]})^2, \quad (\iota = 1, 2, \dots, n_x; s = 0, 1), \quad (4.52g)$$

then  $J_\infty(t) \leq \gamma(t)$ , and desirable weighting matrices in the triggering function in (4.6) and corresponding controller gains are given by

$$\Omega_0 = \gamma\bar{\Omega}_0^{-1}, \quad \Omega_1 = \gamma\bar{\Omega}_1^{-1}, \quad K_0 = Y_0\bar{\Omega}_0^{-1}, \quad K_1 = Y_1\bar{\Omega}_1^{-1}.$$

**Proof.** To guarantee closed-loop stability of the proposed LMI-based MPC, two cases should be considered under the stochastic event-triggered scheme in

(4.2) and (4.3) at  $t \in \mathbb{Z}^+$ :  $\xi_t = 1$  and  $\xi_t = 0$ . For  $\xi_t = 1$ , by using the Schur complement equivalence with  $Y_1 \triangleq K_1 \bar{\Omega}_1$ , equation (4.52a) can be written as

$$\begin{aligned} & \begin{bmatrix} \bar{\Omega}_1 - \gamma^{-1} \bar{\Omega}_1^T Q \bar{\Omega}_1 - \gamma^{-1} (K_1 \bar{\Omega}_1)^T R K_1 \bar{\Omega}_1 & 0 \\ 0 & \vartheta I \end{bmatrix} \\ & - [(A \bar{\Omega}_1 + B K_1 \bar{\Omega}_1) \gamma I]^T (\beta_0 \bar{\Omega}_0^{-1} + (1 - \beta_0) \bar{\Omega}_1^{-1}) \\ & \times [(A \bar{\Omega}_1 + B K_1 \bar{\Omega}_1) \gamma I] \succeq 0. \end{aligned} \quad (4.53)$$

Substituting  $\bar{\Omega}_0 \triangleq \gamma \Omega_0^{-1}$ ,  $\bar{\Omega}_1 \triangleq \gamma \Omega_1^{-1}$ , and  $\vartheta \triangleq \gamma \varsigma$  into (4.53), and pre- and post-multiplying it by  $\text{diag}\{\gamma^{-\frac{1}{2}} \Omega_1, \gamma^{-\frac{1}{2}} I\}$  yield that

$$\begin{aligned} & \begin{bmatrix} \Omega_1 - (Q + K_1^T R K_1) & 0 \\ 0 & \varsigma I \end{bmatrix} - [(A + B K_1) I]^T \\ & \times (\beta_0 \Omega_0 + (1 - \beta_0) \Omega_1) [(A + B K_1) I] \succeq 0. \end{aligned} \quad (4.54)$$

For  $\xi_t = 0$ , by using the Schur complement equivalence with  $Y_0 \triangleq K_0 \bar{\Omega}_0$ , equation (4.52b) can be written as

$$\begin{aligned} & \begin{bmatrix} \bar{\Omega}_0 - \gamma^{-1} \bar{\Omega}_0^T Q \bar{\Omega}_0 - \gamma^{-1} (K_0 \bar{\Omega}_0)^T R K_0 \bar{\Omega}_0 & 0 \\ 0 & \vartheta I \end{bmatrix} \\ & - [(A \bar{\Omega}_0 + B K_0 \bar{\Omega}_0) \gamma I]^T ((1 - \alpha_0) \bar{\Omega}_0^{-1} + \alpha_0 \bar{\Omega}_1^{-1}) \\ & \times [(A \bar{\Omega}_0 + B K_0 \bar{\Omega}_0) \gamma I] \succeq 0. \end{aligned} \quad (4.55)$$

Substituting  $\bar{\Omega}_0 = \gamma \Omega_0^{-1}$ ,  $\bar{\Omega}_1 = \gamma \Omega_1^{-1}$ , and  $\vartheta = \gamma \varsigma$  into (4.55), and pre- and post-multiplying it by  $\text{diag}\{\gamma^{-\frac{1}{2}} \Omega_0, \gamma^{-\frac{1}{2}} I\}$  yield that

$$\begin{aligned} & \begin{bmatrix} \Omega_0 - (Q + K_0^T R K_0) & 0 \\ 0 & \varsigma I \end{bmatrix} - [(A + B K_0) I]^T \\ & \times ((1 - \alpha_0) \Omega_0 + \alpha_0 \Omega_1) [(A + B K_0) I] \succeq 0. \end{aligned} \quad (4.56)$$

For (4.52c), substituting  $\bar{\Omega}_0 = \gamma \Omega_0^{-1}$  and  $\bar{\Omega}_1 = \gamma \Omega_1^{-1}$  into it, we have that

$$\Omega_1 \succeq \Omega_0. \quad (4.57)$$

Then, pre- and post-multiplying (4.54) and (4.56) by  $[x(i|t)^T \omega(i|t)^T]^T$  and its transpose, and combining them with (4.57), the following condition can be guaranteed for the monotonicity of performance cost  $J_\infty(t)$  and closed-loop stability:

$$\mathbb{E}\{V_L(x(i+1|t)) - V_L(x(i|t))\} \leq -\mathbb{E}\{l(x(i|t), u(i|t)) - \varsigma \omega(i|t)^T \omega(i|t)\}, \quad (4.58)$$

where  $i, t \in \mathbb{Z}^+$ . By summing (4.58) from  $i = 0$  to  $i = \infty$ , we have that

$$\mathbb{E}\{V_L(x(\infty|t)) - V_L(x(t))\} \leq -\mathbb{E}\left\{\sum_{i=0}^{\infty} (l(x(i|t), u(i|t)) - \varsigma\omega(i|t)^T\omega(i|t))\right\},$$

where  $x(t) = x(0|t)$ . Consequently, we have that

$$J_{\infty}(t) \leq \mathbb{E}\{V_L(x(t))\}, \quad t \in \mathbb{Z}^+. \quad (4.59)$$

Note that the optimization problem in (4.52) should be solved at triggering instants only, i.e.,  $\xi_{t_j} = 1$ . That is,  $\mathbb{E}\{V_L(x(t_j))\} = x(t_j)^T\Omega_1x(t_j)$  at the triggering instant  $t_j$ . Let  $\bar{\Omega}_1 = \gamma\Omega_1^{-1}$ , then (4.52d) can be written as

$$x(t_j)^T\Omega_1x(t_j) \leq \gamma(t_j),$$

where  $\gamma(t_j)$  is regarded as an upper bound of  $J_{\infty}(t_j)$ , then (4.59) is guaranteed at  $t = t_j$ . To guarantee it at  $t \in \mathbb{Z}_{>t_j}$ , for (4.52e), using the Schur complement equivalence with  $Y_1 = K_1\bar{\Omega}_1$ , we have that

$$\begin{bmatrix} (1-\varepsilon)\bar{\Omega}_1 & 0 \\ 0 & \frac{\varepsilon}{\bar{\omega}}I \end{bmatrix} - [A\bar{\Omega}_1 + BK_1\bar{\Omega}_1 \ I]^T\bar{\Omega}_1^{-1}[A\bar{\Omega}_1 + BK_1\bar{\Omega}_1 \ I] \succeq 0. \quad (4.60)$$

Substituting  $\bar{\Omega}_1 = \gamma\Omega_1^{-1}$  into (4.60), and pre- and post-multiplying it by  $\text{diag}\{\gamma^{-1}\Omega_1, I\}$  yield that

$$\begin{bmatrix} (1-\varepsilon)\frac{1}{\gamma}\Omega_1 & 0 \\ 0 & \frac{\varepsilon}{\bar{\omega}}I \end{bmatrix} - [A + BK_1 \ I]^T\frac{1}{\gamma}\Omega_1[A + BK_1 \ I] \succeq 0. \quad (4.61)$$

Consider  $x(1|t) = Ax(t) + Bu_L(x(t)) + \omega(t)$ ,  $t \in \mathbb{Z}^+$ . Invoking the S-procedure, if and only if (4.61) is satisfied with  $0 < \varepsilon < 1$ , then the following condition is guaranteed

$$\frac{1}{\gamma}x(t)^T\Omega_1x(t) \geq \frac{1}{\bar{\omega}}\omega(t)^T\omega(t) \implies \frac{1}{\gamma}x(1|t)^T\Omega_1x(1|t) \leq \frac{1}{\gamma}x(t)^T\Omega_1x(t).$$

Then, according to Lemmas (4.4)-(4.4),  $\mathcal{X}_L \triangleq \{x|x^T\Omega_1x \leq \gamma\}$  is a robust positively invariant set. That is, equation (4.52d) satisfying for  $t \in \mathbb{Z}_{>t_j}$ . Thus, equation (4.59) is guaranteed by (4.52d) and (4.52e).

For (4.52f), using the Schur complement equivalence, we have that

$$(Y_s\bar{\Omega}_s^{-1}Y_s^T)^{[\ell\ell]} \leq (\bar{u}^{[\ell]})^2, \quad (4.62)$$

where  $\ell = 1, 2, \dots, n_u$ ;  $s = 0, 1$ . From (4.52c)-(4.52e), it follows that

$$x(i|t_j)^T \bar{\Omega}_0^{-1} x(i|t_j) \leq x(i|t_j)^T \bar{\Omega}_1^{-1} x(i|t_j) \leq 1, \quad i \in \mathbb{Z}^+.$$

Using the Cauchy-Schwarz inequality, it is shown that

$$\begin{aligned} (Y_s \bar{\Omega}_s^{-1} Y_s^T)^{[\ell\ell]} &= \left\| \left( Y_s \bar{\Omega}_s^{-\frac{1}{2}} \right)^{[\ell]} \right\|^2 \\ &\geq \left\| \left( Y_s \bar{\Omega}_s^{-\frac{1}{2}} \right)^{[\ell]} \right\|^2 \left\| \left( \bar{\Omega}_s^{-\frac{1}{2}} x(i|t_j) \right)^{[\ell]} \right\|^2 \\ &\geq \left| \left( Y_s \bar{\Omega}_s^{-1} x(i|t_j) \right)^{[\ell]} \right|^2 = |u(i|t_j)^{[\ell]}|^2. \end{aligned} \quad (4.63)$$

Combining (4.62) and (4.63), the input constraint in (4.1) is guaranteed. Likewise, the state constraint in (4.1) is guaranteed by (4.52g).  $\blacksquare$

Different from the tube-based MPC designed in Section 4.3,  $\Omega_0$  and  $\Omega_1$  here need to be updated on-line through the optimization problem in (4.52) at each triggering instant. It is seen from (4.52d) ( $x(t_j)$  is related to the disturbances) and (4.52e) ( $\bar{\omega}$  is the upper bound of  $\|\omega\|^2$ ), that  $\Omega_0$  and  $\Omega_1$  are able to directly reflect uncertain disturbances in (4.6). Hence, a ‘‘closed-loop’’ connection is also built between the checking function  $\mu$  and uncertain disturbances through the triggering function  $g$ , the triggering indicator  $\xi_{t_i}$ , and the updating law for Markov transition probabilities in (4.11).

**Remark 4.3.** *It is stressed here that only initial values  $\alpha_0$  and  $\beta_0$  are used in the optimization problem in (4.52), rather than  $\alpha_{t_i}$  and  $\beta_{t_i}$  which are dependent on  $t_i$ , since there is a conflict between recursive feasibility of the LMI-based MPC optimization problem in (4.52) and the updating law for  $\alpha_{t_i}$  and  $\beta_{t_i}$ . How to design more general  $\alpha_{t_i}$  and  $\beta_{t_i}$  to reduce this conservatism is a highly interesting but challenging problem, which is left for further investigation.*

**Remark 4.4.** *There are two reasons for considering both tube-based and LMI-based MPC approaches. The first and most important one is to show the generality of the proposed event-triggered scheme that such a novel event-triggered*



scheme can be implemented by these two robust MPC approaches and the completeness of the research work. Secondly, as the computational burden of determining Minkowski sums and convex hulls is scaling rapidly with respect to the dimension of the system, the tube-based MPC approach proposed here may not work efficiently for high-order systems. By contrast, the proposed LMI-based MPC approach is much less computational demanding due to the numerical tractability of LMIs, although some conservatism is inevitably introduced by the worst-case performance cost in LMIs. Hence, the two proposed stochastic event-triggered robust MPC approaches are complementary and some numerical evaluations are provided to show this in the simulation.

#### 4.4.2 Recursive Feasibility and Stability Analysis

**Theorem 4.5.** *Suppose that  $\Upsilon^*(t_j) \triangleq \{\gamma^*(t_j), \vartheta^*(t_j), \bar{\Omega}_0^*(t_j), \bar{\Omega}_1^*(t_j), Y_0^*(t_j), Y_1^*(t_j), U^*(t_j), X^*(t_j)\}$  is the optimal solution of the optimization problem in (4.52) at any triggering instant  $t_j$ . Then, for the system in (2.1), if the event-triggered controller is designed as in (4.51) with the stochastic event-triggered scheme in (4.2) and (4.3),  $\Upsilon^*(t_j)$  is feasible at the triggering instant  $t_{j+1}$ . Moreover, the closed-loop system is exponentially mean-square stable.*

**Proof.** (Recursive feasibility) According to Theorem 4.4, only (4.52d) is dependent on the state  $x(t_{j+1})$ , hence, to prove recursive feasibility, we just need to prove that  $x(t_{j+1})^T \bar{\Omega}_1^*(t_j)^{-1} x(t_{j+1}) \leq 1$ . Since (4.52d) and (4.52e) can guarantee that  $\mathcal{X}_L$  is a robust positively invariant set, we have that  $x(t_{j+1})^T \Omega_1^*(t_j) x(t_{j+1}) \leq \gamma(t_j)$ , where  $\Omega_1^*(t_j) = \gamma^*(t_j) \bar{\Omega}_1^*(t_j)^{-1}$ , which implies that (4.52d) is satisfied at the triggering instant  $t_{j+1}$ . Hence,  $\Upsilon^*(t_j)$  is feasible at the triggering instant  $t_{j+1}$ .

(Stability) Since recursive feasibility of the optimization problem in (4.52) is guaranteed based on the above analysis, equation (4.58) is always satisfied by (4.52a)-(4.52c). Then, at the checking instant  $t_l \in \mathbb{Z}_{>t_j}$ , if the triggering

condition is not satisfied, i.e.,  $\xi_{t_l} = 0$ , there must exist  $0 < \epsilon < 1$  satisfying

$$\begin{aligned}\mathbb{E}\{V_L(x(t_j + 1) \mid \xi_{t_j} = 1)\} &\leq \epsilon V_L^*(x(t_j)), \\ &\vdots \\ \mathbb{E}\{V_L(x(t_l) \mid \xi_{t_l-1} = 0)\} &\leq \epsilon V_L(x(t_l - 1)).\end{aligned}$$

It follows that

$$\mathbb{E}\{\|x(t_l)\|^2\} \leq \tau \epsilon^{(t_l - t_j)} \|x(t_j)\|^2. \quad (4.64)$$

where  $\tau > 0$ . Furthermore, we have that  $\mathbb{E}\{\|x(t)\|^2\} \leq \tau \epsilon^t \|x(0)\|^2$ ,  $t \in \mathbb{Z}_{>0}$  for initial state  $x(0)$ . If the triggering condition is satisfied, i.e.,  $\xi_{t_l} = 1$ , equation (4.64) is still guaranteed since  $V_L^*(x(t_l)) - V_L^*(x(t_j)) \leq V_L(x(t_l)) - V_L^*(x(t_j))$ . Hence, according to Definition 4.1, the exponential mean-square stability of the closed-loop system is guaranteed.  $\blacksquare$

## 4.5 Simulation Examples

In this section, three examples are used to show the advantages of the proposed stochastic event-triggered robust MPC approaches. For each example, we execute a Monte Carlo simulation with 1000 samples. To show the results, let  $\bar{\Delta}$  represent the average inter-execution time,  $\bar{T}_1$  represent the average number of  $\xi_{t_l} = 1$  and  $\bar{\mu}_{11}$  represent the corresponding average waiting time, and  $\bar{T}_0$  represent the average number of  $\xi_{t_l} = 0$  and  $\bar{\mu}_{01}$  represent the corresponding average waiting time.

**Example 4.1.** Consider the cart and spring-damper system in [88]. The discrete-time model of this system is given by

$$\begin{bmatrix} x_1(t+1) \\ x_2(t+1) \end{bmatrix} = \begin{bmatrix} 1 & T_c \\ -T_c \frac{k_0}{M} e^{-x_1(t)} & 1 - h_d \frac{k_0}{M} \end{bmatrix} \begin{bmatrix} x_1(t) \\ x_2(t) \end{bmatrix} + \begin{bmatrix} 0 \\ \frac{T_c}{M} \end{bmatrix} u(t) + \begin{bmatrix} \omega_1(t) \\ \omega_2(t) \end{bmatrix}. \quad (4.65)$$

The mass of the cart is  $M = 1.0$  kg; the spring linear factor is  $k_0 = 0.33$  N/m; the damper factor is  $h_d = 1.1$  Ns/m; the sampling period is  $T_c = 0.4$  s; the prediction horizon is  $N = 4$ . The state and control input constraints

Table 4.1: Average inter-execution time  $\bar{\Delta}$  and performance cost  $\bar{J}$

	$\theta = 0.2$		$\theta = 0.6$	
	$\bar{\Delta}$	$\bar{J}$	$\bar{\Delta}$	$\bar{J}$
LMI-based MPC	1.81	1.1372	2.31	1.1897
Tube-based MPC	2.12	0.9817	2.75	0.9935

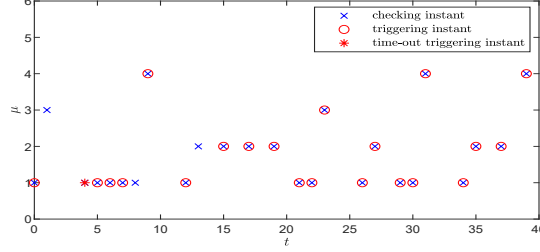


Figure 4.4: Triggering instants of the proposed LMI-based MPC.

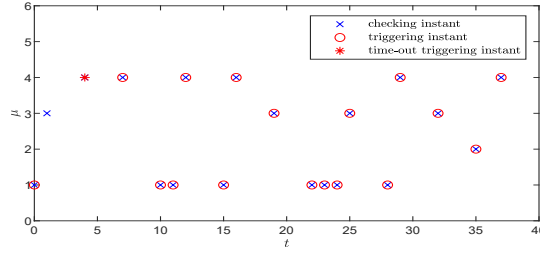


Figure 4.5: Triggering instants of the proposed tube-based MPC.

are given as  $|x_1| \leq 2.56$  m and  $|u| \leq 4.5$  N; the disturbance constraint set is  $\mathcal{W} = [-0.2, 0.2] \times [-0.2, 0.2]$  and thus  $\bar{\omega} = 0.08$ . The nonlinear function in (4.65) is linearized at the equilibrium point  $x_{eq} = [0, 0]^T$ . With tube-based MPC, a local feedback control is designed as  $K_T = [-1.1575 \quad 0.9481]$  by using the LQR technique with weighting matrices  $Q = I_2$  and  $R = I$ . Set the Hill coefficient  $n = 1$ , the initial transition probabilities  $\alpha_0 = 0.8$  and  $\beta_0 = 0.3$ , and the simulation step  $T_{sim} = 40$ .

To show the effects of the triggering parameter  $\theta$  on the inter-execution time and control performance, different values of  $\theta$  are considered and the results are presented in Table 4.1. It is clear that, for a larger  $\theta$ , the average inter-execution time is longer with slight control performance loss. Furthermore, tube-based MPC outperforms LMI-based MPC in terms of the inter-

Table 4.2: Triggering results with  $\theta = 0.2$ 

LMI-based MPC		Tube-based MPC	
$\bar{T}_1 = 20.55$	$\bar{\mu}_{11} = 1.64$	$\bar{T}_1 = 18.25$	$\bar{\mu}_{11} = 1.81$
$\bar{T}_0 = 3.23$	$\bar{\mu}_{01} = 1.65$	$\bar{T}_0 = 4.58$	$\bar{\mu}_{01} = 1.76$

execution time and control performance since it utilizes a robust positively invariant set containing all uncertainties instead of considering a min-max approach, namely, minimizing the worst-case performance cost with the upper bound of disturbances in the LMI-based MPC. The distributions of checking and triggering instants with  $\theta = 0.2$  in one of realizations are shown in Figures. 4.4-4.5. Most of checking instants are triggering instants, which shows the accuracy of the designed estimation strategy of checking instants. The triggering results are concluded in Table 4.2. Taken together, the results in this example verify that the proposed stochastic triggering strategy effectively links event verification and triggering to achieve adaptive waiting time.

**Example 4.2.** Consider the seventh-order Aircraft Model 6 provided in [84]. The sampling period is  $T_c = 0.2$ ; the prediction horizon is  $N = 8$ ; the initial state is  $x(0) = [-1.29, 3.76, -2.15, 0.83, 1.05, 0.58, -0.95]^T$ ; the triggering parameter  $\theta = 0.2$ .

Table 4.3: Running results

	Average computation time	Running results
LMI-based MPC	6.82 seconds	succeed
Tube-based MPC	more than 72 hours	fail

For this high-order system, we try to exploit the proposed stochastic event-triggered tube-based MPC and LMI-based MPC. The running results are shown in Table 4.3. Together with Figure 4.6, it is seen that the proposed LMI-based MPC is able to handle large systems with less computational resources, and drive the system to a neighborhood of the origin in the presence of disturbances. However, as mentioned in Remark 4.4, it is very difficult to implement a tube-based model predictive controller due to the computational

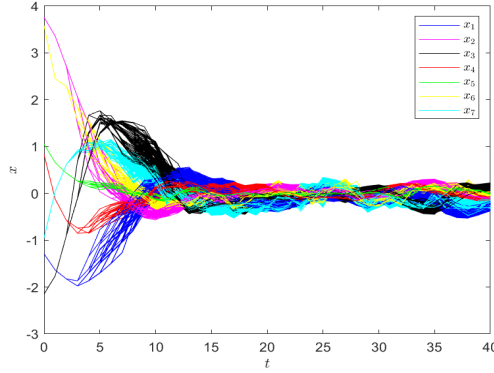


Figure 4.6: State trajectories of the proposed LMI-based MPC.

complexity associated with the robust positively invariant set. In this sense, tube-based MPC fails for this example.

**Example 4.3.** Consider the linear system as in (3.31). The simulation step is  $T_{\text{sim}} = 30$ ; the prediction horizon is  $N = 6$ ; the upper bound of disturbances is  $\bar{\omega} = 0.729$ ; the initial state is  $x(0) = [-21, 1]^T$ ; the triggering parameter  $\theta = 0.3$ .

To show the advantage of the proposed stochastic event-triggered scheme, comparisons with the existing methods in [60] and [89] are carried out. The average inter-execution time  $\bar{\Delta}$  and performance cost  $\bar{J}$  are shown in Table 4.4. It is seen that the two proposed event-triggered robust MPC approaches obtain longer inter-execution times, although the proposed LMI-based MPC shows some conservatism on control performance. The triggering results are concluded in Table 4.5. As shown in (4.5), the triggering condition needs to be checked at each sampling instant, and thus  $\bar{\mu}_{11}$  and  $\bar{\mu}_{01}$  for [60] can be set to “1”. As for self-triggered MPC, the event verification is removed,  $\bar{\mu}_{11}$  for [89] can be regarded as the same as  $\bar{\Delta}$  and  $\bar{\mu}_{01}$  is not considered. Table 4.5 shows that the proposed stochastic event-triggered scheme in (4.2) and (4.3) removes persistent monitoring of the triggering condition and achieves adaptive waiting time for the subsequent event verification and triggering.

Table 4.4: Comparison results with existing results

	$\bar{\Delta}$	$\bar{J}$
Stochastic LMI-based MPC	2.01	70.41
Stochastic tube-based MPC	2.11	43.40
Event-triggered MPC in [60]	1.07	45.19
Self-triggered MPC in [89]	1.88	53.84

Table 4.5: Triggering results

	$\bar{T}_1$	$\bar{\mu}_{11}$	$\bar{T}_0$	$\bar{\mu}_{01}$
Stochastic LMI-based MPC	14.94	1.57	4.45	1.60
Stochastic tube-based MPC	14.22	1.58	4.97	1.59
Event-triggered MPC in [60]	28.04	1.00	2.56	1.00
Self-triggered MPC in [89]	15.96	1.88	-	-

## 4.6 Summary

In this chapter, a novel stochastic triggering strategy for both tube-based MPC and LMI-based MPC has been proposed. A Markov chain with updating transition probabilities has been designed to link event verification with action triggering, and thus removing persistent monitoring and verification in conventional event-triggered schemes and improving the flexibility and robustness of self-triggered schemes. Recursive feasibility and closed-loop robust stability of both tube-based MPC and LMI-based MPC have been proved. Finally, the comparison simulation results have verified the effectiveness of the proposed stochastic triggering strategy.

# Chapter 5

## Event-Triggered Robust MPC: A Data-Driven Approach\*

This chapter investigates an event-triggered robust data-driven MPC for unknown systems, which is totally different from last three chapters under known system models. With initially measured input-output data, we target at constructing a terminal inequality constraint to complete the analysis of recursive feasibility and closed-loop stability in a data-driven case, and designing an event-triggered scheme to reduce resource consumption. According to Willems' fundamental lemma from behavioral systems theory in [72], a data-driven prediction model is generated and a terminal set is designed for the MPC optimization problem without any prior identification. By monitoring a feedback from the robust data-driven MPC controller to the event trigger, a mismatch between the data-driven model and the original plant is detected, and both deterministic and stochastic criteria are provided to select the threshold of the event-triggered scheme, respectively.

This chapter is organized as follows. Section 5.1 describes the system model and formulates an event-triggered robust data-driven MPC problem. Section 5.2 designs a terminal set for the data-driven MPC optimization problem. Section 5.3 provides both deterministic and stochastic event-triggered schemes. Section 5.4 analyzes recursive feasibility and stability. Section 5.5 verifies the

---

\*A version of this chapter has been submitted to *IEEE Transactions on Automatic Control* as: Li Deng, Zhan Shu, and Tongwen Chen, Event-triggered robust MPC with terminal inequality constraints: A data-driven approach, Aug. 2022.

proposed approach by numerical examples. Section 5.6 concludes this chapter.

## 5.1 Problem Formulation

Consider the following linear discrete-time system:

$$x(t+1) = Ax(t) + Bu(t), \quad (5.1a)$$

$$y(t) = Cx(t) + Du(t), \quad (5.1b)$$

$$\tilde{y}(t) = y(t) + \omega(t), \quad (5.1c)$$

where  $x(t) \in \mathbb{R}^{n_x}$  is the system state,  $u(t) \in \mathbb{R}^{n_u}$  is the control input,  $y(t) \in \mathbb{R}^{n_y}$  is the output of the plant, and  $\tilde{y}(t)$  is the output measurement with the additive stochastic noise  $\omega(t) \in \mathbb{R}^{n_y}$  at instant  $t \in \mathbb{Z}$ , respectively. Assume that the matrix pair  $(A, B)$  is controllable and the matrix pair  $(A, C)$  is observable. This work mainly focuses on the case that all system matrices are unknown and only input-output data samples are available.

**Assumption 5.1.** *The noise  $\omega(t)$  is independently and identically distributed and satisfies  $\|\omega(t)\|^2 \leq \bar{\omega}$ , where  $\bar{\omega} \in \mathbb{R}_{>0}$ .*

System (5.1) is subject to the following input and output constraints:

$$u \in \mathcal{U}, \quad y \in \mathcal{Y}, \quad (5.2)$$

where  $\mathcal{Y} \triangleq \{y \in \mathbb{R}^{n_y} \mid H_y y \preceq h_y\}$ ,  $\mathcal{U} \triangleq \{u \in \mathbb{R}^{n_u} \mid H_u u \preceq h_u\}$ , and  $H_y \in \mathbb{R}^{l_y \times n_y}$ ,  $H_u \in \mathbb{R}^{l_u \times n_u}$ ,  $h_y \in \mathbb{R}^{l_y}$ , and  $h_u \in \mathbb{R}^{l_u}$  are known matrices and vectors.

To avoid the state estimation and use available input-output data directly, we recall the input-output representation of system (5.1) as in [90]:

$$y(t) + \sum_{i=1}^n a_i y(t-i) = \sum_{i=1}^n b_i u(t-i),$$

where  $n \in \mathbb{Z}_{\geq n_x}$  represents the system order;  $a_i, b_i \in \mathbb{R}$  are the coefficients of  $y(t-i)$  and  $u(t-i)$ , respectively. Then, an input-output state-space model



with additive stochastic noises is obtained as

$$z(t+1) = \hat{A}z(t) + \hat{B}u(t), \quad (5.3a)$$

$$\tilde{z}(t) = z(t) + \begin{bmatrix} \omega_{[t-n,t-1]} \\ \mathbf{0}_{n_u n} \end{bmatrix}, \quad (5.3b)$$

where  $\omega_{[t-n,t-1]} \triangleq [\omega_{t-n}^T \ \dots \ \omega_{t-1}^T]^T$ ;  $z(t) = \begin{bmatrix} y_{[t-n,t-1]} \\ u_{[t-n,t-1]} \end{bmatrix}$  is an augmented state related to the past  $n$ -step input-output data; system matrices  $\hat{A} \in \mathbb{R}^{n(n_y+n_u) \times n(n_y+n_u)}$  and  $\hat{B} \in \mathbb{R}^{n(n_y+n_u) \times n_u}$  are unknown.

In this work, a robust MPC using a data-driven approach will be designed to handle the constraints in (5.2). Commonly, classical model-based MPC is always dependent on the following prediction model corresponding to (5.3a) to predict future trajectories:

$$\bar{z}(t+1) = \hat{A}\bar{z}(t) + \hat{B}\bar{u}(t), \quad (5.4)$$

where  $\bar{z}(t) = \begin{bmatrix} \bar{y}_{[t-n,t-1]} \\ \bar{u}_{[t-n,t-1]} \end{bmatrix}$  is an augmented predicted state related to the past  $n$ -step predicted input-output data. Since  $\hat{A}$  and  $\hat{B}$  are unknown and only input-output measurements are available, it is impossible to use prediction model (5.4) directly in a data-driven optimization problem. Hence, we will have the aid of the following definition and lemma regarding persistence of excitation to construct a non-parametric predictive model based on available input-output data.

**Definition 5.1.** [72] *A sequence  $u_{[i,i+L-1]}$ ,  $i \in \mathbb{Z}$  with  $u_i \in \mathbb{R}^{n_u}$  is said to be persistently exciting of order  $\tilde{L}$  if  $\text{rank}(U_{i,\tilde{L},L-\tilde{L}+1}) = n_u \tilde{L}$ , where  $U_{i,\tilde{L},L-\tilde{L}+1}$  is the Hankel matrix associated to  $u_{[i,i+L-1]}$  and*

$$U_{i,\tilde{L},L-\tilde{L}+1} \triangleq \begin{bmatrix} u_i & u_{i+1} & \cdots & u_{i+L-\tilde{L}} \\ u_{i+1} & u_{i+2} & \cdots & u_{L-\tilde{L}+1} \\ \vdots & \vdots & \ddots & \vdots \\ u_{i+\tilde{L}-1} & u_{i+\tilde{L}} & \cdots & u_{i+L-1} \end{bmatrix}$$

with  $\tilde{L}, L \in \mathbb{Z}_{>0}$  and  $\tilde{L} \leq L$ .

**Lemma 5.1.** [72] Suppose  $\{u_{[0,L-1]}^o, y_{[0,L-1]}^o\}$  is a trajectory of system (5.1) and  $U_{0,\tilde{L},L-\tilde{L}+1}$  and  $Y_{0,\tilde{L},L-\tilde{L}+1}$  are the corresponding Hankel matrices, where  $u_{[0,L-1]}^o$  is persistently exciting of order  $\tilde{L}$ . Then,  $\{u_{[0,\tilde{L}-1]}, y_{[0,\tilde{L}-1]}\}$  is a trajectory of this system if and only if there exists  $g \in \mathbb{R}^{L-\tilde{L}+1}$  such that

$$\begin{bmatrix} u_{[0,\tilde{L}-1]} \\ y_{[0,\tilde{L}-1]} \end{bmatrix} = \begin{bmatrix} U_{0,\tilde{L},L-\tilde{L}+1} \\ Y_{0,\tilde{L},L-\tilde{L}+1} \end{bmatrix} g. \quad (5.5)$$

Lemma 5.1 indicates that all trajectories with length  $\tilde{L}$  of system (5.1) can be obtained from linear combinations of their past trajectories. This is an appealing data-driven characterization for system (5.1) without any prior identification. Let  $\{u_{[-n,L-n-1]}^o, \tilde{y}_{[-n,L-n-1]}^o\}$  be the collected past input-output data of system (5.1). To employ Lemma 5.1 for robust data-driven MPC with the prediction horizon  $N$ , according to Definition 5.1, the input data  $u_{[-n,L-n-1]}^o$  are supposed to satisfy the following assumption.

**Assumption 5.2.** The input data  $u_{[-n,L-n-1]}^o$  is persistently exciting of order  $N + n$ .

With available past data  $\{u_{[-n,L-n-1]}^o, \tilde{y}_{[-n,L-n-1]}^o\}$ , Assumption 5.2 guarantees that Hankel matrices  $U_{-n,n+N,L-(n+N)+1}$  and  $\tilde{Y}_{-n,n+N,L-(n+N)+1}$  have full row rank. Then, we can use these data to generate a prediction trajectory by Lemma 5.1 later.

It is well-known that terminal constraints play an important role in recursive feasibility and stability of MPC. However, it is very challenging to construct some terminal ingredients without the knowledge of a model. This is the main reason why most data-driven MPC approaches cannot guarantee the recursive feasibility and closed-loop stability ([73, 74, 75]). Very recently, by utilizing terminal equality constraints, a new data-driven MPC approach has been proposed in [76] such that recursive feasibility and closed-loop stability can be analyzed theoretically. However, the implementation of a terminal equality constraint is rather restrictive. As it is generally easier to drive a state to a specified set than into a specified point, we relax a terminal equality constraint into a terminal inequality constraint for the robust data-driven

MPC optimization problem formulated by:

$$\begin{aligned} & \min_{\bar{u}_{[-n,N-1]}(t), \bar{y}_{[-n,N-1]}(t), g(t), \varepsilon_{[-n,N-1]}(t)} J(\tilde{z}(t)) \\ \text{s.t. } & \begin{bmatrix} \bar{u}_{[-n,N-1]}(t) \\ \bar{y}_{[-n,N-1]}(t) + \varepsilon_{[-n,N-1]}(t) \end{bmatrix} = \begin{bmatrix} U_{-n,n+N,L-(n+N)+1} \\ \tilde{Y}_{-n,n+N,L-(n+N)+1} \end{bmatrix} g(t) \end{aligned} \quad (5.6a)$$

$$\begin{bmatrix} \bar{y}_{[-n,-1]}(t) \\ \bar{u}_{[-n,-1]}(t) \end{bmatrix} = \tilde{z}(t) \quad (5.6b)$$

$$\bar{u}_i(t) \in \mathcal{U}, \quad i \in \mathbb{Z}_{[0,N-1]} \quad (5.6c)$$

$$\bar{y}_i(t) \in \mathcal{Y}, \quad i \in \mathbb{Z}_{[0,N-1]} \quad (5.6d)$$

$$\begin{bmatrix} \bar{y}_{[N-n,N-1]}(t) \\ \bar{u}_{[N-n,N-1]}(t) \end{bmatrix} \in \mathcal{Z}_f \quad (5.6e)$$

where  $\bar{u}_i(t)$  is the predicted control input at  $t+i$  and  $\bar{u}(t) = \bar{u}_0(t)$ ;  $\bar{y}_i(t)$  is the predicted output at  $t+i$  and  $\bar{y}(t) = \bar{y}_0(t)$ ; the prediction horizon  $N$  should satisfy  $N \in \mathbb{Z}_{\geq n}$ . A data-driven model in (5.6a) is used to replace classical prediction model (5.4) and predict input-output behavior based on Lemma 5.1. The available output measurement  $\tilde{y}_{[-n,L-n-1]}^o$  is subject to bounded additive noises, which implies that the Hankel matrices  $U_{-n,n+N,L-(n+N)+1}$  and  $\tilde{Y}_{-n,n+N,L-(n+N)+1}$  may not span the trajectory space strictly. Thus, to improve the prediction accuracy, a slack variable  $\varepsilon_{[-n,N-1]}(t)$  in (5.6a) is introduced to compensate the noisy part and guarantee the feasibility of this optimization problem. Equation (5.6b) is regarded as the initial condition since  $\tilde{z}(t)$  consists of past  $n$ -step input-output measurements  $u_{[t-n,t-1]}$ ,  $\tilde{y}_{[t-n,t-1]}$ . Equations (5.6c) and (5.6d) are input and output constraints. Equation (5.6e) is the terminal inequality constraint, where  $\mathcal{Z}_f$  is a terminal set to be designed. As will be seen later, the inequality constraint in (5.6e) can lead to a larger feasible region and a lower bound for the prediction horizon than a terminal equality constraint.

The cost function is defined as

$$J(\tilde{z}(t)) = \sum_{i=0}^{N-1} l(\bar{u}_{i-1}(t), \bar{y}_{i-1}(t)) + V(\bar{z}_N(t)) + \lambda_\varepsilon \|\varepsilon_{[-n,N-1]}(t)\|^2 + \lambda_g \bar{\omega} \|g(t)\|^2,$$

where  $l(\bar{u}_i(t), \bar{y}_i(t)) \triangleq \bar{y}_i(t)^\top Q \bar{y}_i(t) + \bar{u}_i(t)^\top R \bar{u}_i(t)$  with  $Q \succ 0$  and  $R \succ 0$ ;  $\bar{z}_N(t) = \begin{bmatrix} \bar{y}_{[N-n,N-1]}(t) \\ \bar{u}_{[N-n,N-1]}(t) \end{bmatrix}$  and  $V(\bar{z}_N(t))$  is a terminal cost to be designed;

$\lambda_\varepsilon, \lambda_g \in \mathbb{R}_{>0}$  are given weights for regularization terms  $\|\varepsilon_{[-n, N-1]}(t)\|^2$  and  $\|g(t)\|^2$ .

**Remark 5.1.** *When the output measurements are corrupted by noises, the optimization problem in (5.6) may become infeasible if the form of (5.5) is directly used for prediction. Hence, the slack variable  $\varepsilon_{[-n, N-1]}(t)$  is introduced to ensure feasibility of (5.6) at all instants.*

Seen from (5.6), the proposed robust data-driven MPC is able to guarantee input and output constraints (5.2) for unknown system (5.1) without any prior identification, but it may introduce heavier computational burden and thus require more computational resources than that of the model-based MPC due to the introduction of a large amount of data. As a matter of fact, if the latest solved control sequence of the robust data-driven MPC controller could regulate the system well, it is unnecessary to solve the optimization problem in (5.6) again. Hence, an event-triggered scheme is introduced below to reduce the number of times of solving (5.6), leading to the reduction of resource consumption.

Define the output error as  $e(t) \triangleq \tilde{y}(t) - \bar{y}(t)$ . If the predicted output  $\bar{y}(t)$  actually coincides with the actual output  $y(t)$  of the original plant, that is,  $e(t)$  tending to  $\omega(t)$ , it indicates that the data-driven model in (5.6a) is nearly consistent with the original system in (5.1) and the current control action  $u(t)$  could regulate the system well. Hence, the key idea of our design is that the event verification should be dependent on the deviation of the predicted output  $\bar{y}$  from the actual output  $y$ , namely, the output error  $e$ . To this end, define an appropriate triggering function  $\varphi : \mathbb{R}^{n_y} \rightarrow \mathbb{R}$  related to  $e$ . Then, the event-triggered condition is formulated by

$$\varphi(e(t)) > \kappa \iff \xi(t) = 1, \quad (5.7)$$

where  $\kappa$  is a triggering threshold to be designed based on the known information of noises;  $\xi(t)$  is a binary triggering indicator. Denote the triggering instant sequence  $\{t_j : j \in \mathbb{Z}^+\} \subseteq \mathbb{Z}^+$ . Accordingly, the triggering instant is

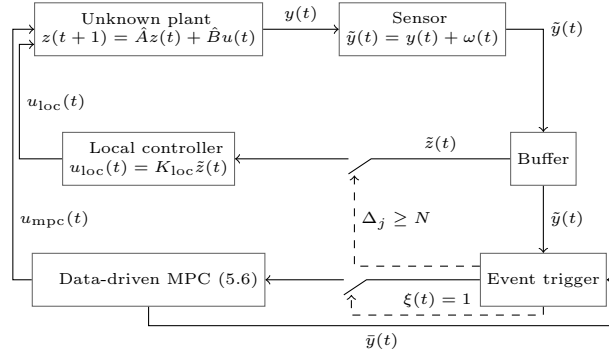


Figure 5.1: Architecture of the proposed event-triggered data-driven MPC.

generated by

$$t_{j+1} = \min\{t \in \mathbb{Z}_{>t_j} \mid \varphi(e(t)) > \kappa\},$$

where  $t_0 = 0$  as  $j = 0$ .

Define the inter-execution time between triggering instants  $t_j$  and  $t_{j+1}$  as  $\Delta_j \triangleq t_{j+1} - t_j$ ,  $j \in \mathbb{Z}^+$ . In most existing event-triggered MPC, to preserve the optimality and closed-loop stability, the inter-execution time is always limited in the prediction horizon  $N$ , i.e., if the inter-execution time exceeds  $N$ , then the event is triggered automatically at this instant. To remove this limitation without losing closed-loop stability, an extra local controller applied for  $\Delta_j \geq N$ , is embedded in the event-triggered control structure:

$$u_{\text{loc}}(t) = K_{\text{loc}} \tilde{z}(t), \quad (5.8)$$

where  $K_{\text{loc}}$  is a local controller gain to be designed. Accordingly, the designed event-triggered controller is of the form

$$u(t) = \begin{cases} u_{\text{mpc}}(t), & t_j \leq t < t_j + N, \\ u_{\text{loc}}(t), & t_j + N \leq t < t_{j+1}, \end{cases} \quad (5.9)$$

where  $u_{\text{mpc}}(t)$  represents the robust data-driven MPC controller.

The control architecture of the proposed event-triggered robust data-driven MPC is illustrated in Figure 5.1. The designed event trigger controls an inner loop and an outer loop: If  $\varphi(e(t)) > \kappa$ , the outer loop will start to work and the robust data-driven MPC controller will solve the optimization problem in

(5.6); else, the robust data-driven MPC controller will transmit its feasible control to the plant when  $\Delta_j < N$ , or the buffer will transmit  $\tilde{z}(t)$  to the local controller and the inner loop will start to work when  $\Delta_j \geq N$ .

The main objective of this chapter is to design robust data-driven MPC controller  $u_{\text{mpc}}$  together with the corresponding terminal set  $\mathcal{Z}_f$  and an extra local controller  $u_{\text{loc}}$  by using measured input-output data only, and form a feedback from the robust data-driven MPC controller to the event trigger such that the event-triggered condition in (5.7) is carefully generated and the corresponding event-triggered controller in (5.9) is synthesized to save the on-line computational resources.

## 5.2 Terminal Set $\mathcal{Z}_f$ Design

In this section, a suitable terminal set  $\mathcal{Z}_f$  will be constructed for the robust data-driven MPC optimization problem in (5.6) based on available data  $\{u_{[-n, L-n-1]}^o, \tilde{y}_{[-n, L-n-1]}^o\}$ . Define the terminal cost as:  $V(\bar{z}) = \bar{z}^T P \bar{z}$ , and the form of the terminal set as:

$$\mathcal{Z}_f \triangleq \{\bar{z} \in \underbrace{\mathbb{R}^{n_y} \times \cdots \times \mathbb{R}^{n_y}}_n \times \underbrace{\mathbb{R}^{n_u} \times \cdots \times \mathbb{R}^{n_u}}_n \mid \bar{z}^T P \bar{z} \leq \alpha\},$$

where  $P \succ 0$  is a terminal weighting matrix and  $\alpha \in \mathbb{R}_{>0}$  is to be designed. According to model-based robust MPC, to guarantee the stability,  $P$  should be designed such that the following condition holds

$$(\hat{A} + \hat{B}\hat{K})^T P (\hat{A} + \hat{B}\hat{K}) - P \preceq -(\mathcal{Q} + \hat{K}^T R \hat{K}), \quad (5.10)$$

where  $\mathcal{Q} = \text{diag}\{\underbrace{Q, \dots, Q}_n, \underbrace{R, \dots, R}_n\}$ ;  $\hat{K} \in \mathbb{R}^{n_u \times n(n_y + n_u)}$  is a terminal control gain to be constructed. Since  $\hat{A}$  and  $\hat{B}$  are unknown in robust data-driven MPC, it is impossible to directly use (5.10) to find a suitable  $P$ . Hence, the key to overcome this issue is to avoid the need of these unknown system matrices or to find their equivalent representations with available data  $\{u_{[-n, L-n-1]}^o, \tilde{y}_{[-n, L-n-1]}^o\}$ . Based on persistently exciting data, reference [91] provided some

data-dependent representations of linear systems without any explicit system matrix identification, which paves a way to solve this issue of our work. Motivated by [91], we can derive a data-based closed-loop representation as will be shown in the first subsection. Accordingly, the terminal weighting matrix  $P$  and control gain  $\hat{K}$  will be designed and the corresponding terminal set will be determined in the later subsections.

Before proceeding, we present the following lemma, which is a useful tool to facilitate our discussion.

**Lemma 5.2.** [92] *For arbitrary matrices  $X_1, X_2, E$  with  $E \succ 0$  and a scalar  $\delta > 0$ , it is true that  $X_1 E X_2^T + X_2 E X_1^T \preceq \delta X_1 E X_1^T + \delta^{-1} X_2 E X_2^T$ .*

## 5.2.1 Data-Based Closed-Loop Representation

To construct a data-based closed-loop representation, it is unnecessary to use all available data to increase the computational burden. We can pick  $\{u_{[\rho_1-n, \rho_1-n+L_1-1]}^o, \tilde{y}_{[\rho_1-n, \rho_1-n+L_1-1]}^o\}$  from available data  $\{u_{[-n, L-n-1]}^o, \tilde{y}_{[-n, L-n-1]}^o\}$ , where  $L_1 \in \mathbb{Z}_{\geq n_u + (n_y + n_u)n}$  and  $\rho_1 \in \mathbb{Z}_{[0, L-L_1]}$ . Note that all available data are used when  $\rho_1 = 0$  and  $L_1 = L$ . Then, we have the following two Hankel matrices

$$\tilde{Z}_{\rho_1, L_1} = Z_{\rho_1, L_1} + \begin{bmatrix} W_{\rho_1-n, n, L_1} \\ \mathbf{0}_{n_u n \times L_1} \end{bmatrix}, \quad (5.11)$$

$$\tilde{Z}_{\rho_1+1, L_1} = Z_{\rho_1+1, L_1} + \begin{bmatrix} W_{\rho_1-n+1, n, L_1} \\ \mathbf{0}_{n_u n \times L_1} \end{bmatrix}, \quad (5.12)$$

where  $Z_{\rho_1, L_1} = \begin{bmatrix} Y_{\rho_1-n, n, L_1} \\ U_{\rho_1-n, n, L_1} \end{bmatrix}$ . Regarding the picked data  $\{u_{[\rho_1-n, \rho_1-n+L_1-1]}^o, \tilde{y}_{[\rho_1-n, \rho_1-n+L_1-1]}^o\}$ , we have the following assumption, which shows a natural requirement that the information loss caused by noise is not significant. In this case, we can use the data to generate a data-based closed-loop representation.

**Assumption 5.3.** *There exist scalars  $\gamma_1 > 0$  and  $\gamma_2 > 0$  such that*

$$\begin{bmatrix} \mathbf{0}_{n_u \times L_1} \\ \begin{bmatrix} W_{\rho_1-n, n, L_1} \\ \mathbf{0}_{n_u n \times L_1} \end{bmatrix} \end{bmatrix} \begin{bmatrix} \mathbf{0}_{n_u \times L_1} \\ \begin{bmatrix} W_{\rho_1-n, n, L_1} \\ \mathbf{0}_{n_u n \times L_1} \end{bmatrix} \end{bmatrix}^T \preceq \gamma_1 \begin{bmatrix} U_{\rho_1, L_1} \\ \tilde{Z}_{\rho_1, L_1} \end{bmatrix} \begin{bmatrix} U_{\rho_1, L_1} \\ \tilde{Z}_{\rho_1, L_1} \end{bmatrix}^T, \quad (5.13)$$

$$\begin{bmatrix} W_{\rho_1-n+1,n,L_1} \\ \mathbf{0}_{n_u n \times L_1} \end{bmatrix} \begin{bmatrix} W_{\rho_1-n+1,n,L_1} \\ \mathbf{0}_{n_u n \times L_1} \end{bmatrix}^T \preceq \gamma_2 \tilde{Z}_{\rho_1+1,L_1} \tilde{Z}_{\rho_1+1,L_1}^T, \quad (5.14)$$

where  $U_{\rho_1,L_1} = U_{\rho_1,\tilde{L},L_1}$  with  $\tilde{L} = 1$ .

Motivated by the remarkable results in [91], an equivalent representation of  $\hat{A} + \hat{B}\hat{K}$  can be obtained as in the following lemma.

**Lemma 5.3.** *For the picked data  $\{u^o_{[\rho_1-n,\rho_1-n+L_1-1]}, \tilde{y}^o_{[\rho_1-n,\rho_1-n+L_1-1]}\}$  with Assumption 5.2, system (5.3a) with a control law  $u = \hat{K}z$  can be parameterized as:*

$$\hat{A} + \hat{B}\hat{K} = (\tilde{Z}_{\rho_1+1,L_1} + M_{\rho_1,L_1})G, \quad (5.15)$$

where  $G \in \mathbb{R}^{L_1 \times n(n_y+n_u)}$  satisfies

$$\begin{bmatrix} \hat{K} \\ I_{n(n_y+n_u)} \end{bmatrix} = \begin{bmatrix} U_{\rho_1,L_1}G \\ \tilde{Z}_{\rho_1,L_1}G \end{bmatrix} \quad (5.16)$$

$$\text{and } M_{\rho_1,L_1} \triangleq \hat{A} \begin{bmatrix} W_{\rho_1-n,n,L_1} \\ \mathbf{0}_{n_u n \times L_1} \end{bmatrix} - \begin{bmatrix} W_{\rho_1-n+1,n,L_1} \\ \mathbf{0}_{n_u n \times L_1} \end{bmatrix}.$$

**Proof.** Under Assumption 5.2, for any given  $\hat{K}$ , there exists  $G \in \mathbb{R}^{L_1 \times n(n_y+n_u)}$  satisfying (5.16) (by Rouché-Capelli theorem in [93]). Then, we have that

$$\begin{aligned} \hat{A} + \hat{B}\hat{K} &= \begin{bmatrix} \hat{B} & \hat{A} \end{bmatrix} \begin{bmatrix} \hat{K} \\ I_{n(n_y+n_u)} \end{bmatrix} = \begin{bmatrix} \hat{B} & \hat{A} \end{bmatrix} \begin{bmatrix} U_{\rho_1,L_1}G \\ \tilde{Z}_{\rho_1,L_1}G \end{bmatrix} \\ &= \begin{bmatrix} \hat{B} & \hat{A} \end{bmatrix} \left[ \begin{array}{c} U_{\rho_1,L_1}G \\ \begin{bmatrix} Y_{\rho_1-n,n,L_1} \\ U_{\rho_1-n,n,L_1} \end{bmatrix} G + \begin{bmatrix} W_{\rho_1-n,n,L_1} \\ \mathbf{0}_{n_u n \times L_1} \end{bmatrix} G \end{array} \right] \\ &= \left( Z_{\rho_1+1,L_1} + \hat{A} \begin{bmatrix} W_{\rho_1-n,n,L_1} \\ \mathbf{0}_{n_u n \times L_1} \end{bmatrix} \right) G \\ &= (\tilde{Z}_{\rho_1+1,L_1} + M_{\rho_1,L_1})G. \end{aligned}$$

■

Although a suitable representation of  $\hat{A} + \hat{B}\hat{K}$  is obtained in Lemma 5.3, it is difficult to know  $M_{\rho_1,L_1}$  in (5.15) since the noise data  $\{\omega^o_{[\rho_1-n,\rho_1-n+L_1-1]}\}$  are unavailable. Hence, we provide the following lemma to deal with  $M_{\rho_1,L_1}$  based on Assumption 5.3.



**Lemma 5.4.** *Under Assumptions 5.2-5.3, there exist scalars  $\gamma_1 < \delta_1 < 1$  and  $\delta_2 > 0$  such that*

$$M_{\rho_1, L_1} M_{\rho_1, L_1}^T \preceq \gamma_3 \tilde{Z}_{\rho_1+1, L_1} \tilde{Z}_{\rho_1+1, L_1}^T, \quad (5.17)$$

where  $\gamma_3 = \gamma_4 + \gamma_5 \gamma_2$ ,  $\gamma_4 = \frac{(1+\delta_2)}{(1-\delta_1)(\delta_1-\gamma_1)}$ , and  $\gamma_5 = (1+\delta_2^{-1}) + \frac{\delta_1 \gamma_1 (1+\delta_2)}{(1-\delta_1)(\delta_1-\gamma_1)(1-\delta_1 \gamma_1)}$ .

**Proof.** By pre- and post-multiplying (5.13) by  $[\hat{B} \ \hat{A}]$  and its transpose, we have that

$$\hat{A} \begin{bmatrix} W_{\rho_1-n, n, L_1} \\ \mathbf{0}_{n_u n \times L_1} \end{bmatrix} \begin{bmatrix} W_{\rho_1-n, n, L_1} \\ \mathbf{0}_{n_u n \times L_1} \end{bmatrix}^T \hat{A}^T \preceq \gamma_1 S_{\rho_1, L_1} S_{\rho_1, L_1}^T, \quad (5.18)$$

where  $S_{\rho_1, L_1} \triangleq \hat{A} \tilde{Z}_{\rho_1, L_1} + \hat{B} U_{\rho_1, L_1}$ . By applying Lemma 5.2, (5.18) can be rewritten as

$$\begin{aligned} & \left( \frac{\delta_1}{\gamma_1} - 1 \right) \hat{A} \begin{bmatrix} W_{\rho_1-n, n, L_1} \\ \mathbf{0}_{n_u n \times L_1} \end{bmatrix} \begin{bmatrix} W_{\rho_1-n, n, L_1} \\ \mathbf{0}_{n_u n \times L_1} \end{bmatrix}^T \hat{A}^T \\ & \preceq \delta_1 S_{\rho_1, L_1} S_{\rho_1, L_1}^T - \hat{A} \begin{bmatrix} W_{\rho_1-n, n, L_1} \\ \mathbf{0}_{n_u n \times L_1} \end{bmatrix} \begin{bmatrix} W_{\rho_1-n, n, L_1} \\ \mathbf{0}_{n_u n \times L_1} \end{bmatrix}^T \hat{A}^T \\ & = \frac{\delta_1}{1-\delta_1} \left( S_{\rho_1, L_1} S_{\rho_1, L_1}^T + \hat{A} \begin{bmatrix} W_{\rho_1-n, n, L_1} \\ \mathbf{0}_{n_u n \times L_1} \end{bmatrix} \begin{bmatrix} W_{\rho_1-n, n, L_1} \\ \mathbf{0}_{n_u n \times L_1} \end{bmatrix}^T \hat{A}^T \right) \\ & \quad - \frac{\delta_1}{1-\delta_1} \left( \delta_1 S_{\rho_1, L_1} S_{\rho_1, L_1}^T + \delta_1^{-1} \hat{A} \begin{bmatrix} W_{\rho_1-n, n, L_1} \\ \mathbf{0}_{n_u n \times L_1} \end{bmatrix} \begin{bmatrix} W_{\rho_1-n, n, L_1} \\ \mathbf{0}_{n_u n \times L_1} \end{bmatrix}^T \hat{A}^T \right) \\ & \preceq \frac{\delta_1}{1-\delta_1} \left( S_{\rho_1, L_1} S_{\rho_1, L_1}^T + \hat{A} \begin{bmatrix} W_{\rho_1-n, n, L_1} \\ \mathbf{0}_{n_u n \times L_1} \end{bmatrix} \begin{bmatrix} W_{\rho_1-n, n, L_1} \\ \mathbf{0}_{n_u n \times L_1} \end{bmatrix}^T \hat{A}^T \right) \\ & \quad - \frac{\delta_1}{1-\delta_1} \left( S_{\rho_1, L_1} \begin{bmatrix} W_{\rho_1-n, n, L_1} \\ \mathbf{0}_{n_u n \times L_1} \end{bmatrix}^T \hat{A}^T + \hat{A} \begin{bmatrix} W_{\rho_1-n, n, L_1} \\ \mathbf{0}_{n_u n \times L_1} \end{bmatrix} S_{\rho_1, L_1}^T \right) \\ & = \frac{\delta_1}{1-\delta_1} Z_{\rho_1+1, L_1} Z_{\rho_1+1, L_1}^T, \end{aligned}$$

where  $\gamma_1 < \delta_1 < 1$ . Then, we have that

$$\hat{A} \begin{bmatrix} W_{\rho_1-n, n, L_1} \\ \mathbf{0}_{n_u n \times L_1} \end{bmatrix} \begin{bmatrix} W_{\rho_1-n, n, L_1} \\ \mathbf{0}_{n_u n \times L_1} \end{bmatrix}^T \hat{A}^T \preceq \gamma_4 Z_{\rho_1+1, L_1} Z_{\rho_1+1, L_1}^T. \quad (5.19)$$

Combining (5.14) and (5.19) and applying Lemma 5.2 with  $\delta_2 > 0$  yield that

$$\begin{aligned}
M_{\rho_1, L_1} M_{\rho_1, L_1}^T &\preceq (1 + \delta_2) \hat{A} \begin{bmatrix} W_{\rho_1-n, n, L_1} \\ \mathbf{0}_{n_u n \times L_1} \end{bmatrix} \begin{bmatrix} W_{\rho_1-n, n, L_1} \\ \mathbf{0}_{n_u n \times L_1} \end{bmatrix}^T \hat{A}^T \\
&\quad + (1 + \delta_2^{-1}) \begin{bmatrix} W_{\rho_1-n+1, n, L_1} \\ \mathbf{0}_{n_u n \times L_1} \end{bmatrix} \begin{bmatrix} W_{\rho_1-n+1, n, L_1} \\ \mathbf{0}_{n_u n \times L_1} \end{bmatrix}^T \\
&\preceq \gamma_4 \left( (1 - (1 - \delta_1 \gamma_1)) Z_{\rho_1+1, L_1} Z_{\rho_1+1, L_1}^T \right. \\
&\quad \left. + (1 - (1 - \delta_1 \gamma_1)^{-1}) \begin{bmatrix} W_{\rho_1-n+1, n, L_1} \\ \mathbf{0}_{n_u n \times L_1} \end{bmatrix} \begin{bmatrix} W_{\rho_1-n+1, n, L_1} \\ \mathbf{0}_{n_u n \times L_1} \end{bmatrix}^T \right) \\
&\quad + \gamma_5 \begin{bmatrix} W_{\rho_1-n+1, n, L_1} \\ \mathbf{0}_{n_u n \times L_1} \end{bmatrix} \begin{bmatrix} W_{\rho_1-n+1, n, L_1} \\ \mathbf{0}_{n_u n \times L_1} \end{bmatrix}^T \\
&\preceq \gamma_4 \tilde{Z}_{\rho_1+1, L_1} \tilde{Z}_{\rho_1+1, L_1}^T + \gamma_5 \gamma_2 \tilde{Z}_{\rho_1+1, L_1} \tilde{Z}_{\rho_1+1, L_1}^T \\
&= \gamma_3 \tilde{Z}_{\rho_1+1, L_1} \tilde{Z}_{\rho_1+1, L_1}^T.
\end{aligned}$$

This completes the proof. ■

## 5.2.2 Terminal Weighting Matrix $P$ and Control Gain $\hat{K}$

The following theorem gives the desirable terminal weighting matrix  $P$  and the corresponding terminal control gain  $\hat{K}$ .

**Theorem 5.1.** *Under Assumptions 5.2-5.3, for a given scalar  $\delta_3 > 0$ , if there exist matrices  $F$ ,  $\bar{P} \succ 0$ , and  $\bar{H} \succ 0$  such that*

$$\begin{bmatrix} \bar{P} - (1 + \delta_3^{-1}) \gamma_3 \tilde{Z}_{\rho_1+1, L_1} \tilde{Z}_{\rho_1+1, L_1}^T & \tilde{Z}_{\rho_1+1, L_1} F \\ (\tilde{Z}_{\rho_1+1, L_1} F)^T & (1 + \delta_3)^{-1} \bar{H} \end{bmatrix} \succeq 0 \quad (5.20a)$$

$$\begin{bmatrix} I_{L_1} & F \\ F^T & \bar{H} \end{bmatrix} \succeq 0 \quad (5.20b)$$

$$\begin{bmatrix} \bar{H} & \bar{H}^T & (U_{\rho_1, L_1} F)^T \\ \bar{H} & \mathcal{Q}^{-1} & 0 \\ U_{\rho_1, L_1} F & 0 & R^{-1} \end{bmatrix} \succeq 0 \quad (5.20c)$$

$$\bar{H} \succeq 2\bar{P} \quad (5.20d)$$

$$\bar{H} = \tilde{Z}_{\rho_1, L_1} F \quad (5.20e)$$

then (5.10) is satisfied with  $P = \bar{P}^{-1}$  and  $G = F\bar{H}^{-1}$ , and the terminal control

gain is given by

$$\hat{K} = U_{\rho_1, L_1} F \bar{H}^{-1}. \quad (5.21)$$

**Proof.** For (5.20a), using the Schur complement and substituting  $F = G\bar{H}$  and  $\bar{P} = P^{-1}$  yield that

$$(1 + \delta_3)(\tilde{Z}_{\rho_1+1, L_1} G) \bar{H} (\tilde{Z}_{\rho_1+1, L_1} G)^T + (1 + \delta_3^{-1}) \gamma_3 \tilde{Z}_{\rho_1+1, L_1} \tilde{Z}_{\rho_1+1, L_1}^T - P^{-1} \preceq 0. \quad (5.22)$$

According to (5.20b),  $G\bar{H}G^T \preceq I_{L_1}$  holds. Then, combining it with (5.17) in Lemma 5.4 yields that  $(M_{\rho_1, L_1} G) \bar{H} (M_{\rho_1, L_1} G)^T \preceq \gamma_3 \tilde{Z}_{\rho_1+1, L_1} \tilde{Z}_{\rho_1+1, L_1}^T$ , which implies that (5.22) can guarantee that

$$(1 + \delta_3)(\tilde{Z}_{\rho_1+1, L_1} G) \bar{H} (\tilde{Z}_{\rho_1+1, L_1} G)^T + (1 + \delta_3^{-1})(M_{\rho_1, L_1} G) \bar{H} (M_{\rho_1, L_1} G)^T - P^{-1} \preceq 0. \quad (5.23)$$

Then, applying Lemma 5.2 to (5.23) yields that

$$((\tilde{Z}_{\rho_1+1, L_1} + M_{\rho_1, L_1}) G) \bar{H} ((\tilde{Z}_{\rho_1+1, L_1} + M_{\rho_1, L_1}) G)^T - P^{-1} \preceq 0. \quad (5.24)$$

For (5.20c), using the Schur complement yields that

$$\bar{H} \succeq \bar{H}^T \mathcal{Q} \bar{H} + (U_{\rho_1, L_1} F)^T R U_{\rho_1, L_1} F. \quad (5.25)$$

Pre- and post-multiplying (5.25) by  $(\bar{H}^{-1})^T$  and its transpose, and substituting (5.21) into it yield that

$$\bar{H}^{-1} \succeq \mathcal{Q} + (U_{\rho_1, L_1} F \bar{H}^{-1})^T R U_{\rho_1, L_1} F \bar{H}^{-1} = \mathcal{Q} + \hat{K}^T R \hat{K}. \quad (5.26)$$

According to (5.20d),  $\bar{H}^{-1} \preceq P - \bar{H}^{-1}$  holds. Together with (5.26), it indicates that  $(P - \mathcal{Q} - \hat{K}^T R \hat{K})^{-1} \preceq \bar{H}$ . Combining this with (5.24), the following condition is guaranteed:

$$((\tilde{Z}_{\rho_1+1, L_1} + M_{\rho_1, L_1}) G) (P - \mathcal{Q} - \hat{K}^T R \hat{K})^{-1} ((\tilde{Z}_{\rho_1+1, L_1} + M_{\rho_1, L_1}) G)^T - P^{-1} \preceq 0. \quad (5.27)$$

Using the Schur complement, equation (5.27) is equivalent to

$$((\tilde{Z}_{\rho_1+1,L_1} + M_{\rho_1,L_1})G)^T P((\tilde{Z}_{\rho_1+1,L_1} + M_{\rho_1,L_1})G) - (P - Q - \hat{K}^T R \hat{K}) \preceq 0.$$

According to Lemma 5.3, i.e.,  $\hat{A} + \hat{B}\hat{K} = (\tilde{Z}_{\rho_1+1,L_1} + M_{\rho_1,L_1})G$ , equation (5.10) is guaranteed. In addition, equations (5.20e) and (5.21) are consistent with (5.16).  $\blacksquare$

**Remark 5.2.** *Theorem 5.1 involves two important parameters:  $\delta_3$  and  $\gamma_3$ . It is seen from Lemma 5.4 that  $\gamma_3$  is related to  $\delta_1$ ,  $\delta_2$ ,  $\gamma_1$ , and  $\gamma_2$ . Although selecting different parameters may lead to different terminal sets, no big difference on the entire control performance would be caused as these sets work on terminal states only. Hence, here, we are not excessively concerned with the value comparison between these parameters.*

### 5.2.3 The Value of $\alpha$

Based on the designed terminal weighting matrix  $P$  and control gain  $\hat{K}$ ,  $\alpha$  can be obtained by the method in [94] as follows:

$$\begin{aligned} & \max_{\alpha} \alpha \\ \text{s.t.} \quad & \|P^{(-\frac{1}{2})} H_{z,\ell}^T\|^2 \alpha \leq h_{z,\ell}^2, \quad \ell = 1, \dots, n(l_y + l_u) \end{aligned} \quad (5.28a)$$

$$\|P^{(-\frac{1}{2})} \hat{K}^T H_{u,j}^T\|^2 \alpha \leq h_{u,j}^2, \quad j = 1, \dots, l_u \quad (5.28b)$$

where  $H_z = \text{diag}\{\underbrace{H_y, \dots, H_y}_n, \underbrace{H_u, \dots, H_u}_n\}$  and  $h_z = [\underbrace{h_y, \dots, h_y}_n; \underbrace{h_u, \dots, h_u}_n]$ ;  $H_{z,\ell}$  and  $h_{z,\ell}$  correspond to the  $\ell$ th row of  $H_z$  and  $h_z$ , respectively. Since problem (5.28) is a linear program with one variable  $\alpha$ , a variety of efficient solution methods are available to solve it and  $\alpha$  is easy to obtain.

### 5.2.4 Terminal Inequality Constraint

Define a feasible region of the optimization problem in (5.6) as:

$$\begin{aligned} \mathcal{F}(\mathcal{Z}_f, N) = & \{\bar{z}_0 \in \underbrace{\mathbb{R}^{n_y} \times \dots \times \mathbb{R}^{n_y}}_n \times \underbrace{\mathbb{R}^{n_u} \times \dots \times \mathbb{R}^{n_u}}_n \mid \text{there exists } \bar{u}_i \in \mathcal{U}, \\ & i \in \mathbb{Z}_{[0, N-1]} \text{ such that } \bar{y}_i \in \mathcal{Y} \text{ and } \bar{z}_N \in \mathcal{Z}_f\}. \end{aligned}$$

Given a terminal equality set

$$\mathcal{Z}_0 \triangleq \{\bar{z} \in \underbrace{\mathbb{R}^{n_y} \times \cdots \times \mathbb{R}^{n_y}}_n \times \underbrace{\mathbb{R}^{n_u} \times \cdots \times \mathbb{R}^{n_u}}_n \mid \bar{z} = \mathbf{0}_{n(n_y+n_u) \times 1}\},$$

the corresponding feasible region with the terminal equality constraint is  $\mathcal{F}(\mathcal{Z}_0, N)$ . Obviously,  $\mathcal{Z}_0 \subseteq \mathcal{Z}_f$ . Then, we have the following two propositions to show the advantages of terminal inequality constraints over terminal equality counterparts.

**Proposition 5.1.** *Consider a terminal equality set  $\mathcal{Z}_0$  and a terminal inequality set  $\mathcal{Z}_f$  with  $\mathcal{Z}_0 \subseteq \mathcal{Z}_f$ . If there exist two feasible regions  $\mathcal{F}(\mathcal{Z}_0, N)$  and  $\mathcal{F}(\mathcal{Z}_f, N)$  with the same prediction horizon  $N \in \mathbb{Z}_{\geq n}$ , then it holds that  $\mathcal{F}(\mathcal{Z}_0, N) \subseteq \mathcal{F}(\mathcal{Z}_f, N)$ .*

**Proof.** For every initial state  $\bar{z}_t \in \mathcal{F}(\mathcal{Z}_0, N)$ ,  $\bar{z}_t$  can be steered to  $\mathcal{Z}_0$  in  $N$  steps. Since  $\mathcal{Z}_0 \subseteq \mathcal{Z}_f$ ,  $\bar{z}_t$  can also be steered to  $\mathcal{Z}_f$  in  $N$  steps, which implies that the optimization problem with the terminal set  $\mathcal{Z}_f$  is feasible with the initial state  $\bar{z}_t$ . Hence,  $\bar{z}_t \in \mathcal{F}(\mathcal{Z}_f, N)$ . This proves that  $\mathcal{F}(\mathcal{Z}_0, N) \subseteq \mathcal{F}(\mathcal{Z}_f, N)$  because  $\bar{z}_t \in \mathcal{F}(\mathcal{Z}_0, N)$  is arbitrary. ■

**Proposition 5.2.** *Consider a terminal equality set  $\mathcal{Z}_0$  and a terminal inequality set  $\mathcal{Z}_f$  with  $\mathcal{Z}_0 \subseteq \mathcal{Z}_f$ . For two feasible regions  $\mathcal{F}(\mathcal{Z}_0, N_0)$  and  $\mathcal{F}(\mathcal{Z}_f, N_f)$ , where  $N_0 \in \mathbb{Z}_{\geq \underline{N}_0}$ ,  $N_f \in \mathbb{Z}_{\geq \underline{N}_f}$ , and  $\underline{N}_0$  and  $\underline{N}_f$  are the minimum lower bounds of  $N_0$  and  $N_f$ , respectively, it holds that  $\underline{N}_0 \geq \underline{N}_f$ . Specifically,  $\underline{N}_0 = \underline{N}_f$  if and only if  $\mathcal{F}(\mathcal{Z}_0, \underline{N}_f)$  exists.*

**Proof.** According to Proposition 5.1, since  $\mathcal{Z}_0 \subseteq \mathcal{Z}_f$ ,  $\mathcal{F}(\mathcal{Z}_f, \underline{N}_0)$  always exists and it holds that  $\mathcal{F}(\mathcal{Z}_0, \underline{N}_0) \subseteq \mathcal{F}(\mathcal{Z}_f, \underline{N}_0)$ , which implies that  $\underline{N}_f \in \mathbb{Z}_{\geq \underline{N}_0}$ . Since  $\underline{N}_f$  is the minimum lower bound of  $N_f$ , we have  $\mathbb{Z}_{\geq \underline{N}_0} \subseteq \mathbb{Z}_{\geq \underline{N}_f}$ . Hence,  $\underline{N}_0 \geq \underline{N}_f$ .

Two cases should be considered for  $\mathcal{F}(\mathcal{Z}_0, \underline{N}_f)$  under the condition  $\mathcal{Z}_0 \subseteq \mathcal{Z}_f$ . First, there is no such an initial state  $\bar{z}_t \in \mathcal{F}(\mathcal{Z}_f, \underline{N}_f)$  that can be steered to  $\mathcal{Z}_0$  in  $\underline{N}_f$  steps, i.e.,  $\mathcal{F}(\mathcal{Z}_0, \underline{N}_f)$  does not exist, which implies that  $\underline{N}_f < \underline{N}_0$ . Second, there exist some initial states  $\bar{z}_t \in \mathcal{F}(\mathcal{Z}_f, \underline{N}_f)$  that can be steered

to  $\mathcal{Z}_0$  in  $\underline{N}_f$  steps, i.e.,  $\mathcal{F}(\mathcal{Z}_0, \underline{N}_f)$  exists, which implies that  $N_0 \in \mathbb{Z}_{\geq \underline{N}_f}$ . Since  $\underline{N}_0$  is the minimum lower bound of  $N_0$ , we have  $\mathbb{Z}_{\geq \underline{N}_f} \subseteq \mathbb{Z}_{\geq \underline{N}_0}$ . Note that  $\mathbb{Z}_{\geq \underline{N}_0} \subseteq \mathbb{Z}_{\geq \underline{N}_f}$  always holds. Hence,  $\underline{N}_f = \underline{N}_0$  if and only if  $\mathcal{F}(\mathcal{Z}_0, \underline{N}_f)$  exists.  $\blacksquare$

Propositions 5.1 and 5.2 indicate that compared with a terminal equality constraint, a terminal inequality constraint can lead to a larger feasible region and a lower bound for the prediction horizon  $N$ .

**Remark 5.3.** *In the above analysis, we just consider a terminal equality constraint with the origin. We can also consider a more general case for a desired equilibrium  $\bar{z}^e$ . That is to define a terminal inequality set as*

$$\mathcal{Z}_f \triangleq \left\{ \bar{z} \in \underbrace{\mathbb{R}^{n_y} \times \dots \times \mathbb{R}^{n_y}}_n \times \underbrace{\mathbb{R}^{n_u} \times \dots \times \mathbb{R}^{n_u}}_n \mid (\bar{z} - \bar{z}^e)^T P (\bar{z} - \bar{z}^e) \leq \alpha \right\}$$

and the corresponding terminal equality set as

$$\mathcal{Z}_0 \triangleq \left\{ \bar{z} \in \underbrace{\mathbb{R}^{n_y} \times \dots \times \mathbb{R}^{n_y}}_n \times \underbrace{\mathbb{R}^{n_u} \times \dots \times \mathbb{R}^{n_u}}_n \mid \bar{z} = \bar{z}^e \right\}.$$

Similar results can also be obtained as Propositions 5.1-5.2 for these two terminal sets.

### 5.3 Event-Triggered Scheme Design

Most existing event-triggered schemes are derived and implemented based on an explicit model of the plant, and studies based on data-driven approaches remain few. If we extend model-based event-triggered schemes directly, it may not work well due to the unavoidable mismatch between the data-driven model and the original plant. The  $n$ -step strategy proposed in [76], that is, solving the data-driven MPC optimization problem for every  $n$ -step regardless of this mismatch, has the same problem. Specifically, if there is a significant mismatch between the data-driven model and the original plant, even if the optimization problem can be solved, the obtained predicted trajectory usually does not satisfy the dynamics of the original system. Hence, in a data-driven

framework, we need to design a novel event-triggered scheme that can not only take this mismatch into consideration, but also save computational resources effectively, which is undoubtedly a great challenge.

Seen from Figure 5.1, there is a feedback from the robust data-driven MPC controller to the event trigger which can be used to characterize the mismatch between the data-driven model and the original plant, namely, the output error  $e(t)$ . As mentioned in Section 5.1, if  $e(t)$  actually coincides with the actual noise  $\omega(t)$ , then it indicates that the data-driven model is nearly consistent with the original plant. Thus, the output error  $e(t)$  can be regarded as an empirically observed counterpart of the actual noise  $\omega(t)$  and we can link this connection to the event verification. Although true noises in the control process are unknown to both controller and event trigger, we can use Assumption 5.1 on noises to design the event trigger in (5.7) to decide when to solve (5.6).

### 5.3.1 Triggering Threshold

Define the triggering function as  $\varphi(e(t)) = \|e(t)\|$ , which can be regarded as an empirical index related to noises and is sampled from the control process. Comparatively, the theoretical index is  $\varphi(\omega(t)) = \|\omega(t)\|$ , which is a random variable because  $\omega(t)$  is assumed to be independently and identically distributed. Hence, by checking if empirically observed indexes  $\varphi(e(t))$  coincide with theoretically derived properties, we are able to detect significant mismatches between the data-driven model and the original plant. Accordingly, based on Assumption 5.1, we can construct both deterministic and stochastic criteria to select the triggering threshold  $\kappa$  in (5.7).

First, if there is no access to any information of stochastic distribution of noises, a deterministic event-triggered condition can be considered, i.e., directly pre-specifying the threshold  $\kappa$  based on the condition  $\|\omega(t)\|^2 \leq \bar{\omega}$ :

$$0 \leq \kappa \leq \sqrt{\bar{\omega}} + \epsilon, \quad (5.29)$$

where  $\epsilon \geq 0$  is a prescribed scalar which is used to compensate for tracking or

other unknown errors.

Second, if some information about stochastic distribution of noises is known, a stochastic event-triggered condition can be generated to choose  $\kappa$  from a statistical point of view such that

$$\mathbb{P}(\|e(t)\| > \kappa) < \eta, \quad (5.30)$$

i.e., the probability of triggering is less than a desired confidence level  $\eta$ . We are able to adopt the following Markov's inequality to design  $\kappa$  in (5.30).

**Lemma 5.5.** [82] *If  $X$  is a random variable with  $\mathbb{E}(\|X\|^r) < \infty$  for  $r > 0$  and  $\kappa > 0$ , then*

$$\mathbb{P}(\|X\| > \kappa) \leq \frac{\mathbb{E}(\|X\|^r)}{\kappa^r}.$$

According to Lemma 5.5, if we can derive the mean, variance, or higher moments of the random variable  $\|\omega(t)\|$  based on known information of noises, given a desired confidence level  $\eta$ , the threshold  $\kappa$  can be designed by

$$\kappa = \sqrt[r]{\frac{\mathbb{E}(\|\omega(t)\|^r)}{\eta}}, \quad (5.31)$$

where the parameter  $r$  represents the  $r$ -th moment of  $\|\omega(t)\|$  and can be selected based on known information of noises.

As the event-triggered condition is dependent on the output errors, the feedback from the robust data-driven MPC controller to the event trigger plays a significant role in our design. Note that this feedback not only affects the event verification, but also can be used to tune parameters  $\lambda_\varepsilon$  and  $\lambda_g$  of the robust data-driven MPC optimization problem in (5.6) manually, since an inappropriate  $\lambda_\varepsilon$  or  $\lambda_g$  may lead to large output errors.

### 5.3.2 Event-Triggered Controller

The event-triggered controller in (5.9) to be designed consists of a robust MPC controller and a local controller. At the triggering instant  $t_j$ , the robust data-driven MPC optimization problem is solved and the optimal solution



$\{\bar{u}_{[-n, N-1]}^*(t_j), \bar{y}_{[-n, N-1]}^*(t_j), g^*(t_j), \varepsilon_{[-n, N-1]}^*(t_j)\}$  is obtained. Then, for  $t_j \leq t < t_j + N$ , the control input applied to the plant is  $u(t) = \bar{u}_{t-t_j}^*(t_j)$ ; for  $t_j + N \leq t < t_{j+1}$ , namely,  $\Delta_j \geq N$ , the local controller in (5.8) starts to work. To guarantee recursive feasibility of robust data-driven MPC and stability of the system, the local controller gain is determined by the terminal control gain of robust MPC, namely,  $K_{\text{loc}} = \hat{K}$ . Consequently, the event-triggered controller is designed by

$$u(t) = \begin{cases} \bar{u}_{t-t_j}^*(t_j), & t_j \leq t < t_j + N, \\ \hat{K}\bar{z}(t), & t_j + N \leq t < t_{j+1}. \end{cases} \quad (5.32)$$

Note that the local controller works for  $\Delta_j \geq N$  only. If the triggering threshold  $\kappa$  is sufficiently small or the prediction horizon  $N$  is sufficiently large, then it is impossible that the inter-execution time  $\Delta_j$  exceeds the prediction horizon  $N$  and thus the local controller may never be used.

## 5.4 Recursive Feasibility and Stability Analysis

In this section, recursive feasibility of the proposed event-triggered robust data-driven MPC and stability of the system in (5.3) are analyzed. The analysis of recursive feasibility is based on the solutions of the optimization problem after a period of time. Assume that the data-driven MPC controller can store all predicted data. At  $t \in \mathbb{Z}_{>0}$ , pick  $\{\bar{u}_{[\rho_2-n, \rho_2-n+L_2-1]}, \bar{y}_{[\rho_2-n, \rho_2-n+L_2-1]}\}$  from past predicted data, where  $L_2 \in \mathbb{Z}_{\geq n_u + (n_y + n_u)n}$  and  $\rho_2 \in \mathbb{Z}_{[n, t-L_2+1]}$ , and obtain the associated Hankel matrices  $\bar{U}_{\rho_2, L_2}$  and  $\bar{Z}_{\rho_2, L_2}$ . Then, we provide the following lemma for the prediction model in (5.4).

**Lemma 5.6.** *Let  $\begin{bmatrix} \bar{U}_{\rho_2, L_2} \\ \bar{Z}_{\rho_2, L_2} \end{bmatrix}$  be full-row rank. The prediction model in (5.4) with a state feedback  $\bar{u} = \hat{K}\bar{z}$  has an equivalent representation:*

$$\bar{z}(t+1) = \Xi \bar{z}(t), \quad (5.33)$$

where  $\Xi \triangleq \bar{Z}_{\rho_2+1, L_2} \begin{bmatrix} \bar{U}_{\rho_2, L_2} \\ \bar{Z}_{\rho_2, L_2} \end{bmatrix}^\dagger \begin{bmatrix} U_{\rho_1, L_1} G \\ \tilde{Z}_{\rho_1, L_1} G \end{bmatrix}$ .

**Proof.** According to Theorem 1 in [91], we have the following representation for unknown system matrices:

$$[\hat{B} \ \hat{A}] = \bar{Z}_{\rho_2+1, L_2} \begin{bmatrix} \bar{U}_{\rho_2, L_2} \\ \bar{Z}_{\rho_2, L_2} \end{bmatrix}^\dagger. \quad (5.34)$$

Then, substituting  $\bar{u} = \hat{K}\bar{z}$ , (5.34), and (5.16) into (5.4) yields (5.33).  $\blacksquare$

**Remark 5.4.** Although both (5.15) and (5.33) show an equivalent representation of  $\hat{A} + \hat{B}\hat{K}$ , they have different roles: (5.15) is helpful to the design of the terminal set with available data and cannot be calculated since  $M_{\rho_1, L_1}$  is unknown; while (5.33) is used for the analysis of recursive feasibility after the whole design is completed, and can be calculated with the predicted data.

At  $t \in \mathbb{Z}_{>t_j}$ , by using (5.33), the candidate predicted output  $\bar{y}_{[0, N-1]}(t)$  and input  $\bar{u}_{[0, N-1]}(t)$  can be constructed based on the latest optimal solution  $\{\bar{u}_{[0, N-1]}^*(t_j), \bar{y}_{[0, N-1]}^*(t_j)\}$ . If  $\Delta_j < N$ , we have that

$$\begin{cases} \bar{y}_i(t_{j+1}) = \begin{cases} \bar{y}_{i+\Delta_j}^*(t_j), & i \in \mathbb{Z}_{[0, N-1-\Delta_j]}, \\ \Lambda_y \Xi^{\Delta_j - N + i + 1} \bar{z}_N^*(t_j), & i \in \mathbb{Z}_{[N-\Delta_j, N-1]}, \end{cases} \\ \bar{u}_i(t_{j+1}) = \begin{cases} \bar{u}_{i+\Delta_j}^*(t_j), & i \in \mathbb{Z}_{[0, N-1-\Delta_j]}, \\ \hat{K} \Xi^{\Delta_j - N + i} \bar{z}_N^*(t_j), & i \in \mathbb{Z}_{[N-\Delta_j, N-1]}, \end{cases} \end{cases} \quad (5.35)$$

where  $\Lambda_y = [\mathbf{0}_{n_y \times n_y(n-1)} \ I_{n_y} \ \mathbf{0}_{n_y \times n_u n}]$ . If  $\Delta_j \geq N$ , we have

$$\begin{cases} \bar{y}_i(t_{j+1}) = \Lambda_y \Xi^{\Delta_j - N + i + 1} \bar{z}_N^*(t_j), \\ \bar{u}_i(t_{j+1}) = \hat{K} \Xi^{\Delta_j - N + i} \bar{z}_N^*(t_j), \end{cases} \quad i \in \mathbb{Z}_{[0, N-1]}. \quad (5.36)$$

### 5.4.1 Recursive Feasibility

**Theorem 5.2.** Under Assumptions 5.1-5.3, if the optimization problem in (5.6) is feasible at  $t_j$ , then it is feasible at  $t_{j+1}$ .

**Proof.** Based on the optimal solution of the triggering instant  $t_j$ , a feasible candidate solution  $\{\bar{u}_{[-n, N-1]}(t_{j+1}), \bar{y}_{[-n, N-1]}(t_{j+1}), g(t_{j+1}), \varepsilon_{[-n, N-1]}(t_{j+1})\}$  can be constructed at  $t_{j+1}$ . For  $i \in \mathbb{Z}_{[-n, -1]}$ ,  $\bar{y}_i(t_{j+1}) = \bar{y}_{i+\Delta_j}^*(t_j) + e(t_{j+1} + i)$

and  $\bar{u}_i(t_{j+1}) = \bar{u}_{i+\Delta_j}^*(t_j)$  such that constraint (5.6b) is satisfied. Then, according to (5.35) or (5.36),  $\bar{y}_{[0,N-1]}(t_{j+1})$  and  $\bar{u}_{[0,N-1]}(t_{j+1})$  are constructed and satisfy that

$$\begin{bmatrix} \bar{u}_{[-n,N-1]}(t_{j+1}) \\ \bar{y}_{[-n,N-1]}(t_{j+1}) \end{bmatrix} = \Omega^{\Delta_j} \begin{bmatrix} \bar{u}_{[-n,N-1]}^*(t_j) \\ \bar{y}_{[-n,N-1]}^*(t_j) \end{bmatrix} + \begin{bmatrix} \mathbf{0}_{(n+N)n_u \times 1} \\ e_{[t_{j+1}-n,t_{j+1}-1]} \\ \mathbf{0}_{Nn_y \times 1} \end{bmatrix}, \quad (5.37)$$

where

$$\Omega = \begin{bmatrix} [\mathbf{0}_{(n+N-1)n_u \times n_u} & I_{(n+N-1)n_u} & \mathbf{0}_{(n+N-1)n_u \times (n+N)n_y}] \\ & \hat{K} \Lambda_{yu} & \\ [\mathbf{0}_{(n+N-1)n_y \times (n+N)n_u} & \mathbf{0}_{(n+N-1)n_y \times n_y} & I_{(n+N-1)n_y}] \\ & \Lambda_y \Xi \Lambda_{yu} & \end{bmatrix},$$

$$\Lambda_{yu} = \begin{bmatrix} \mathbf{0}_{n_y n \times (n+N)n_u} & [\mathbf{0}_{n_y n \times Nn_y} & I_{n_y n}] \\ [\mathbf{0}_{n_u n \times Nn_u} & I_{n_u n}] & \mathbf{0}_{n_u n \times (n+N)n_y} \end{bmatrix}.$$

Assumption 5.2 indicates that the matrix  $\begin{bmatrix} U_{-n,n+N,L-(n+N)+1} \\ \tilde{Y}_{-n,n+N,L-(n+N)+1} \end{bmatrix}$  has full row rank, thus it admits a right inverse. Accordingly,  $\varepsilon_{[-n,N-1]}(t_{j+1})$  and  $g(t_{j+1})$  are chosen as

$$\varepsilon_{[-n,N-1]}(t_{j+1}) = \Lambda_\varepsilon \Omega^{\Delta_j} \begin{bmatrix} \mathbf{0}_{(n+N)n_u \times 1} \\ \varepsilon_{[-n,N-1]}^*(t_j) \end{bmatrix}, \quad (5.38)$$

$$g(t_{j+1}) = \begin{bmatrix} U_{-n,n+N,L-(n+N)+1} \\ \tilde{Y}_{-n,n+N,L-(n+N)+1} \end{bmatrix}^\dagger \left( \Omega^{\Delta_j} \begin{bmatrix} U_{-n,n+N,L-(n+N)+1} \\ \tilde{Y}_{-n,n+N,L-(n+N)+1} \end{bmatrix} \right. \\ \left. g^*(t_j) + \begin{bmatrix} -\Lambda_g \Omega^{\Delta_j} \begin{bmatrix} \mathbf{0}_{(n+N)n_u \times 1} \\ \varepsilon_{[-n,N-1]}^*(t_j) \end{bmatrix} \\ e_{[t_{j+1}-n,t_{j+1}-1]} \\ \mathbf{0}_{Nn_y \times 1} \end{bmatrix} \right), \quad (5.39)$$

where  $\Lambda_\varepsilon = [\mathbf{0}_{(n+N)n_y \times (n+N)n_u} & I_{(n+N)n_y}]$  and  $\Lambda_g = [I_{(n+N)n_u} & \mathbf{0}_{(n+N)n_u \times (n+N)n_y}]$ . Combining (5.37), (5.38), and (5.39) indicates that constraint (5.6a) is guaranteed.

If  $\Delta_j < N$ , for  $i \in \mathbb{Z}_{[0,N-1-\Delta_j]}$ , since  $\bar{u}_{i+\Delta_j}^*(t_j) \in \mathcal{U}$  and  $\bar{y}_{i+\Delta_j}^*(t_j) \in \mathcal{Y}$ , it follows  $\bar{u}_i(t_{j+1}) \in \mathcal{U}$  and  $\bar{y}_i(t_{j+1}) \in \mathcal{Y}$ . For  $i \in \mathbb{Z}_{[N-\Delta_j,N-1]}$ , since  $\bar{z}_N^*(t_j) \in \mathcal{Z}_f$ , we have that  $\bar{z}_N^*(t_j)^\top (\hat{A} + \hat{B}\hat{K})^\top P (\hat{A} + \hat{B}\hat{K}) \bar{z}_N^*(t_j) \leq \bar{z}_N^*(t_j)^\top P \bar{z}_N^*(t_j)$ , which implies that constraint (5.6e) is guaranteed. Combining it with (5.28a) yields

that

$$\begin{aligned} \|P^{(-\frac{1}{2})} H_{z,\ell}^T\|^2 \alpha &= \|P^{(-\frac{1}{2})} H_{z,\ell}^T\|^2 \|\bar{z}_N^*(t_j)^T P^{\frac{1}{2}}\|^2 \\ &\geq \|H_{z,\ell} \bar{z}_N^*(t_j)\|^2, \quad \ell = 1, \dots, n(l_y + l_u), \end{aligned}$$

which implies that  $H_y \bar{y}_i(t_{j+1}) \leq h_y$ . According to (5.28b), we have  $H_u \bar{u}_i(t_{j+1}) \leq h_u$ . Hence, constraints (5.6c) and (5.6d) are guaranteed. If  $\Delta_j \geq N$ , according to (5.36), similar results are obtained to guarantee constraints (5.6c)-(5.6e). Therefore, at  $t_{j+1}$ , the optimization problem in (5.6) is feasible with the constructed candidate solution.  $\blacksquare$

## 5.4.2 Input-to-State Stability

To analyze the stability, a variant of definition on input-to-state stability in [95] is given. Before proceeding, we need to introduce the following notations: A function  $\sigma: \mathbb{R}_{\geq 0} \rightarrow \mathbb{R}_{\geq 0}$  is a  $\mathcal{K}$  function if it is continuous, strictly increasing, and  $\sigma(0) = 0$ ; A function  $\beta$  is a  $\mathcal{K}_\infty$  function if it is a  $\mathcal{K}$  function and  $\beta(x) \rightarrow \infty$  as  $x \rightarrow \infty$ .

**Definition 5.2.** *System (5.3) with data-driven model (5.6a) is input-to-state stable (ISS) with  $e(t)$  and  $g(t)$  as the inputs, if there exist a positive definite function  $J(\tilde{z}(t))$ ,  $\mathcal{K}_\infty$  functions  $\beta_1$ ,  $\beta_2$ , and  $\beta_3$ , and  $\mathcal{K}$  functions  $\sigma_1$  and  $\sigma_2$  such that  $\beta_1(\|\tilde{z}(t)\|) \leq J(\tilde{z}(t)) \leq \beta_2(\|\tilde{z}(t)\|)$  and  $J(\tilde{z}(t+1)) - J(\tilde{z}(t)) \leq -\beta_3(\|\tilde{z}(t)\|) + \sigma_1(\|e(t)\|) + \sigma_2(\|g(t)\|)$ .*

**Theorem 5.3.** *Under Assumptions 5.1-5.3, system (5.3) with data-driven model (5.6a) is ISS under the event-triggered condition in (5.7).*

**Proof.** According to the candidate solution, the candidate cost  $J(\tilde{z}(t_{j+1}))$  can

be derived by

$$\begin{aligned}
J(\tilde{z}(t_{j+1})) &= J^*(\tilde{z}(t_j)) - \sum_{i=0}^{N-1} l(\bar{u}_{i-1}^*(t_j), \bar{y}_{i-1}^*(t_j)) - V(\bar{z}_N^*(t_j)) \\
&\quad + \sum_{i=0}^{N-1} l(\bar{u}_{i-1}(t_{j+1}), \bar{y}_{i-1}(t_{j+1})) + V(\bar{z}_N(t_{j+1})) \\
&\quad + \lambda_\varepsilon (\|\varepsilon_{[-n, N-1]}(t_{j+1})\|^2 - \|\varepsilon_{[-n, N-1]}^*(t_j)\|^2) \\
&\quad + \lambda_g \bar{\omega} (\|g(t_{j+1})\|^2 - \|g^*(t_j)\|^2). \tag{5.40}
\end{aligned}$$

Firstly, we need to derive some useful bounds for the terms in (5.40). Accordingly, input-to-state stability will be proved.

**1) Bound of  $\|\varepsilon_{[-n, N-1]}^*(t_j)\|^2$**

At the triggering instant  $t_j$ , since  $\tilde{Y}_{-n, n+N, L-(n+N)+1} = Y_{-n, n+N, L-(n+N)+1} + W_{-n, n+N, L-(n+N)+1}$  and the predicted output  $\bar{y}_{[-n, N-1]}^*(t_j)$  is assumed to satisfy  $\bar{y}_{[-n, N-1]}^*(t_j) = Y_{-n, n+N, L-(n+N)+1} g^*(t_j)$ . According to (5.6a) and (5.6b), we have that

$$\begin{aligned}
\begin{bmatrix} \varepsilon_{[-n, -1]}^*(t_j) \\ \varepsilon_{[0, N-1]}^*(t_j) \end{bmatrix} &= \begin{bmatrix} \tilde{Y}_{-n, n, L-(n+N)+1} \\ \tilde{Y}_{0, N, L-(n+N)+1} \end{bmatrix} g^*(t_j) - \begin{bmatrix} \tilde{y}_{[t_j-n, t_j-1]} \\ \bar{y}_{[0, N-1]}^*(t_j) \end{bmatrix} \\
&= \begin{bmatrix} W_{-n, n, L-(n+N)+1} g^*(t_j) - e_{[t_j-n, t_j-1]} \\ W_{0, N, L-(n+N)+1} g^*(t_j) \end{bmatrix}, \tag{5.41}
\end{aligned}$$

which demonstrates that the slack variable  $\varepsilon_{[-n, N-1]}(t_j)$  can account for the noisy part. Since  $\|W_{i, L-(n+N)+1}\|^2 \leq \text{trace}(W_{i, L-(n+N)+1} W_{i, L-(n+N)+1}^T) = (L - (n + N) + 1)\bar{\omega}$ ,  $i \in \mathbb{Z}$ , by applying Lemma 5.2 to (5.41), we have that

$$\begin{aligned}
\|\varepsilon_{[-n, N-1]}^*(t_j)\|^2 &\leq ((1 + \delta_4)n + N)(L - (n + N) + 1)\bar{\omega} \|g^*(t_j)\|^2 \\
&\quad + (1 + \delta_4^{-1}) \|e_{[t_j-n, t_j-1]}\|^2. \tag{5.42}
\end{aligned}$$

**2) Bound of  $\|\varepsilon_{[-n, N-1]}(t_{j+1})\|^2 - \|\varepsilon_{[-n, N-1]}^*(t_j)\|^2$**

According to (5.38), we have that

$$\|\varepsilon_{[-n, N-1]}(t_{j+1})\|^2 \leq \|\Omega^{\Delta_j}\|^2 \|\varepsilon_{[-n, N-1]}^*(t_j)\|^2.$$

Since (5.10) is guaranteed, it follows that  $\lim_{\Delta_j \rightarrow \infty} \|\Xi^{\Delta_j}\|^2 = 0$ , which implies that  $\lim_{\Delta_j \rightarrow \infty} \|\Omega^{\Delta_j}\|^2 = 0$ . Note that  $\|\Omega\|^2 \geq 1$  since “1” is a singular value of

$\Omega$  and  $\|\Lambda_\varepsilon\|^2 = 1$ . Hence, there must exist  $\theta \in \mathbb{Z}_{\geq 1}$  such that  $\|\Omega^\theta\|^2 \geq 1$  and  $\|\Omega^\theta\|^2 \geq \|\Omega^{\Delta_j}\|^2$  for all  $\Delta_j \in \mathbb{Z}_{\geq 1}$ . Hence, we have that

$$\|\varepsilon_{[-n, N-1]}(t_{j+1})\|^2 - \|\varepsilon_{[-n, N-1]}^*(t_j)\|^2 \leq (\|\Omega^\theta\|^2 - 1)\|\varepsilon_{[-n, N-1]}^*(t_j)\|^2. \quad (5.43)$$

### 3) Bound of $\|g(t_{j+1})\|^2 - \|g^*(t_j)\|^2$

According to (5.39), we have

$$\begin{aligned} \|g(t_{j+1})\|^2 &\leq \frac{\mu_1}{\mu_2}(1 + \delta_5)\|\Omega^\theta\|^2\|g^*(t_j)\|^2 + \frac{1}{\mu_2}(1 + \delta_5^{-1})\|\Omega^{\Delta_j}\|^2 \\ &\times \|\varepsilon_{[-n, N-1]}^*(t_j)\|^2 + \frac{1}{\mu_2}(1 + \delta_5^{-1})\|\hat{A}^{\Delta_j}\|^2\|e_{[t_j-n, t_j-1]}\|^2, \end{aligned} \quad (5.44)$$

where  $\hat{A}$  is obtained by (5.34), and

$$\begin{aligned} \begin{bmatrix} e_{[t_{j+1}-n, t_{j+1}-1]} \\ \mathbf{0}_{nn_u \times 1} \end{bmatrix} &= \hat{A}^{\Delta_j} \begin{bmatrix} e_{[t_j-n, t_j-1]} \\ \mathbf{0}_{nn_u \times 1} \end{bmatrix}, \\ \mu_1 &= \lambda_{\max} \left( \begin{bmatrix} U_{-n, n+N, L-(n+N)+1} \\ \tilde{Y}_{-n, n+N, L-(n+N)+1} \end{bmatrix} \begin{bmatrix} U_{-n, n+N, L-(n+N)+1} \\ \tilde{Y}_{-n, n+N, L-(n+N)+1} \end{bmatrix}^T \right), \\ \mu_2 &= \lambda_{\min} \left( \begin{bmatrix} U_{-n, n+N, L-(n+N)+1} \\ \tilde{Y}_{-n, n+N, L-(n+N)+1} \end{bmatrix} \begin{bmatrix} U_{-n, n+N, L-(n+N)+1} \\ \tilde{Y}_{-n, n+N, L-(n+N)+1} \end{bmatrix}^T \right). \end{aligned}$$

Note that  $\frac{\mu_1}{\mu_2}\|\Omega^\theta\|^2 \geq 1$  and  $\|\Lambda_g\|^2 = 1$ .

### 4) Bound of $V(\bar{z}_N(t_{j+1})) - V(\bar{z}_N(t_j))$

Since  $\bar{z}_N(t_{j+1}) = \Xi^{\Delta_j} \bar{z}_N^*(t_j)$ , combining this with (5.10) and (5.33) yields that

$$\begin{aligned} V(\bar{z}_N(t_{j+1})) - V(\bar{z}_N(t_j)) &\leq - \sum_{i=0}^{h-1} \bar{z}_N(t_j)^T \Xi^{iT} (\mathcal{Q} + \hat{K}^T R \hat{K}) \Xi^i \bar{z}_N(t_j) \\ &\leq - \sum_{i=0}^{h-1} l(\bar{u}_{N-i-1}(t_{j+1}), \bar{y}_{N-i-1}(t_{j+1})), \end{aligned} \quad (5.45)$$

where  $h \triangleq \min\{N, \Delta_j\}$ .

### 5) ISS

Let  $\mathcal{G} = \text{diag}\{\underbrace{\mathbf{0}_{n_y \times n_y}, \dots, \mathbf{0}_{n_y \times n_y}}_{n-1}, \mathcal{Q}, \underbrace{\mathbf{0}_{n_u \times n_u}, \dots, \mathbf{0}_{n_u \times n_u}}_{n-1}, R\}$ . Then, we have that  $l(\bar{u}_{i-1}^*(t_j), \bar{y}_{i-1}^*(t_j)) = \bar{z}_i^*(t_j)^T \mathcal{G} \bar{z}_i^*(t_j)$ . Accordingly, there exists a  $q > 0$  such that  $l(\bar{u}_{i-1}^*(t_j), \bar{y}_{i-1}^*(t_j)) \geq q\|\bar{z}_i^*(t_j)\|^2$ . According to (5.6a) and (5.6b),

we have that  $\bar{z}_0^*(t_j) = \tilde{z}(t_j)$  and  $\bar{y}_{-1}(t_{j+1}) = \tilde{Y}_{-1,L-(n+N)+1}g(t_{j+1}) - \varepsilon_{-1}(t_{j+1})$ . Note that the optimal cost at the triggering instant  $t_{j+1}$  satisfies  $J^*(\tilde{z}(t_{j+1})) \leq J(\tilde{z}(t_{j+1}))$ . Then, substituting (5.42), (5.43), (5.44), and (5.45) into (5.40) yields that

$$\begin{aligned} & J^*(\tilde{z}(t_{j+1})) - J^*(\tilde{z}(t_j)) \\ & \leq -q\|\tilde{z}^*(t_j)\|^2 + \psi_1\|e_{[t_j-n,t_j-1]}\|^2 + \psi_2\|g^*(t_j)\|^2, \end{aligned} \quad (5.46)$$

where

$$\begin{aligned} \psi_1 &= \frac{1}{\mu_2}(\psi_3 + \lambda_g\bar{\omega})(1 + \delta_5^{-1})\|\hat{A}^{\Delta_j}\|^2 + \psi_4(1 + \delta_4^{-1}), \\ \psi_2 &= \frac{\mu_1}{\mu_2}(\psi_3 + \lambda_g\bar{\omega})(1 + \delta_5)\|\Omega^\theta\|^2 + \psi_5 - \lambda_g\bar{\omega}, \\ \psi_3 &= (1 + \delta_6)\lambda_{\max}(Q)\|\tilde{Y}_{-1,L-(n+N)+1}\|^2, \\ \psi_4 &= \frac{1}{\mu_2}(\psi_3 + \lambda_g\bar{\omega})(1 + \delta_5^{-1})\|\Omega^{\Delta_j}\|^2 + ((1 + \delta_6^{-1})\lambda_{\max}(Q) + \lambda_\varepsilon)\|\Omega^\theta\|^2 - \lambda_\varepsilon, \\ \psi_5 &= \psi_4((1 + \delta_4)n + N)(L - (n + N) + 1)\bar{\omega}. \end{aligned}$$

According to Definition 2, system (5.3) with data-driven model (5.6a) is ISS. ■

## 5.5 Simulation Example

**Example 5.1.** Consider the four tank system provided in [76]:

$$\begin{aligned} x(t+1) &= \begin{bmatrix} 0.921 & 0 & 0.041 & 0 \\ 0 & 0.918 & 0 & 0.033 \\ 0 & 0 & 0.924 & 0 \\ 0 & 0 & 0 & 0.937 \end{bmatrix} x(t) + \begin{bmatrix} 0.017 & 0.001 \\ 0.001 & 0.023 \\ 0 & 0.061 \\ 0.072 & 0 \end{bmatrix} u(t) \\ y(t) &= \begin{bmatrix} 1 & 0 & 0 & 0 \\ 0 & 1 & 0 & 0 \end{bmatrix} x(t). \end{aligned}$$

An input-output trajectory of length  $L = 400$  is measured, where the input is chosen randomly from the unit interval and the output is subject to uniformly distributed noises in  $[-0.002, 0.002]^2$ ; the simulation step is  $T_{\text{sim}} = 200$ ; the control goal is to track the setpoints:  $y_s = [0.65; 0.77]$  and  $u_s = [1; 1]$ . We execute a Monte Carlo simulation with 100 samples. To verify the effectiveness

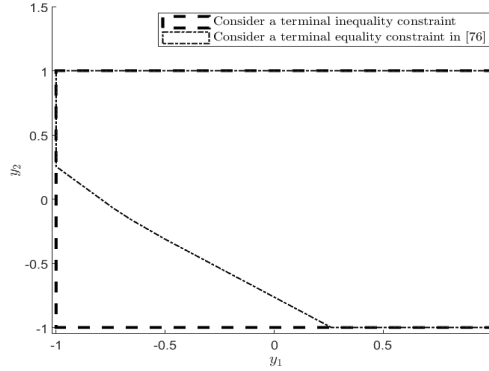


Figure 5.2: Feasible regions with different terminal constraints.

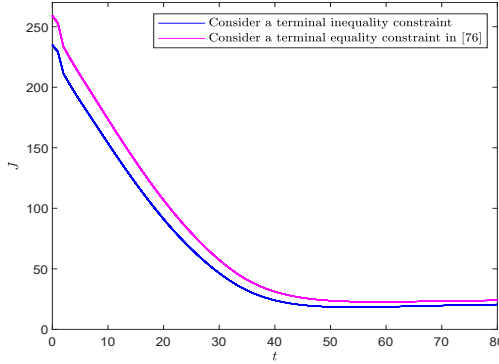


Figure 5.3: Evolutions of  $J$  with different terminal constraints.

of the proposed approach, we compare it with a multistep data-driven MPC strategy with a terminal equality constraint in [76] and have the two following groups of comparisons.

**A. A terminal inequality constraint vs. a terminal equality constraint**

To construct a terminal inequality constraint, we pick some data with  $L_1 = 200$  and  $\rho_1 = 0$  from the initial input-output trajectory, and choose  $\gamma_1 = 0.08$ ,  $\gamma_2 = 10$ ,  $\delta_1 = 0.5$ , and  $\delta_2 = 0.1$ . Then, by solving problems (5.20) and (5.28) off-line, the terminal ingredients are obtained. Although the introduction of the slack variable  $\varepsilon_{[-n, N-1]}(t)$  ensures the feasibility of the optimization problem in (5.6) at all instants, it also lowers the effects of terminal constraints on the feasibility of (5.6). Hence, to focus on such effects, we firstly select a feasible  $\varepsilon_{[-n, N-1]}(t)$  by solving (5.6) and then depict the



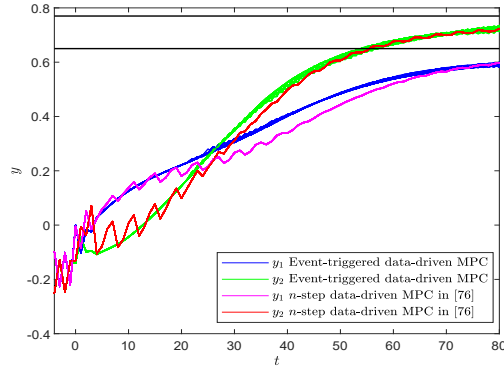


Figure 5.4: Output trajectories with different triggering strategies.

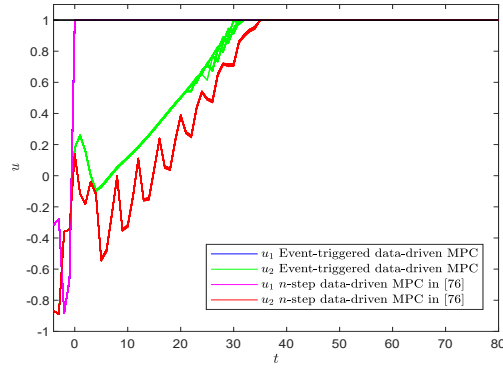


Figure 5.5: Control input trajectories with different triggering strategies.

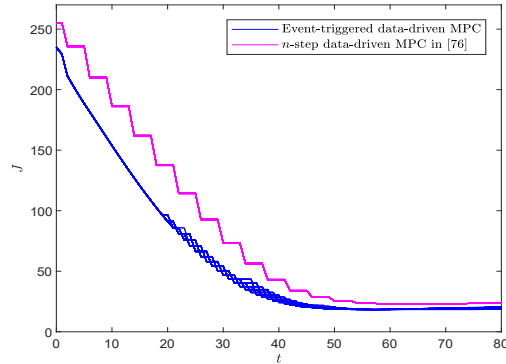


Figure 5.6: Evolutions of  $J$  with different triggering strategies.

feasible regions for different terminal constraints, respectively, which are shown in Figure 5.2. It is seen that the feasible region with a terminal inequality constraint is larger than that with a terminal equality constraint. Seen from Figure 5.3, the evolution of the performance cost  $J$  of the optimization problem

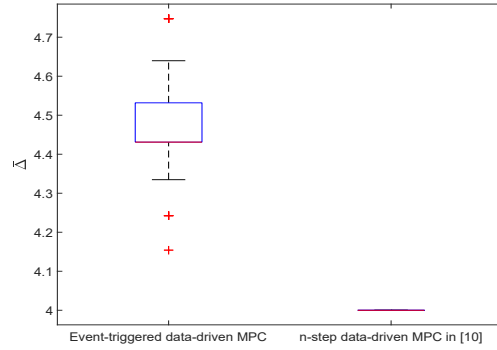


Figure 5.7: Average inter-execution time comparison.

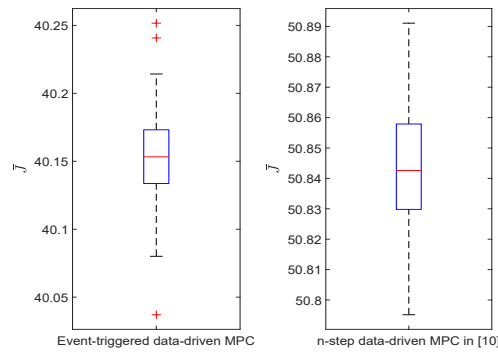


Figure 5.8: Performance cost comparison.

with a terminal inequality constraint is better.

### B. Event-triggered scheme vs. $n$ -step strategy

To show the advantages of the proposed event-triggered scheme over the multistep strategy provided in [76], the deterministic event-triggered scheme in (5.29) with  $\kappa = 0.03$  is considered. Seen from Figures 5.4-5.6, the  $n$ -step strategy in [76] provides worse control performance and causes wider fluctuations of outputs before the system is controlled well; by using the designed event-triggered scheme, the optimization problem is solved frequently at the beginning and then the number of triggering instants become decreasing after the system is in good control, while the instants of solving the optimization problem in the  $n$ -step strategy are fixed, which reflects the flexibility of the proposed approach. Box plots in Figures 5.7-5.8 are used to show average inter-execution times and control performance costs, which implies that the

proposed event-triggered data-driven MPC controller can obtain a longer average inter-execution time and better control performance than that in [76].

## 5.6 Summary

In this chapter, an event-triggered robust MPC approach with a terminal inequality constraint has been proposed for unknown systems by using initially measured input-output data only. Compared with a terminal equality constraint, the constructed terminal inequality constraint for the data-driven MPC optimization problem can lead to a larger feasible region and a lower bound for the prediction horizon, and simplify the analysis of recursive feasibility and input-to-state stability. An event-triggered scheme has been designed to trigger the solution of the data-driven MPC optimization problem when necessary, leading to the reduction of resource consumption. Simulation results have verified the effectiveness of the proposed approach.

# Chapter 6

## An Application to Constrained Queueing Networks \*

This chapter investigates an event-triggered stochastic MPC approach for the scheduling problem of constrained queueing networks. Motivated by the idea of event verification in Chapter 4, a novel event-triggered scheme combining event checking and triggering with the arrival frequency and the number of new packets is designed to achieve non-persistent event monitoring and verification. Under this scheme, a stochastic MPC optimization problem which considers the constituency and positiveness constraints, the dynamic topology, and the stochasticity in packet arrival is solved when necessary, leading to reduced computational burden and improved utilization of communication resources. With a constructed stability region of arrival rates, the stability of queueing networks is discussed by the relation between the inter-execution time and objective function.

This chapter is organized as follows. Section 6.1 describes a queueing network with constraints and formulates a control strategy for the scheduling problem. Section 6.2 designs an event-triggered stochastic MPC approach. Section 6.3 discusses the stability of queueing networks. Section 6.4 verifies the proposed approach by numerical examples. Section 6.5 concludes this chapter.

---

\*A version of this chapter has been submitted to *IEEE Transactions on Network Science and Engineering* as: Li Deng, Zhan Shu, and Tongwen Chen, Event-triggered stochastic model predictive control for constrained queueing networks, Jun. 2023.

## 6.1 Problem Formulation

Consider a discrete-time, packet-level network consisting of  $n_q$  queues and  $n_u$  links:

$$q(t+1) = q(t) + R(t)u(t) + a(t), \quad (6.1)$$

where  $q(t) \in \mathbb{Z}^{+n_q}$  is the queue vector which includes the number of packets waiting in each queue in time slot  $t \in \mathbb{Z}^+$ , namely,  $q(t)^{[i]}$ ,  $i = 1, 2, \dots, n_q$  represents the length of  $i$ th queue;  $u(t) \in \{0, 1\}^{n_u}$  is the binary control vector and  $\{0, 1\}^{n_u}$  represents the set of  $n_u$ -dimensional vectors with elements being 0 or 1;  $a(t) \in \mathbb{Z}^{+n_q}$  is a stochastic arrival vector and  $\bar{a} \triangleq \mathbb{E}\{a(t)\}$  is called the arrival rate;  $R(t) \in \mathbb{Z}^{n_q \times n_u}$  is the routing matrix that reflects the number of packets received from or sent to other queues or leaving the queue system in time slot  $t$ . In practice, not every communication link could be activated during the same time slot due to some limitations, such as resources and reliability. Hence, the control vector  $u(t)$  is used to activate some suitable links and make rational use of resources, that is, activating some columns of  $R(t)$ . As a result, some columns of  $R(t)$  are set to 0, whereas others are the same as in  $R(t)$ .

### 6.1.1 Constraints

Due to the complexity of queueing networks, the link activation process, network topology, and queue lengths are subject to the following constraints:

- Constituency constraint:

$$Cu(t) \leq c, \quad (6.2)$$

where  $C \in \mathbb{Z}^{+n_c \times n_u}$  and  $c \in \mathbb{Z}^{+n_c}$ . Some links may not be activated simultaneously because they share the same channels. Hence, this constraint is used to prohibit these links from being activated simultaneously.

- **Dynamic topology:** The routing matrix  $R(t)$  is time-varying, which is governed by an irreducible and aperiodic discrete-time Markov chain (DTMC) in combination with a Bernoulli trial. A diagonal weight matrix  $M(t) \in \{0, 1\}^{n_u \times n_u}$  is introduced to describe the success probability of activated communication links and each diagonal element of  $M(t)$  is Bernoulli distributed, i.e.,  $M(t) \sim \mathcal{B}(W_{r(t)})$  and  $\mathbb{E}\{M(t)\} = W_{r(t)}$ , where  $W_{r(t)}$  is picked from a predetermined set  $\{W_1, \dots, W_{n_r}\}$  and  $r(t) \in \text{DTMC}(\Upsilon, P, r(0))$  with a Markov state set  $\Upsilon = \{1, \dots, n_r\}$ , a transition probability matrix  $P$ , and an initial state  $r(0)$ . Accordingly, a dynamic topology is described by

$$R(t) = RM(t) \tag{6.3}$$

subject to  $M(t) \sim \mathcal{B}(W_{r(t)})$

$$W_{r(t)} \in \{W_1, \dots, W_{n_r}\}$$

$$r(t) \in \text{DTMC}(\Upsilon, P, r(0)),$$

where  $R$  is an invariant matrix containing all possible communication routes among queues and satisfies  $\sum_{\ell=1}^{n_q} (R\mathbf{1}_{n_u})^{[\ell]} < 0$ ;  $\mathbf{1}_n$  represents  $n$ -dimensional column vector with all elements being 1.

- **Positiveness constraint:** For any time slot  $t \in \mathbb{Z}^+$ ,  $q(t) \geq 0$  should be guaranteed. As one single packet can only traverse one single link in a time slot, to avoid that the system routes a single packet through multiple queues in a time slot, the maximum number of packets leaving from each queue should be less than the total packets in this queue, that is,

$$-\tilde{R}(t)u(t) \leq q(t), \tag{6.4}$$

where  $\tilde{R}(t)$  is equal to  $R(t)$  without its positive elements, i.e., all positive elements of  $R(t)$  are set to zero.

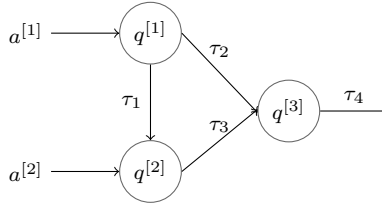


Figure 6.1: An example of a queueing network.

For illustration, we refer to a network composed of 2 arrivals, 3 nodes, and 4 links in Figure 6.1. It is shown that

$$R = \begin{bmatrix} -\tau_1 & -\tau_2 & 0 & 0 \\ \tau_1 & 0 & -\tau_3 & 0 \\ 0 & \tau_2 & \tau_3 & -\tau_4 \end{bmatrix}.$$

If it is required that the first link and second link cannot be activated in the same time slot, then the constituency matrices can be determined by

$$C = [1 \ 1 \ 0 \ 0], \quad c = 1.$$

Consider the dynamic topology of this network with the following matrices:

$$P = \begin{bmatrix} 0.2 & 0.8 \\ 0.5 & 0.5 \end{bmatrix}, \quad \Upsilon = \{1, 2\},$$

$$W_1 = \text{diag}\{1, 0, 1, 0\}, \quad W_2 = \text{diag}\{0.9, 0.1, 0.3, 0.6\}.$$

It indicates that, in time slot  $t$ , if  $r(t) = 1$ , then  $M(t) \sim \mathcal{B}(W_1)$ , implying that the success probabilities of routing packets follow the corresponding diagonal element of  $W_1$ , for example, the success probability that the first queue sends  $\tau_1$  packets to the second queue is 1 if the 1st link is activated and the success probability that the first queue sends  $\tau_2$  packets to the third queue is 0 even if the 2nd link is activated; for the next time slot  $t + 1$ , the probability from “ $r(t) = 1$ ” to “ $r(t + 1) = 1$ ” is 0.2 and the probability from “ $r(t) = 1$ ” to “ $r(t + 1) = 2$ ” is 0.8 according to the transition probability matrix  $P$ .

### 6.1.2 Control Strategy

To deal with constraints (6.2)-(6.4) of the queueing network in (6.1), MPC is applied to generate dynamic link activation schedules in each time slot. Let

$N \in \mathbb{Z}^+_{\geq 1}$  be the prediction horizon of MPC. To reduce the computational burden brought by MPC and improve utilization of communication resources, an event-triggered scheme with an adaptive checking strategy dependent on new arrival is constructed to decide whether the MPC optimization problem should be solved or not in time slot  $t$ , different from the commonly used event-triggered scheme with a persistent event verification.

Denote the checking time slot sequence as  $\{t_l : l \in \mathbb{Z}^+\} \subseteq \mathbb{Z}^+$ . Given a checking time slot  $t_l$ , we introduce a waiting horizon  $\mu : \mathbb{Z}^+ \rightarrow \mathbb{Z}^+_{[1, N]}$ , to determine the next checking time slot, that is,

$$t_{l+1} = t_l + \mu(t_l), \quad (6.5)$$

where  $t_0 = 0$  as  $l = 0$ . The waiting horizon  $\mu(t_l)$  is to be designed based on the arrival frequency of new packets.

Define a queue error  $e(t) \triangleq q(t) - q(t-1)$  and an appropriate triggering function  $\varphi : \mathbb{Z}^{+n_q} \rightarrow \mathbb{Z}^+$  related to  $e$ . Denote the triggering time slot sequence as  $\{t_j : j \in \mathbb{Z}^+\} \subseteq \mathbb{Z}^+$ . Accordingly, the triggering time slot is generated by

$$t_{j+1} = \min\{t \in \mathbb{Z}^+_{(t_j, t_j+N]} \mid \varphi(e(t_l)) > 0\}, \quad (6.6)$$

where  $t_0 = 0$  as  $j = 0$ . Here, the prediction horizon  $N$  is set as the upper bound of the inter-execution time, which is essential in event-triggered MPC to preserve the optimality and stability.

Then, an event-triggered controller  $\kappa : \mathbb{Z}^+ \times \mathbb{Z}^{+n_q} \times \Upsilon \rightarrow \{0, 1\}^{n_u}$  to be designed is of the form

$$u(t) = \kappa(t_j, q(t), r(t)), \quad t \in \mathbb{Z}^+_{[t_j, t_{j+1})}. \quad (6.7)$$

The control structure with the proposed approach is illustrated in Figure 6.2. The designed event trigger consisting of two parts is connected with the queueing network and locally implemented. In the ‘Packet monitoring’ part, whether the current time slot  $t$  is the checking time slot  $t_l$  or not is determined. If it is, i.e.,  $t = t_l$ , then the triggering condition will be checked; else, a feasible control decision constructed by the optimal solution of the



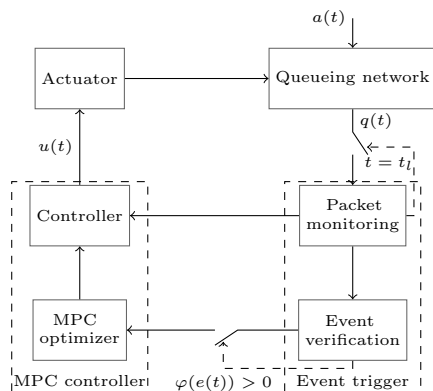


Figure 6.2: Architecture with the proposed event-triggered scheme.

optimization problem in triggering time slot  $t_j$  and stored in the ‘Controller’ will be applied. In the ‘Event verification’ part, if the triggering condition is satisfied, the optimization problem will be solved by the ‘MPC optimizer’; else, the feasible control decision will be executed.

To improve resource utilization while processing more packets for a constrained queueing network with a dynamic topology, this chapter is to design an event-triggered MPC approach involving the waiting horizon  $\mu$  and corresponding triggering function  $\varphi$  such that the triggering condition is checked in some specific time slots and the control decision is optimized accordingly through an on-line stochastic optimization problem if the condition is satisfied in these time slots.

## 6.2 Main Results

As we know, MPC needs to solve the optimization problem in each time slot and only the first element of the optimal control sequence is applied to the system, which indeed requires much computational resources. Hence, we plan to design an event-triggered scheme with an adaptive checking strategy to decide when necessary to solve the MPC optimization problem, leading to reduction of the computational burden brought by MPC and improvement of utilization of communication resources.

### 6.2.1 MPC Optimization Problem

To incorporate a dynamic topology into the MPC optimization problem, for the current time slot  $t$  with a Markov state  $r(t)$ , the expected future routing matrix in time slot  $t + \ell$  is expressed by

$$\hat{R}_\ell(r(t)) \triangleq \mathbb{E}\{R(t + \ell) \mid r(t)\} = ((P^\ell)^{[r(t)]} \otimes I_{n_q}) \begin{bmatrix} RW_1 \\ RW_2 \\ \vdots \\ RW_{n_r} \end{bmatrix}, \quad (6.8)$$

where the symbol  $\otimes$  denotes the Kronecker product. In [96], a quadratic objective function was considered, which increased the complexity for the MPC optimization problem and stability analysis. Hence, in this work, to reduce the complexity of it, a linear objective function is defined according to the positiveness of  $q(t)$ :

$$J(q(t), r(t)) \triangleq \mathbb{E}\left\{ \sum_{\ell=1}^N q_\ell(t)^\top \gamma \right\}, \quad (6.9)$$

where  $q_\ell(t)$  is the predicted queue in time slot  $t + \ell$  and  $q(t) = q_0(t)$ ;  $\gamma$  is a weighting vector with positive elements and satisfies  $(R\mathbf{1}_{n_u})^\top \gamma < 0$ . Naturally, this linear objective function shows clear physical significance, as minimizing  $J$  indicates minimizing the amount of packets in the queueing network, which forces the control decision to process as many packets as possible. Substituting (6.1) and (6.8) into (6.9) yields that

$$J(q(t), r(t)) = (Nq(t) + \sum_{\ell=1}^N \ell \bar{a})^\top \gamma + \hat{J}(q(t), r(t)),$$

where

$$\hat{J}(q(t), r(t)) \triangleq \sum_{\ell=0}^{N-1} (N - \ell) (\hat{R}_\ell(r(t)) u_\ell(t))^\top \gamma.$$

It is seen that in time slot  $t$ ,  $Nq(t)$  and  $\sum_{\ell=1}^N \ell \bar{a}$  are deterministic and do not depend on the control decision  $u(t)$ , which indicates that these two terms have no effect on the minimization of  $J(q(t), r(t))$ . Hence, the minimization

problem of  $J(q(t), r(t))$  is equal to minimize  $\hat{J}(q(t), r(t))$ . Then, a stochastic MPC optimization problem for the queueing network in (6.1) with constraints (6.2)-(6.4) is formulated by

$$\begin{aligned} & \min_{\mathbf{u}(t)} \hat{J}(q(t), r(t)) \\ (C \otimes I_N) \mathbf{u}(t) & \leq c \otimes \mathbf{1}_N \end{aligned} \quad (6.10a)$$

$$\mathbf{u}(t) \in \{0, 1\}^{n_u \cdot N} \quad (6.10b)$$

$$- \begin{bmatrix} \tilde{R}_0(r(t)) & & & & \\ \hat{R}_0(r(t)) & \tilde{R}_1(r(t)) & & & \\ \vdots & \vdots & \ddots & & \\ \hat{R}_0(r(t)) & \hat{R}_1(r(t)) & \cdots & \tilde{R}_{N-1}(r(t)) & \end{bmatrix} \mathbf{u}(t) \leq \begin{bmatrix} q(t) \\ q(t) + \bar{a} \\ \vdots \\ q(t) + (N-1)\bar{a} \end{bmatrix} \quad (6.10c)$$

where  $\mathbf{u}(t) \triangleq [u_0(t)^T \ u_1(t)^T \ \cdots \ u_{N-1}(t)^T]^T$ ;  $\tilde{R}_\ell(r(t))$  is equal to  $\hat{R}_\ell(r(t))$  without its positive elements, i.e., all positive elements of  $\hat{R}_\ell(r(t))$  are set to zero. Equation (6.10a) is the constituency constraint as in (6.2) and (6.10b) is the binary condition on the whole control sequence  $\mathbf{u}(t)$ . It is seen that the positiveness constraint in (6.4) neglects all information of the current arrival packets, namely, setting  $a(t) = 0$ , which can guarantee  $q_1(t) \geq 0$  farthest. If we continue to neglect the arrival packets in the future queue vectors, it is too conservative. Hence, for  $\ell = 2, 3, \dots, N$ , we consider soft constraints  $\mathbb{E}\{q_\ell(t) \mid q(t), r(t)\} \geq 0$ . Then, the positiveness constraints on queue vectors of the future  $N$  time slots can be expressed by

$$\begin{aligned} q(t) + \tilde{R}_0(r(t))u_0(t) & \geq 0 \\ q(t) + \hat{R}_0(r(t))u_0(t) + \tilde{R}_1(r(t))u_1(t) + \bar{a} & \geq 0 \\ & \vdots \\ q(t) + \hat{R}_0(r(t))u_0(t) + \cdots + \tilde{R}_{N-1}(r(t))u_{N-1}(t) + (N-1)\bar{a} & \geq 0 \end{aligned}$$

Consequently, we obtain positiveness constraint (6.10c).

According to (6.10), the optimal control sequence is obtained by

$$\mathbf{u}^*(t) = \arg \min_{\mathbf{u}(t)} \hat{J}(q(t), r(t)). \quad (6.11)$$

## 6.2.2 Event-Triggered Scheme with An Adaptive Checking Strategy

In most existing event-triggered schemes, the event-triggered condition is checked in each time slot no matter how the system changes, undoubtedly showing some conservatism. For a queue network, if there are few or no new packets arrived in some time slots, feasible control decisions of the latest optimal solutions may regulate the system well and it is unnecessary to check the event-triggered condition and solve the MPC optimization problem in these time slots. To achieve this idea, we try to design an adaptive checking strategy for the event-triggered scheme. Since a control decision is largely affected by new arrivals, the idea of designing the event-triggered scheme in (6.5) and (6.6) will take this influence into account. To this end, we use the arrival frequency and the number of new packets to construct the waiting horizon  $\mu$  and the triggering function  $\varphi$ , respectively.

### 6.2.2.1 Waiting Horizon

Given a positive integer  $H$ , for each element of the arrival vector, namely,  $a(t)^{[i]}$ ,  $i = 1, 2, \dots, n_q$ , define a binary vector  $\sigma(t)_i \in \{0, 1\}^H$  and each element of it represents the status of new packets arrival in past  $H$  time slots, i.e., if there is any packet arrived in time slot  $t-l$ ,  $l = 0, 1, \dots, H-1$ , then  $\sigma(t)_i^{[l]} = 1$ ; otherwise,  $\sigma(t)_i^{[l]} = 0$ . Then, we present the following assumption.

**Assumption 6.1.** *There is at least one queue that receives the new arrival packets in past  $H$  time slots.*

Note that we only consider the non-zero elements of the average arrival vector, that is,  $\bar{a}^{[i]} \neq 0$ ,  $i = 1, 2, \dots, n_q$ . Then, for a suitable  $H$ , Assumption 6.1 is easy to satisfy.

Accordingly, in the checking time slot  $t_l$ , the frequency of new arrivals in the  $i$ th queue in past  $H$  time slots is obtained by

$$\hat{\mu}(t_l)_i = \frac{H}{\sigma(t_l)_i^T \sigma(t_l)_i}, \quad (6.12)$$

where  $\sigma(t_l)_i^T \sigma(t_l)_i$  reflects the total arrival times of new packets in past  $H$  time slots. Then, a waiting horizon for the next checking time slot is estimated by

$$\mu(t_l) = \min \{ \min \{ \lfloor \hat{\mu}(t_l)_1 \rfloor, \dots, \lfloor \hat{\mu}(t_l)_{n_q} \rfloor \}, N \}. \quad (6.13)$$

That is, the waiting horizon  $\mu(t_l)$  is generated based on the minimum frequency of new arrivals in all queues. Specifically, if new packets arrive frequently, then the waiting horizon is short; otherwise, the waiting horizon is long.

**Lemma 6.1.** *For given initial values  $H$  and  $N$ , under Assumption 6.1, the waiting horizon satisfies*

$$1 \leq \mu(t_l) \leq \min\{N, H\}. \quad (6.14)$$

**Proof.** According to Assumption 6.1, we have that  $\min\{\lfloor \hat{\mu}(t_l)_1 \rfloor, \dots, \lfloor \hat{\mu}(t_l)_{n_q} \rfloor\} \leq H$ . For the  $i$ th queue, in past  $H$  time slots, the maximum number of arrival times is  $H$ , i.e.,  $\max\{\sigma(t_l)_i^T \sigma(t_l)_i\} = H$ , thus it holds that  $\lfloor \hat{\mu}(t_l)_i \rfloor \geq 1$ . Hence, we have that

$$1 \leq \min\{\lfloor \hat{\mu}(t_l)_1 \rfloor, \dots, \lfloor \hat{\mu}(t_l)_{n_q} \rfloor\} \leq H.$$

Combining it with (6.13) yields that (6.14). ■

### 6.2.2.2 Triggering Function

The triggering function is constructed by

$$\varphi(e(t_l)) = e(t_l)^T \gamma. \quad (6.15)$$

Since

$$e(t_l) = R(t_l - 1)u(t_l - 1) + a(t_l - 1), \quad (6.16)$$

the triggering function is dependent on the packet variations of queues, that is, the sum of errors between leaving and entering packets in these queues. In time slot  $t$ , if  $\varphi(e(t)) > 0$ , then it is necessary to solve the optimization problem to obtain an optimal control decision; else, it is unnecessary to solve the optimization problem and the feasible control can be used.

From (6.13) and (6.15), instead of checking the triggering condition in each time slot as in a traditional event-triggered scheme, the proposed event-triggered scheme can adapt to check it according to the arrival frequency of new packets, which is more flexible. This scheme does not only reasonably schedule packets with limited resources, but also as a novel feature, adaptively predict a waiting horizon for the next checking time slot.

### 6.2.2.3 Inter-Execution Time

Define  $\Delta_j \triangleq t_{j+1} - t_j$ ,  $j \in \mathbb{Z}^+$  as the inter-execution time between the triggering time slot  $t_j$  and  $t_{j+1}$ . Then, we have the following theorem to quantify it.

**Theorem 6.1.** *Under the designed event-triggered scheme in (6.5) and (6.6), in the checking time slot  $t_l \in \mathbb{Z}^+_{(t_j, t_{j+1}]}$ , if  $t_{j+1} = t_l$ , then the inter-execution time satisfies*

$$\Delta_j = \begin{cases} \mu(t_j) + \sum_{s=1}^{\delta} \mu(t_{l-s}), & \text{if } \delta \in \mathbb{Z}^+_{\geq 1}, \\ \mu(t_j), & \text{otherwise.} \end{cases} \quad (6.17)$$

Moreover, we have that

$$1 \leq \Delta_j \leq N, \quad j \in \mathbb{Z}^+. \quad (6.18)$$

**Proof.** In the checking time slot  $t_l \in \mathbb{Z}^+_{(t_j, t_{j+1}]}$ , we need to consider two cases as in Figure 6.3.

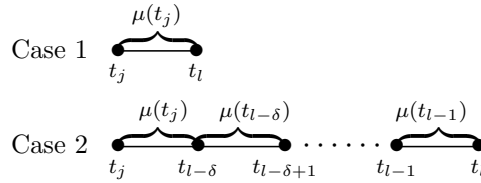


Figure 6.3: Illustration of inter-execution time.

For case 1,  $t_j = t_{l-1}$  and  $t_{j+1} = t_l$ , then

$$\Delta_j = t_l - t_j = \mu(t_j).$$

For case 2,  $t_j = t_{l-\delta-1}$  and  $t_{j+1} = t_l$ , then

$$\Delta_j = t_l - t_j = \mu(t_j) + \mu(t_{l-\delta}) + \cdots + \mu(t_{l-1}).$$

Combining the above two cases yields (6.17). Accordingly, we have that  $\Delta_j \geq \mu(t_j)$ . Seen from (6.6),  $N$  is the upper bound of  $\Delta_j$ . Hence, we have (6.18). ■

**Remark 6.1.** *The parameters  $H$  and  $N$  are crucial in the implementation of the designed event-triggered scheme. A bigger value of  $H$  may make the estimation of the waiting horizon more accurate, but it should not be too big which may not reflect the latest status of packet arrival. A bigger value of the MPC prediction horizon  $N$  will lead to better control performance but larger computational burden. However, the effects of them on the designed event-triggered scheme is challenging to quantify, which is left for future research.*

### 6.2.3 Event-Triggered Controller

Under the designed event-triggered scheme in (6.5) and (6.6), the event-triggered MPC controller in (6.7) is designed by

$$u(t) = u_{t-t_j}^*(t_j), \quad t \in \mathbb{Z}_{[t_j, t_{j+1})}^+. \quad (6.19)$$

It indicates that, in the time slot  $t \in \mathbb{Z}_{>t_j}^+$ , if the event-triggered condition in (6.6) is not satisfied, then a feasible control decision  $u_{t-t_j}^*(t_j)$  would be applied; else, the MPC optimization problem in (6.10) would be solved and a new control sequence  $\mathbf{u}^*(t)$  would be obtained.

It is seen that the MPC optimization problem in (6.10) is essentially a stochastic problem, which means that  $u_{t-t_j}(t_j)$  in (6.19) may not be able to guarantee the positiveness constraint of the queue vector  $q(t)$ . Hence, a positive requirement is incorporated into the queueing network in (6.1) to avoid  $q(t) < 0$ :

$$q(t+1)^{[i]} = \max\{(q(t) + R(t)u(t) + a(t))^{[i]}, 0\}, \quad i = 1, \dots, n_q, \quad (6.20)$$

which implies that the length of the  $i$ th queue would be forced to be zero if it would become negative after using the feasible control decision  $u_{t-t_j}^*(t_j)$ .

**Remark 6.2.** Note that due to the stochasticity of a dynamic topology, not only the event-triggered MPC controller in (6.19) but also many max-weight policies in [97, 98, 99] cannot absolutely guarantee the positiveness constraint. Hence, it is indeed necessary to incorporate (6.20).

## 6.3 Stability of Queueing Networks

A queueing network is stable if its queue vector reaches a steady state and does not blow to infinity. Generally, stability cannot always be guaranteed for any arrival rates. As stated in [100], for a control policy, there exists a stability region of arrival rates for which the system is stable under this policy.

**Definition 6.1.** The queueing network in (6.1) with a dynamic topology is stable if there exists a function  $J : \mathbb{Z}^{+n_q} \times \Upsilon \rightarrow \mathbb{Z}^+$  such that

$$\mathbb{E}\{J(q(t+1), r(t+1)) \mid q(t)\} < \infty$$

for all  $\bar{a} \in \mathcal{A}$ , where  $\mathcal{A}$  is called the stability region.

**Lemma 6.2.** [101, Section 1.8.1] If  $X_1, X_2, X_3, \dots$  are independent and identically distributed with finite mean, and  $T$  is a stopping time with  $\mathbb{E}\{T\} < \infty$ , then  $\sum_{j=1}^T \mathbb{E}\{X_j\} = \mathbb{E}\{T\}\mathbb{E}\{X_1\}$ , where a stopping time is a random variable whose value is completely determined by the past and present events of the stochastic process  $X_1, X_2, X_3, \dots$ , that is,  $T = n$  being determined by  $X_1, \dots, X_n$ .

### 6.3.1 Stability Region

The designed control policy can stabilize the system for a given arrival rate  $\bar{a}$  if it can compensate the arrival rate on average:

$$\begin{aligned} \lim_{\ell \rightarrow \infty} \frac{1}{\ell} \sum_{t=1}^{\ell} (q(t+1) - q(t))^T \gamma &= \lim_{\ell \rightarrow \infty} \frac{1}{\ell} \sum_{t=1}^{\ell} (R(t)u(t) + a(t))^T \gamma \\ &= \lim_{\ell \rightarrow \infty} \frac{1}{\ell} \sum_{t=1}^{\ell} (R(t)u(t))^T \gamma + \bar{a}^T \gamma \\ &= 0. \end{aligned} \tag{6.21}$$



Since the designed event-triggered MPC controller in (6.19) can guarantee constituency constraint (6.2), it indicates that all possible control decisions fall into the following set:

$$\mathcal{U} \triangleq \{u \in \{0, 1\}^{n_u} \mid Cu \leq c\}.$$

Consider this constraint set and the dynamic topology into (6.21) and then we have that

$$\lim_{\ell \rightarrow \infty} \frac{1}{\ell} \sum_{t=1}^{\ell} R(t)u(t) = \sum_{i \in \Upsilon} \pi_i RW_i v, \quad v \in \text{Conv}(\mathcal{U}), \quad (6.22)$$

where  $\text{Conv}(\mathcal{U})$  represents the convex hull of  $\mathcal{U}$  and  $0 \leq \pi_i \leq 1$  is the steady state probability of  $r(t) = i$ ,  $i \in \Upsilon$ . According to (6.21) and (6.22), we define the following stability region:

$$\mathcal{A} \triangleq \left\{ \bar{a} \in \mathbb{Z}^{+n_q} \mid \left( \sum_{i \in \Upsilon} \pi_i RW_i v + \bar{a} \right)^T \gamma \leq 0, \quad v \in \text{Conv}(\mathcal{U}) \right\}. \quad (6.23)$$

Seen from (6.23), the stability region is decided by the weighting vector  $\gamma$  in (6.9) and the properties of the queueing network, such as the constituency constraint in (6.2) and the dynamic topology in (6.3).

### 6.3.2 Terminal Feasible Control Set

According to the designed stability region, we have the following lemma, which is useful to construct a suitable feasible solution and discuss the stability.

**Lemma 6.3.** *For a specified  $\bar{a} \in \mathcal{A}$ , if the prediction horizon  $N$  can satisfy*

$$\hat{R}_N(r(t)) = \sum_{i \in \Upsilon} \pi_i RW_i \quad (6.24)$$

*for any  $r(t) = i$ ,  $i \in \Upsilon$ , then there exists a terminal control set such that*

$$\mathcal{V} \triangleq \left\{ v \in \text{Conv}(\mathcal{U}) \mid (\hat{R}_N(r(t))v + \bar{a})^T \gamma \leq 0 \right\}. \quad (6.25)$$

**Proof.** According to (6.23), for a specified  $\bar{a} \in \mathcal{A}$ , there exists a control set such that

$$\left\{ v \in \text{Conv}(\mathcal{U}) \mid \left( \sum_{i \in \Upsilon} \pi_i R W_i v + \bar{a} \right)^\top \gamma \leq 0 \right\}. \quad (6.26)$$

Substituting (6.24) into (6.26) yields (6.25). ■

In the triggering time slot  $t_j$ , suppose that  $\mathbf{u}^*(t_j)$  is the optimal solution of the optimization problem in (6.10). Then, in the time slot  $t \in \mathbb{Z}^+_{(t_j, t_{j+1}]}$ , a feasible control sequence can be constructed as  $\mathbf{u}(t) \triangleq [u_0(t)^\top \cdots u_{N-1}(t)^\top]^\top$ , where

$$u_\ell(t) = \begin{cases} u_{\ell+(t-t_j)}^*(t_j), & \ell \in \mathbb{N}_{[0, N-1-(t-t_j)]}, \\ v(q_{\ell+(t-t_j)}(t_j)), & \ell \in \mathbb{N}_{[N-(t-t_j), N-1]}, \end{cases} \quad (6.27)$$

$$v(q_\ell(t_j)) \triangleq \arg \min_{v \in \mathcal{V}} (\hat{R}_\ell(r(t_j))v + \bar{a})^\top \gamma. \quad (6.28)$$

Hence,  $v(q_\ell(t_j))$  in (6.28) can be regarded as a terminal feasible control strategy.

### 6.3.3 Stability Analysis

The stability of the queueing network in (6.1) is discussed by the relation between the inter-execution time and objective function, which is shown in the following theorem.

**Theorem 6.2.** *Given the prediction horizon  $N$  satisfying (6.24), under the designed event-triggered scheme in (6.5) and (6.6), the queueing network in (6.1) with a dynamic topology is stable for all  $\bar{a} \in \mathcal{A}$  by the designed event-triggered MPC controller in (6.19).*

**Proof.** In the triggering time slot  $t_j$ , suppose that  $J^*(q(t_j), r(t_j))$  is the optimal objective value obtained by solving the optimization problem in (6.10). Then, in the next triggering time slot  $t_{j+1}$ , a feasible value  $J(q(t_{j+1}), r(t_{j+1}))$  can be constructed based on the feasible control sequence in (6.27). Then, consider the expectation of the difference between  $J(q(t_{j+1}), r(t_{j+1}))$  and  $J^*(q(t_j), r(t_j))$ .

$r(t_j)$ ) conditioned on  $q(t_j)$ :

$$\begin{aligned}
& \mathbb{E}\{J(q(t_{j+1}), r(t_{j+1})) - J^*(q(t_j), r(t_j)) \mid q(t_j)\} \\
&= \mathbb{E}\left\{N(q(t_{j+1}) - q(t_j))^{\text{T}}\gamma - \sum_{\ell=0}^{\Delta_j-1} (N - \ell)(\hat{R}_\ell(r(t_j))u_\ell^*(t_j) + a(t_j + \ell))^{\text{T}}\gamma \right. \\
&\quad \left. \mid q(t_j)\right\} + \sum_{\ell=0}^{N-1-\Delta_j} \mathbb{E}\{\Delta_j(\hat{R}_{\ell+\Delta_j}(r(t_j))u_{\ell+\Delta_j}^*(t_j) + a(t_j + \ell + \Delta_j))^{\text{T}}\gamma \mid q(t_j)\} \\
&\quad + \sum_{\ell=N-\Delta_j}^{N-1} \mathbb{E}\{(N - \ell)(\hat{R}_{\ell+\Delta_j}(r(t_j))v(q_{\ell+\Delta_j}(t_j)) + a(t_j + \ell + \Delta_j))^{\text{T}}\gamma \mid q(t_j)\}.
\end{aligned} \tag{6.29}$$

Since  $q(t_{j+1}) = q(t_j) + \sum_{\ell=0}^{\Delta_j-1} \hat{R}_\ell(r(t_j))u_\ell^*(t_j) + a(t_j + \ell)$ , we have that

$$\begin{aligned}
& \mathbb{E}\left\{N(q(t_{j+1}) - q(t_j))^{\text{T}}\gamma - \sum_{\ell=0}^{\Delta_j-1} (N - \ell)(\hat{R}_\ell(r(t_j))u_\ell^*(t_j) + a(t_j + \ell))^{\text{T}}\gamma \mid q(t_j)\right\} \\
&= \sum_{\ell=1}^{\Delta_j-1} \mathbb{E}\{\ell(\hat{R}_\ell(r(t_j))u_\ell^*(t_j) + a(t_j + \ell))^{\text{T}}\gamma \mid q(t_j)\}.
\end{aligned} \tag{6.30}$$

Since  $(R\mathbf{1}_{n_u})^{\text{T}}\gamma < 0$ , it follows that

$$(\hat{R}_\ell(r(t_j))u_\ell^*(t_j))^{\text{T}}\gamma \leq 0, \quad \ell \in \mathbb{Z}^+.$$

Then, for the optimal solution  $\mathbf{u}^*(t)$ , there exists  $0 \leq \rho \leq -(R\mathbf{1}_{n_u})^{\text{T}}\gamma$  such that

$$\max_{\ell=1, \dots, N-1} (\hat{R}_\ell(r(t_j))u_\ell^*(t_j))^{\text{T}}\gamma = -\rho. \tag{6.31}$$

Since the triggering condition is not satisfied between two triggering time slots, together with (6.15) and (6.16) yields that

$$(\hat{R}_\ell(r(t_j))u_\ell^*(t_j) + a(t_j + \ell))^{\text{T}}\gamma \leq 0, \quad \ell = 0, \dots, \Delta_j - 2. \tag{6.32}$$

Then, we have that

$$\begin{aligned}
& \sum_{\ell=1}^{\Delta_j-1} \mathbb{E}\{\ell(\hat{R}_\ell(r(t_j))u_\ell^*(t_j) + a(t_j + \ell))^T \gamma \mid q(t_j)\} \\
&= \sum_{\ell=1}^{\Delta_j-2} \mathbb{E}\{\ell(\hat{R}_\ell(r(t_j))u_\ell^*(t_j) + a(t_j + \ell))^T \gamma \mid q(t_j)\} \\
&\quad + \mathbb{E}\{(\Delta_j - 1)(\hat{R}_{\Delta_j-1}(r(t_j))u_{\Delta_j-1}^*(t_j) + a(t_j + \Delta_j - 1))^T \gamma \mid q(t_j)\} \\
&\leq 0 - (\bar{\Delta} - 1)\rho + (\bar{\Delta} - 1)\bar{a}^T \gamma.
\end{aligned} \tag{6.33}$$

where  $\bar{\Delta} \triangleq \mathbb{E}\{\Delta_j\}$ . Based on (6.31), by Lemma 6.2, we have that

$$\begin{aligned}
& \sum_{\ell=0}^{N-1-\Delta_j} \mathbb{E}\{\Delta_j(\hat{R}_{\ell+\Delta_j}(r(t_j))u_{\ell+\Delta_j}^*(t_j) + a(t_j + \ell + \Delta_j))^T \gamma \mid q(t_j)\} \\
&\leq \mathbb{E}\{(N - \Delta_j)\} \mathbb{E}\{\Delta_j\} (-\rho + \bar{a}^T \gamma) \\
&= (N\bar{\Delta} - \bar{\Delta}^2)(-\rho + \bar{a}^T \gamma).
\end{aligned} \tag{6.34}$$

With the prediction horizon  $N$  satisfying (6.24), combining (6.25) and (6.28) yields that

$$\sum_{\ell=N-\Delta_j}^{N-1} \mathbb{E}\{(N - \ell)(\hat{R}_{\ell+\Delta_j}(r(t_j))v(q_{\ell+\Delta_j}(t_j)) + a(t_j + \ell + \Delta_j))^T \gamma \mid q(t_j)\} \leq 0. \tag{6.35}$$

Note that  $J^*(q(t_{j+1}), r(t_{j+1})) \leq J(q(t_{j+1}), r(t_{j+1}))$ . Then, substituting (6.30), (6.33), (6.34), and (6.35) into (6.29) yields that

$$\begin{aligned}
& \mathbb{E}\{J^*(q(t_{j+1}), r(t_{j+1})) - J^*(q(t_j), r(t_j)) \mid q(t_j)\} \\
&\leq (N\bar{\Delta} - \bar{\Delta}^2 + \bar{\Delta} - 1)(-\rho + \bar{a}^T \gamma).
\end{aligned} \tag{6.36}$$

Seen from (6.36), it seems that  $\rho$  would be very small if  $J^*(q(t_j), r(t_j))$  is sufficiently large. Note that, as  $J^*(q(t_j), r(t_j))$  increases,  $q(t_j)^T \gamma$  increases as well, which implies that constraint (6.10c) in the optimization problem is certainly satisfied, that is,

$$\begin{aligned}
q(t_j)^T \gamma &\geq - \left( \sum_{\ell=0}^{N-2} (\hat{R}_\ell(r(t_j))u_\ell(t_j))^T \gamma \right) - (\tilde{R}_{N-1}(r(t_j))u_{N-1}(t_j))^T \gamma \\
&\quad - (N - 1)\bar{a}^T \gamma \\
&\geq N\rho - (N - 1)\bar{a}^T \gamma.
\end{aligned} \tag{6.37}$$

Since the objective of the optimization problem in (6.10) is to minimize  $\hat{J}(q(t_j), r(t_j))$ , it indicates that  $\max_{\ell=1, \dots, N-1} (\hat{R}_\ell(r(t_j))u_\ell^*(t_j))^T \gamma$  would become as small as possible to process more packets if  $q(t_j)^T \gamma$  is sufficiently large. Hence, instead of becoming small,  $\rho$  would become as large as possible if  $J^*(q(t_j), r(t_j))$  is sufficiently large. In this case, there exists an  $\epsilon \geq 0$  such that

$$\begin{aligned} \mathbb{E}\{J^*(q(t_{j+1}), r(t_{j+1})) - J^*(q(t_j), r(t_j)) \mid q(t_j)\} &\leq -\epsilon, \\ \text{if } q(t_j)^T \gamma &\geq N\rho - (N-1)\bar{a}^T \gamma, \end{aligned}$$

where  $\rho = \frac{\epsilon}{(N\Delta - \Delta^2 + \Delta - 1)} + \bar{a}^T \gamma$ . Then, there exists a scalar  $0 < \xi \leq 1$  satisfying

$$\begin{aligned} \mathbb{E}\{J^*(q(t_{j+1}), r(t_{j+1})) \mid q(t_j)\} &\leq \xi J^*(q(t_j), r(t_j)), \\ \text{if } q(t_j)^T \gamma &\geq N\rho - (N-1)\bar{a}^T \gamma, \end{aligned}$$

which indicates that

$$\mathbb{E}\{J^*(q(t_{j+1})) \mid q(t_j)\} < \infty. \quad (6.38)$$

Note that if  $\rho$  is small which implies that  $q(t_j)^T \gamma < \infty$  for  $\bar{a} \in \mathcal{A}$ , then (6.38) is certainly guaranteed. Since the triggering condition is not satisfied between two triggering time slots, i.e.,  $e(t)^T \gamma \leq 0$ ,  $t \in \mathbb{Z}^+_{(t_j, t_{j+1})}$ , we have that

$$\mathbb{E}\{J^*(q(t+1)) \mid q(t_j)\} < \infty, t \in \mathbb{Z}^+_{(t_j, t_{j+1})}$$

Combining this with (6.38), according to Definition 6.1, the queueing network in (6.1) with a dynamic topology is stable for all  $\bar{a} \in \mathcal{A}$  by the designed event-triggered MPC controller in (6.19).  $\blacksquare$

**Remark 6.3.** *Since we focus on the expectation of the difference of the objective function between two triggering time slots, to simplify the analysis and avoid the confusion, we ignore the extreme cases (namely,  $\Delta_j = 1$  and  $\Delta_j = N$ ) in the proof of Theorem 6.2. If  $\Delta_j = 1$  or  $\Delta_j = N$ , then some terms including  $\Delta_j - 2$  or  $N - 1 - \Delta_j$  would be removed and (6.36) is still guaranteed.*

## 6.4 Simulation Examples

In this section, two examples are used to show the advantages of the proposed approach and each example is executed by a Monte Carlo simulation with 100 samples.

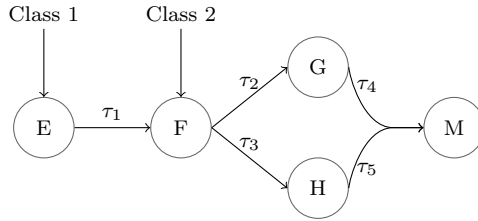


Figure 6.4: Airport scheduling.

**Example 6.1.** This example is concerned with an airport scheduling problem. Figure 6.4 is a schematic showing two classes of customers who wish to travel from different airports (E, F) to a common destination M. To avoid airport congestion problems, we should consider the variability and the finite number of flight seats between airports, and then make optimal control decisions to allow customers to the destination M as many as possible.

A queueing network model can be used to describe this process. Let the queue vector represent the number of customers at different airports, namely,  $q = [q_E \ q_F \ q_G \ q_H]^T$ . Once customers arrive at the destination and then leave, so it is no need to consider airport M in the queue vector. Seen from Figure 6.4, the routing matrix is obtained as

$$R = \begin{bmatrix} -\tau_1 & 0 & 0 & 0 \\ \tau_1 & -\tau_2 & -\tau_3 & 0 \\ 0 & \tau_2 & 0 & -\tau_4 \\ 0 & 0 & \tau_3 & -\tau_5 \end{bmatrix},$$

where  $\tau_1 = 2$ ,  $\tau_2 = 3$ ,  $\tau_3 = 5$ ,  $\tau_4 = 5$ , and  $\tau_5 = 3$ . The variability and the finite number of flight seats between airports are described by the constituency

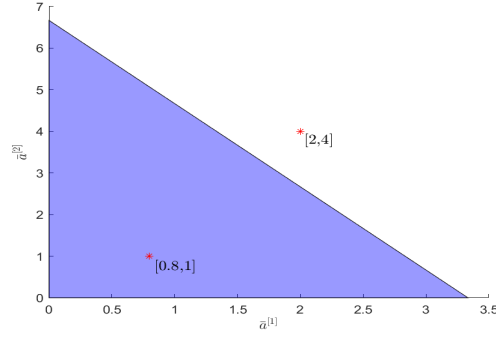


Figure 6.5: Stability region.

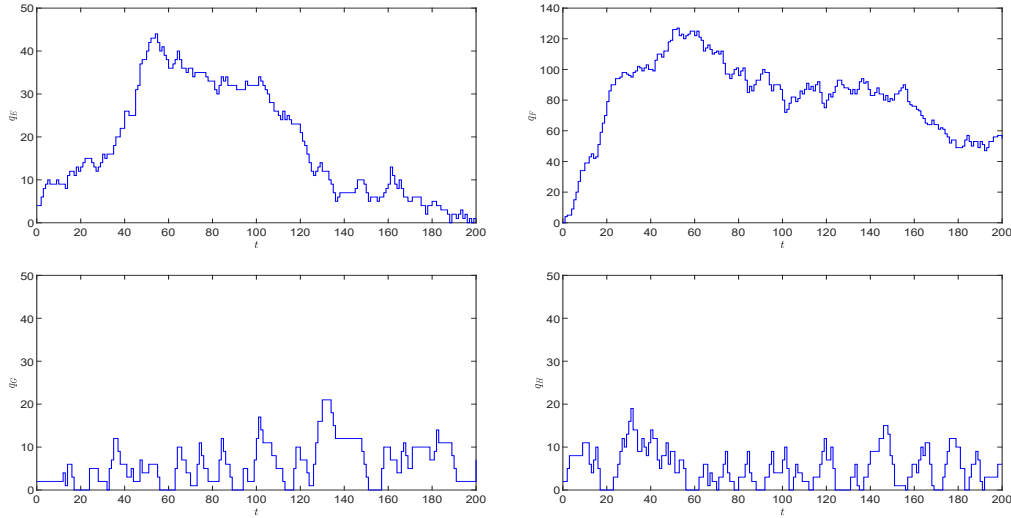


Figure 6.6: The number of customers at airports in one realization.

constraint and a dynamic topology of this model, which are given by

$$C = \begin{bmatrix} 1 & 1 & 1 & 0 \\ 0 & 1 & 1 & 1 \end{bmatrix}, \quad c = \begin{bmatrix} 2 \\ 2 \end{bmatrix}, \quad P = \begin{bmatrix} 0.5 & 0.3 & 0.2 \\ 0.4 & 0.3 & 0.3 \\ 0.2 & 0.6 & 0.2 \end{bmatrix},$$

$$W_1 = \text{diag}\{0.9, 0.6, 0.3, 0.8\}, \quad W_2 = \text{diag}\{0.3, 1, 0.7, 0.1\},$$

$$W_3 = \text{diag}\{0.5, 0.7, 0.5, 0.9\}.$$

The parameters of the proposed approach are selected as follows:  $\gamma = [2 \ 1 \ 1 \ 1]^T$ ,  $N = 9$ , and  $H = 6$ . The initial queue vector is  $q(0) = [4 \ 0 \ 2 \ 2]^T$ . The simulation step is  $T_{\text{step}} = 200$ .

Seen from Figure 6.4, the two customer classes consist of an arrival vector. Assume this arrival vector be Poisson distribution. According to (6.23),

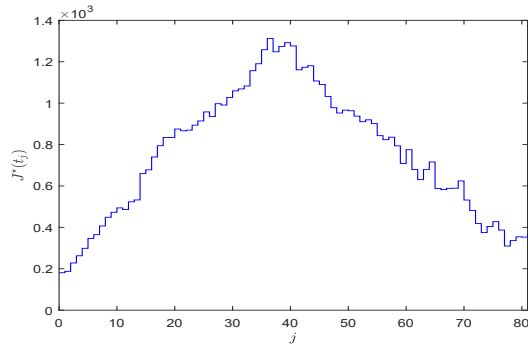


Figure 6.7: Evolution of  $J^*(q(t_j))$  in one realization.

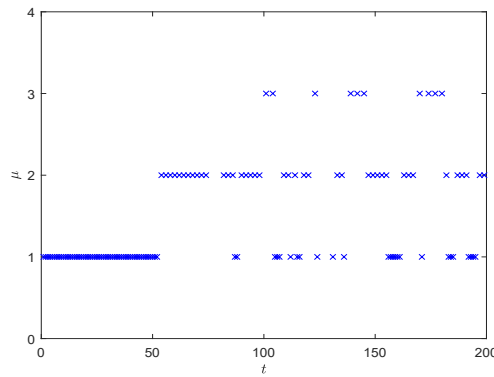


Figure 6.8: Checking time slots in one realization.

the stability region  $\mathcal{A}$  with respect to  $\bar{a}^{[1]}$  and  $\bar{a}^{[2]}$  is depicted in Figure 6.5, which includes all possible values of  $\bar{a}^{[1]}$  and  $\bar{a}^{[2]}$  for which this system is stable. To show the effects of this stability region on the control performance and the designed event-triggered scheme, we consider an unstable point  $\bar{a} = [2 \ 4 \ 0 \ 0]^T \notin \mathcal{A}$  for  $t \leq 50$  and a stable point  $\bar{a} = [0.8 \ 1 \ 0 \ 0]^T \in \mathcal{A}$  for  $t > 50$ . The trajectories of the number of customers at airports in one realization are shown in Figure 6.6. It is seen that, the number of customers at airports E, F presents an increasing trend with an unstable arrival rate and then shows a decreasing trend if a stable arrival rate is considered while the number of customers at airports G, H keeps comparatively stable. Figure 6.7 depicts the evolution of  $J^*(q(t_j))$  in one realization, which shows that there are more than 80 events triggered and the objective value shows a similar trend as the number of customers at airports E, F since it is largely dependent on  $q_E$  and



Table 6.1: Triggering results for  $t \in [50, 200]$

$\bar{\Delta}$	$\bar{\mu}$	$\bar{J}_{\text{diff}}$
3.36	1.88	-18.88

$q_F$ . The triggering results for  $t \in [50, 200]$  are presented in Table 6.1, where  $J_{\text{diff}}$  represents the average difference of optimal objective functions between two triggering time slots in one realization:

$$J_{\text{diff}} = \frac{1}{T_{\text{event}}} \sum_{j=0}^{T_{\text{event}}-1} (J^*(q(t_{j+1})) - J^*(q(t_j))),$$

$T_{\text{event}}$  represents the number of triggered events,  $\bar{J}_{\text{diff}}$  represents the average value of  $J_{\text{diff}}$  in all realizations,  $\bar{\Delta}$  is the average inter-execution time, and  $\bar{\mu}$  is the average waiting horizon to check the triggering condition. The results in this table verify that the stability can be guaranteed for  $\bar{a} \in \mathcal{A}$ . Figure 6.8 depicts the checking time slots. It is observed that the waiting horizon is always equal to 1 when a large arrival rate is considered while it would become longer when the arrival rate is small. Therefore, the designed triggering scheme can estimate a waiting horizon and adapt to check the triggering condition according to the arrival frequency so that to avoid some unnecessary checkings, which is different from most commonly used triggering schemes that need to check the triggering condition in each time slot no matter how low the arrival rate is.

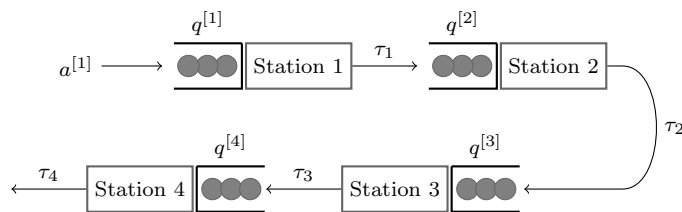


Figure 6.9: A product line.

**Example 6.2.** A product line with 4 stations, 4 buffers, and 4 links shown in Figure 6.9 is a queueing network. A raw material arrival stream which characterizes different product demands, will visit the first station, then the

second, and so on until it is processed by the last station and leaves the system. All stations can work asynchronously according to link activation. Seen from Figure 6.9, we can obtain the following routing matrix:

$$R = \begin{bmatrix} -\tau_1 & 0 & 0 & 0 \\ \tau_1 & -\tau_2 & 0 & 0 \\ 0 & \tau_2 & -\tau_3 & 0 \\ 0 & 0 & \tau_3 & -\tau_4 \end{bmatrix}.$$

It is required that the second link and fourth link cannot be activated in the same time slot, which means that the constituency constraint is given by  $C = [0 \ 1 \ 0 \ 1]$  and  $c = 1$ . For the dynamic topology, a transition probability matrix of DTMC and all diagonal weight matrices of describing the success probability of each activated communication link are given as follows:

$$P = \begin{bmatrix} 0.2 & 0.1 & 0.5 & 0.2 \\ 0.5 & 0.2 & 0 & 0.3 \\ 0.1 & 0.4 & 0.3 & 0.2 \\ 0 & 0.2 & 0.2 & 0.6 \end{bmatrix},$$

$$W_1 = \text{diag}\{1, 1, 1, 1\}, \quad W_2 = \text{diag}\{0.6, 0.4, 0.1, 0.5\},$$

$$W_3 = \text{diag}\{0.1, 0.9, 0.8, 0.9\}, \quad W_4 = \text{diag}\{0.2, 0.3, 0.2, 1\}.$$

The parameters of the routing matrix are  $\tau_1 = 5$ ,  $\tau_2 = 10$ ,  $\tau_3 = 5$ , and  $\tau_4 = 10$ . Set  $N = 13$ ,  $\gamma = [1 \ 1 \ 1 \ 1]^T$ , and  $H = 8$ . The simulation step is  $T_{\text{step}} = 200$ . According to (6.23), we know that the raw material arrival stream should satisfy  $0 \leq \bar{a}^{[1]} \leq 8.63$ . The raw material arrival stream is assumed to be Poisson distribution with  $\bar{a}^{[1]} = 2$ . Assume that initially all queues are empty.

In this example, we compare MPC approaches with the max-weight policy in [97]. Figures 6.10-6.11 depict the trajectories of buffers and total amount of materials in all buffers in one realization, respectively. It is seen that, MPC approaches show a much slower growth than the max-weight policy in [97], which implies that MPC approaches provide better control decisions to process more materials than the max-weight policy in [97] since MPC is able to avoid the myopic problem of max-weight policy.

To compare and evaluate these three approaches, namely, classical MPC, the proposed event-triggered MPC, and the max-weight policy in [97], a com-

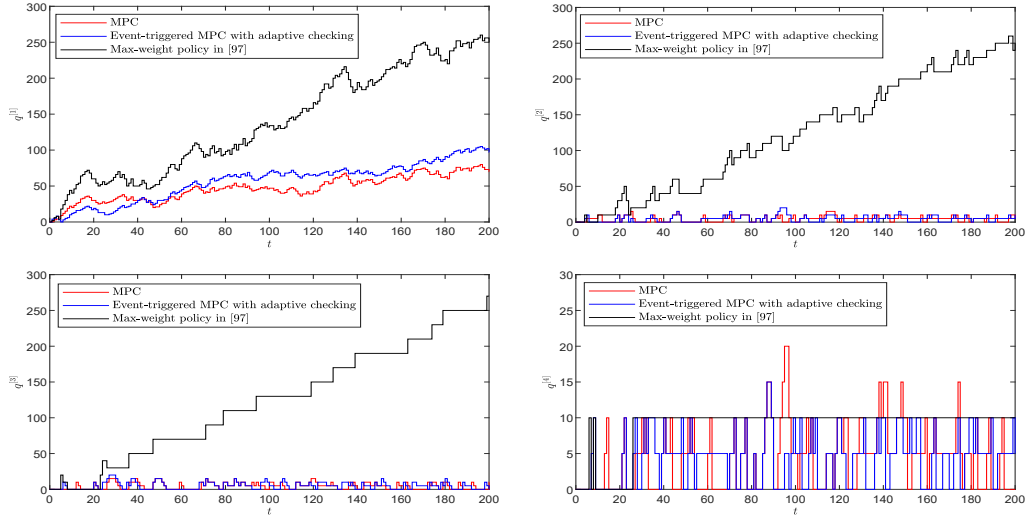


Figure 6.10: Trajectories of buffers in one realization.

Table 6.2: Comparison results with [97]

	$\bar{\Delta}$	CPI
MPC	1	$1.34 \times 10^4$
Event-triggered MPC with adaptive checking	1.52	$0.73 \times 10^4$
Max-weight policy in [97]	1	$0.79 \times 10^4$

prehensive performance index (CPI) is calculated by

$$\text{CPI} = \frac{\bar{Q}\bar{T}_{\text{com}}}{\bar{\Delta}},$$

where  $\bar{Q}$  is the average value of  $Q$  (namely, total amount of materials in all buffers at  $t = 200$ ) and  $\bar{T}_{\text{com}}$  is the average computation time in 100 realizations. Naturally, a larger  $\bar{\Delta}$ , a smaller  $\bar{Q}$ , and a smaller  $\bar{T}_{\text{com}}$  indicate a better approach. Roughly, the smaller the CPI is, the better the approach is. Table 6.2 provides comparison results with classical MPC and the max-weight policy in [97]. Among them, the proposed event-triggered MPC can obtain the best CPI, which implies that it has the best comprehensive performance. Taken together, the proposed strategy can not only require less computational resources than classical MPC, but also process more materials than the max-weight policy in [97].

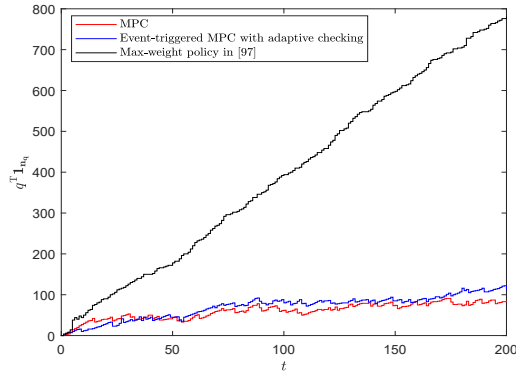


Figure 6.11: The amount of materials in all buffers in one realization.

## 6.5 Summary

In this chapter, an event-triggered stochastic MPC approach has been proposed for the scheduling problem of constrained queueing networks with a dynamic topology. A novel event-triggered scheme combining event checking and triggering with the arrival frequency and the number of new packets, has been designed to achieve adaptive and non-persistent event monitoring and verification, which can decide when it is necessary to solve the stochastic MPC optimization problem with constituency and positiveness constraints, leading to reduced computational burden and improved utilization of communication resources. The stability of queueing networks has been analyzed according to the relation between the inter-execution time and objective function. Simulation results have shown the benefits of the proposed approach.

# Chapter 7

## Conclusions and Future Work

In this chapter, remarks are provided to conclude this thesis, and then some potential research directions are pointed out for future work.

### 7.1 Conclusions

This thesis focuses on the design of event-triggered robust MPC to reduce computational burden as well as guarantee recursive feasibility and robust stability for linear time-invariant systems with bounded disturbances. The outcomes of the studies in this thesis are summarized as follows:

1. In Chapter 2, an event-triggered tube-based MPC approach based on the concept of minimal robust positively invariant sets has been proposed. According to the known probability distribution of bounded disturbances, an event-triggered condition dependent on the state error between the predicted state and the actual state has been derived to achieve a prescribed expectation of inter-execution times, while not sacrificing the quadratic performance significantly.
2. In Chapter 3, based on the distances between actual states and a robust positively invariant set, an event trigger including two-step checks has been designed to ensure necessary events, resulting in a larger average inter-execution time. The effects of designed parameters on the inter-execution time have been analyzed. The designed two-step triggering

scheme has been extended to multi-agent systems and the consensus among all agents has been achieved.

3. In Chapter 4, a stochastic triggering strategy for both tube-based MPC and LMI-based MPC has been proposed. The designed strategy has linked event verification with action triggering, and thus removing persistent monitoring and verification in conventional event-triggered schemes and improving the flexibility and robustness of self-triggered schemes. Recursive feasibility and closed-loop robust stability of both tube-based MPC and LMI-based MPC have been proved.
4. In Chapter 5, an event-triggered data-driven MPC design with a terminal inequality constraint has been investigated for unknown systems with initially measured input-output data. Compared with terminal equality constraints, the constructed terminal inequality constraint for the data-driven MPC optimization problem can lead to a larger feasible region and simplify the analysis of recursive feasibility and stability. According to a mismatch between the data-driven model and the original plant, an event-triggered scheme with a local controller has been designed to trigger the solution of the data-driven MPC optimization problem when necessary, reducing resource consumption.
5. In Chapter 6, an event-triggered stochastic MPC approach has been applied for the scheduling problem of constrained queueing networks with a dynamic topology. Combining event checking and triggering with the arrival frequency and the number of new packets, an event-triggered scheme has been designed to achieve adaptive and non-persistent event monitoring and verification, leading to reduced computational burden and improved utilization of communication resources. The stability of queueing networks has been analyzed according to the relation between the inter-execution time and objective function.

For all proposed approaches, the effectiveness has been demonstrated by numerical examples and the theoretical analysis of recursive feasibility and robust stability has been provided.

## 7.2 Future Work

Based on the obtained results in this thesis, some extension work can be considered as follows:

1. Improve the analysis of the event-triggered scheme with event verification in Chapter 4. There are two topics for future research. One is to consider Markov transition probabilities  $\alpha_{t_l}$  and  $\beta_{t_l}$  into MPC optimization problems to reduce the conservatism. In Chapter 4, only initial values  $\alpha_0$  and  $\beta_0$  are used in the optimization problem in (4.52), rather than  $\alpha_{t_l}$  and  $\beta_{t_l}$  which are dependent on  $t_l$ , since there is a conflict between recursive feasibility of the LMI-based MPC optimization problem in (4.52) and the updating law for  $\alpha_{t_l}$  and  $\beta_{t_l}$ . Another topic, which would be highly meaningful but also challenging, is to analyze the relation between the performance cost and inter-execution time based on the designed Markov chain.
2. Study more effective data-driven predictive models for robust data-driven MPC. Although some results about data-driven MPC have been obtained in Chapter 5, they are preliminary. There are decision variables on both sides of the equation in (5.6a), which may make the predicted states deviate too much from the actual states. A data-driven predictive model with less decision variables may make the predicted states closer to the actual states and reduce computational burden, which needs further investigation.

The future research directions on the improvement of event-triggered control and MPC are summarized with the following aspects:

1. Combine MPC and reinforcement learning algorithms. Most existing data-driven MPC approaches require that the input data should be persistently exciting, which is a strong assumption. Reinforcement learning may be a good choice to remove this data requirement and improve the accuracy of prediction models. For MPC, reinforcement learning can be used to tune the uncertain parameters of MPC, thus improving control performance. For reinforcement learning, MPC can be used as a function approximator to provide safety and stability guarantees of learning. Hence, the combination of MPC and reinforcement learning is an interesting area of research and deserves further study.
2. Develop event-triggered learning methods. Two aspects can be considered. On the one hand, it is difficult for event-triggered control to choose suitable triggering parameters when the system is uncertain or complex. With some advanced learning algorithms, it is possible to learn an optimal event-triggered scheme or update triggering parameters adaptively. On the other hand, learning regularly and permanently is wasteful from a resource point of view. In this case, designing an event-triggered scheme to decide when to learn is worth investigating.



# Bibliography

- [1] B. Kouvaritakis and M. Cannon, *Model Predictive Control: Classical, Robust and Stochastic*. Springer, 2016.
- [2] D. Q. Mayne, “Model predictive control: Recent developments and future promise,” *Automatica*, vol. 50, no. 12, pp. 2967–2986, 2014.
- [3] M. Cannon and B. Kouvaritakis, “Optimizing prediction dynamics for robust MPC,” *IEEE Transactions on Automatic Control*, vol. 50, no. 11, pp. 1892–1897, 2005.
- [4] L. Imsland, N. Bar, and B. A. Foss, “More efficient predictive control,” *Automatica*, vol. 41, no. 8, pp. 1395–1403, 2005.
- [5] B. Kouvaritakis, J. A. Rossiter, and J. Schuurmans, “Efficient robust predictive control,” *IEEE Transactions on Automatic Control*, vol. 45, no. 8, pp. 4283–4287, 2000.
- [6] P. Bumroongsri and S. Kheawhom, “An ellipsoidal off-line model predictive control strategy for linear parameter varying systems with applications in chemical processes,” *Systems & Control Letters*, vol. 61, no. 3, pp. 435–442, 2012.
- [7] Z. Wan and M. V. Kothare, “An efficient off-line formulation of robust model predictive control using linear matrix inequalities,” *Automatica*, vol. 39, no. 5, pp. 837–846, 2003.
- [8] B. Ding, Y. Xi, M. T. Cychowski, and T. O’Mahony, “A synthesis ap-

- proach for output feedback robust constrained model predictive control,” *Automatica*, vol. 44, pp. 258–264, 2008.
- [9] J. Hu and B. Ding, “An efficient offline implementation for output feedback min-max MPC,” *International Journal of Robust & Nonlinear Control*, vol. 29, pp. 492–506, 2019.
- [10] W. P. M. H. Heemels, K. H. Johansson, and P. Tabuada, “An introduction to event-triggered and self-triggered control,” *IEEE Conference on Decision and Control*, pp. 3270–3285, 2012.
- [11] Y. L. Wang, P. Shi, C. C. Lim, and Y. Liu, “Event-triggered fault detection filter design for a continuous-time networked control system,” *IEEE Transactions on Cybernetics*, vol. 46, no. 12, pp. 3414–3426, 2016.
- [12] W. P. M. H. Heemels and M. C. F. Donkers, “Model-based periodic event-triggered control for linear systems,” *Automatica*, vol. 49, pp. 698–711, 2013.
- [13] D. Maity and J. S. Baras, “Optimal event-triggered control of nondeterministic linear systems,” *IEEE Transactions on Automatic Control*, vol. 65, no. 2, pp. 604–619, 2020.
- [14] P. Tallapragada and N. Chopra, “Event-triggered dynamic output feedback control for LTI systems,” *IEEE Conference on Decision and Control*, pp. 6597–6602, 2012.
- [15] H. Yu and P. J. Antsaklis, “Event-triggered output feedback control for networked control systems using passivity: Achieving  $\mathcal{L}_2$  stability in the presence of communication delays and signal quantization,” *Automatica*, vol. 49, no. 1, pp. 30–38, 2013.
- [16] J. Sijts, M. Lazar, and W. P. M. H. Heemels, “On integration of event-based estimation and robust MPC in a feedback loop,” *Proceedings of*

*the 13th ACM international conference on hybrid systems: Computation and control*, pp. 31–40, 2010.

- [17] F. D. Brunner, W. Heemels, and F. Allgöwer, “Event-triggered and self-triggered control for linear systems based on reachable sets,” *Automatica*, vol. 101, pp. 15–26, 2019.
- [18] A. Girard, “Dynamic triggering mechanisms for event-triggered control,” *IEEE Transactions on Automatic Control*, vol. 60, no. 7, pp. 1992–1997, 2015.
- [19] Q. Li, B. Shen, Z. Wang, T. Huang, and J. Luo, “Synchronization control for a class of discrete time-delay complex dynamical networks: A dynamic event-triggered approach,” *IEEE Transactions on Cybernetics*, vol. 49, no. 5, pp. 1979–1986, 2019.
- [20] B. A. Khashoeei, D. J. Antunes, and W. P. M. H. Heemels, “Output-based event-triggered control with performance guarantees,” *IEEE Transactions on Automatic Control*, vol. 62, no. 7, pp. 3646–3652, 2017.
- [21] P. Yang, X. Chen, X. Zhao, and M. Yan, “Fixed time event-triggered tracking control for interconnected nonlinear uncertain systems: An observer-based approach,” *International Journal of Control, Automation and Systems*, vol. 20, pp. 2641–2654, 2022.
- [22] Z. Karimi, A. A. Jalali, and Y. Batmani, “Event-triggered dynamic surface control of uncertain nonlinear networked systems subject to transmission delays,” *International Journal of Robust & Nonlinear Control*, vol. 33, no. 3, pp. 2479–2495, 2023.
- [23] L. Wu, Y. Gao, J. Liu, and H. Li, “Event-triggered sliding mode control of stochastic systems via output feedback,” *Automatica*, vol. 82, pp. 79–92, 2017.

- [24] F. Li and Y. Liu, “Event-triggered stabilization for continuous-time stochastic systems,” *IEEE Transactions on Automatic Control*, vol. 65, no. 10, pp. 4031–4046, 2020.
- [25] D. Ding, Z. Wang, B. Shen, and G. Wei, “Event-triggered consensus control for discrete-time stochastic multi-agent systems: The input-to-state stability in probability,” *Automatica*, vol. 62, pp. 284–291, 2015.
- [26] X. Wang and M. D. Lemmon, “Event-triggering in distributed networked control systems,” *IEEE Transactions on Automatic Control*, vol. 56, no. 3, pp. 586–601, 2011.
- [27] Y. Zou, X. Su, and Y. Niu, “Event-triggered distributed predictive control for the cooperation of multi-agent systems,” *IET Control Theory & Applications*, vol. 11, no. 1, pp. 10–16, 2017.
- [28] Z. Wang and T. Chen, “Data and event-driven control of a class of networked non-linear control systems,” *IET Control Theory & Applications*, vol. 9, no. 7, pp. 1034–1041, 2015.
- [29] H. Li, W. Yan, Y. Shi, and Y. Wang, “Periodic event-triggering in distributed receding horizon control of nonlinear systems,” *Systems & Control Letters*, vol. 86, pp. 16–23, 2015.
- [30] M. Wang, J. Sun, and J. Chen, “Input-to-state stability of perturbed nonlinear systems with event-triggered receding horizon control scheme,” *IEEE Transactions on Industrial Electronics*, vol. 66, no. 8, pp. 6393–6403, 2019.
- [31] B. A. Khashoeei, D. J. Antunes, and W. P. M. H. Heemels, “A consistent threshold-based policy for event-triggered control,” *IEEE Control Systems Letters*, vol. 2, no. 3, pp. 447–452, 2018.
- [32] M. Cucuzzella and A. Ferrara, “Event-triggered second order sliding

- mode control of nonlinear uncertain systems,” *European Control Conference*, pp. 295–300, 2016.
- [33] P. Chen and Y. T. Cheng, “Event-triggered communication and  $H_\infty$  control co-design for networked control systems,” *Automatica*, vol. 49, no. 5, pp. 1326–1332, 2013.
- [34] A. Selivanov and E. Fridman, “Event-triggered  $H_\infty$  control: A switching approach,” *IEEE Transactions on Automatic Control*, vol. 61, no. 10, pp. 3221–3226, 2016.
- [35] H. Yang, X. Guo, L. Dai, and Y. Xia, “Event-triggered predictive control for networked control systems with network-induced delays and packet dropouts,” *International Journal of Robust & Nonlinear Control*, vol. 28, no. 4, pp. 1350–1365, 2018.
- [36] R. Yang and W. X. Zheng, “Output-based event-triggered predictive control for networked control systems,” *IEEE Transactions on Industrial Electronics*, vol. 67, no. 12, pp. 10 631–10 640, 2020.
- [37] P. Tabuada, “Event-triggered real-time scheduling of stabilizing control tasks,” *IEEE Transactions on Automatic Control*, vol. 52, no. 9, pp. 1680–1685, 2007.
- [38] X. Xiao, L. Zhou, D. W. C. Ho, and G. Lu, “Event-triggered control of continuous-time switched linear systems,” *IEEE Transactions on Automatic Control*, vol. 64, no. 4, pp. 1710–1717, 2019.
- [39] Y. Qi and M. Cao, “Finite-time boundedness and stabilisation of switched linear systems using event-triggered controllers,” *IET Control Theory & Applications*, vol. 11, no. 18, pp. 3240–3248, 2017.
- [40] Z. Fei, C. Guan, and X. Zhao, “Event-triggered dynamic output feedback control for switched systems with frequent asynchronism,” *IEEE Transactions on Automatic Control*, vol. 65, no. 7, pp. 3120–3127, 2020.

- [41] B.-C. Zheng, L. Guo, and K. Li, “Event-triggered sliding mode fault-tolerant consensus for a class of leader-follower multi-agent systems,” *International Journal of Control, Automation and Systems*, vol. 19, pp. 2664–2673, 2021.
- [42] Z. Wu, Y. Xu, R. Lu, Y. Wu, and T. Huang, “Event-triggered control for consensus of multiagent systems with fixed/switching topologies,” *IEEE Transactions on Systems, Man, and Cybernetics: Systems*, vol. 48, no. 10, pp. 1736–1746, 2018.
- [43] N. Wu, D. Li, Y. Xi, and B. de Schutter, “Distributed event-triggered model predictive control for urban traffic lights,” *IEEE Transactions on Intelligent Transportation Systems*, vol. 22, no. 8, pp. 4975–4985, 2021.
- [44] S. Du, Q. Zhang, H. Han, H. Sun, and J. Qiao, “Event-triggered model predictive control of wastewater treatment plants,” *Journal of Water Process Engineering*, vol. 47, 2022.
- [45] T. Bai, A. Johansson, K. H. Johansson, and J. Mårtensson, “Event-triggered distributed model predictive control for platoon coordination at Hubs in a transport system,” *IEEE Conference on Decision and Control*, pp. 1198–1204, 2021.
- [46] D. Lehmann, E. Henriksson, and K. H. Johansson, “Event-triggered model predictive control of discrete-time linear systems subject to disturbances,” *European Control Conference*, pp. 1156–1161, 2013.
- [47] K. Zhu, Y. Song, D. Ding, G. Wei, and H. Liu, “Robust MPC under event-triggered mechanism and round-robin protocol: An average dwell-time approach,” *Information Sciences*, vol. 457, pp. 126–140, 2018.
- [48] X. Tang and L. Deng, “Multi-step output feedback predictive control for uncertain discrete-time T-S fuzzy system via event-triggered scheme,” *Automatica*, vol. 107, pp. 362–370, 2019.

- [49] J. Zhang, S. Chai, and B. Zhang, “Model-based event-triggered dynamic output predictive control of networked uncertain systems with random delay,” *International Journal of Systems Science*, vol. 51, no. 1, pp. 20–34, 2020.
- [50] G. P. Incremona, A. Ferrara, and L. Magni, “Asynchronous networked MPC with ISM for uncertain nonlinear systems,” *IEEE Transactions on Automatic Control*, vol. 62, no. 9, pp. 4305–4317, 2017.
- [51] A. S. Kolarijani, S. C. Bregman, P. M. Esfahani, and T. Keviczky, “A decentralized event-based approach for robust model predictive control,” *IEEE Transactions on Automatic Control*, vol. 65, no. 8, pp. 3517–3529, 2020.
- [52] S. Ghorbani, A. A. Safavi, and S. V. Naghavi, “Event-triggered robust model predictive control for Lipschitz nonlinear networked control systems subject to communication delays,” *Transactions of the Institute of Measurement and Control*, vol. 43, no. 5, pp. 1126–1142, 2021.
- [53] S. Liu, Y. Song, G. Wei, D. Ding, and Y. Liu, “Event-triggered dynamic output feedback RMPC for polytopic systems with redundant channels: Input-to-state stability,” *Journal of the Franklin Institute*, vol. 354, no. 7, pp. 2871–2892, 2017.
- [54] H. Chen, M. Liu, and S. Zhang, “Event-triggered distributed dynamic state estimation with imperfect measurements over a finite horizon,” *IET Control Theory & Applications*, vol. 11, no. 15, pp. 2607–2622, 2017.
- [55] Y. Xu, S. Chai, P. Shi, B. Zhang, and Y. Wang, “Resilient and event-triggered control of stochastic jump systems under deception and denial of service attacks,” *International Journal of Robust & Nonlinear Control*, vol. 33, no. 3, pp. 1821–1837, 2023.

- [56] H. Li and Y. Shi, “Event-triggered robust model predictive control of continuous-time nonlinear systems,” *IEEE Transactions on Automatic Control*, vol. 50, no. 5, pp. 1507–1513, 2014.
- [57] C. Liu, J. Gao, H. Li, and D. Xu, “Aperiodic robust model predictive control for constrained continuous-time nonlinear systems: An event-triggered approach,” *IEEE Transactions on Cybernetics*, vol. 48, no. 5, pp. 1397–1405, 2018.
- [58] S. A. K. Hashimoto and D. V. Dimarogonas, “Event-triggered intermittent sampling for nonlinear model predictive control,” *Automatica*, vol. 81, pp. 148–155, 2017.
- [59] Y. Zou, X. Su, S. Li, Y. Niu, and D. Li, “Event-triggered distributed predictive control for asynchronous coordination of multi-agent systems,” *Automatica*, vol. 99, pp. 92–98, 2019.
- [60] C. Liu, H. Li, Y. Shi, and D. Xu, “Codesign of event trigger and feedback policy in robust model predictive control,” *IEEE Transactions on Automatic Control*, vol. 65, no. 1, pp. 302–309, 2020.
- [61] X. Hu, H. Yu, F. Hao, and Y. Luo, “Event-triggered model predictive control for disturbed linear systems under two-channel transmissions,” *International Journal of Robust & Nonlinear Control*, vol. 30, pp. 6701–6719, 2020.
- [62] Z. Sun, Y. Xia, L. Dai, and P. Campoy, “Tracking of unicycle robots using event-based MPC with adaptive prediction horizon,” *IEEE/ASME Transactions on Mechatronics*, vol. 25, no. 2, pp. 739–749, 2020.
- [63] F. D. Brunner, D. Antunes, and F. Allgöwer, “Stochastic thresholds in event-triggered control: A consistent policy for quadratic control,” *Automatica*, vol. 89, pp. 376–381, 2018.



- [64] B. Demirel, A. S. Leong, V. Gupta, and D. E. Quevedo, “Tradeoffs in stochastic event-triggered control,” *IEEE Transactions on Automatic Control*, vol. 64, no. 6, pp. 2567–2574, 2019.
- [65] J. Wu, X. Ren, D. Han, D. Shi, and L. Shi, “Finite-horizon Gaussianity-preserving event-based sensor scheduling in Kalman filter applications,” *Automatica*, vol. 72, pp. 100–107, 2016.
- [66] S. Weerakkody, Y. Mo, B. Sinopoli, D. Han, and L. Shi, “Multi-sensor scheduling for state estimation with event-based, stochastic triggers,” *IEEE Transactions on Automatic Control*, vol. 61, no. 9, pp. 2695–2701, 2016.
- [67] F. D. Brunner, W. P. M. H. Heemels, and F. Allgöwer, “Robust event-triggered MPC with guaranteed asymptotic bound and average sampling rate,” *IEEE Transactions on Automatic Control*, vol. 62, no. 11, pp. 5694–5709, 2017.
- [68] X. Yang, H. Wang, and Q. Zhu, “Event-triggered predictive control of nonlinear stochastic systems with output delay,” *Automatica*, vol. 140, 2022.
- [69] U. Rosolia, X. Zhang, and F. Borrelli, “Robust learning model-predictive control for linear systems performing iterative tasks,” *IEEE Transactions on Automatic Control*, vol. 67, no. 2, pp. 856–869, 2022.
- [70] L. Hewing, J. Kabzan, and M. N. Zeilinger, “Cautious model predictive control using Gaussian process regression,” *IEEE Transactions on Control Systems Technology*, vol. 28, no. 6, pp. 2736–2743, 2020.
- [71] M. Zanon and S. Gros, “Safe reinforcement learning using robust MPC,” *IEEE Transactions on Automatic Control*, vol. 66, no. 8, pp. 3638–3652, 2021.

- [72] J. C. Willems, P. Rapisarda, I. Markovskiy, and B. L. D. Moor, “A note on persistency of excitation,” *Systems & Control Letters*, vol. 54, no. 4, pp. 325–329, 2005.
- [73] J. R. Salvador, D. M. P. na, T. Alamo, and A. Bemporad, “Data-based predictive control via direct weight optimization,” *IFAC PapersOnLine*, pp. 356–361, 2018.
- [74] J. Coulson, J. Lygeros, and F. Dörfler, “Distributionally robust chance constrained data-enabled predictive control,” *IEEE Transactions on Automatic Control*, vol. 67, no. 7, pp. 3289–3304, 2022.
- [75] L. Huang, J. Coulson, J. Lygeros, and F. Dörfler, “Decentralized data-enabled predictive control for power system oscillation damping,” *IEEE Transactions on Control Systems Technology*, vol. 30, no. 3, pp. 1065–1077, 2022.
- [76] J. Berberich, J. Köhler, M. A. Müller, and F. Allgöwer, “Data-driven model predictive control with stability and robustness guarantees,” *IEEE Transactions on Automatic Control*, vol. 66, no. 4, pp. 1702–1717, 2021.
- [77] J. W. Lee, “Exponential stability of constrained receding horizon control with terminal ellipsoid constraints,” *IEEE Transactions on Automatic Control*, vol. 45, no. 1, pp. 83–88, 2000.
- [78] J. Yoo and K. H. Johansson, “Event-triggered model predictive control with a statistical learning,” *IEEE Transactions on Systems, Man, and Cybernetics: Systems*, vol. 51, no. 4, pp. 2571–2581, 2021.
- [79] Z. Li, X. Yuan, Y. Wang, and C.-H. Xie, “Subspace predictive control with the data-driven event-triggered law for linear time-invariant systems,” *Journal of the Franklin Institute*, vol. 356, no. 15, pp. 8167–8181, 2019.

- [80] D. Q. Mayne, M. M. Seron, and S. V. Raković, “Robust model predictive control of constrained linear systems with bounded disturbances,” *Automatica*, vol. 41, no. 2, pp. 219–224, 2005.
- [81] S. V. Raković, E. C. Kerrigan, K. I. Kouramas, and D. Q. Mayne, “Invariant approximations of the minimal robust positively invariant set,” *IEEE Transactions on Automatic Control*, vol. 50, no. 3, pp. 406–410, 2005.
- [82] R. D. Yates and D. J. Goodman, *Probability and Stochastic Processes: A Friendly Introduction for Electrical and Computer Engineers (Third edition)*. John Wiley & Sons, Inc, 2014.
- [83] H. Robbins and S. Monro, “A stochastic approximation method,” *Institute of Mathematical Statistics*, vol. 22, no. 3, pp. 400–407, 1951.
- [84] F. Leibfritz, *COMPL<sub>e</sub>ib: Constrained Matrix-optimization Problem Library—A Collection of Test Examples for Nonlinear Semidefinite Programs, Control System Design and Related Problems*, 2003.
- [85] D. R. Cox and H. D. Miller, *The Theory of Stochastic Processes*. New York: Wiley, 1965.
- [86] A. Alessandri, M. Baglietto, and G. Battistelli, “On estimation error bounds for receding-horizon filters using quadratic boundedness,” *IEEE Transactions on Automatic Control*, vol. 49, no. 8, pp. 1350–1355, 2004.
- [87] L. Magni, D. M. Raimondo, and R. Scattolini, “Regional input-to-state stability for nonlinear model predictive control,” *IEEE Transactions on Automatic Control*, vol. 51, no. 9, pp. 1548–1553, 2006.
- [88] H. Li and Y. Shi, “Networked min-max model predictive control of constrained nonlinear systems with delays and packet dropouts,” *International Journal of Control*, vol. 86, no. 4, pp. 610–624, 2013.

- [89] C. Liu, H. Li, J. Gao, and D. Xu, “Robust self-triggered min-max model predictive control for discrete-time nonlinear systems,” *Automatica*, vol. 89, pp. 333–339, 2018.
- [90] G. C. Goodwin and K. S. Sin, *Adaptive Filtering Prediction and Control*. North Chelmsford, MA, USA: Courier Corporation, 2014.
- [91] C. D. Persis and P. Tesi, “Formulas for data-driven control: Stabilization, optimality, and robustness,” *IEEE Transactions on Automatic Control*, vol. 65, no. 3, pp. 909–924, 2020.
- [92] I. R. Petersen, “A stabilization algorithm for a class of uncertain linear systems,” *Systems & Control Letters*, vol. 8, no. 4, pp. 351–357, 1987.
- [93] I. R. Shafarevich and A. O. Remizov, *Linear Algebra and Geometry*. New York: Springer, 2012.
- [94] C. Conte, C. N. Jones, M. Morari, and M. N. Zeilinger, “Distributed synthesis and stability of cooperative distributed model predictive control for linear systems,” *Automatica*, vol. 69, pp. 117–125, 2016.
- [95] Z. P. Jiang and Y. Wang, “Input-to-state stability for discrete-time nonlinear systems,” *Automatica*, vol. 37, no. 6, pp. 857–869, 2001.
- [96] R. Schoeffauer and G. Wunder, “Model-predictive control for discrete-time queueing networks with varying topology,” *IEEE Transactions on Control of Network Systems*, vol. 8, no. 3, pp. 1528–1539, 2021.
- [97] M. Kasparick and G. Wunder, “Stable wireless network control under service constraints,” *IEEE Transactions on Control of Network Systems*, vol. 5, no. 3, pp. 946–956, 2018.
- [98] M. Bramson, B. D’Auria, and N. Walton, “Stability and instability of the maxweight policy,” *Mathematics of Operations Research*, vol. 46, no. 4, pp. 1611–1638, 2021.

- [99] S. Meyn, *Control Techniques for Complex Networks*. Cambridge University Press, 2007.
- [100] L. Tassiulas and A. Ephremides, “Stability properties of constrained queueing systems and scheduling policies for maximum throughput in multihop radio networks,” *IEEE Transaction on Automatic Control*, vol. 37, no. 12, pp. 1936–1948, 1992.
- [101] S. I. Resnick, *Adventures in Stochastic Processes*. Boston: Birkhäuser, 1992.